

---

# **Correlation between vertebral *Hox* code and vertebral morphology in archosaurs:**

implications for vertebral evolution  
in sauropodomorph dinosaurs



Dissertation zur Erlangung des Doktorgrades  
der Fakultät für Geowissenschaften  
der Ludwig-Maximilians-Universität München

vorgelegt von

**Christine Stephanie Böhmer**

M. Sc. Geological Sciences

München, 10.10.2013

---

Erstgutachter: PD Dr. Oliver W. M. Rauhut  
(Ludwig-Maximilians-Universität München,  
Bayerische Staatssammlung für Geologie und Paläontologie München)

Zweitgutachter: Prof. Dr. Gert Wörheide  
(Ludwig-Maximilians-Universität München,  
Bayerische Staatssammlung für Geologie und Paläontologie München)

Datum der mündlichen Prüfung: 20.12.2013

*“The farther backward you can look, the farther forward you are likely to see.”*

Winston Churchill

*Meinen Eltern und Großeltern in Dankbarkeit gewidmet.*

*Thank you for your unending support of my unending education.*

## Abstract

---

The evolution of the vertebral column is marked by profound morphological changes that have a strong impact on organismal biology. The vital functions of the axial skeleton range from protecting the neural structures through sustaining the body posture to physiological aspects such as breathing. Archosaurs (crocodiles, birds and dinosaurs), as a group, display a striking variety of body plans and vertebral morphologies.

This dissertation aims to contribute to the understanding of the pattern and the genetic basis for the evolution of the vertebral column in archosaurs. The transdisciplinary project comprises five chapters. Framed by a general introduction (chapter 1) and the conclusion (chapter 5), the second chapter considers, from a morphofunctional point of view, the question of (1) why differences in the vertebral column evolved. The present thesis revealed a strong link between the digitally simulated flexion pattern of the presacral vertebral column and the axial movements of modern archosaurs during related activities such as feeding and locomotion: this correlation allowed the inference of the feeding range and locomotor options in the extinct archosaur *Plateosaurus*. This long-necked dinosaur was primarily adapted as mid-level browser, obtaining food that was at or above the horizontal level of its head. There is currently no evidence to unambiguously interpret the locomotion style of *Plateosaurus*. The morphofunctional analysis supported both a quadrupedal and a bipedal posture.

The third chapter addresses, from a molecular biology point of view, the question (2) of how modern taxa develop their vertebral columns. It provides insights into the genetic basis for the embryonic development of the vertebral column in modern archosaurs, which includes the highly conserved *Hox* genes. The *Hox* gene expression pattern was detected in the Nile crocodile (*Crocodylus niloticus*) via whole-mount *in situ* hybridisation experiments. *Hox* paralog genes 4 and 5 are expressed in the cervical region of the crocodile. The anterior expression limit of *HoxC-6* marks the cervicothoracic transition. The expression of *Hox* paralog genes 7 and 8 is restricted to the dorsal series. The same *Hox* genes are expressed along the anteroposterior body axis of crocodiles, chickens and mice, but the pattern of expression is different. The comparative analysis revealed two general processes that are accompanied by evolutionary differences in the axial skeleton: 1) expansion and condensation as well as 2) a shift of genetic activity corresponding to different vertebral counts.

The strong association between the anterior limits of the expression of specific *Hox* genes and the borders between morphological regions of the vertebral axis in a variety of vertebrate species stimulated the work presented in the fourth chapter. It considers the question (3) of whether we can infer that the development of the vertebral column took place in extinct animals. The direct correlation between vertebral *Hox* code and quantifiable vertebral morphology shows that the genetic code is deducible from vertebral morphology in modern crocodiles, chickens and mice. Applying these findings to the fossil relative *Plateosaurus* revealed that the hypothetical *Hox* code for the dinosaur would be generally similar to the crocodylian *Hox* gene expression pattern, but with the variation that the anterior region is expanded, as in birds.

The integrative analysis (morphology, genes and fossils) of the vertebrae greatly enhanced our knowledge of evolutionary processes and provided valuable information about the possible reasons, genetic basis and pattern for evolutionary changes of the vertebral column in extant and extinct archosaurs.

---

## Zusammenfassung

---

Im Laufe der Evolution hat die Wirbelsäule tiefgreifende morphologische Veränderungen erfahren, die sich signifikant auf die Biologie der Organismen ausgewirkt haben. Die lebenswichtigen Funktionen des Axialskeletts reichen vom Schutz der neuralen Strukturen, über die Stützung des Körpers, bis hin zu physiologischen Aufgaben wie beispielsweise der Atmung. Archosauria (Krokodile, Vögel und Dinosaurier) zeigen eine bemerkenswerte Vielfalt an Körperbauplänen und Wirbelmorphologien.

Das Ziel der Dissertation besteht darin, einen entscheidenden Beitrag zum Verständnis der Muster und der genetischen Basis für die Evolution der Wirbelsäule bei Archosauriern zu liefern. Das interdisziplinäre Projekt umfasst fünf Kapitel. Neben einer allgemeinen Einleitung (Kapitel 1) und den Schlussbemerkungen (Kapitel 5), widmet sich das zweite Kapitel aus morphofunktionaler Sicht der Frage (1) warum sich Unterschiede in der Wirbelsäule während der Evolution entwickelt haben. Die vorliegende Arbeit zeigt einen engen Zusammenhang zwischen dem digital simulierten Flexionsmuster der präsakralen Wirbelsäule und den axialen Bewegungen moderner Archosaurier während relevanter Aktivitäten wie beispielsweise Nahrungsaufnahme und Lokomotion. Diese Korrelation ermöglichte es, auf die Nahrungsreichweite sowie die Fortbewegungsmöglichkeiten des ausgestorbenen Archosauriers *Plateosaurus* rückzuschließen. Dieser langhalsige Dinosaurier war primär als Laubäser auf mittlerem Niveau angepasst, der Nahrung auf oder oberhalb seiner horizontalen Kopfhöhe aufgenommen hat. Es konnte kein eindeutiger Hinweis auf die Fortbewegungsweise von *Plateosaurus* erbracht werden. Die Ergebnisse der morphofunktionalen Analyse unterstützen sowohl eine quadrupedale als auch eine bipedale Haltung.

Das dritte Kapitel behandelt aus molekularbiologischer Sicht die Frage (2) wie moderne Arten ihre Wirbelsäule entwickeln. Es liefert Einsichten in die genetische Basis der embryonalen Entwicklung der Wirbelsäule von modernen Archosauriern; die hoch konservativen *Hox* Gene. Das Expressionsmuster der *Hox* Gene wurde beim Nilkrokodil (*Crocodylus niloticus*) mittels whole-mount *in situ* Hybridisierungsexperimenten nachgewiesen. Die *Hox* Gene der paralogen Gruppe 4 und 5 werden in der Halswirbelsäule des Krokodils exprimiert. Die anteriore Expressionsgrenze von *HoxC-6* markiert den Übergang von Hals- zu Brustwirbelsäule. Die *Hox* Gene der paralogen Gruppe 7 und 8 sind auf die Brust- und Lendenwirbelsäule begrenzt. Die gleichen *Hox* Gene werden entlang der anteroposterioren Körperachse des Krokodils, des Huhns und der Maus exprimiert. Das Muster der Expression ist jedoch unterschiedlich. Die vergleichende Analyse hat zwei generelle Prozesse aufgezeigt, die mit den evolutionären Veränderungen des Axialskeletts in Zusammenhang stehen: 1) die Expansion und Kondensation sowie 2) eine Verschiebung der genetischen Aktivität entsprechend der unterschiedlichen Wirbelanzahl.

Der enge Zusammenhang zwischen den anterioren Expressionsgrenzen von spezifischen *Hox* Genen und den Grenzen zwischen morphologischen Regionen der Wirbelsäule bei einer Vielzahl von Wirbeltierarten regte die Arbeit an, die im vierten Kapitel vorgestellt wird. Es widmet sich der Frage (3) ob man auf die Entwicklung der Wirbelsäule von ausgestorbenen Tieren rückschließen kann. Die direkte Korrelation zwischen dem *Hox* Code und der quantifizierbaren Wirbelmorphologie zeigt, dass der jeweilige genetische Code von der Wirbelform des modernen Krokodils, Huhns und der Maus ableitbar ist. Diese Ergebnisse wurden auf den fossilen Verwandten *Plateosaurus* angewendet und lieferten den hypothetischen *Hox* Code für den Dinosaurier. Er wäre generell ähnlich zum *Hox* Gen-Expressionsmuster des Krokodils mit der Variation, dass die anteriore Region wie beim Vogel expandiert wäre.

Die integrative Analyse (Morphologie, Gene und Fossilien) der Wirbel hat unsere Kenntnis über evolutionäre Prozesse grundlegend erweitert. Sie hat wertvolle Informationen über die möglichen Ursachen, die genetische Basis sowie das Muster der evolutionären Veränderungen der Wirbelsäule heutiger und ausgestorbener Archosaurier geliefert.

---

## Table of contents

Abstract .....	4
Zusammenfassung.....	5
Chapter 1: General introduction .....	10
1.1. General aspects .....	10
1.2. Research overview .....	11
1.2.1. Morphology - Part I .....	12
1.2.2. Genes - Part II .....	13
1.2.3. Fossils - Part III .....	13
1.3. Aims and outline of the dissertation .....	14
1.3.1. Superior goal .....	14
1.3.2. Overview of manuscripts.....	14
1.4. Background.....	16
1.4.1. Archosaurs - a variety of body plans .....	16
1.4.2. Biomechanics in dinosaurs .....	17
1.4.3. Development of the vertebral column.....	18
1.4.4. <i>Hox</i> genes and axial patterning .....	19
1.4.5. <i>Hox</i> genes, development and cancer .....	20
1.4.6. Evolution and development .....	20
1.5. References .....	22
Chapter 2: Vertebral evolution in archosaurs: new insights from morphofunctional analysis of <i>Alligator</i> , <i>Plateosaurus</i> and <i>Struthio</i> .....	31
2.1. Introduction.....	32
2.2. Materials and methods .....	34
2.2.2. Morphological analysis.....	35
2.2.1. Digital mounting and mobility range analysis .....	37
2.2.3. Morphofunctional pattern .....	38
2.3. Results .....	40
2.3.1. Comparative anatomical description .....	40

2.3.2.	Morphological analysis.....	43
2.3.2.1.	Vertebral dimensions .....	43
2.3.2.2.	Landmark analysis .....	44
2.3.3.	Mobility range analysis.....	49
2.3.3.1.	Osteological neutral pose (ONP) and maximal flexion.....	49
2.3.3.2.	Flexibility.....	52
2.3.4.	Morphofunctional pattern .....	55
2.4.	Discussion .....	62
2.4.1.	Mobility range analysis.....	62
2.4.2.	Feeding and locomotion behaviour .....	63
2.5.	Conclusion .....	69
2.6.	References.....	71
	Acknowledgements.....	76
	Appendix.....	77
Chapter 3:	New insights into the vertebral <i>Hox</i> code of archosaurs .....	78
3.1.	Introduction.....	79
3.2.	Materials and methods .....	82
3.2.1.	Embryo collection.....	82
3.2.2.	RNA extraction and cDNA synthesis.....	83
3.2.3.	Primer design, sequencing and riboprobe synthesis .....	83
3.2.4.	<i>In situ</i> hybridisation .....	85
3.2.5.	Sectioning .....	87
3.3.	Results .....	87
3.3.1.	Sequence analysis.....	87
3.3.2.	Histology and section analysis.....	87
3.3.3.	<i>Hox</i> gene expression in archosaurs .....	88
3.4.	Discussion .....	92
3.4.1.	<i>Hox</i> gene expression in archosaurs .....	92

3.4.2. <i>Hox</i> gene expression domains and axial evolution .....	96
3.5. Conclusion .....	97
3.6. References .....	99
Acknowledgements .....	103
Appendix.....	104
 Chapter 4: Correlation between <i>Hox</i> code and vertebral morphology in archosaurs: implications for vertebral evolution in sauropodomorph dinosaurs.....	
	113
4.1. Introduction.....	114
4.2. Materials and methods .....	116
4.2.1. Whole-mount <i>in situ</i> hybridisation.....	116
4.2.2. Morphological analysis.....	117
4.3. Results .....	119
4.3.1. <i>Hox</i> gene expression in modern archosaurs .....	119
4.3.2. Vertebral morphology in modern archosaurs.....	121
4.3.2.1. Qualitative morphology.....	121
4.3.2.2. Quantitative morphology (landmark analysis).....	125
4.3.2.3. Morphological pattern (Principal Coordinates and Cluster Analysis) .....	125
4.3.3. Correlation between <i>Hox</i> gene expression and vertebral morphology.....	128
4.3.4. Vertebral morphology and <i>Hox</i> gene expression in extinct archosaur.....	129
4.3.4.1. Vertebral morphology in <i>Plateosaurus</i> .....	130
4.3.4.2. <i>Hox</i> gene expression in <i>Plateosaurus</i> .....	133
4.4. Discussion .....	135
4.4.1. <i>Hox</i> gene expression correlates with vertebral morphology.....	135
4.4.2. Modification of <i>Hox</i> gene expression associated with vertebral evolution.....	137
4.5. Conclusion .....	137
4.6. References.....	139
Acknowledgements.....	142
Appendix.....	143

Chapter 5 ..... 150

5.1. Synopsis ..... 150

5.1.1. Morphology ..... 150

5.1.2. Genes ..... 150

5.1.3. Fossils ..... 151

5.2. Concluding remarks ..... 152

5.3. Future directions ..... 152

5.4. References ..... 154

Acknowledgments ..... 155

## Chapter 1

### General introduction

#### 1.1. General aspects

The axial skeleton (vertebrae and ribs) is the key trait of vertebrates, and it serves many vital functions, from protecting the neural structures and sustaining the body posture through locomotion and food acquisition to physiological aspects such as breathing. The great diversity of vertebral structures and counts results from specific functional adaptations. It is striking that major evolutionary events, such as the transition from water onto land and back again to the sea, the diverse colonisation of terrestrial environments, including the conquest of the air, and the evolution of bipedalism, were accompanied by substantial changes in the axial skeleton. The essential significance of the axial skeleton is not only restricted to fossil non-hominid vertebrate life; it also strongly affects present human life and health. Besides spinal traumas, congenital defects and degenerative diseases of the vertebral column, such as scoliosis, spondylosis and tumours, also have severe effects on human physiology (e.g. Prescher 1998, Tsou et al. 1980). The opportunity to gain new insights into fundamental questions regarding the functioning of the human skeleton and related diseases comes, in part, from understanding the evolution of the vertebral column. Thus, analysing the axial skeleton in our close and distant ancestors will greatly enhance our knowledge of evolutionary processes and also of the genetic basis of phenotypic evolution.

Despite the great variety of vertebral morphology and number, the developmental process of anteroposterior segmentation along the embryonic body axis is a highly conservative mechanism. A special group of regulatory genes, the *Hox* genes, provide a generative programme for the establishment of the regionalised vertebral column in animals as different as fish, birds and mammals (including humans) (Burke et al. 1995, Kessel and Gruss 1990, Kosaki et al. 2002, Morin-Kensicki et al. 2002). This implies that variation in the vertebral column is due to modifications in the pattern of *Hox* gene expression. Comparing the *Hox* code in animals with different axial body plans suggests that evolutionary differences in the vertebral skeleton are associated with changes in the expression of *Hox* genes.

The link between the genetic expression pattern and the morphological pattern was emphasised by mutations in specific *Hox* genes. Defects in or loss of *Hox* gene function result in drastic transformations or severe malformations of vertebrae (e.g. Redline et al. 1992, Wellik and Capecchi 2003). A unique or highly distinct *Hox* code may specify different vertebral morphologies (Gaunt 1994, Johnson and O'Higgins 1996). If the morphological variation of vertebrae can be used as a

proxy for *Hox* gene expression pattern, the genetic basis for vertebral evolution may be also inferred in extinct taxa for which genetic evidence cannot directly be obtained. For the first time, this would allow researchers to comprehensively trace the evolutionary history of the axial skeleton through a holistic approach, integrating comparative morphology, developmental genetics and palaeontology.

## 1.2. Research overview

The evolution of the vertebral skeleton is marked by profound changes, resulting in its huge diversity. The different states among animals are visible in the morphology of vertebrae, in the genes and fossil bones. Transitional fossils in particular open many windows to the evolutionary history of life. Almost all mammals have seven cervical vertebrae, irrespective of their neck length (Galis 1999). A long neck is acquired by a change in the length of the individual vertebrae during evolution. Fossils are the direct record of such changes, because transitional forms exactly show the gradual elongation of the vertebrae (Figure 1.1.). Tracing the process of change with respect to the vertebral column is complicated if the number of vertebrae is different (e.g. Buchholtz 2007, Müller et al. 2010). In contrast to mammalian taxa, reptiles, including dinosaurs and birds, display a high variability in cervical count (Müller et al. 2010). Crocodiles have nine cervical vertebrae, some dinosaurs had up to 19 cervicals and birds vary between 13 and 25 cervical vertebrae. These changes are problematic to study, as it is difficult to establish homologies between vertebrae within an anatomical region (Figure 1.1.).

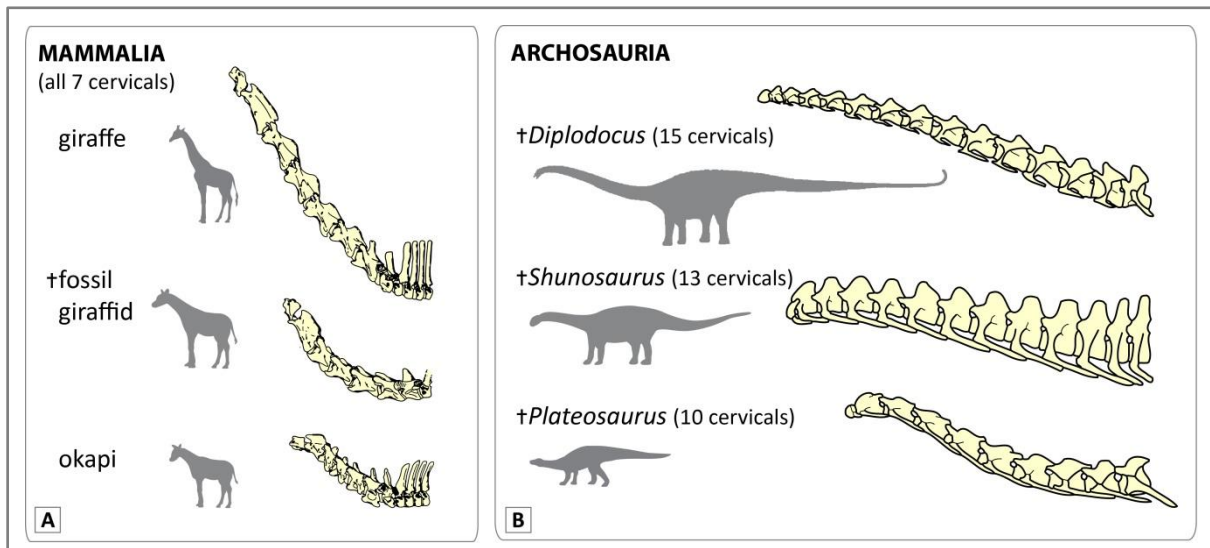


**Figure 1.1.: Evolution of long necks.** (A) The cervical vertebrae of the okapi, a fossil giraffid and the modern giraffe illustrate the evolution of long necks through elongating the individual vertebrae (vertebrae are redrawn after Prothero 2007). (B) Archosaurs (crocodiles, birds and dinosaurs) display a high degree of plasticity. One of the most conspicuous characters of sauropodomorph dinosaurs is the extremely long neck. The cervical vertebrae of the basal sauropodomorph *Plateosaurus*, the basal sauropod *Shunosaurus* and the neosauropod *Diplodocus* show the evolution of long necks associated with increasing the number of vertebrae (vertebrae not to scale). Cross (†) denotes extinct taxon.

This dissertation will address this problem and aims to contribute to the understanding of the pattern and the genetic basis for the evolution of the vertebral column in archosaurs (crocodiles, birds and dinosaurs). All three aspects - morphology, genes and fossils - are integrated in order to gain insights into (1) why differences in the vertebral column evolved, (2) how modern taxa develop their vertebral column and (3) if we can infer how the development of the vertebral column took place in extinct animals (Figure 1.2.).

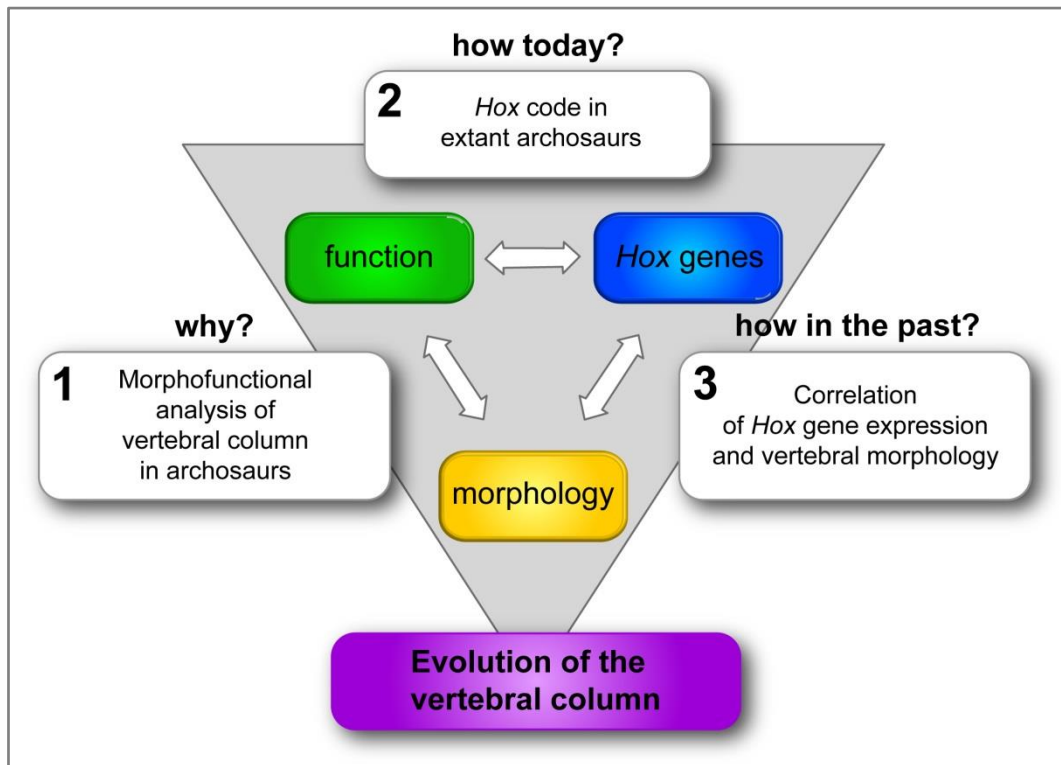


**Figure 1.2.: Research overview.** This thesis investigates three major questions regarding the evolution of the vertebral column in archosaurs (crocodiles, birds and dinosaurs): 1) Why did differences in the vertebral column evolve? The vertebral morphology is related to its biomechanical function. 2) How do modern taxa develop their vertebral column? *Hox* genes specify the vertebral morphology as a function of their taxon-specific expression pattern. 3) Can we infer how the development of the vertebral column took place in extinct animals? A correlation between vertebral morphology and *Hox* gene expression is indicated in extant archosaurs. This may allow the use of morphological variation of vertebrae as an expression pattern proxy in fossil archosaurs.

### 1.2.1. Morphology - Part I

Comparing vertebral morphology reveals that the differences between animals lie in differences in shape (including the presence or absence of attached structures), the size and the number of bones, which is related to different biological roles of the axial skeleton. An extraordinary group of gigantic, Mesozoic reptiles displaying an amazing variability of vertebral morphologies and count, are the sauropodomorph dinosaurs. Linked to the gigantism of these dinosaurs is the evolutionary development of an anatomical key feature: the extremely long neck (Sander et al. 2011 and references therein). There is strong evidence to show that the elongated neck facilitated their evolutionary success, by allowing efficient exploitation of the vegetation, among other things (Sander

et al. 2011 and references therein). Due to the incompleteness of many basal taxa and the phylogenetic uncertainty at the base of the clade, it is difficult to trace the anatomical changes that led to the distinct body plan through sauropodomorph evolution (Rauhut et al. 2011). One of the best-known early taxa is the basal sauropodomorph dinosaur *Plateosaurus* from the Late Triassic. We still lack detailed knowledge about its feeding strategy and locomotion style (e.g. Mallison (2010), Remes (2008) contra Christian and Preuschoft (1996), Fechner (2009) and references therein). Understanding the adaptive value of axial morphology to biological mechanisms and connected behaviour, such as feeding and locomotion, is part of the focus of the first section (chapter 2) of this thesis.

### 1.2.2. Genes - Part II

Evolutionary changes of vertebral morphology and count do not require the evolution of new genes, but likely involve co-opting existing genes in new ways (Carroll 2008, Carroll et al. 2005, Pearson et al. 2005); in keeping with the credo: “Old genes can learn new tricks.” (Carroll 2005). To date, the patterns of *Hox* gene expression along the axial skeleton have been analysed in a variety of vertebrate animals (including fish, mammals and squamates) (Burke et al. 1995, Cohn and Tickle 1999, Kessel and Gruss 1990, Morin-Kensicki et al. 2002, Ohya et al. 2005, Woltering et al. 2009). The *Hox* code in archosaurs is by far the least completely known. Identifying the *Hox* gene expression pattern in the vertebral column of the Nile crocodile is the challenge posed in the second section (chapter 3). Comparing the crocodylian *Hox* code with the genetic programme in chickens and mice will provide new insights into how evolutionary differences in the axial skeleton correspond to changes in the *Hox* gene expression pattern.

### 1.2.3. Fossils - Part III

Genetic activity and embryonic development are powerful sources in the study of evolution. Analysing how *Hox* genes affect the vertebral morphology during embryogenesis in extant animals allows for the use of phenotypic changes during evolution to indirectly reconstruct the underlying genetic programme of development. The observation that specific *Hox* gene expression boundaries coincide with anatomical boundaries along the vertebral column stimulates the work described in chapter 3 of this thesis. The anterior expression limit of *HoxC-6* marks the transition from cervical to thoracic vertebrae in a variety of vertebrate species that differ in cervical number (Burke et al. 1995). Likewise, *Hox-10* and *Hox-11* paralog genes regulate the formation of the boundary between lumbar and sacral vertebrae in vertebrates (Wellik and Capecchi 2003). Thus, the strong link between the genetic expression patterns and the morphological patterns indicates that morphological similarity within an individual vertebral column seems to be directly and causally related to *Hox* gene expression (Johnson and O'Higgins 1996). In the third section of this thesis (chapter 4), the

correlation between *Hox* gene expression and vertebral morphology is tested first in the cervical vertebral column of extant archosaurs. Second, the correlation observed in modern crocodiles and birds will allow a reconstruction of the vertebral *Hox* code in extinct relatives such as the dinosaur *Plateosaurus*.

### **1.3. Aims and outline of the dissertation**

#### **1.3.1. Superior goal**

In order to study the morphological variation of the vertebral column in archosaurs, and to understand how novel or modified structures were generated during evolution, a transdisciplinary approach was necessary. Each of the following three chapters was written to stand on its own as an independent publication. Some redundancy is unavoidable, as the same superior goal (the evolution of the vertebral column in archosaurs) was illuminated from several aspects.

#### **1.3.2. Overview of manuscripts**

Chapter 2 is a morphofunctional analysis of the presacral vertebral column in archosaurs. It reveals a strong link between the morphofunctional pattern and the neck and trunk movements observed in extant archosaurs. This allowed to infer the feeding range and locomotor options in the extinct sauropodomorph dinosaur *Plateosaurus*. The aim of the study was to assess the biological role of the vertebral column in modern and fossil archosaurs in order to understand why changes in vertebral number and morphology appeared during evolution.

In chapter 3, the genetic basis for the embryonic development of the vertebral column in modern archosaurs was analysed. The highly conserved *Hox* genes are the key determinants for the establishment of the anteroposterior patterning, including the regionalisation of the vertebral column in vertebrates. *Hox* gene expression was analysed in the Nile crocodile (*Crocodylus niloticus*) with whole-mount *in situ* hybridisation experiments. Subsequently, the comparative analysis of the *Hox* code in the crocodile, the chicken and the mouse provided new evidence that evolutionary differences in the axial skeleton correspond to changes in *Hox* gene expression domains. The objective of the project is to gain insight into the genetic mechanisms by which changes in vertebral number and morphology in extant archosaurs occurred.

Based on the strong link between genetic and morphological pattern in the vertebral column, as revealed in the previous section, the correlation of *Hox* gene expression and quantifiable vertebral morphology in archosaurs is investigated in chapter 4. Although archosaurs display a great variety of vertebral morphologies and count, it appears that equivalent *Hox* genes are active in the neck during embryonic development. This implies that variation in the cervical vertebral column is due to

modifications in the pattern of gene expression. The aim of the study was to test the correlation in modern crocodiles and birds and to apply the results to extinct archosaurs. The study of morphological variation of vertebrae as an *Hox* gene expression pattern proxy provided an opportunity to confidently infer the genetic basis for vertebral evolution in fossil groups with highly variable vertebral counts, such as sauropodomorph dinosaurs.

#### Author contributions

Chapter 2: **Christine Böhmer**, Oliver W. M. Rauhut, Katrin Reis: Vertebral evolution in archosaurs: new insights from morphofunctional analysis of *Alligator*, *Plateosaurus* and *Struthio*.

CB and OWMR conceived of the study. CB designed and conducted the analyses, interpreted the data and drafted the manuscript. All authors contributed to discussions and the final manuscript.

Manuscript to be submitted as standalone publication.

Chapter 3: **Christine Böhmer**, Oliver W. M. Rauhut, Gert Wörheide: New insights into the vertebral *Hox* code of archosaurs and implications for amniote evolution.

OWMR designed the study. CB performed the experiments, interpreted the data and wrote the manuscript. GW provided analytical tools and reagents. All authors contributed to data interpretation, manuscript editing and discussions.

Manuscript to be submitted as standalone publication.

Chapter 4: **Christine Böhmer**, Oliver W. M. Rauhut, Igor Schneider, Neil H. Shubin, Gert Wörheide: Correlation between *Hox* code and vertebral morphology in archosaurs: implications for vertebral evolution in sauropodomorph dinosaurs.

OWMR designed the study. CB conducted the analyses, interpreted the data and drafted the manuscript. OWMR and GW contributed to data interpretation, discussions and the final manuscript. GW provided analytical tools and reagents. All authors contributed to manuscript editing and discussions.

Manuscript to be submitted as standalone publication.

## 1.4. Background

### 1.4.1. Archosaurs - a variety of body plans

Archosaurs ("ruling reptiles", Cope 1869) represent one of the fundamental divisions of the vertebrate group. They comprise a major group within Reptilia that includes crocodylians, birds and many extinct relatives such as dinosaurs (e.g. Sereno 1991) (Figure 1.3.). The origin of this ancient group lies in the Late Permian or Early Triassic, approximately 250 million years ago (Brusatte et al. 2011). Since then, the archosaurian clade has greatly diversified, achieving global distribution and often playing the dominant role in terrestrial ecosystems (Brusatte et al. 2011). The crown group Archosauria is understood to be divided into two major lineages (Benton 2004, Brusatte et al. 2010): the bird line, Avemetatarsalia (Benton 1999) and the crocodile line, Crurotarsi (Sereno 1991). The latter is considered more morphologically conservative, whereas the morphological variety of birds and dinosaurs is huge (Nesbitt and Norell 2006). One extraordinary group of archosaurs are the long-necked sauropodomorph dinosaurs, the largest terrestrial animals ever that dominated ecosystems over more than 140 million years (reviewed in Sander et al. 2011, Upchurch et al. 2004). They display an amazing variety of vertebral morphologies and count, which is thought to have contributed to the evolution of their gigantic body masses and ultimately resulted in a high rate of diversification,

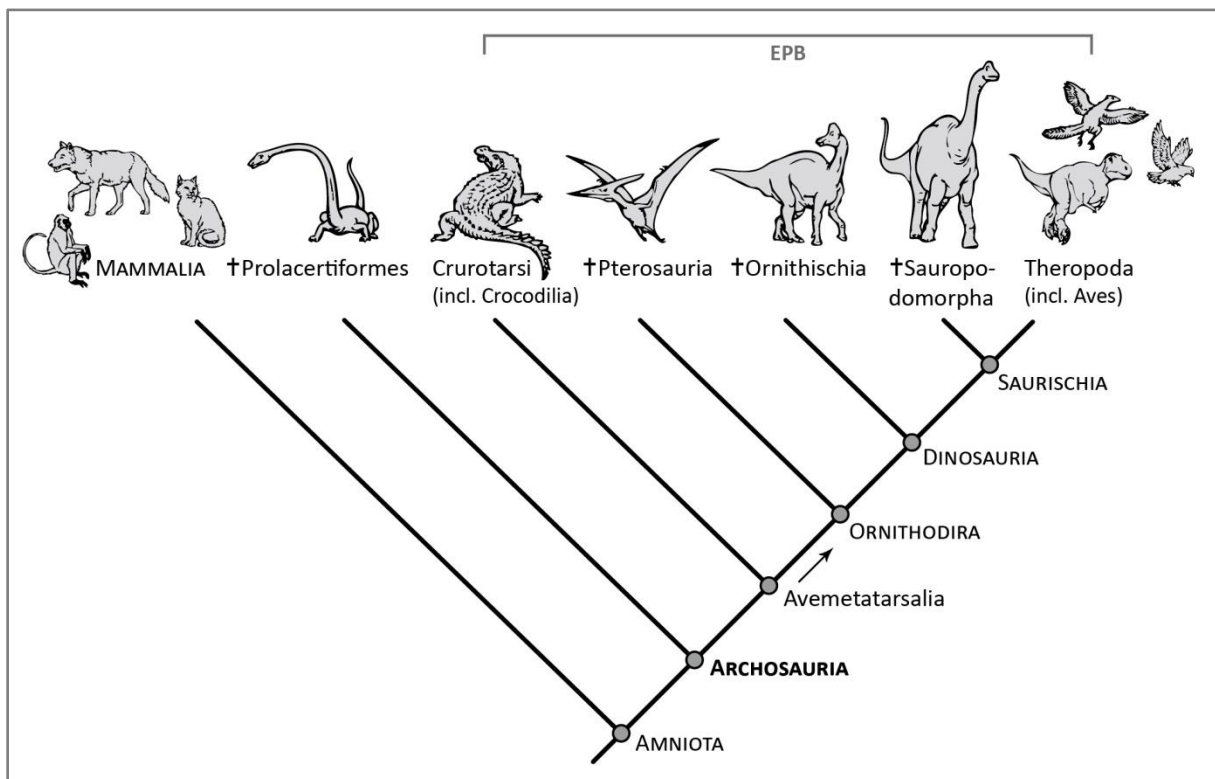


**Figure 1.3.: Phylogenetic framework for Archosauria (mammals as outgroup).** The topology illustrates the relationships between extant and extinct archosaurs. According to the extant phylogenetic bracket (EPB) approach applied in this study, modern crocodiles and birds bracket sauropodomorph dinosaurs. (Tree and animal figures are redrawn and modified from Fastovsky and Weishampel 2009).

reflecting the evolutionary success of this group (Bonaparte 1999, Sander et al. 2011, Wilson 1999). Vertebral characters are even more important than cranial characters in sauropodomorph taxonomy and phylogeny. Although the vertebrae are of both great ecological and systematic significance in the study of sauropodomorph dinosaurs, the exact mode and pattern of vertebral evolution in these extinct organisms is largely unknown.

Fossils are generally represented with little more than bones and teeth as primary data (Witmer 1995). In order to comprehensively analyse the evolution of the vertebral column and, in particular, to understand the associated genetic mechanisms, a methodology for reconstructing information not preserved in the fossil record is necessary: the extant phylogenetic bracket approach (Witmer 1995). This method allows inference of traits of extinct taxa by considering their closest extant relatives (Witmer 1995). Crocodylians and birds are the only surviving representatives of archosaurs among modern vertebrates. They form the bracket around sauropodomorph dinosaurs (Figure 1.3.). Thus, understanding the vertebral development in the modern taxa helps to formulate a hypothesis about the process in fossil archosaurs.

#### **1.4.2. Biomechanics in dinosaurs**

The preserved remains of extinct animals mainly consist of the skeletal system, which includes all the bones and joints in the body. The preserved structure (external and internal) of fossil bones as well as the form of articulation between bones contains direct information regarding the forces that acted on them during life (Kummer 2005, Lauder 1995, Thomason 1995). With regard to the vertebrae, these forces depend mainly on posture, locomotion style and feeding strategy (Hildebrand and Goslow 2004). Thus, the application of the principles of mechanics to fossil bones may provide answers to a large variety of questions concerning dinosaur palaeobiology (reviewed in Alexander 2006).

In this context, sauropodomorph dinosaurs are highly interesting because of their extraordinary body size, with dimensions that are close to the theoretical size limit for terrestrial vertebrates and far beyond the size of present terrestrial animals (Sander and Clauss 2008). However, it is not only the gigantism of these extinct archosaurs that is interesting; their unique body plan, displaying a very small head at the end of an extreme long neck and a huge trunk ending in a very long tail (Galton and Upchurch 2004, Sander et al. 2011, Upchurch et al. 2004) poses particular challenges to the structure of the axial column (Kummer 1975). For instance, one strategy that is supposed to reduce the weight of vertebrae is the development of postcranial pneumaticity, similar to the pneumatisation of the avian skeleton (e.g. Benson et al. 2012, Butler et al. 2012, Kummer 1975, Wedel 2005, Yates et al. 2012).

With regard to the biomechanics of the vertebral column of sauropodomorph dinosaurs, several studies have focused on the posture as well as the static and dynamic forces that act on the axial skeleton (e.g. Alexander 1989, 2006, Christian and Dzemski 2007, Christian and Preuschoft 1996, Martin 1987, Preuschoft et al. 2011, Rauhut et al. 2011, Stevens and Parrish 1999). However, there is still controversy regarding the biological implications of these results; that is, the interpretation of the neck posture and associated feeding strategy as well as the posture of the whole body and associated locomotor options in sauropodomorph dinosaurs.

### 1.4.3. Development of the vertebral column

Despite the great diversity in vertebrate body plan, the basic embryonic development is highly conserved. Early on, during embryogenesis, three different cell regions (germ layers) are formed in animal embryos (gastrulation) that give rise to distinct types of tissue: the outer ectoderm, the middle mesoderm and the inner endoderm (Gilbert 1991, Wolpert et al. 2007). The ectoderm forms the epidermis and the nervous system, whereas the endoderm gives rise to the respiratory and digestive systems (Gilbert 1991, Wolpert et al. 2007). The mesoderm forms internal organs such as the kidney and heart, connective tissues and the skeletomuscular system (Christ and Ordahl 1995, Gilbert 1991, Wolpert et al. 2007).

The middle layer is subdivided into several parts, with one region of cells called paraxial mesoderm producing cartilage, bone and muscles (Gilbert 1991, Wolpert et al. 2007). The paraxial mesoderm cells run longitudinally as two strips along each side of the notochord and neural tube (Dietrich et al. 1997, Gilbert 1991, Pourquie 2003) (Figure 1.4.). Postcranially, at the body level, the dynamic process of somitogenesis initiates the formation of repeated segments called somites (vertebrae precursors) (Dequéant and Pourquie 2008, Dubrulle and Pourquie 2002, Tam et al. 2000). The periodic formation of somites is understood to work as a molecular oscillator or segmentation “clock” (Cooke and

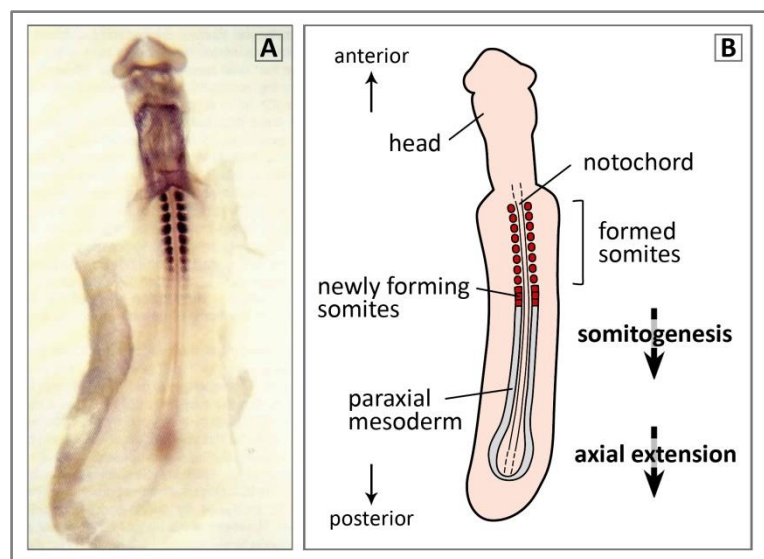


**Figure 1.4.: Somite formation in the chicken.** (A) Chick embryo (2 days of incubation) in ventral view with formed somites at the anterior end and unsegmented paraxial mesoderm at the posterior end (photograph from Brand-Saberi et al. 1996). (B) Schematic representation of somitogenesis. The somites develop successively from the unsegmented paraxial mesoderm that flanks the notochord. The process of somite formation proceeds from anterior to posterior.

Zeeman 1976, Dequéant and Pourquie 2008, Palmeirim et al. 1997, Pourquie 2003). The periodicity and final number of somites is specific for species (Eckalbar et al. 2012, Gomez et al. 2008). Depending on their position along the anteroposterior axis, the homologous somites differentiate into vertebrae displaying different morphologies (Burke and Nowicki 2001, Pourquie 2003), whereby two adjacent somites contribute to one vertebra (theory of resegmentation) (Bagnall et al. 1988 and references therein, Remak 1855). The sequential expression of *Hox* genes in the somites is the molecular basis for defining the particular shape of the vertebrae (Pourquie 2003, Wellik 2007). The *Hox* genes are thought to act as developmental switches (“master control genes”) because the same gene family is at work in animals exhibiting a variety of vertebral morphologies (Gehring et al. 1994, Kmita and Duboule 2003).

#### 1.4.4. *Hox* genes and axial patterning

Despite significant differences in appearance, most animals share several families of genes that regulate major aspects of body pattern (common genetic “toolkit”) (Carroll 2000). These developmental or regulatory genes encode transcription factors and most signalling pathways that participate in the evolutionary conserved gene regulatory networks (GRNs) (reviewed in Ben-Tabou de-Leon and Davidson 2007, Carroll 2000, Davidson and Erwin 2006). The hierarchically organised GRNs control the various phases of development of the animal body plan (Ben-Tabou de-Leon and Davidson 2007, Carroll 2000, Davidson and Erwin 2006). The *Hox* genes, as part of the genetic network, provide cells of the axial and paraxial tissues with specific positional identities along the anteroposterior body axis (Deschamps and van Nes 2005, McGinnis and Krumlauf 1992).

All *Hox* genes share a characteristic 180-bp homeobox encoding a structurally conserved DNA-binding domain in these proteins, the homeodomain (McGinnis et al. 1984). The *Hox* proteins are sequence-specific transcription factors that bind to specific sequences in the DNA and directly regulate the transcription of other genes (Ben-Tabou de-Leon and Davidson 2007, Gehring et al. 1994). In *Drosophila*, eight *Hox* genes among two complexes, the Bithorax Complex (according to Lewis 1978) and the Antennapedia Complex (according to Kaufman et al. 1980), “choreograph” the embryonic development of this animal. They specify the morphological identities of segments in the mesoderm along the anteroposterior body axis (Kaufman et al. 1980, Lewis 1978, Miller et al. 2001). This pioneering discovery stimulated intensive work about homologous genes in other organisms. Indeed, *Hox* genes have also been found in cnidarians and all bilaterian animals (Gehring et al. 1994, Lemons and McGinnis 2006). A systematic nomenclature for *Hox* genes in vertebrates has been proposed by Scott (1992, 1993).

In vertebrates, the expression of different *Hox* genes is associated with the vertebral morphologies along the anteroposterior axis (Burke et al. 1995, Burke and Nowicki 2001, Krumlauf 1994). *Hox*

genes specify distinct vertebral identities along the axial skeleton (Burke et al. 1995). Mutations in *Hox* genes cause homeotic transformations of the vertebral column, resulting in changes of vertebral morphology (e.g. Jeannotte et al. 1993, Mallo et al. 2010, McGinnis and Krumlauf 1992, Scott et al. 1989, Wellik 2007). The importance of these highly conserved genes in the anteroposterior patterning of the vertebrate body plan indicates how crucial *Hox* genes are for understanding the development and evolution of the axial column in vertebrates.

#### 1.4.5. *Hox* genes, development and cancer

*Hox* gene expression is not only involved in the establishment of the primary body axis - that is, the regionalised vertebral column in vertebrates - but *Hox* genes are also important for the development of the secondary axis of the vertebrate embryo, particularly the limbs (e.g. Coates and Cohn 1998, Cohn et al. 1997, Nelson et al. 1996, Tickle 2007). Furthermore, *Hox* genes are expressed in specific tissues and organs of the embryo, such as the kidney (e.g. Cantile et al. 2011, Patterson and Potter 2003, Wellik 2011), the heart (e.g. Makki and Capecchi 2012, Searcy and Yutzey 1998), the central nervous system (e.g. Akin and Nazarali 2005, Krumlauf et al. 1993, Nolte and Krumlauf 2007) and blood cells (e.g. Magli et al. 1997).

Due to the involvement of *Hox* genes in normal embryonic development, they also play an important role in abnormal development and malignant transformations such as cancers (Abate-Shen 2002, Boncinelli 1997, Cillo et al. 1999, Galis 1999, Lappin et al. 2006), which can be considered as anomalous structures growing inside the body (Cantile et al. 2007). From an architectural viewpoint, this follows the equivalent rules that regulate normal embryonic development (Cantile et al. 2007, Cillo 2007). Recent studies suggested that specific *Hox* genes are perturbed in certain types of human cancers, including kidney cancer, breast and prostate cancer as well as leukaemia (e.g. Cantile et al. 2003, Cantile et al. 2011, Chen et al. 2012, Drabkin et al. 2002). Understanding the evolution and function of developmental patterning genes has the potential to help explain the genetic basis of defects, which can serve as potential prognostic tool (Cantile et al. 2011, Veraksa et al. 2000). It has even been suggested that specific *Hox* genes should be targeted in order to achieve a therapeutic effect in cancer patients (Cantile et al. 2007).

#### 1.4.6. Evolution and development

The great diversity of life as a result of evolution is fundamentally linked to embryonic development and the underlying genetic mechanisms that elaborate the phenotype. Thus, the relationship between regulatory genes and phenotypic variation has become of central interest in evolutionary research. In the past three decades, the integration of evolutionary biology and developmental biology in the field of evolutionary developmental biology (Evo-Devo) has revolutionised our

understanding of evolutionary processes (Hall 2003). Analysing the role of regulatory genes, such as *Hox* genes, in animal diversification established the idea that differences in the spatial pattern and temporal timing of gene expression of a shared set of genes (“genetic toolkit”) are the primary causes of morphological evolution (Carroll et al. 2005, Futuyma 2007, Wolpert et al. 2007).

The great potential of the linkage between morphology and genetics through development in vertebrates has gained importance over the last two decades (e.g. Sanchez-Villagra 2010, Thewissen et al. 2012 and references therein). There is a slow but steadily increasing number of attempts to integrate developmental genetics and paleontological data in evolutionary scenarios. With each new study it is becoming clearer and clearer how revealing the synthesis of disciplines is for our understanding of the evolution of life, including human evolution. The most prominent examples concern the origin of the tetrapod limbs (e.g. Fröbisch and Shubin 2011, Schneider and Shubin 2013, Shubin et al. 1997, Shubin et al. 2009) and the evolution of the limbs in archosaurs (e.g. de Bakker et al. 2013, Galis et al. 2005, Tamura et al. 2011, Vargas and Fallon 2005). Other case studies involve the evolution of limb loss that happened independently in a variety of species (e.g. Kohlsdorf et al. 2008, Shapiro et al. 2003, Thewissen et al. 2006) and the formation of teeth and integumental structures such as feathers (e.g. Braga and Heuze 2007, Jernvall and Thesleff 2012, Wu et al. 2004). Recently, the evolutionary history of the vertebral column has been the scope of several studies that attempted to combine modern and fossil data (e.g. Asher et al. 2011, Buchholtz 2007, Filler 2007, Guinard and Marchand 2010, Müller et al. 2010). These works give direction to the identification of patterns of vertebral evolution and suggest possible genetic pathways that may control the evolvability. However, genetic information is only available for modern animals, and interpretation of genetic mechanisms in fossil groups has been largely conjectural. Due to the modular structure of the axial skeleton and the high conservation of *Hox* gene activity along the anteroposterior body axis, the vertebral column can serve as a promising model to establish a direct correlation between developmental genes and phenotypic variation.

## 1.5. References

- Abate-Shen, C., 2002. Deregulated homeobox gene expression in cancer: cause or consequence? *Nature Reviews Cancer* **2**: 777-785.
- Akin, Z.N., Nazarali, A.J., 2005. Hox genes and their candidate downstream targets in the developing central nervous system. *Cellular and Molecular Neurobiology* **25**: 697-741.
- Alexander, R.M., 1989. Dynamics of dinosaurs and other extinct giants. Columbia University Press, New York, 167 pp.
- Alexander, R.M., 2006. Dinosaur biomechanics. *Proceedings of the Royal Society London B* **273**: 1849-1855.
- Asher, R.J., Lin, K.H., Kardjilov, N., Hautier, L., 2011. Variability and constraint in the mammalian vertebral column. *Journal of Evolutionary Biology* **24**: 1080-1090.
- Bagnall, K.M., Higgins, S.J., Sanders, E.J., 1988. The contribution made by a single somite to the vertebral column: experimental evidence in support of resegmentation using the chick-quail chimaera model. *Development* **103**: 69-85.
- Ben-Tabou de-Leon, S., Davidson, E.H., 2007. Gene regulation: gene control network in development. *Annual Review of Biophysics and Biomolecular Structure* **36**: 191.
- Benson, R.B.J., Butler, R.J., Carrano, M.T., O'Connor, P.M., 2012. Air-filled postcranial bones in theropod dinosaurs: physiological implications and the 'reptile'–bird transition. *Biological Reviews* **87**: 168-193.
- Benton, M.J., 1999. *Scleromochlus taylori* and the origin of dinosaurs and pterosaurs. *Philosophical Transactions of the Royal Society London B* **354**: 1423-1446.
- Benton, M.J., 2004. Origin and Relationships of Dinosauria, in: Weishampel, D.B., Dodson, P., Osmólska, H. (Eds.), *The Dinosauria*. University of California Press, Berkeley, California, pp. 7-19.
- Bonaparte, J.F., 1999. Evolución de las vértebras presacras en Sauropodomorpha. *Ameghiniana* **36**: 115-187.
- Boncinelli, E., 1997. Homeobox genes and disease. *Current Opinion in Genetics & Development* **7**: 331-337.
- Braga, J., Heuze, Y., 2007. Quantifying variation in human dental development sequences: An EVO-DEVO perspective, in: Bailey, S., Hublin, J.-J. (Eds.), *Dental Perspectives on Human Evolution: State of the Art Research in Dental Paleoanthropology*. Springer Netherlands, pp. 247-261.
- Brand-Saberri, B., Wilting, J., Ebensperger, C., Christ, B., 1996. The formation of somite compartments in the avian embryo. *The International Journal of Developmental Biology* **40**: 411-420.
- Brusatte, S.L., Benton, M.J., Desojo, J.B., Langer, M.C., 2010. The higher-level phylogeny of Archosauria (Tetrapoda: Diapsida). *Journal of Systematic Palaeontology* **8**: 3-47.
- Brusatte, S.L., Benton, M.J., Lloyd, G.T., Ruta, M., Wang, S.C., 2011. Macroevolutionary patterns in the evolutionary radiation of archosaurs (Tetrapoda: Diapsida). *Earth and Environmental Science Transactions of the Royal Society of Edinburgh* **101**: 367-382.

- Buchholtz, E.A., 2007. Modular evolution of the Cetacean vertebral column. *Evolution & Development* **9**: 278-289.
- Burke, A.C., Nelson, C.E., Morgan, B.A., Tabin, C., 1995. *Hox* genes and the evolution of vertebrate axial morphology. *Development* **121**: 333-346.
- Burke, A.C., Nowicki, J.L., 2001. *Hox* genes and axial specification in vertebrates. *American Zoologist* **41**: 687-697.
- Butler, R.J., Barrett, P.M., Gower, D.J., 2012. Reassessment of the evidence for postcranial skeletal pneumaticity in Triassic archosaurs, and the early evolution of the avian respiratory system. *PLoS One* **7**: e34094.
- Cantile, M., Pettinato, G., Procino, A., Feliciello, I., Cindolo, L., Cillo, C., 2003. In vivo expression of the whole HOX gene network in human breast cancer. *European Journal of Cancer* **39**: 257-264.
- Cantile, M., Schiavo, G., Franco, R., Cindolo, L., Procino, A., D'Armiento, M., Facchini, G., Terracciano, L., Botti, G., Cillo, C., 2011. Expression of lumbosacral HOX genes, crucial in kidney organogenesis, is systematically deregulated in clear cell kidney cancers. *Anticancer Drugs* **22**: 392-401.
- Cantile, M., Schiavo, G., Terracciano, L., Cillo, C., 2007. The HOX gene network as a potential target for cancer therapy. *Current Cancer Therapy Reviews* **3**: 17-24.
- Carroll, S.B., 2000. Endless forms: the evolution of gene regulation and morphological diversity. *Cell* **101**: 577-580.
- Carroll, S.B., 2005. Endless forms most beautiful: the new science of evo devo and the making of the animal kingdom. W. W. Norton & Company, Inc., New York, 350 pp.
- Carroll, S.B., 2008. Evo-devo and an expanding evolutionary synthesis: a genetic theory of morphological evolution. *Cell* **134**: 25-36.
- Carroll, S.B., Grenier, J.K., Weatherbee, S.D., 2005. From DNA to Diversity. Molecular Genetics and the Evolution of animal Design. Blackwell Publishing, Malden, 258 pp.
- Chen, J.L., Li, J., Kiriluk, K.J., Rosen, A.M., Paner, G.P., Antic, T., Lussier, Y.A., Vander Griend, D.J., 2012. Deregulation of a Hox protein regulatory network spanning prostate cancer initiation and progression. *Clinical Cancer Research* **18**: 4291-4302.
- Christ, B., Ordahl, C.P., 1995. Early stages of chick somite development. *Anatomy and Embryology* **191**: 381-396.
- Christian, A., Dzemski, G., 2007. Reconstruction of the cervical skeleton posture of *Brachiosaurus brancai* Janensch, 1914 by an analysis of the intervertebral stress along the neck and a comparison with the results of different approaches. *Fossil Record* **10**: 38-49.
- Christian, A., Preuschoft, H., 1996. Deducing the body posture of extinct large vertebrates from the shape of the vertebral column. *Palaeontology* **39**: 801-812.
- Cillo, C., 2007. Deregulation of the Hox gene network and cancer, in: Papageorgiou, S. (Ed.), Hox gene expression. Landes Bioscience and Springer Science+Business Media, LLC, New York, pp. 121-133.
- Cillo, C., Faiella, A., Cantile, M., Boncinelli, E., 1999. Homeobox genes and cancer. *Experimental Cell Research* **248**: 1-9.

- Coates, M.I., Cohn, M.J., 1998. Fins, limbs, and tails: outgrowths and axial patterning in vertebrate evolution. *Bioessays* **20**: 371-381.
- Cohn, M.J., Patel, K., Krumlauf, R., Wilkinson, D.G., Clarke, J.D., Tickle, C., 1997. Hox9 genes and vertebrate limb specification. *Nature* **387**: 97-101.
- Cohn, M.J., Tickle, C., 1999. Developmental basis of limblessness and axial patterning in snakes. *Nature* **399**: 474-479.
- Cooke, J., Zeeman, E.C., 1976. A clock and wavefront model for control of the number of repeated structures during animal morphogenesis. *Journal of Theoretical Biology* **58**: 455-476.
- Cope, E.D., 1869. Synopsis of the extinct Batrachia, Reptilian and Aves of North America. *Transactions of the American Philosophical Society* **14**: 1-252.
- Davidson, E.H., Erwin, D.H., 2006. Gene regulatory networks and the evolution of animal body plans. *Science* **311**: 796-800.
- de Bakker, M.A., Fowler, D.A., den Oude, K., Dondorp, E.M., Navas, M.C., Horbanczuk, J.O., Sire, J.Y., Szczerbinska, D., Richardson, M.K., 2013. Digit loss in archosaur evolution and the interplay between selection and constraints. *Nature* **500**: 445-448.
- Dequéant, M.L., Pourquie, O., 2008. Segmental patterning of the vertebrate embryonic axis. *Nature Review Genetics* **9**: 370-382.
- Deschamps, J., van Nes, J., 2005. Developmental regulation of the Hox genes during axial morphogenesis in the mouse. *Development* **132**: 2931-2942.
- Dietrich, S., Schubert, F.R., Lumsden, A., 1997. Control of dorsoventral pattern in the chick paraxial mesoderm. *Development* **124**: 3895-3908.
- Drabkin, H.A., Parsy, C., Ferguson, K., Guilhot, F., Lacotte, L., Roy, L., Zeng, C., Baron, A., Hunger, S.P., Varella-Garcia, M., Gemmill, R., Brizard, F., Brizard, A., Roche, J., 2002. Quantitative HOX expression in chromosomally defined subsets of acute myelogenous leukemia. *Leukemia* **16**: 186-195.
- Dubrulle, J., Pourquie, O., 2002. From head to tail: links between the segmentation clock and antero-posterior patterning of the embryo. *Current Opinion in Genetics & Development* **12**: 519-523.
- Eckalbar, W.L., Lasku, E., Infante, C.R., Elsey, R.M., Markov, G.J., Allen, A.N., Corneveaux, J.J., Losos, J.B., DeNardo, D.F., Huentelman, M.J., Wilson-Rawls, J., Rawls, A., Kusumi, K., 2012. Somitogenesis in the anole lizard and alligator reveals evolutionary convergence and divergence in the amniote segmentation clock. *Developmental Biology* **363**: 308-319.
- Fastovsky, D.E., Weishampel, D.B., 2009. Dinosaurs. A concise Natural History. Cambridge University Press, New York, 379 pp.
- Fechner, R., 2009. Morphofunctional evolution of the pelvic girdle and hindlimb of Dinosauromorpha on the lineage to Sauropoda. Dissertation, Ludwig-Maximilians-Universität München, Fakultät für Geowissenschaften, Munich, 197 pp.
- Filler, A.G., 2007. Homeotic evolution in the mammalia: diversification of therian axial seriation and the morphogenetic basis of human origins. *PLoS One* **2**: e1019.

- Fröbisch, N.B., Shubin, N.H., 2011. Salamander limb development: Integrating genes, morphology, and fossils. *Developmental Dynamics* **240**: 1087-1099.
- Futuyma, D.J., 2007. *Evolution*. Spektrum Akademischer Verlag, München, 610 pp.
- Galis, F., 1999. Why do almost all mammals have seven cervical vertebrae? Developmental constraints, *Hox* genes, and cancer. *Journal of Experimental Zoology Part B Molecular and Developmental Evolution* **285**: 19-26.
- Galis, F., Kundrát, M., Metz, J.A.J., 2005. Hox genes, digit identities and the theropod/bird transition. *Journal of Experimental Zoology Part B Molecular and Developmental Evolution* **304**: 198-205.
- Galton, P.M., Upchurch, P., 2004. Prosauropoda, in: Weishampel, D.B., Dodson, P., Osmólska, H. (Eds.), *The Dinosauria*. University of California Press, Berkeley, California, pp. 232-258.
- Gaunt, S.J., 1994. Conservation in the *Hox* code during morphological evolution. *International Journal of Developmental Biology* **38**: 549-552.
- Gehring, W.J., Affolter, M., Burglin, T., 1994. Homeodomain proteins. *Annual Review of Biochemistry* **63**: 487-526.
- Gilbert, S.F., 1991. *Developmental Biology*. Sinauer Association, Inc., Massachusetts, 891 pp.
- Gomez, C., Ösbudak, E.M., Wunderlich, J., Baumann, D., Lewis, J., Pourquié, O., 2008. Control of segment number in vertebrate embryos. *Nature* **454**: 335-339.
- Guinard, G., Marchand, D., 2010. Modularity and complete natural homeoses in cervical vertebrae of extant and extinct penguins (Aves: Sphenisciformes). *Evolutionary Biology* **37**: 210-226.
- Hall, B.K., 2003. Evo-Devo: evolutionary developmental mechanisms. *The International Journal of Developmental Biology* **47**: 491-495.
- Hildebrand, M., Goslow, G.E., 2004. *Vergleichende und funktionelle Anatomie der Wirbeltiere*. Springer Verlag, Berlin und Heidelberg, 713 pp.
- Jeannotte, L., Lemieux, M., Charron, J., Poirier, F., Robertson, E.J., 1993. Specification of axial identity in the mouse: role of the *Hoxa-5* (*Hox1.3*) gene. *Genes & Development* **7**: 2085-2096.
- Jernvall, J., Thesleff, I., 2012. Tooth shape formation and tooth renewal: evolving with the same signals. *Development* **139**: 3487-3497.
- Johnson, D.R., O'Higgins, P., 1996. Is there a link between changes in the vertebral "*hox* code" and the shape of vertebrae? A quantitative study of shape change in the cervical vertebral column of mice. *Journal of Theoretical Biology* **183**: 89-93.
- Kaufman, T.C., Kewis, R., Wakimoto, B., 1980. Cytogenetic analysis of chromosome 3 in *Drosophila melanogaster*: the homeotic gene complex in polytene chromosome interval 84A-B. *Genetics* **94**: 115-133.
- Kessel, M., Gruss, P., 1990. Murine developmental control genes. *Science* **249**: 374-379.
- Kmita, M., Duboule, D., 2003. Organizing axes in time and space; 25 years of colinear tinkering. *Science* **301**: 331-333.

- Kohlsdorf, T., Cummings, M.P., Lynch, V.J., Stopper, G.F., Takahashi, K., Wagner, G.P., 2008. A Molecular Footprint of Limb Loss: Sequence Variation of the Autopodial Identity Gene *Hoxa-13*. *Journal of Molecular Evolution* **67**: 581-593.
- Kosaki, K., Kosaki, R., Suzuki, T., Yoshihashi, H., Takahashi, T., Sasaki, K., Tomita, M., McGinnis, W., Matsuo, N., 2002. Complete mutation analysis panel of the 39 human HOX genes. *Teratology* **65**: 50-62.
- Krumlauf, R., 1994. *Hox* genes in vertebrate development. *Cell* **78**: 191-201.
- Krumlauf, R., Marshall, H., Studer, M., Nonchev, S., Sham, M.H., Lumsden, A., 1993. Hox homeobox genes and regionalisation of the nervous system. *Journal of Neurobiology* **24**: 1328-1340.
- Kummer, B., 1975. Grundsätzliche Bemerkungen zum Einfluß der Körpergröße und der Graviation auf die Konstitution des Bewegungsapparates landbewohnender Tetrapoden. *Aufsätze und Reden der Senckenbergischen naturforschenden Gesellschaft* **27**: 69-84.
- Kummer, B., 2005. Biomechanik. Form und Funktion des Bewegungsapparates. Deutscher Ärzte-Verlag, Köln, 604 pp.
- Lappin, T.R., Grier, D.G., Thompson, A., Halliday, H.L., 2006. HOX genes: seductive science, mysterious mechanisms. *The Ulster Medical Journal* **75**: 23-31.
- Lauder, G.V., 1995. On the inference of function from structure, in: Thomason, J. (Ed.), *Functional morphology in vertebrate paleontology*. Cambridge University Press, Cambridge, pp. 1-18.
- Lemons, D., McGinnis, W., 2006. Genomic evolution of *Hox* gene clusters. *Science* **313**: 1918-1922.
- Lewis, E.B., 1978. A gene complex controlling segmentation in *Drosophila*. *Nature* **276**: 565-570.
- Magli, M.C., Largman, C., Lawrence, H.J., 1997. Effects of HOX homeobox genes in blood cell differentiation. *Journal of Cellular Physiology* **173**: 168-177.
- Makki, N., Capecchi, M.R., 2012. Cardiovascular defects in a mouse model of HOXA1 syndrome. *Human Molecular Genetics* **21**: 26-31.
- Mallison, H., 2010. The digital Plateosaurus II: An assessment of the range of motion of the limbs and vertebral column and of previous reconstructions using a digital skeletal mount. *Acta Palaeontologica Polonica* **55**: 433-458.
- Mallo, M., Wellik, D.M., Deschamps, J., 2010. *Hox* genes and regional patterning of vertebrate body plan. *Developmental Biology* **344**: 7-15.
- Martin, J., 1987. Mobility and feeding of Cetiosaurus (Saurischia, Sauropoda) - why the long neck?, in: Currie, P.J., Koster, E.H. (Eds.), *Fourth Symposium on Mesozoic Terrestrial Ecosystems. Short Papers, Occasional Papers of the Royal Tyrrell Museum of Paleontology*, pp. 154-159.
- McGinnis, W., Garber, R.L., Wirz, J., Kuroiwa, A., Gehring, W.J., 1984. A homologous protein-coding sequence in *Drosophila* homeotic genes and its conservation in other metazoans. *Cell* **37**: 403-408.
- McGinnis, W., Krumlauf, R., 1992. Homeobox genes and axial patterning. *Cell* **68**: 283-302.
- Miller, D.F., Holtzman, S.L., Kalkbrenner, A., Kaufman, T.C., 2001. Homeotic Complex (Hox) gene regulation and homeosis in the mesoderm of the *Drosophila melanogaster* embryo: the roles of signal transduction and cell autonomous regulation. *Mechanisms of Development* **102**: 17-32.

- Morin-Kensicki, E.M., Melancon, E., Eisen, J.S., 2002. Segmental relationship between somites and vertebral column in zebrafish. *Development* **129**: 3851-3860.
- Müller, J., Scheyer, T.M., Head, J.J., Barrett, P.M., Werneburg, I., Ericson, P.G.P., Pol, D., Sánchez-Villagra, M.R., 2010. Homeotic effects, somitogenesis and the evolution of vertebral numbers in recent and fossil amniotes. *Proceedings of the National Academy of Sciences* **107**: 2118-2123.
- Nelson, C.E., Morgan, B.A., Burke, A.C., Laufer, E., DiMambro, E., Murtaugh, L.C., Gonzales, E., Tessarollo, L., Parada, L.F., Tabin, C., 1996. Analysis of Hox gene expression in the chick limb bud. *Development* **122**: 1449-1466.
- Nesbitt, S.J., Norell, M.A., 2006. Extreme convergence in the body plans of an early suchian (Archosauria) and ornithomimid dinosaurs (Theropoda). *Proceedings of the Royal Society London B* **273**: 1045-1048.
- Nolte, C., Krumlauf, R., 2007. Expression of Hox genes in the nervous system of vertebrates, in: Papageorgiou, S. (Ed.), Hox gene expression. Landes Bioscience and Springer Science+Business Media, LLC, New York, pp. 14-41.
- Ohya, Y.K., Kuraku, S., Kuratani, S., 2005. Hox code in embryos of Chinese soft-shelled turtle *Pelodiscus sinensis* correlates with the evolutionary innovation in the turtle. *Journal of Experimental Zoology Part B Molecular and Developmental Evolution* **304**: 107-118.
- Palmeirim, I., Henrique, D., Ish-Horowicz, D., Pourquie, O., 1997. Avian hairy gene expression identifies a molecular clock linked to vertebrate segmentation and somitogenesis. *Cell* **91**: 639-648.
- Patterson, L.T., Potter, S.S., 2003. Hox genes and kidney patterning. *Current Opinion in Nephrology and Hypertension* **12**: 19-23.
- Pearson, J.C., Lemons, D., McGinnis, W., 2005. Modulating Hox gene functions during animal body patterning. *Nature Reviews Genetics* **6**: 893-904.
- Pourquie, O., 2003. The segmentation clock: converting embryonic time into spatial pattern. *Science* **301**: 328-330.
- Prescher, A., 1998. Anatomy and pathology of the aging spine. *European Journal of Radiology* **27**: 181-195.
- Preuschoft, H., Hohn, B., Stoinski, S., Witzel, U., 2011. Why so huge? Biomechanical reasons for the acquisition of large size in sauropod and theropod dinosaurs, in: Klein, N., Remes, K., Gee, C.T., Sander, P.M. (Eds.), Biology of the Sauropod Dinosaurs. Understanding the Life of Giants. Indiana University Press, Bloomington, pp. 179-218.
- Prothero, D.R., 2007. Evolution: what the fossils say and why it matters. Columbia University Press, New York, 381 pp.
- Rauhut, O.W.M., Fechner, R., Remes, K., Reis, K., 2011. How to get big in the Mesozoic: the evolution of the sauropodomorph body plan, in: Klein, N., Remes, K., Gee, C.T., Sander, P.M. (Eds.), Biology of the Sauropod Dinosaurs: Understanding the Life of Giants. Indiana University Press, Bloomington, pp. 119-149.
- Redline, R.W., Neish, A., Holmes, L.B., Collins, T., 1992. Homeobox genes and congenital malformations. *Laboratory Investigation* **66**: 659-670.

- Remak, R., 1855. Untersuchungen über die Entwicklung der Wirbelthiere. Reimer, Berlin, 194 pp.
- Remes, K., 2008. Evolution of the pectoral girdle and forelimb in Sauropodomorpha (Dinosauria, Saurischia): osteology, myology and function. Dissertation, Ludwig-Maximilians-Universität München, Fakultät für Geowissenschaften, Munich, 355 pp.
- Sanchez-Villagra, M.R., 2010. Developmental palaeontology in synapsids: the fossil record of ontogeny in mammals and their closest relatives. *Proceedings of the Royal Society London B* **277**: 1139-1147.
- Sander, P.M., Christian, A., Clauss, M., Fechner, R., Gee, C.T., Griebeler, E.-M., Gunga, H.-C., Hummel, J., Mallison, H., Perry, S.F., Preuschoft, H., Rauhut, O.W.M., Remes, K., Tütken, T., Wings, O., Witzel, U., 2011. Biology of the sauropod dinosaurs: the evolution of gigantism. *Biological Reviews* **86**: 117-155.
- Sander, P.M., Clauss, M., 2008. Sauropod gigantism. *Science* **322**: 200-201.
- Schneider, I., Shubin, N.H., 2013. The origin of the tetrapod limb: from expeditions to enhancers. *Trends in Genetics* **29**: 419-426.
- Scott, M.P., 1992. Vertebrate homeobox gene nomenclature. *Cell* **71**: 551-553.
- Scott, M.P., 1993. A rational nomenclature for vertebrate homeobox (HOX) genes. *Nucleic Acids Research* **21**: 1687-1688.
- Scott, M.P., Tamkun, J.W., Hartzell, G.W., 3rd, 1989. The structure and function of the homeodomain. *Biochimica et Biophysica Acta* **989**: 25-48.
- Searcy, R.D., Yutzey, K.E., 1998. Analysis of Hox gene expression during early avian heart development. *Developmental Dynamics* **213**: 82-91.
- Sereno, P.C., 1991. Basal Archosaurs: Phylogenetic Relationships and Functional Implications. *Journal of Vertebrate Paleontology* **11**: 1-53.
- Shapiro, M.D., Hanken, J., Rosenthal, N., 2003. Developmental basis of evolutionary digit loss in the Australian lizard *Hemiergis*. *Journal of Experimental Zoology Part B Molecular and Developmental Evolution* **297**: 48-56.
- Shubin, N., Tabin, C., Carroll, S.B., 1997. Fossils, genes and the evolution of animal limbs. *Nature* **388**: 639-648.
- Shubin, N., Tabin, C., Carroll, S.B., 2009. Deep homology and the origins of evolutionary novelty. *Nature* **457**: 818-823.
- Stevens, K.A., Parrish, J.M., 1999. Neck posture and feeding habits of two Jurassic sauropod dinosaurs. *Science* **284**: 798-800.
- Tam, P.P., Goldman, D., Camus, A., Schoenwolf, G.C., 2000. Early events of somitogenesis in higher vertebrates: allocation of precursor cells during gastrulation and the organization of a meristic pattern in the paraxial mesoderm. *Current Topics in Developmental Biology* **47**: 1-32.
- Tamura, K., Nomura, N., Seki, R., Yonei-Tamura, S., Yokoyama, H., 2011. Embryological evidence identifies wing digits in birds as digits 1, 2, and 3. *Science* **331**: 753-757.

- Thewissen, J.G., Cohn, M.J., Stevens, L.S., Bajpai, S., Heyning, J., Horton, W.E., Jr., 2006. Developmental basis for hind-limb loss in dolphins and origin of the cetacean bodyplan. *Proceedings of the National Academy of Sciences* **103**: 8414-8418.
- Thewissen, J.G.M., Cooper, L.N., Behringer, R.R., 2012. Developmental biology enriches paleontology. *Journal of Vertebrate Paleontology* **32**: 1223-1234.
- Thomason, J., 1995. To what extent can the mechanical environment of a bone be inferred from its internal architecture?, in: Thomason, J. (Ed.), *Functional morphology in vertebrate paleontology*. Cambridge University Press, Cambridge, pp. 249-263.
- Tickle, C., 2007. The Hox gene network in vertebrate limb development, in: Papageorgiou, S. (Ed.), *Hox gene expression*. Landes Bioscience and Springer Science+Business Media, LLC, New York, pp. 42-52.
- Tsou, P.M., Yau, A., Hodgson, A.R., 1980. Embryogenesis and prenatal development of congenital vertebral anomalies and their classification. *Clinical Orthopaedics and Related Research* **152**: 211-231.
- Upchurch, P., Barrett, P.M., Dodson, P., 2004. Sauropoda, in: Weishampel, D.B., Dodson, P., Osmólska, H. (Eds.), *The Dinosauria*. University of California Press, Berkeley, California, pp. 259-322.
- Vargas, A.O., Fallon, J.F., 2005. The digits of the wing of birds are 1, 2, and 3. A review. *Journal of Experimental Zoology Part B Molecular and Developmental Evolution* **304**: 206-219.
- Veraksa, A., Del Campo, M., McGinnis, W., 2000. Developmental patterning genes and their conserved functions: from model organisms to humans. *Molecular Genetics and Metabolism* **69**: 85-100.
- Wedel, M.J., 2005. Postcranial skeletal pneumaticity in sauropods and its implications for mass estimates, in: Curry Rogers, K.A., Wilson, J.A. (Eds.), *The Sauropods: Evolution and Paleobiology*. University of California Press, Berkeley, California, pp. 201-228.
- Wellik, D.M., 2007. Hox patterning of the vertebrate axial skeleton. *Developmental Dynamics* **236**: 2454-2463.
- Wellik, D.M., 2011. Hox genes and kidney development. *Pediatric Nephrology* **26**: 1559-1565.
- Wellik, D.M., Capecchi, M.R., 2003. *Hox10* and *Hox11* genes are required to globally pattern the mammalian skeleton. *Science* **30**: 363-367.
- Wilson, J.A., 1999. A nomenclature for vertebral laminae in sauropods and other saurischian dinosaurs. *Journal of Vertebrate Paleontology* **19**: 639-653.
- Witmer, L.M., 1995. The extant phylogenetic bracket and the importance of reconstructing soft tissues in fossils, in: Thomason, J. (Ed.), *Functional morphology in vertebrate paleontology*. Cambridge University Press, Cambridge, pp. 19-33.
- Wolpert, L., Jessel, T., Lawrence, P., Meyerowitz, E., Robertson, E., Smith, J., 2007. *Principles of Development*. Spektrum Akademischer Verlag, Heidelberg, 559 pp.
- Woltering, J.M., Vonk, F.J., Müller, H., Bardine, N., Tudu, I.L., de Bakker, M.A.G., Knöchel, W., Sirbu, I.O., Durston, A.J., Richardson, M.K., 2009. Axial patterning in snakes and caecilians: evidence for an alternative interpretation of the Hox code. *Developmental Biology* **332**: 82-89.

Wu, P., Hou, L., Plikus, M., Hughes, M., Scehnet, J., Suksaweang, S., Widelitz, R., Jiang, T.X., Chuong, C.M., 2004. Evo-Devo of amniote integuments and appendages. *The International Journal of Developmental Biology* **48**: 249-270.

Yates, A.M., Wedel, M.J., Bonnan, M.F., 2012. The early evolution of postcranial skeleton pneumaticity in sauropodomorph dinosaurs. *Acta Palaeontologica Polonica* **57**: 85-100.

## Chapter 2

### Vertebral evolution in archosaurs: new insights from morphofunctional analysis of *Alligator*, *Plateosaurus* and *Struthio*

#### Abstract

---

Vertebral number and morphology have far-reaching consequences for organismal function and ecology. The vertebral column serves many different functions, from food acquisition through sustaining the body posture to locomotion. Archosaurs (crocodiles, birds and dinosaurs) display a variety of body plans and vertebral morphologies. Since the form of the axial column is related to its function, the patterns of morphological and functional variation may provide insights into biological mechanisms and connected behaviour, such as feeding strategy and locomotion style.

Here we establish morphofunctional subregions in the presacral vertebral column of extant and extinct archosaurs, based on the osteological flexibility between successive vertebrae. Comparing the flexion pattern with the neck (feeding) and trunk movement (locomotion) of the living animal revealed a strong link between osteological flexibility and axial movements. The relation between the morphofunctional pattern and the neck and trunk movements observed in modern archosaurs, allows the inference of the feeding range and locomotor options in the extinct taxon *Plateosaurus*. The morphofunctional subregions served as proxy to assess the biological role to which the vertebral mobility is adapted in the dinosaur, which enables us to interpret niche partitioning or habitat preferences in one of the first long-necked dinosaurs.

---

## 2.1. Introduction

The morphological diversity and variety of body plans of the Archosauria, including the sole surviving crocodiles and birds as well as extinct forms such as sauropodomorph dinosaurs, is striking (Figure 2.1.). However, all three groups evolved large or even gigantic body sizes. The largest extant bird, the ostrich (about 150 kg), is a long-necked, bipedal, cursorial herbivore (occasional omnivore) with a small head and a highly reduced tail (Jackson et al. 2004). In contrast, one of the largest modern crocodylians, the alligator (about 500 kg), is a short-necked, quadrupedal, semiaquatic carnivore with a large head and a powerful tail (Murphy and Schlager 2004).

Sauropodomorph dinosaurs (sauropods and their ancestors) are an extraordinary group of reptiles, because their gigantic body size has remained unsurpassed in all other terrestrial animals (Sander et al. 2011). The largest well-described sauropod dinosaur *Argentinosaurus* reached an estimated weight of up to 70 metric tonnes (Mazzetta et al. 2004). One of the largest non-sauropod sauropodomorph dinosaurs is *Plateosaurus* (about 1 t) (Rauhut et al. 2011) (Figure 2.1.). The basal sauropodomorph had a relatively long neck and tail and a small head, lived on land and fed mainly on plants (Galton and Upchurch 2004, Huene 1926). Although *Plateosaurus* has been the subject of previous studies (e.g. Bonaparte 1999, Christian et al. 1996, Gunga et al. 2007, Mallison 2010a, b, Moser 2003, Sander and Klein 2005), its feeding strategy and locomotion style remain controversial.

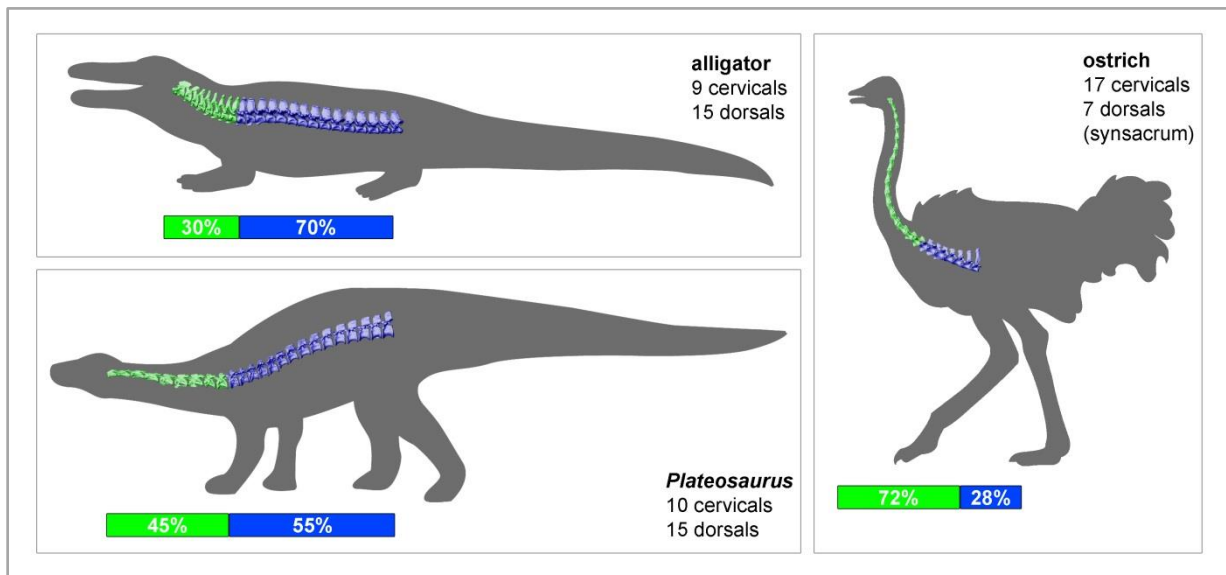


**Figure 2.1.: Body plans of extant and extinct archosaurs.** The silhouette drawings of the archosaurs show the presacral axial skeleton (not to scale). The 3D models of the cervical (green) (excl. atlas) and dorsal (blue) vertebrae are posed to conform to the (potential) living pose. The vertebral formula in alligator (SAPM No. 3) and *Plateosaurus* (GPIT/RE/7288) is very similar. Whereas the ostrich (SAPM No. 1) reveals a highly specialised axial skeleton. Several dorsal and sacral vertebrae are bound to the synsacrum (not displayed). The bars represent the relative percentage of the length of the cervical and dorsal region in the presacral vertebral column of each taxon. Some sauropod taxa for comparison (data from Rauhut et al. 2011): *Shunosaurus* (54%:46%), *Mamenchisaurus* (76%:24%).

Analyses of the fossil skeleton lead to controversial assumptions concerning bipedalism or quadrupedalism of the animal (e.g. Mallison (2010b), Remes (2008) contra Christian and Preuschoft (1996), Fechner (2009) and references therein). The bones indicate that *Plateosaurus* could have adopted both a bipedal and a quadrupedal posture, but there is no unambiguous evidence for the exact locomotion behaviour.

The evolutionary development of a very long neck is linked to the gigantism of sauropodomorphs (Sander et al. 2011). In general, an elongated neck enables a greater reaching distance and thus, increases the feeding envelope (Preuschoft et al. 2011). In order to efficiently exploit the vegetation, two feeding behaviours can be distinguished: either the increased feeding range is primarily used in vertical direction or the feeding range is increased in horizontal direction. Both hypotheses are supported for different sauropod taxa (high- and low-browsing), which indicates a certain degree of niche partitioning in these dinosaurs (Sander et al. 2011 and references therein). *Plateosaurus* was able to rear up on its hind limbs to reach food in great heights, and the overall mobility of the animal allowed the head to come down to the ground for feeding (Barrett and Upchurch 2007, Mallison 2010b). To which feeding strategy is the long neck of the basal sauropodomorph dinosaur primarily adapted? Is *Plateosaurus* one of the first high-browsers during tetrapod evolution, as suggested by Bakker (1978) and Galton (1985)? Its browsing height would have overlapped with some of the few contemporaneous sauropods (Barrett and Upchurch 2007). Alternatively, the long neck may have been an adaptation to increase the horizontal feeding range in order to efficiently exploit a wider volume of vegetation without moving the massive body.

Since the form of the axial skeleton is related to its function, vertebral morphology reflects the specific functional adaptations (Koob and Long 2000, Slijper 1946, Wainwright 2000). The presacral vertebral column of archosaurs is a key architectural element of resistance against the loads imposed by gravity, as well as the stresses imposed during feeding, locomotion and other activities. In addition to maintaining maximum stability, the axial column must provide mobility as well as protection of the neural structures. The differentiation of the axial skeleton into distinct cervical and dorsal regions correlates with morphological and functional features. Support and trajectory of the head during feeding and other activities are major factors in the form of the neck. The structure of the trunk appears to be the result of the axial bracing system in order to support and move the body during a variety of activities.

An analysis of vertebral mobility in various birds has shown that cervical flexibility determines the biological role to which neck movement is adapted (van der Leeuw et al. 2001). It has been previously recognised that the cervical column of birds can be divided in subregions, according to the dorsoventral bending capabilities (Boas 1929, Sivers 1934). The characteristic flexion pattern is

related to differences in functional demands imposed by feeding and, thus, provides information about the neck movement pattern (van der Leeuw et al. 2001). In this study, vertebral flexibility is used as proxy for function of the cervical and dorsal vertebral column. Differences in the distribution of flexibility (functional partitioning) along the presacral axial skeleton in the investigated archosaur taxa may correspond to differences in the feeding strategy and locomotion style. In order to understand the role of the presacral axial system in feeding and locomotion behaviour, the relationship between vertebral morphology and function is first analysed in extant species, in which the predicted behaviour can be verified by observations of the living animal. Second, the comparison between the morphofunctionality of the axial system of the extant models provides the opportunity to reconstruct the anatomy and behaviour of their extinct relative *Plateosaurus*. This study will allow a better understanding of the relationship between organismal structure and function of modern crocodiles and birds, which eventually will elucidate the palaeobiology of the extinct archosaur.

The aims of this study are 1) to establish functional subregions in the presacral vertebral column of extant and extinct archosaurs based on the osteological flexibility between successive vertebrae, 2) to evaluate the vertebral morphology with respect to the functional subregions and 3) to assess the biological role to which the vertebral mobility is adapted in extant and extinct archosaurs.

## 2.2. Materials and methods

The osteology of the presacral vertebrae in the American alligator (*Alligator mississippiensis*), the sauropodomorph dinosaur *Plateosaurus engelhardti* and the ostrich (*Struthio camelus*) were comparatively investigated (Table 2.1.). Additionally, the general anatomy of the analysed archosaurs was compared with regard to the axial skeleton. Simple length ratios were measured in order to use them as proxies for general body proportions, such as the relative skull size and the relative neck length. The ratios are thought to be linked to the biological significance of the body parts in terms of importance in activities like feeding and locomotion.

Taxon	Presacral vertebrae	Specimen	3D model
<i>Alligator mississippiensis</i>	9c, 15d	SAPM No. 3	X
<i>Alligator mississippiensis</i>		SAPM No. 4	-
† <i>Plateosaurus engelhardti</i>	10c, 15d	GPIT/RE/7288	X
† <i>Plateosaurus engelhardti</i>		SMNS 13200	-
<i>Struthio camelus</i>	17c, 7d	SAPM No. 1	X
<i>Struthio camelus</i>		SAPM No. 5	-

**Table 2.1:** List of modern and fossil taxa analysed in the present study. Cross (†) denotes extinct taxon. Abbreviations: c = cervical vertebrae, d = dorsal vertebrae. Institutional abbreviations: SAPM = Staatliche Sammlung für Anthropologie und Paläoanatomie München, Germany; GPIT = Geologisches und Paläontologisches Institut der Universität Tübingen, Germany; SMNS = Staatliches Museum für Naturkunde Stuttgart, Germany.

The terminology used in this study (Table 2.2.) is based on the nomenclature proposed by Baumel et al. (1993) for bird, Huene (1926) and Wilson (1999) for dinosaur and Romer (1976) for alligator.

For the following analyses, three-dimensional scans of the presacral vertebrae of *A. mississippiensis*, *P. engelhardti* and *S. camelus* were generated using the laser scanner ModelMaker Z35, integrated with the FaroArm Platinum (Table 2.1.). The software packages KUBE and Geomagic Studio 9.0 were used for post-processing of the raw data. For digital mounting of the 3D vertebrae and for analysing the mobility range the CAD software, Rhinoceros® was used. Additional individuals were used for verification of the collected 3D data.

Abbreviation	Osteological term	Abbreviation	Osteological term
ansa <sup>1</sup>	ansa costotransversaria	para	parapophysis
cent	centrum	poz	postzygapophysis
cond <sup>2</sup>	condylus	prez	prezygapophysis
dia	diapophysis	spin	neural spine
hyp	hypapophysis		

**Table 2.2.: Osteological terms and abbreviations used in the present study.** Note that there are terms that are solely used for <sup>1</sup>bird or <sup>2</sup>alligator. See text for references.

### 2.2.2. Morphological analysis

In order to analyse the morphological variability of the vertebrae within each axial column and subsequently to evaluate the vertebral morphology with regard to osteological flexibility, a combined shape analysis was performed. The morphological differences between the vertebrae were quantitatively analysed via traditional morphometrics and landmark-based geometric morphometrics.

The linear measurements (Figure 2.2.) included maximal vertebral length, maximal vertebral height, centrum length and centrum height as well as the calculated vertebral arch height and zygapophyseal overhang. The maximal vertebral length does not include ribs. The maximal vertebral height includes ventral processes if present. The centrum length was taken as maximum distance between anterior and posterior margin. The centrum height was measured at the anterior margin in alligator and dinosaur. It was

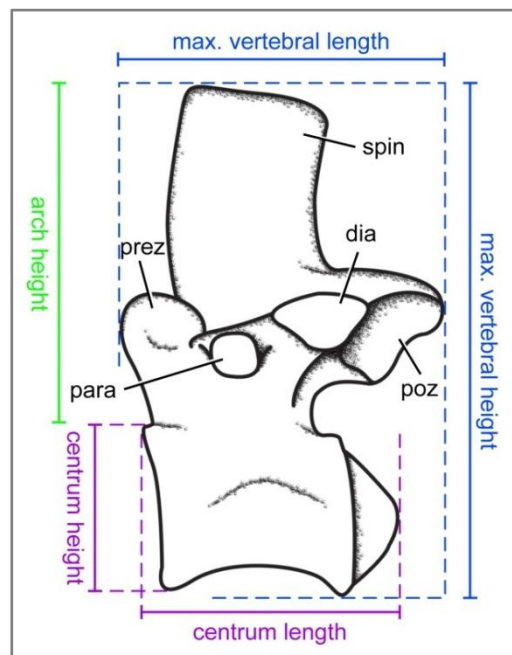


**Figure 2.2.: Measurements shown on the 6<sup>th</sup> dorsal vertebra of alligator in left lateral view.** See text for definition of the measurements. Refer to Table 2.2. for osteological abbreviations.

taken at the posterior margin in the bird. The arch height is the difference between maximal vertebral height and centrum height. The zygapophyseal overhang (not marked in the illustration) is the subtraction of maximal vertebral length and centrum length. All measurements were taken on own photographs of the analysed specimens using Adobe Photoshop CS4.

For the geometric morphometric analysis, two series of landmarks were digitised on the 3D scans. Applying the software Landmark Version 3.0 (Wiley 2005), the first set of 17 homologous points (LM 1-17) was collected (Figure 2.3., Table 2.3.). This represents the overall vertebral shape. In a separate investigation, the second set of 4 landmarks (LM 11, 12, 20, 25) and 8 semilandmarks (sLM 18, 19, 21, 22, 23, 24, 26, 27) was digitised on the articular facet of the left prezygapophysis (Figure 2.3., Table 2.3.). The points characterise the surface shape of the anterior zygapophysis.

The first cervical vertebra was not included in the geometric morphometric analysis because it lacks specific homologies and thus, several landmarks cannot be applied to the atlas.

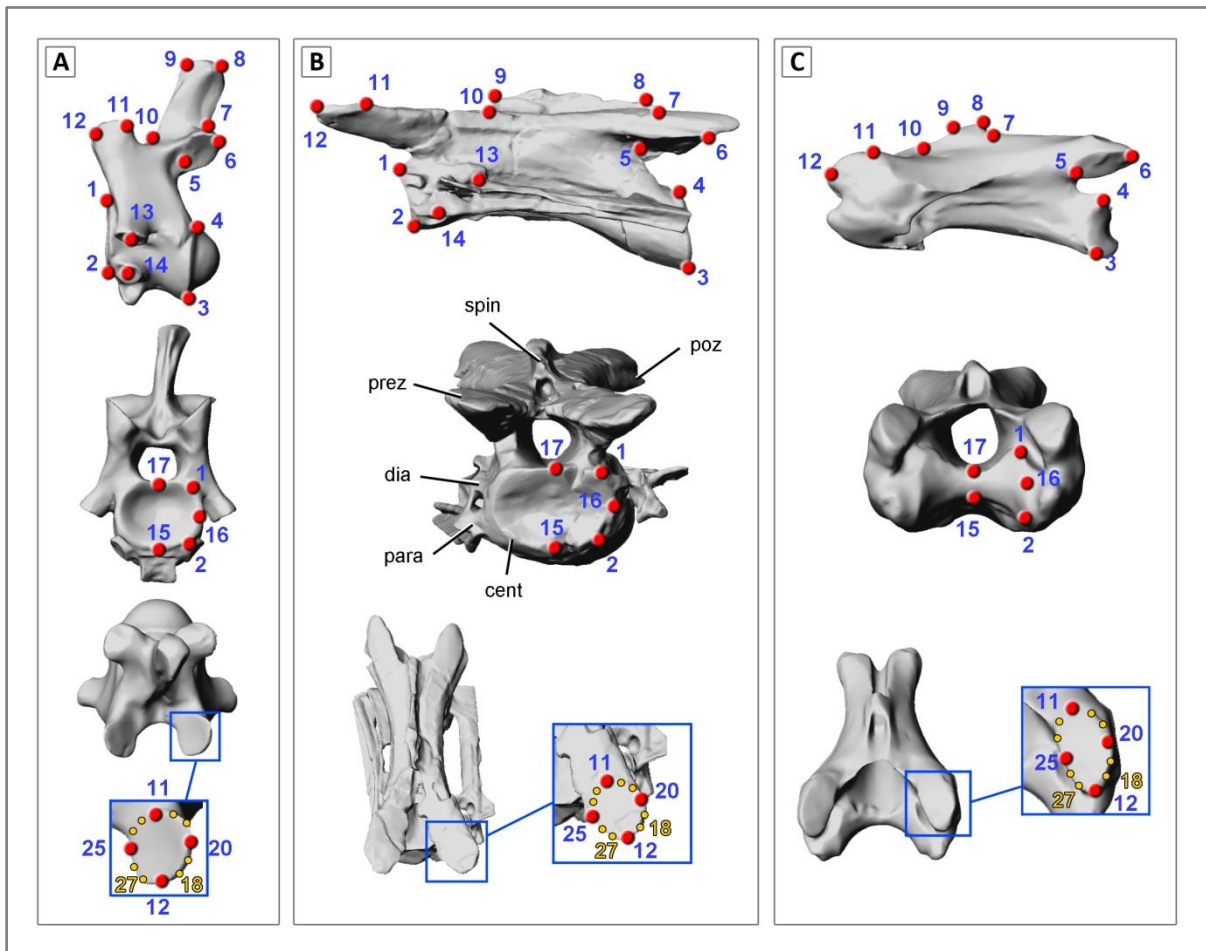


**Figure 2.3.:** Landmark set used in the geometric morphometric analysis. The 3D landmarks (red points) and semilandmarks (orange points) are shown on the fourth cervical vertebra (not to scale) of (A) alligator (SAPM No. 3), (B) *Plateosaurus* (GPIT/RE/7288) and (C) ostrich (SAPM No. 1). Each vertebra is shown in left lateral, anterior and dorsoanterior view including a magnified view of the prezygapophysis (from top to bottom). Refer to Table 2.2. for osteological abbreviations and Table 2.3. for detailed description of the homologous points.

The coordinates of both landmark sets were superimposed using General Procrustes Analysis (GPA) in Morphologika<sup>2</sup> (O'Higgins and Jones 2006). The subsequent Relative Warps Analysis (RWA) summarised the multidimensional information. With the applied settings, this method is equivalent to a Principal Components Analysis. The shape differences were visualised with 3D thin-plate splines. The morphological disparity (MD) was calculated as  $MD = \frac{\sum_{j=1}^N d_j^2}{(N-1)}$  (Foote 1993, Zelditch et al. 2004).

View	Landmark (LM)	Definition
lateral	1	dorsal-anterior edge of the centrum
	2	ventral-anterior edge of the centrum
	3	ventral-posterior edge of the centrum
	4	dorsal-posterior edge of the centrum
	5	anteriormost edge of the articular facet of the postzygapophysis
	6	dorsal-posterior edge of the articular facet of the postzygapophysis
	7	point of maximum curvature between postzygapophysis and neural spine
	8	posterior edge of the neural spine
	9	anterior edge of the neural spine
	10	point of maximum curvature between neural spine and prezygapophysis
	11	posteriormost point of the articular facet of the prezygapophysis
	12	dorsal-anterior edge of the articular facet of the prezygapophysis
	13	centre of the diapophysis
	14	centre of the parapophysis
anterior	15	ventralmost point of the centrum
	16	lateralmost point of the centrum
	17	dorsal most point of the centrum
dorsal	20	lateral point of maximum curvature between LM 11 and LM 12
	25	medial point of maximum curvature between LM 11 and LM 12
	sLM 18, 19, 21, 22, 23, 24, 26, 27	tracing the outline of the articular facet of the prezygapophysis

**Table 2.3.: Description of the 3D landmarks.** The first landmark set includes LM 1-17. The second landmark set comprises LM 11, 12, 20, 25 and semilandmarks (sLM) 18, 19, 21, 22, 23, 24, 26, 27. Both sets were applied to all analysed taxa in order to provide a comparable basis for the morphological study. Although there are transverse processes connecting the cervical ribs with the vertebral centrum, LM 13 and 14 are not applied in the analysis of the ostrich because their placement is not exactly repeatable. In the alligator, the diapophysis and parapophysis are not recognisable on the transverse process of the five last dorsal vertebrae because they are rib-free. In order to avoid missing landmark coordinates, LM 13 and 14 are placed on the anterior and posterior part of the transverse process homologous to the diapophysis and parapophysis in the preceding vertebrae.

### 2.2.1. Digital mounting and mobility range analysis

The 3D models of the presacral vertebra (excluding the first cervical vertebra) in the skeleton of alligator, dinosaur and ostrich were articulated in osteological neutral pose (ONP) (after Stevens and

Parrish 1999). This posture is defined as the neutral state of deflection between successive vertebrae (Stevens and Parrish 1999) (Figure 2.4. B, F, G). At ONP, the central margins of adjacent vertebrae are parallel and the zygapophyses overlap (Stevens and Parrish 1999). The paired articular facets of the postzygapophyses are centred over the facets of the prezygapophyses (Stevens and Parrish 1999).

The osteological flexibility of each presacral vertebral column was assessed by mobility range analyses with regard to three types of intervertebral movement; that is, dorsal, ventral and lateral bending. In order to determine the mechanical capacity of the vertebral joints, the vertebrae were digitally subjected to maximal flexion in each of these directions. Each anterior vertebra was manipulated with respect to its posterior neighbour, to the point that the zygapophyses minimally overlapped for  $\frac{1}{4}$  of their articular surface (Figure 2.4. A, C, D, E, H, I, J). Although that theoretical limit might differ across vertebrate taxa, 25% overlap allows a conservative reconstruction (Dzemiński and Christian 2007). The influence of bony barriers that lead to a modified flexibility range by blocking further bending was also considered (Figure 2.4. H). The flexion was digitally measured as the cutting angle between the longitudinal axes of the centra of adjacent vertebrae. Each measurement was taken three times and averaged. While connective soft-tissue is also relevant to analyses of vertebral flexibility and axial remodelling (Cobley et al. 2013), such information is generally unavailable for fossil species and is not included here for lack of completeness, but for the benefit of comparability.

It has been previously recognised that the cervical column of birds can be divided in subdivisions according to the dorsoventral bending (Boas 1929, Sivers 1934). Based on the differences in maximal dorsal and ventral flexion between successive vertebrae, the presacral vertebral column of the three studied archosaurs is separated into functional subregions, in which either dorsal or ventral flexion is prevalent or in which equal dorsoventral flexion is observed.

### 2.2.3. Morphofunctional pattern

After establishing functional subregions in the presacral vertebral column of alligator, dinosaur and ostrich based on the osteological flexibility between adjacent vertebrae, vertebral morphology is evaluated with respect to these functional subunits. In order to investigate the correlation between vertebral flexibility and mode of life, the resulting morphofunctional patterns were compared in the modern archosaurs that display different feeding strategies and locomotor options. On the basis of this correlation, the biological role to which the vertebral mobility might be adapted was assessed in the extinct archosaur.

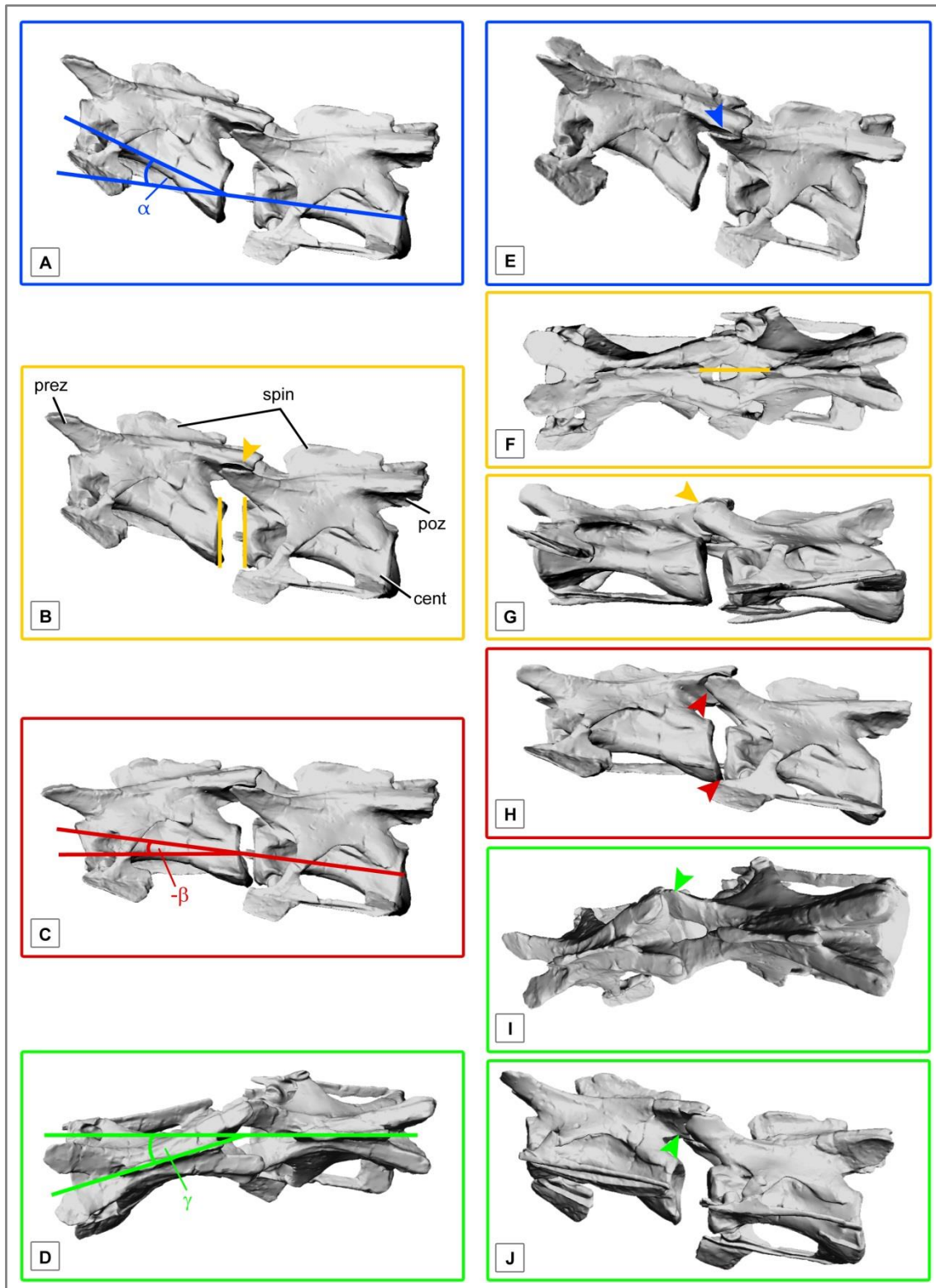


**Figure 2.4.: Applied postures for modelling flexion in archosaurs.** Left row: the 3D models (not to scale) of the sixth and seventh cervical vertebra of *Plateosaurus* (GPIT/RE/7288) in left lateral view at (A) maximal dorsal flexion, (B) osteological neutral pose (ONP), (C) maximal ventral flexion and in dorsal view at (D) maximal lateral flexion. Right row: Details of the respective posture in (E) dorsolateral, (F) dorsal, (G, H, I) ventrolateral and (I) posterodorsal view. If not otherwise indicated, lines mark measured angles and arrows point towards important characters of each posture. At ONP the central margins of adjacent vertebrae are parallel (orange lines), the zygapophyses overlap with centred articular facets (orange arrow) and the longitudinal axes of the neural spines are aligned (B, F, G). The maximal dorsal, ventral and lateral flexion is achieved when the zygapophyses minimally overlap for  $\frac{1}{4}$  of their articular surface or when bony elements blocks further bending (H). Refer to Table 2.2. for osteological abbreviations.

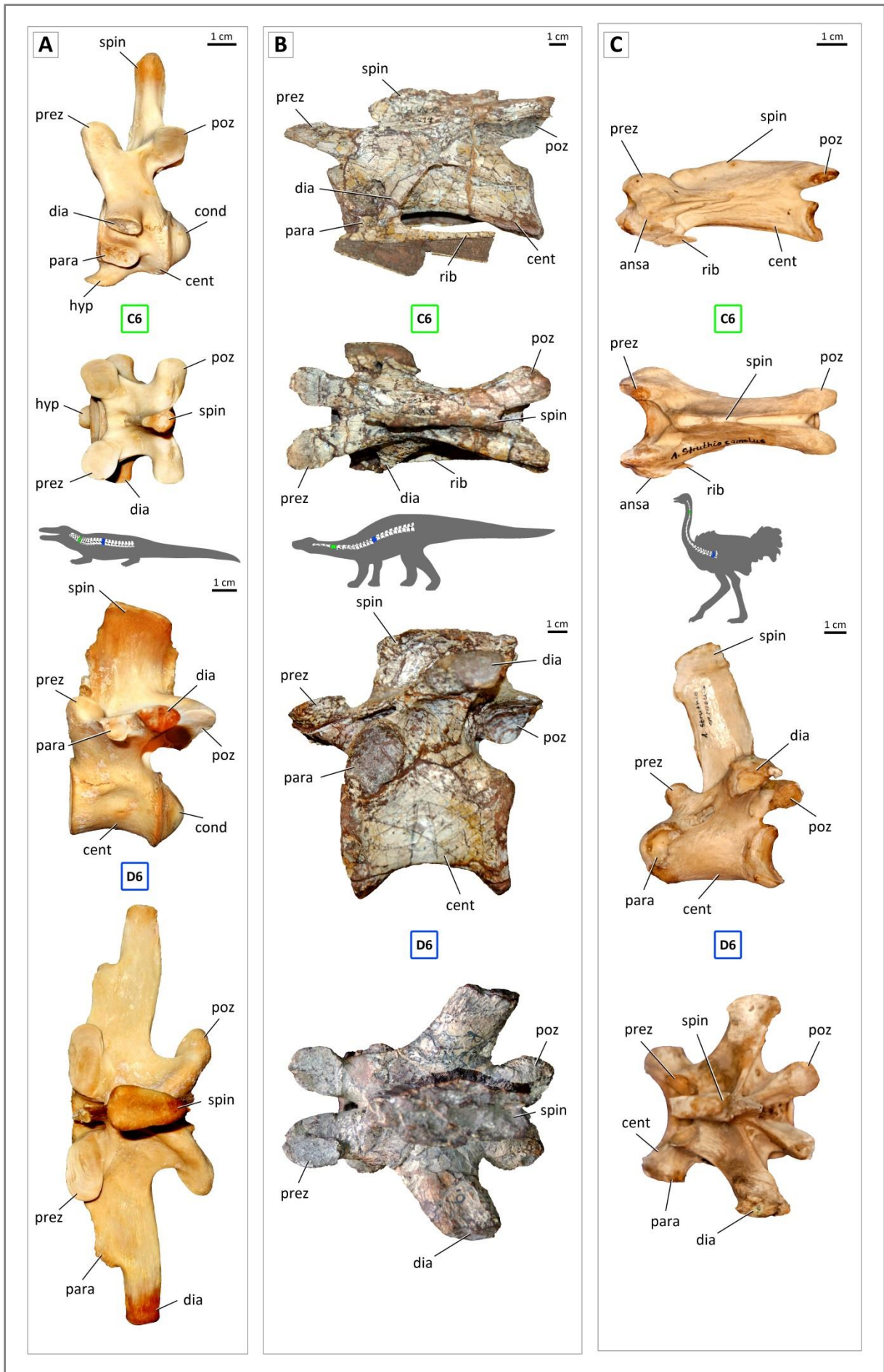
## 2.3. Results

### 2.3.1. Comparative anatomical description

The archosaurian taxa in this study show no significant difference in the number of presacral vertebrae (Table 2.4.). The vertebral formula is very similar in the alligator and *Plateosaurus*, whereas the ostrich displays a specialised axial system typical for birds, because several dorsal and sacral vertebrae are fused with the pelvis into the synsacrum and the ultimate caudal vertebrae are bound to the pygostyle. Comparing several anatomical characteristics between the crocodylian and the bird emphasises the fundamental structural modifications of the axial skeleton that occurred between these two lineages (Table 2.4.). The sauropodomorph dinosaur shares characters of both lineages (Table 2.4.): the alligator has a relatively large head, whereas *Plateosaurus* and the ostrich have a small skull. With regard to the trunk length, the alligator has a very short neck (0.44), whereas

Character	<i>Alligator</i>	<i>Plateosaurus</i>	<i>Struthio</i>
number of presacrals	24p	25p	24p
vertebral formula	9c, 15d, 2s, 30-40ca	10c, 15d, 3s, >30ca	17c, 7d, syn, ca, pyg
head	large	small	small
(skull/femur length ratio)	(3.45)	(0.46)	(0.40)
neck length	short	long	long
(neck/skull length ratio)	(0.92)	(3.06)	(4.00)
neck/back length ratio	0.44	0.78	2.67
# cervicals/dorsals ratio	0.60	0.67	2.43
proatlas	present	present	absent
ribs	cervical (incl. atlas) and dorsal	cervical (incl. atlas) and dorsal	cervical (excl. atlas) and dorsal
cervical vertebral articulation (centrum)	procoelous	amphicoelous	heterocoelous
dorsal vertebral articulation (centrum)	procoelous	platycoelous	heterocoelous
open neurocentral suture	present	absent	absent
pleurocoelous	absent	present	present
vertebral lamination	absent	present	present
locomotion	quadrupedal (different gaits incl. gallop)	?facultative bipedal	bipedal (fastest running biped)
limb posture	not parasagittal	parasagittal	parasagittal

**Table 2.4.: Comparison of anatomical characteristics in extant and extinct archosaurs.** Abbreviations: p = presacral vertebrae, c= cervical vertebrae, d= dorsal vertebrae, s = sacral vertebrae, ca = caudal vertebrae, syn = synsacrum, pyg = pygostyle.



↑ **Figure 2.5.: Comparative anatomy of representative cervical and dorsal vertebrae in extant and extinct archosaurs.** The primary parts of an individual vertebra are present in the axial skeleton of (A) alligator (SAPM No. 3), (B) *Plateosaurus* (GPIT/RE/7288) and (C) ostrich (SAPM No. 1). Each vertebra is represented by a photograph in left lateral and dorsal view. The silhouette drawings of the archosaurs show the presacral axial skeleton and indicate the position of the representative cervical (green) and dorsal (blue) vertebrae. Refer to Table 2.2. for osteological abbreviations.

*Plateosaurus* revealed a neck/back length ratio of 0.78. In the ostrich, the total length of the cervical series is over two times higher than that of the dorsal series (2.67). The relation between the total length of the cervical and dorsal series (neck/back length ratio) is highly variable between the three archosaur taxa analysed. This pattern is not reflected by the ratio between the number of cervical and dorsal vertebrae (Table 2.4.).

The presacral vertebrae of alligator, *Plateosaurus* and ostrich share a basic vertebral architecture, including the presence of a vertebral centrum, neural arch, anterior and posterior zygapophyses, a neural spine and transverse processes (Figure 2.5.). The overall shape of the representative cervical (C6) and dorsal vertebrae (D6) reveals that the cervical series of the dinosaur resembles the avian condition of the neck, whereas the dorsal series shares more similarities with the crocodylian trunk.

In *Plateosaurus*, we identified the presence of the hyposphene-hypantrum complex in the dorsal series, starting at the last cervical vertebrae (Figure 2.6.). The hyposphene is developed as a vertical wall of bone that extends ventrally from between the postzygapophyses, and slots into a notch between the prezygapophyses of the adjacent vertebra (Rauhut 2003). This accessory articulation increases structural rigidity of the vertebral column and prevents torsion between the vertebrae.

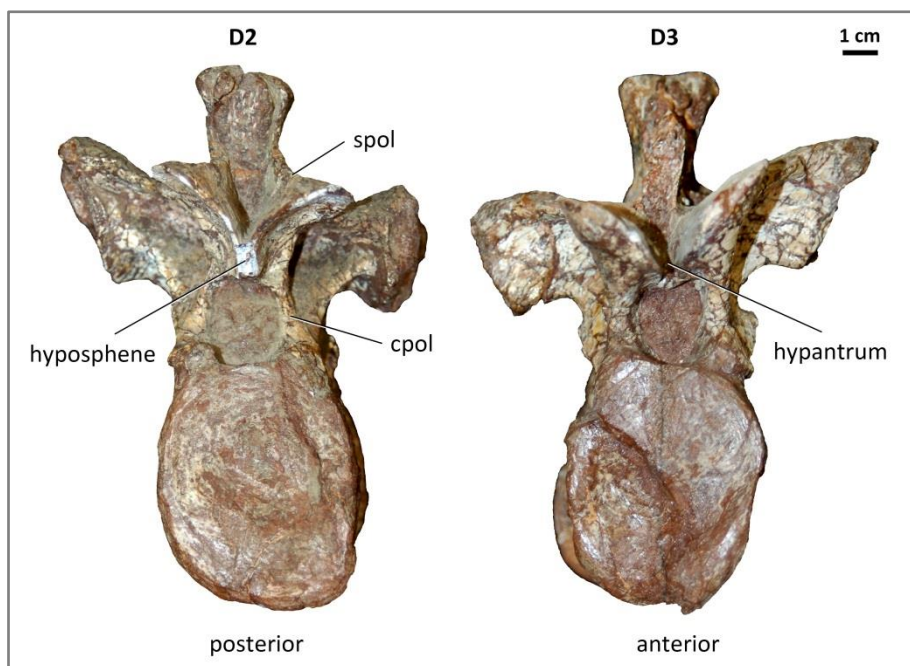


**Figure 2.6.: Hyposphene-hypantrum complex in the dorsal vertebrae of *Plateosaurus*.** The accessory articulation complex involves several laminae in its structure: spol = spinopostzygapophyseal lamina, cpol = centropostzygapophyseal lamina.

### 2.3.2. Morphological analysis

#### 2.3.2.1. Vertebral dimensions

*Plateosaurus* shows a differentiation in maximal vertebral length along the presacral vertebral column, which is also evident in the centrum length (Figure 2.7. A and B). On average, the centra of the cervical vertebrae ( $\varnothing$  119.1 mm) are longer than that of the dorsal vertebrae ( $\varnothing$  93.8 mm). The alligator and the ostrich display a more or less undifferentiated profile of maximal vertebral length and centrum length (Figure 2.7. A and B). In the crocodilian, the centra of the cervical region ( $\varnothing$  31.7 mm) are slightly shorter than the centra of the dorsal region ( $\varnothing$  46.6 mm), whereas the centrum length in the bird shows a very slight decrease from the neck ( $\varnothing$  59.8 mm) to the trunk ( $\varnothing$  52.6 mm).

There is a significant increase in maximal vertebral height along the presacral axial skeleton of *Plateosaurus* (Figure 2.7. C). The profile centrum height displays the same trend, with lower centra in

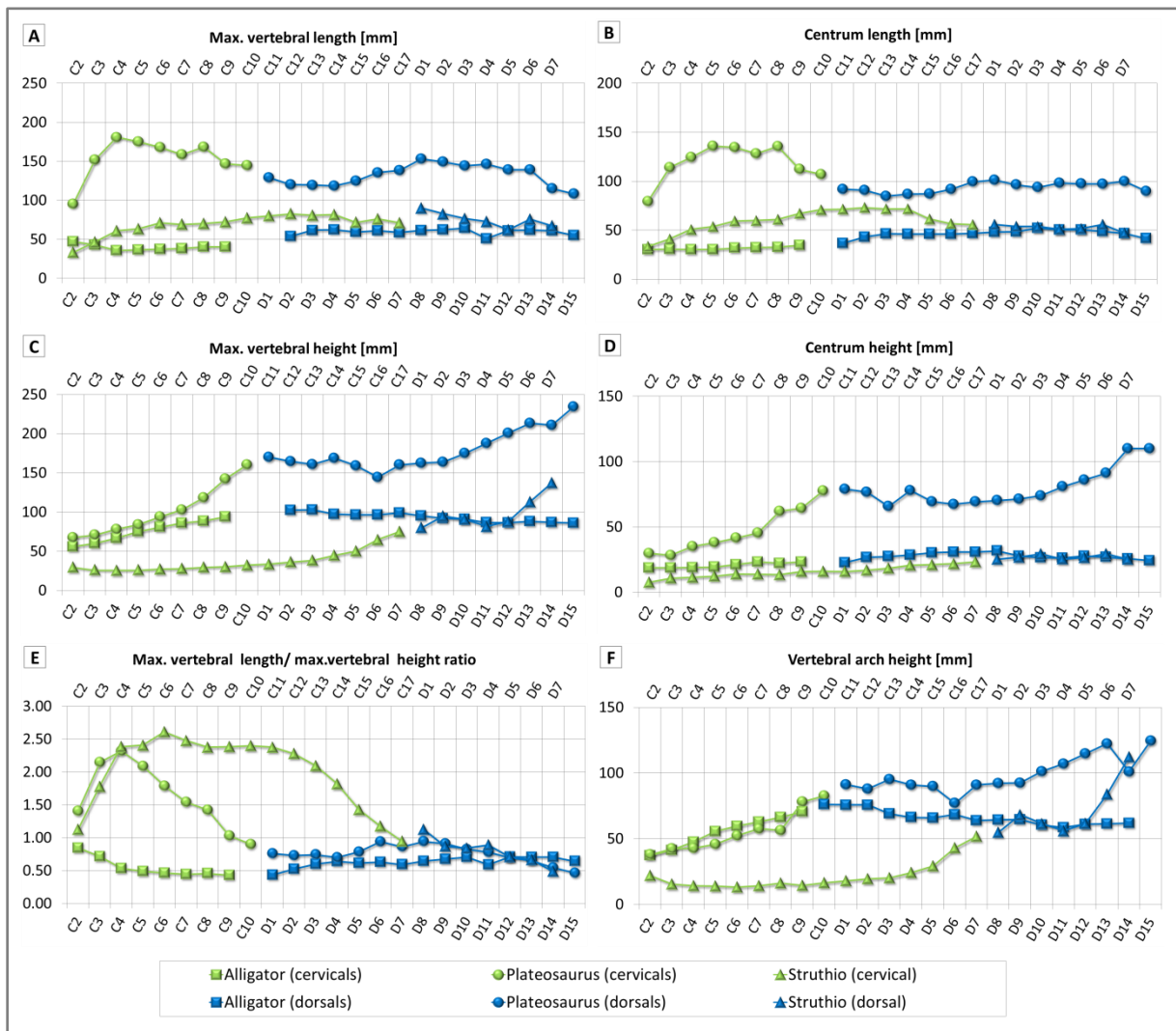


Figure 2.7.: Linear profiles of the presacral vertebrae in extant and extinct archosaurs. The linear measurements are plotted against vertebral position. The lower x-axis labelling of each plot indicates the vertebral position in the alligator and *Plateosaurus*. The upper x-axis labelling gives the position in the ostrich skeleton.

the cervical series ( $\emptyset$  46.9 mm) and taller centra in the dorsal series ( $\emptyset$  80.0 mm) (Figure 2.7. D). The height of the centra in the alligator is relatively constant from the neck ( $\emptyset$  20.7 mm) to the trunk ( $\emptyset$  27.6 mm). In the ostrich, the centra in the cervical region ( $\emptyset$  15.8 mm) are slightly lower than that of the dorsal region ( $\emptyset$  26.8 mm). The significant increase in the maximal vertebral height of the avian vertebrae is mainly due to an increase in the vertebral arch height (Figure 2.7. C and F).

The ratio between maximal vertebral length and height shows that the cervical vertebrae of *Plateosaurus* are significantly longer than high ( $\emptyset$  1.63) (Figure 2.7. E). The maximal vertebral length/height ratio increases towards the middle part of the neck and reaches a minimum at the cervicothoracic transition. The profile shows that the dorsal vertebrae are higher than long ( $\emptyset$  0.76). In the crocodylian, all presacral vertebrae are higher than long ( $\emptyset$  0.60) (Figure 2.7. E). The highest ratio was measured at the second cervical vertebra (0.85). It then slightly decreases towards the middle part of the neck, and remains constant among the following vertebrae. Statistically, the cervical vertebrae of the ostrich are significantly longer than high ( $\emptyset$  2.00) (Figure 2.7. E), whereas the vertebrae of the dorsal region are slightly higher than long ( $\emptyset$  0.80).

#### 2.3.2.2. Landmark analysis

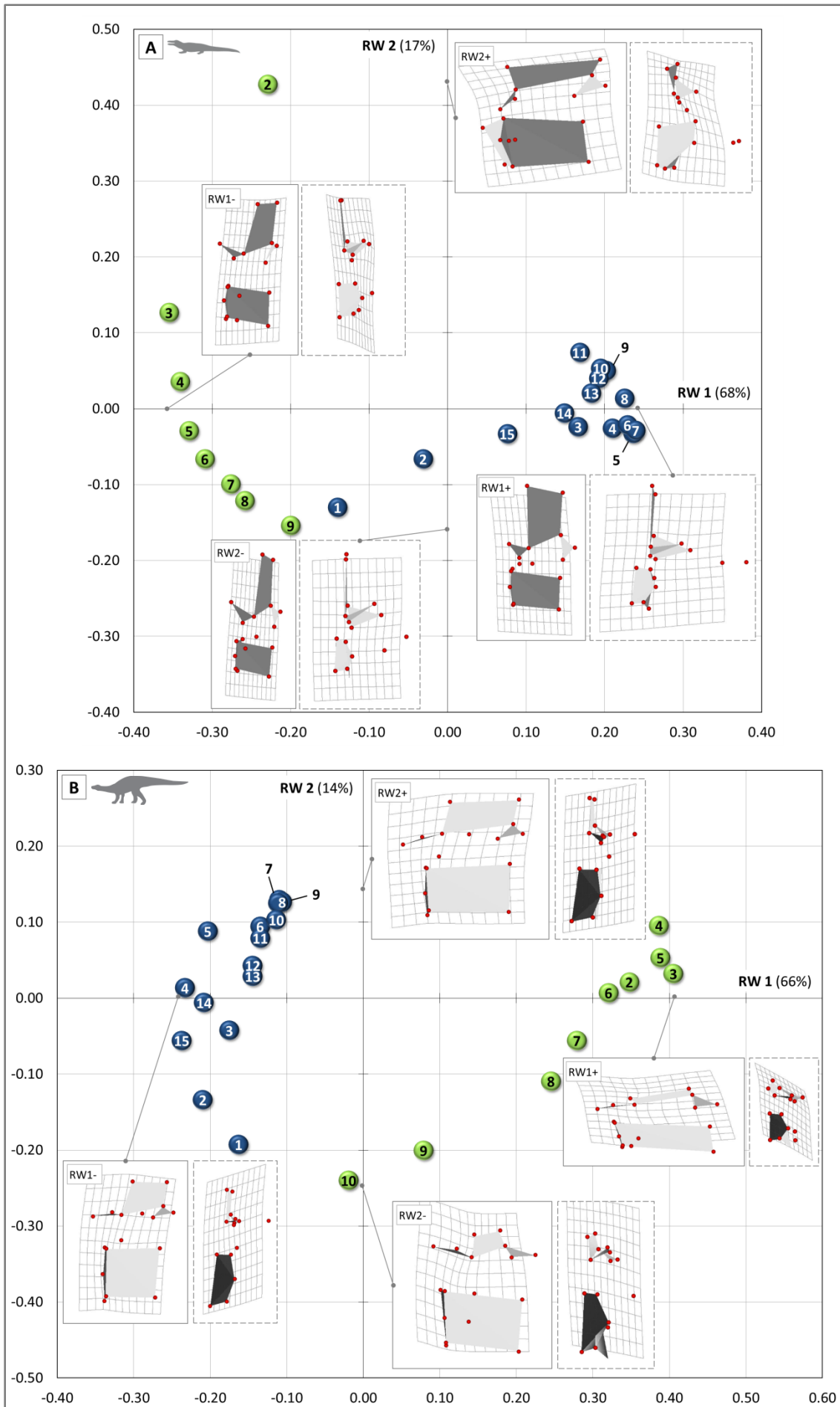
The landmark-based geometric morphometric study allowed to quantitatively assess the varying morphology of the presacral vertebrae in the alligator, *Plateosaurus* and ostrich. The Relative Warps Analysis of the overall vertebral morphology (first landmark set) summarised the shape differences and 3D thin-plate splines visualised the shape changes from the average (Figure 2.8.). In all studied taxa, the first two RW axes (which explain about 80% of the total variation) separate two main morphological clusters (the cervical and dorsal vertebrae). In between is a transitional zone (cervicothoracic transition) with vertebrae that exhibit a gradual changing morphology. The second cervical vertebra is clearly distinct in its specialised shape. However, it is most different from the successive vertebrae in the alligator. The morphological disparity (MD) - the amount of shape variability within a dataset - is almost equal in the analysed specimens (alligator: 1.73, *Plateosaurus*: 1.87, ostrich: 1.78).

The RW 1 captures the morphological change of the neural spine in the three archosaurs. Additionally, it characterises the positional change of the diapophysis and parapophysis in the alligator and *Plateosaurus* (Figure 2.8. A and B). RW 1 also describes the shape difference of the vertebral centrum in the dinosaur and the bird (Figure 2.8. B and C). In general, RW 2 mainly separates the vertebrae according to the morphological changes of the zygapophyses and of the neural spine. Furthermore, it describes the shape differences of the vertebral centrum in the alligator. Thus, several osteological features display the same differentiation of the two main morphological clusters in all studied taxa. However, the direction and the extent of the shape

variation between the cervical and dorsal vertebrae in the archosaurs is quite different. The neural spine of the cervical vertebrae in the crocodilian is slightly more slender than that of the dorsal vertebrae (Figure 2.8. A). In the dinosaur and bird, the shape difference of the neural spine between the two presacral regions is highly distinct (low neural spine of cervical vertebrae and relatively high neural spine of dorsal vertebrae) (Figure 2.8. B and C). In the alligator, the presacral vertebrae do not differ significantly in the morphology of the centrum, whereas the cervical centra of *Plateosaurus* and the ostrich are longer than the dorsal centra. The varying position of the diapophysis and parapophysis throughout the vertebral column show the same pattern in the crocodilian and the dinosaur (relatively ventral position of transverse processes in cervical vertebrae and more dorsal position of the transverse processes in dorsal vertebrae).

Applying the second landmark set, the Relative Warps Analysis summarised the morphological differences of the prezygapophysis (Figure 2.9.). The first two RW axes explain 64-90% of the total variation in the studied archosaurs. Two main morphological clusters (the cervical and dorsal vertebrae) were identified in the alligator (Figure 2.9. A). One outlier is the first dorsal vertebra that groups with the cervical vertebrae. In *Plateosaurus* and the ostrich, the clusters are not as distinct as in the crocodilian (Figure 2.9. B and C). The morphological disparity is with 0.38 in *Plateosaurus* and 0.48 in the ostrich significantly lower than the MD of the alligator (1.06).

The main morphological changes of the prezygapophysis that are captured by RW 1 include whether the zygapophyseal surface is oval or round. Associated with positive RW 1 values, there are anteroposteriorly long and oval prezygapophyses in the dinosaur and the bird (Figure 2.9. B and C). Relatively round zygapophyseal surfaces map to negative RW 1 values. In the alligator, anteroposteriorly long and oval prezygapophyses are associated with negative RW 1 values (Figure 2.9. A). Relatively round zygapophyseal surfaces are plotted around the zero point of the diagram, whereas positive RW 1 values indicate a mediolaterally wide and oval prezygapophysis.



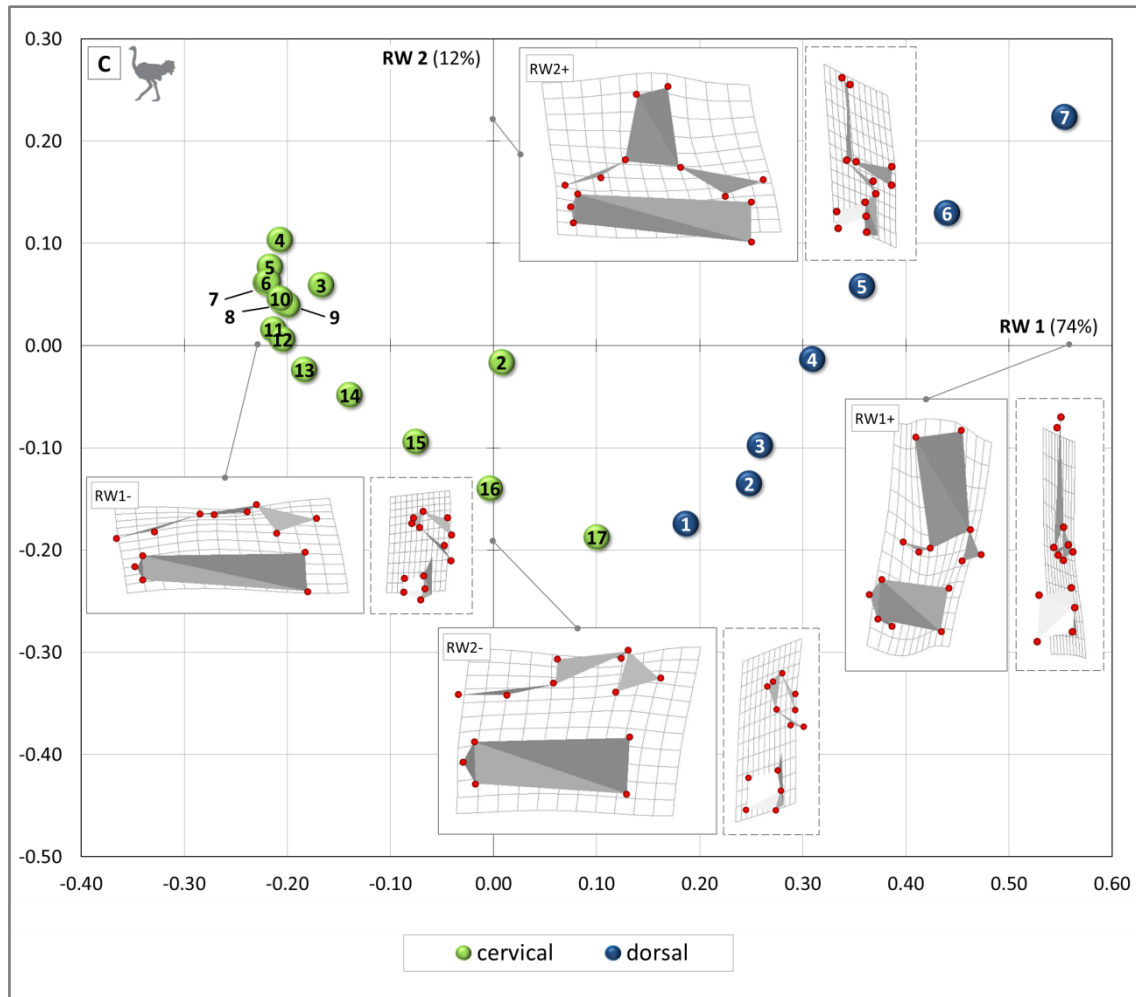


**Figure 2.8.: Relative Warps (RW) Analysis results of the vertebral shape in extant and extinct archosaurs.** Each plot shows the shape differences of the presacral vertebrae along RW 1 and RW 1 in (A) alligator, (B) *Plateosaurus* and (C) ostrich. 3D thin-plate splines visualise the variation between the landmark configurations from the respective average shape (zero point). The left lateral view is indicated by a solid grey frame. The associated anterior view is framed with a dashed grey line (note that not all landmarks are visible in this perspective).

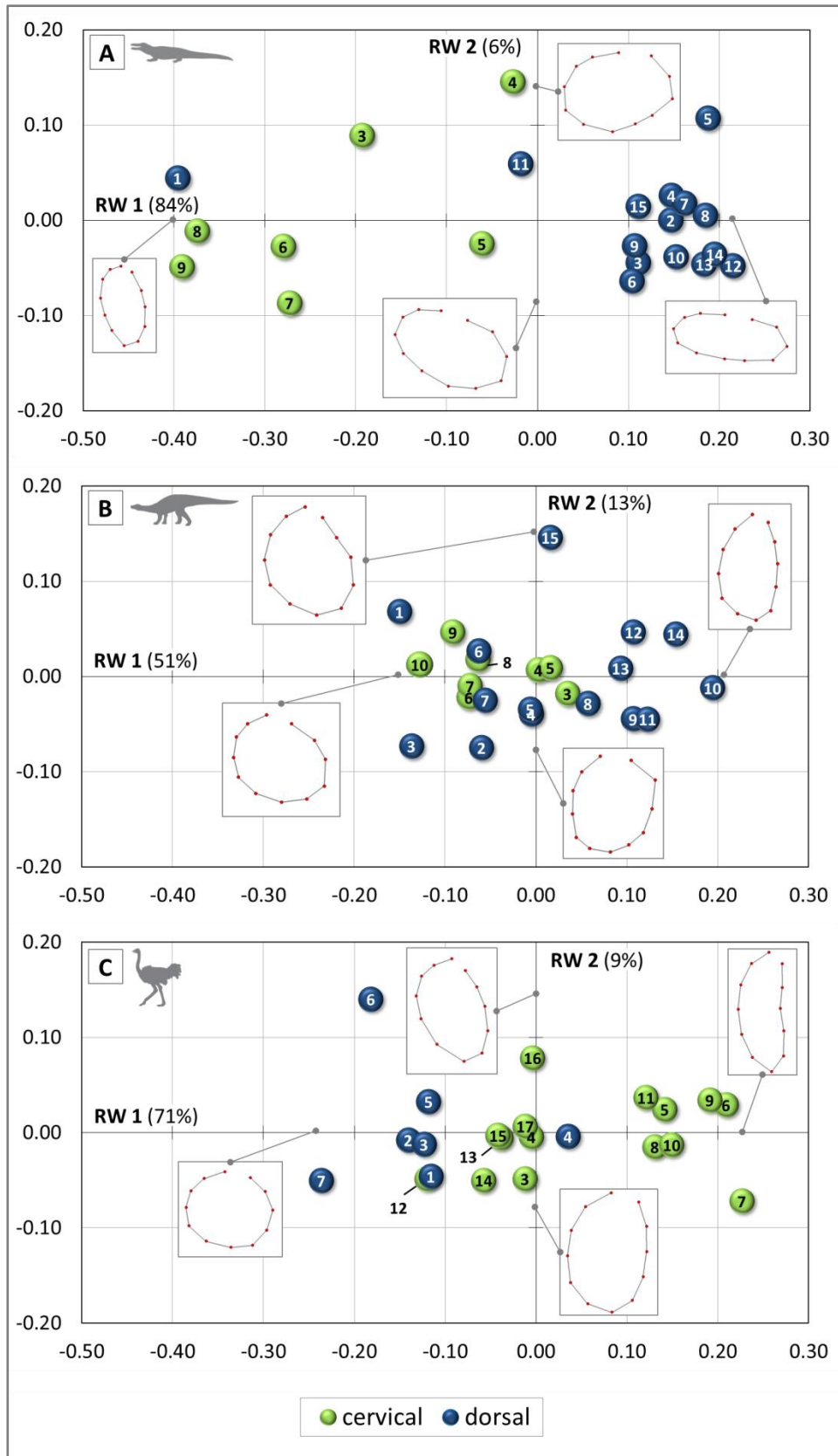


Figure 2.9.: Relative Warps (RW) Analysis results of the prezygapophyseal shape in extant and extinct archosaurs. Each plot shows the shape differences of the left anterior zygapophysis along RW 1 and RW 1 in (A) alligator, (B) *Plateosaurus* and (C) ostrich. 3D thin-plate splines (dorsal view) visualise the variation between the landmark configurations from the respective average shape (zero point). The landmarks are linked with a grey line. There is a gap left between LM 11 and semilandmark 22 for orientation.

### 2.3.3. Mobility range analysis

#### 2.3.3.1. Osteological neutral pose (ONP) and maximal flexion

At ONP, the cervical and dorsal region project anteroposteriorly upwards in all analysed archosaurs (Figure 2.10., Table 2.5.). In the extant taxa, the reconstructed curvature (without consideration of the absolute inclination) of the vertebral column equals the axial form of the living animal as radiological images of the species revealed (Claessens et al. 2009, Wagner 2002). The alligator shows a cervical lordosis (ventral curvature) and a dorsal kyphosis (dorsal curvature), which results in the S-shaped structure of the entire presacral vertebral column (Figure 2.10. A). In contrast, the axial skeleton of the ostrich reveals a cervical kyphosis and a dorsal lordosis (Figure 2.10. C). In *Plateosaurus*, the reconstruction of the cervical and dorsal vertebral series reveals each a kyphosis, and the cervicodorsal transition is lordotic (Figure 2.10. B). The curvature of the dinosaur neck resembles the form of the avian neck, whereas the trunk of *Plateosaurus* is curved as the dorsal vertebrae in the crocodile.

ONP is achieved by optimal articulation of adjacent vertebrae (Stevens and Parrish 1999). At this pose, the vertebral column is biomechanically relaxed and, thus, it has been suggested that ONP corresponds to the neutral resting pose of animals in life (Stevens and Parrish 1999). The latter is

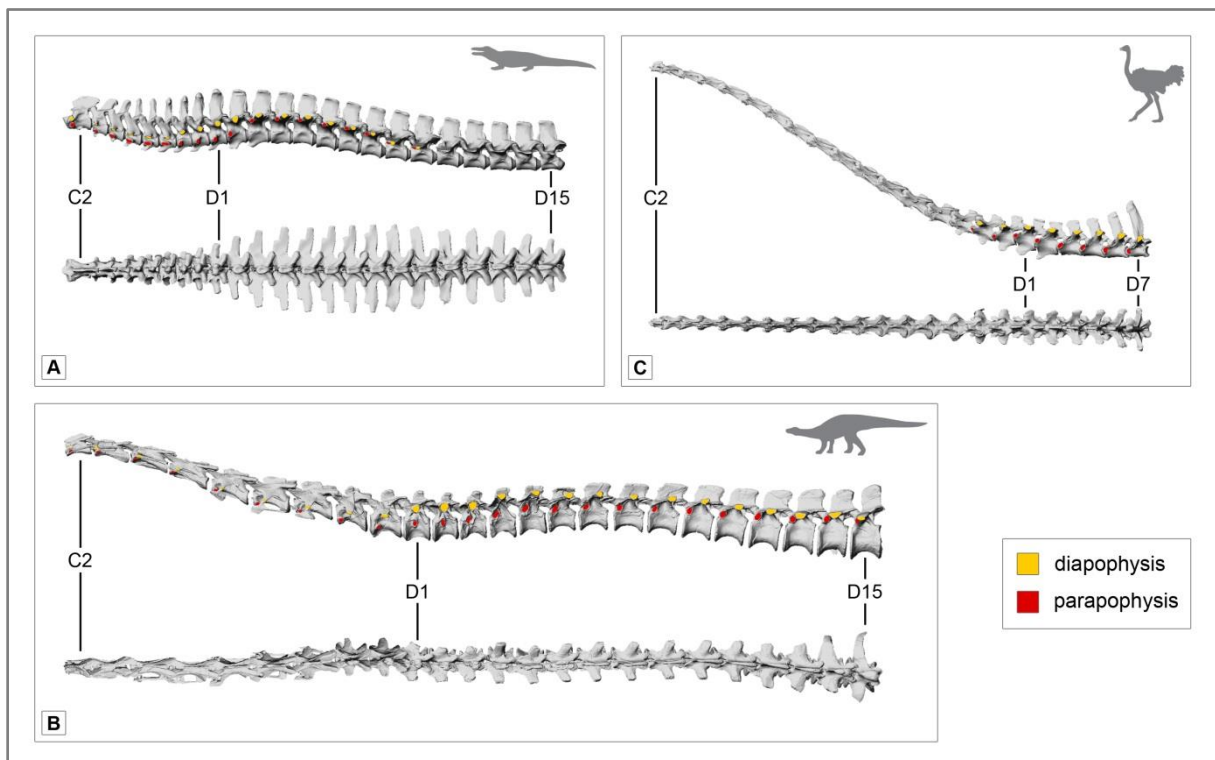


**Figure 2.10.:** Osteological neutral pose (ONP) of the presacral axial column in extant and extinct archosaurs. Digitally articulated 3D models of the cervical (C) and dorsal (D) vertebrae in (A) alligator, (B) *Plateosaurus* and (C) ostrich (not to scale). Each axial skeleton is shown in left lateral (top) and dorsal view (bottom). The positional changes of the diapophysis and the parapophysis are indicated by colour. Note the inclination and curvature of the neck and trunk.

considered as the unrestrained alert posture, in which the vertebral column is predominantly held when the animal is at rest (Graf et al. 1995, Taylor et al. 2009, Vidal et al. 1986). However, it has been shown that ONP does not reflect the unrestrained alert posture (Christian and Dzemski 2007, Dzemski 2006, Dzemski and Christian 2007, Taylor et al. 2009). Comparing the inclination of the vertebral column of alligator and ostrich at ONP (Table 2.5.) with the behaviour of the living animal reveals that the reconstructed pose does not unequivocally reflect the posture during rest.

There is, however, a good correspondence between ONP and resting pose of the cervical and dorsal series in the alligator. In contrast, the ONP of the neck of the ostrich is significantly different from the animal's posture during rest, as previously reported by Dzemski (2006). Thus, our data supports the observation that the reconstructed neck posture is considerably lower than the resting pose in long-necked vertebrates, such as ostriches, and generally differs from the habitual pose in animals that employ significant different neck postures during life (Christian and Dzemski 2007). The data of the extant archosaurs indicates that the ONP of the cervical series in *Plateosaurus* may not represent the habitual posture at rest because of its long neck (similar to the results in ostrich), whereas, the ONP of the dinosaur trunk may represent the habitual pose during rest because its structure is more similar to that of the alligator, in which a correspondence between reconstructed neutral and habitual posture exists.

The osteological neutral posture of the presacral vertebral column served as a basis on which establish the maximal flexion in dorsal, ventral and lateral direction with the theoretical limit of a 25% zygapophyseal overlap between adjacent vertebrae (Figure 2.11.). In total, the cervical vertebrae of the alligator allowed less flexion in all three directions than in *Plateosaurus* (Figure 2.11. A and B). The neck of the ostrich showed the highest dorsoventral flexibility (Figure 2.11. C). The dorsoventral mobility of the dorsal series is relatively similar between the crocodylian and the dinosaur (Figure 2.11. A and B), whereas the short trunk of the bird is less flexible (Figure 2.11. C). *Plateosaurus* revealed the highest lateral flexion in both the cervical and dorsal series (Figure 2.11. B). In the alligator, the neck is less flexible in the lateral direction than the trunk (Figure 2.11. A). In the ostrich, the cervical vertebrae are laterally more mobile than the dorsal vertebrae (Figure 2.11. C).

The reconstructed total flexion of the presacral vertebrae did not consider any ribs, although these structures may alter the maximal mobility. If bony barriers of the vertebra lead to a modified flexibility range by blocking further bending, the specific feature was identified as limiting factor (Table 2.5.). The main limiting structure was the zygapophyseal surface, but the dorsal flexion of the crocodylian neck was also restricted by the neural spine. The spinous process also affected the dorsal flexibility of the trunk in all three archosaurs.

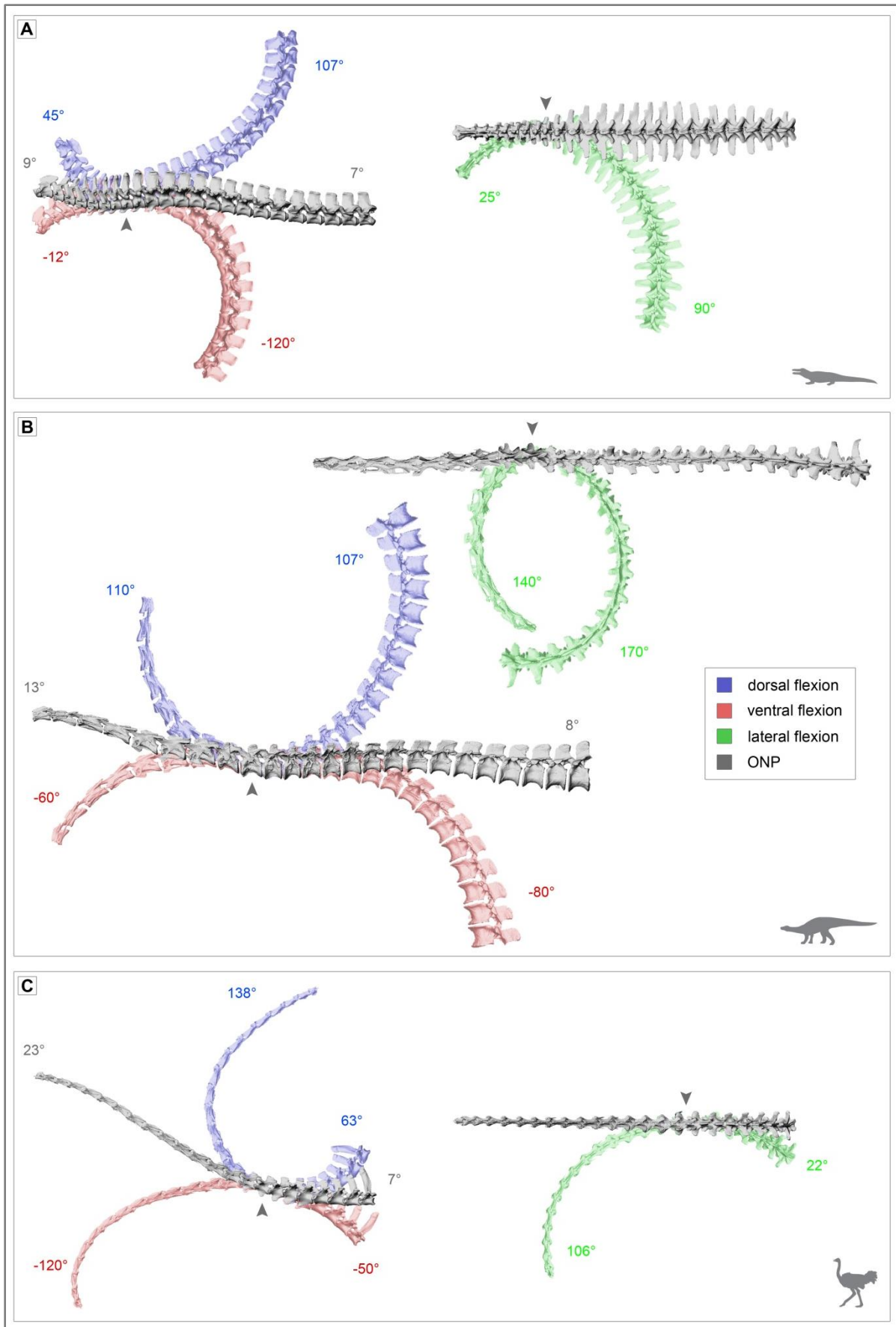


Figure 2.11.: Osteological mobility of the presacral axial column in extant and extinct archosaurs. The total flexion in dorsal, ventral and lateral direction (25% zygapophyseal overlap between adjacent vertebrae) in (A) alligator, (B) *Plateosaurus* and (C) ostrich. The grey arrow marks the last cervical vertebra in each taxon.

<b>Neck</b>	<b>Alligator</b>	<b>Plateosaurus</b>	<b>Struthio</b>
inclination at ONP	9°	13°	23°
(curvature)	(lordosis)	(kyphosis)	(kyphosis)
total dorsal flexion ( $\emptyset$ )	45° (10°)	110° (13°)	138° (10°)
dorsal limitation	neural spine	zygapophyses, centrum	zygapophyses
total ventral flexion ( $\emptyset$ )	-12° (-7°)	-60° (-9°)	-120° (-10°)
ventral limitation	zygapophyses, centrum	zygapophyses, centrum	zygapophyses (centrum)
total lateral flexion ( $\emptyset$ )	25° (8°)	140° (16°)	106° (9°)
lateral limitation	zygapophyses	zygapophyses	zygapophyses (centrum)
<b>trunk</b>			
inclination at ONP	7°	8°	7°
(curvature)	(kyphosis)	(kyphosis)	(lordosis)
total dorsal flexion ( $\emptyset$ )	90° (8°)	107° (10°)	63° (14°)
dorsal limitation	neural spine	neural spine (zygapophyses)	neural spine (zygapophyses)
total ventral flexion ( $\emptyset$ )	-120° (-10°)	-80° (-8°)	-50° (-8°)
ventral limitation	zygapophyses, centrum	zygapophyses, centrum	zygapophyses, centrum (hypapophyses)
total lateral flexion ( $\emptyset$ )	90° (8°)	170° (13°)	22° (8°)
lateral limitation	zygapophyses, transverse process	zygapophyses, centrum	zygapophyses (centrum)

**Table 2.5.: Osteological neutral position (ONP) and osteological mobility of the presacral axial column in extant and extinct archosaurs.** The total flexion in dorsal, ventral and lateral direction was acquired by manipulating the vertebrae to the theoretical limit that the zygapophyses minimally overlap for  $\frac{1}{4}$  of their articular surface. If bony barriers lead to a modified flexibility range by blocking further bending, the specific feature is given as limiting factor.  $\emptyset$  = average between successive vertebrae in the respective axial region.

### 2.3.3.2. Flexibility

The error in measurement of the flexibility between adjacent vertebrae was less than 1.0° in all analysed taxa. The repeated digital manipulation of the axial skeletons for the flexibility analysis revealed an uncertainty of about 3.0°.

In the three archosaurs, the dorsal flexion increases anteroposteriorly in the neck (Figure 2.12.). It is followed by low values throughout the trunk in the alligator and the dinosaur (Figure 2.12. A and B) as well as by relatively high and uniform angles in the dorsal series of the ostrich (Figure 2.12. C). The maximal dorsal mobility is reached in the neck, between the last two cervical vertebrae in the alligator (C8 - C9) and in *Plateosaurus* (C9 - C10), whereas it is between C11 and C12 in the ostrich. The ventral flexion decreases anteroposteriorly in the cervical series of the crocodylian with minimum angles at the base of the neck (Figure 2.12. A). The dorsal series revealed a high ventral mobility with

a peak at the anterior, middle and posterior parts of the trunk. In *Plateosaurus*, the ventral flexion is relatively uniform in the cervical series, but decreases at the base of the neck (Figure 2.12. B). The dorsal series showed low values of mobility in ventral direction. A maximum is reached in the middle part of the trunk. The ventral flexibility of the ostrich is relatively high in the neck (Figure 2.12. C). There are slightly lower values in the middle cervical region and at the cervicothoracic transition (C17 - D1). The trunk revealed a relatively uniform ventral mobility.

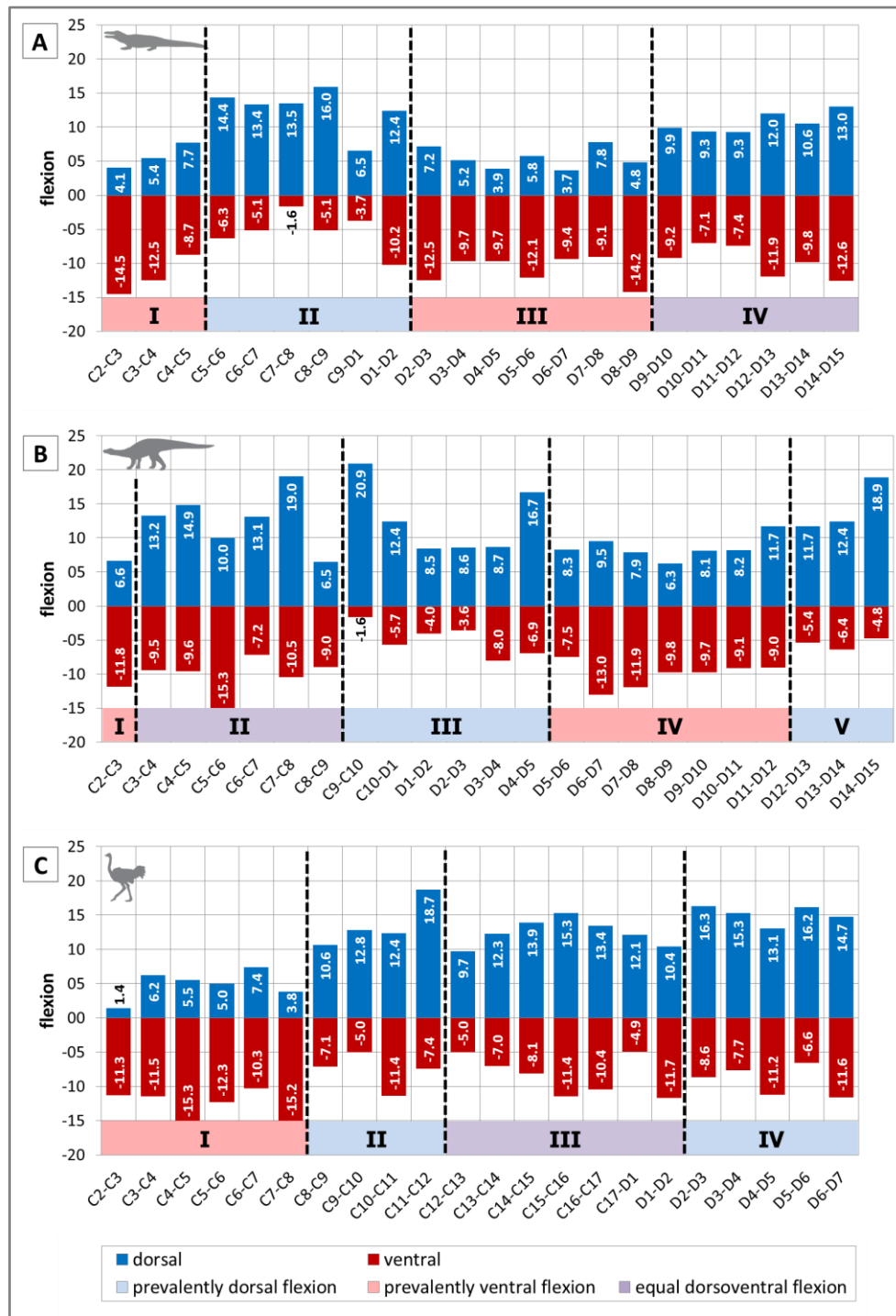


Figure 2.12.: Dorsoventral flexibility of the presacral vertebrae in extant and extinct archosaurs. Flexion between successive vertebrae of ( A ) alligator, ( B ) *Plateosaurus* and ( C ) ostrich. (Error in measurement <math><1.0^\circ</math>). The subregions (I - V) indicate if dorsal, ventral or equal dorsoventral flexion is prevalent.

Studying the differences in dorsal and ventral flexion between successive vertebrae, it is evident that there are regions in which either dorsal or ventral flexion is prevalent, or in which equal dorsoventral flexion is observed (Figure 2.12., Appendix 2.1.). This allows the separation of the presacral vertebral column of the three archosaurs into functional subregions. The most anterior subregion I shows mainly ventral flexion in all analysed taxa. In the alligator, this unit comprises the second to fourth cervical vertebra (C2 - C4) (Figure 2.12. A). *Plateosaurus* only has the vertebra C2 in this subregion (Figure 2.12. B). In the ostrich, subregion I includes the second to seventh cervical vertebra (C2 - C7) (Figure 2.12. C). The following subregion II is characterised by prevalently dorsal flexion in the two modern archosaurs. In the extinct dinosaur, this unit shows relatively equal dorsoventral flexion. The vertebrae C5 to D1 were assigned to subregion II in the crocodylian (Figure 2.12. A). It comprises the cervical vertebrae C8 to C11 in the ostrich (Figure 2.12. C). Almost the entire neck of *Plateosaurus* (C3 - C8) forms the subregion II (Figure 2.12. B). The subsequent subregion III shows uniform dorsoventral flexion in the modern archosaurs. It is characterised by mainly dorsal flexion in the extinct taxon. In the alligator, the vertebrae D2 to D8 exist in this unit (Figure 2.12. A). The posterior part of the neck (C12 - D1) was assigned to this unit in the ostrich (Figure 2.12. C). In *Plateosaurus*, subregion III includes the vertebrae D5 to D11 (Figure 2.12. B). The last unit in the two modern taxa is subregion IV. The extinct dinosaur has one additional domain, subregion V. Subregion IV is characterised by equal dorsoventral flexion in the crocodylian. It comprises the posterior dorsal vertebrae (D9 to D14) (Figure 2.12. A). This unit shows mainly ventral flexion in *Plateosaurus*. The vertebrae D9 to D11 were assigned to this domain (Figure 2.12. B). In the ostrich, subregion IV reveals prevalently dorsal flexion. It includes the dorsal vertebrae D2 to D6 (Figure 2.12. C). In subregion V, which was only identified in *Plateosaurus*, dorsal flexion is prevalent. The dinosaur has the vertebrae D12 to D14 in this unit (Figure 2.12. B).

The dorsoventral flexibility of the neck of the rhea (van der Leeuw et al. 2001) revealed the same overall configuration as the ostrich. The rhea has the second to fifth cervical vertebrae (C2 - C5) in subregion I (prevalently ventral flexion) (van der Leeuw et al. 2001). The vertebrae C6 to C13 were assigned to subregion II (prevalently dorsal flexion) (van der Leeuw et al. 2001). Subregion II, which is characterised by equal dorsoventral flexion, includes the last two cervical vertebrae C14 and C15 (van der Leeuw et al. 2001).

The lateral flexion between adjacent vertebrae is highly uniform throughout the presacral axial column in the crocodile (Figure 2.13. A). In the dinosaur, the lateral mobility is, on average, higher in the neck than in the trunk (Figure 2.13. B). The cervical series of the bird is also more mobile in lateral direction than the dorsal region (Figure 2.13. C). There is no significant correlation between the lateral flexibility and the previously identified functional subregions.

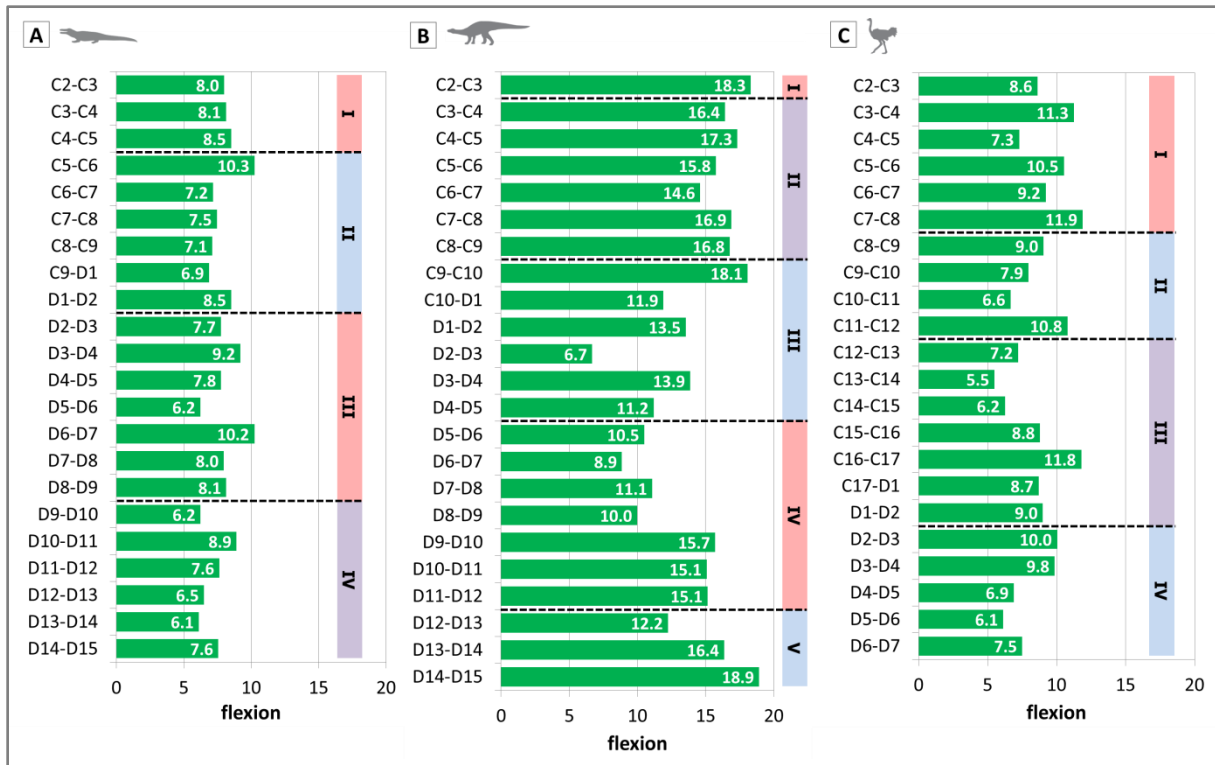


Figure 2.13.: Lateral flexibility of the presacral vertebrae in extant and extinct archosaurs. Flexion between successive vertebrae of ( A) alligator, (B) *Plateosaurus* and (C) ostrich. (Error in measurement  $<1.0^\circ$ ). The subregions (I - V) indicate if dorsal, ventral or equal dorsoventral flexion is prevalent (same colour coding as in Figure 2.12.).

### 2.3.4. Morphofunctional pattern

Based on the differences in dorsoventral flexion, the presacral vertebral column of the archosaurs was differentiated into functional subregions (see section 2.3.3.2). Comparing the functional pattern with the morphological results (see section 2.3.2.1 and 2.3.2.2) reveals that vertebrae that are in the same functional unit share specific morphological characteristics. Although there is no significant correlation, changes in the vertebral flexibility are related with shape and relative size changes.

#### Alligator

In the alligator, the prevalent ventral flexion of the cervical vertebrae in the anteriormost subregion I (C2 - C4) is associated with the specialised shape of the axis and with the relatively similar gross morphology of the third and fourth cervical vertebra (Figure 2.14. A). Starting from C2, in which the maximal length/height ratio reaches almost 1.0, the maximal length of the vertebrae in this unit decreases, whereby the maximal height increases (Figure 2.14. B). This size change is mainly due to a decrease in zygapophyseal overhang and an increase in the vertebral arch height. The centrum length and height is relatively constant. The prezygapophyses are round and broad (Figure 2.14. C).

The vertebrae of subregion II (C5 - D1), in which dorsal flexion is prevalent, share a short and rectangular shape (Figure 2.14. A). They reveal the lowest maximal length/height ratio of about 0.5 (Figure 2.14. B). Throughout this unit, the maximal vertebral length is relatively uniform as the

centrum length and, thus, the zygapophyseal overhang. Whereas the centrum height is also constant, the maximal vertebral height increases significantly because of the increase of the vertebral arch height. The shape of the prezygapophyses in subregion II are mostly oval and long (Figure 2.14. C).

The prevalent ventral flexion between the dorsal vertebrae in subregion III (D2 - D9) is related with a relatively broad vertebral shape with a slight tendency to a quadratic morphology (Figure 2.14. A). The maximal length/height ratio is with about 0.65 higher than in the previous subregion (Figure 2.14. B). The vertebrae in this unit show an increased maximal vertebral length, whereas the maximal vertebral height decreases slightly. As the centrum length and height is uniform in subregion III, the size change is due to an increase of the zygapophyseal overhang and a decrease in the vertebral arch height. The shape of the prezygapophyses in this unit is oval and short but very broad (Figure 2.14. C).

The vertebrae of the posteriormost subregion IV (D10 - D14), in which equal dorsoventral flexion was measured, display a gross morphology that resembles a square (Figure 2.14. A). The maximal length/height ratio reaches a second maximum along the presacral vertebral column with about 0.70 (Figure 2.14. B). The length measurements (maximal vertebral length, centrum length and zygapophyseal overhang) are relatively similar to the dimensions of the previous subregion. However, there is a slight decrease in the maximal vertebral height that is related to a decrease of the vertebral arch height. The prezygapophyses in this unit are mediolaterally wide and oval as in subregion III (Figure 2.14. C).

### Plateosaurus

In the dinosaur, the anteriormost subregion I, in which ventral flexion is prevalent, includes only C2. The axis is very distinct in its morphology, because it is the only vertebra that develops a dens, which has also been observed for the bird and the alligator. The overall shape of the second vertebra is relatively similar to the following cervical vertebrae (Figure 2.15. A). With a maximal length/height ratio of almost 1.5, the vertebra C2 is longer than high (Figure 2.15. B). Compared to the following vertebrae, the centrum length is intermediate, whereas the value of the centrum height is one of the lowest. The axis reveals a relatively short zygapophyseal overhang and a low vertebral arch height.

The equal dorsoventral flexibility of the cervical vertebrae in subregion II (C3 - C8) is associated with a long, narrow, rectangular shape (Figure 2.15. A). Starting from C4, in which the maximal length/height ratio reaches a maximum of almost 2.5, the maximal length of the vertebrae in this unit slightly decreases, whereas the maximal height increases significantly (Figure 2.15. B). The centrum length and height as well as the zygapophyseal overhang and the vertebral arch height reflect this pattern, which indicates that the observed size change is proportional and not modular. The prezygapophyses are circular (Figure 2.15. C).

The vertebrae of subregion III (C9 - D4), in which dorsal flexion prevails, share a quadratic morphology (Figure 2.15. A). The maximal length/height ratios are significantly lower than in the previous units, with values of about 0.8 (Figure 2.15. B). The maximal vertebral length slightly decreases, whereas the maximal vertebral height shows an increase. The centrum length and height show a relatively similar pattern. Whereas the zygapophyseal overhang remains rather constant, the data indicates an increase in the vertebral arch height. The shape of the prezygapophyses is round and relatively broad (Figure 2.15. C).

The prevalent ventral flexion between the dorsal vertebrae in subregion IV (D5 - D11) is related with a rectangular gross morphology (Figure 2.15. A). The maximal length/height ratios are slightly greater than in the previous unit, but do not exceed a value of 1.0 (Figure 2.15. B). The maximal vertebral length and height show a moderate increase. This size change is also reflected in the centrum length and height, as well as zygapophyseal overhang and vertebral arch height. The prezygapophyses in subregion IV vary between round and more oval (anteroposteriorly long) (Figure 2.16. C).

In the posteriormost subregion V, the vertebrae are prevalently flexible in dorsal direction (D12 - D14), which is associated with a similar overall shape as previously observed in subregion III (Figure 2.15. A). The maximal length/height ratio reaches its minimum with about 0.5 in this unit (Figure 2.15. B). The maximal vertebral length decreases, whereby the maximal vertebral height displays an increase. The other measured dimensions reveal the same trend. The shape of the prezygapophyses is anteroposteriorly long and oval (Figure 2.16. C).

### Ostrich

In the ostrich, the prevalent ventral flexion of the cervical vertebrae in the most anterior subregion I (C2 - C7) is linked with the distinct morphology of the axis and with the uniform, long and rectangular shape of the successive vertebrae (Figure 2.16. A). Starting from C2, in which the maximal length/height ratio is about 1.1, the ratio increases and reaches a maximum at C6, with a value of 2.6 (Figure 2.16. B). The maximal vertebral length of the vertebrae in this unit increases, whereas the maximal vertebral height is rather constant. The same pattern is observed for the length and height of the centrum, as well as for the zygapophyseal overhang and the vertebral arch height. The oval shape of the prezygapophyses is anteroposteriorly long and mediolaterally very narrow (Figure 2.16. C).

The vertebra of subregion II (C8 - C11), in which dorsal flexion is prevalent, are relatively similar in their gross morphology to the previous unit (Figure 2.16. A). The maximal vertebral length/height ratio is equally high, with values of about 2.4 (Figure 2.16. B). The maximal vertebral length and height slightly increase. Whereas the centrum gets longer in this subregion, the centrum height remains constant. Accordingly, the zygapophyseal overhang slightly decreases, while the vertebral

arch height shows no significant change. The prezygapophyses are oval, as previously observed in subregion I (Figure 2.16. C).

The equal dorsoventral flexion between the vertebrae in subregion III (C12 - D1) is associated with a long but increasingly quadratic shape (Figure 2.16. A). The maximal length/height ratio decreases significantly in this unit (Figure 2.16. B). The maximal vertebral length is relatively constant, but the maximal vertebral height shows a distinct increase. The centrum length decreases slightly, whereas the centrum height is relatively uniform. The significant change in size is mainly due to an increase of the vertebral arch height. The shape of the prezygapophyses is circular (Figure 2.16. C).

The vertebrae of the posteriormost subregion IV (D2 - D6), in which dorsal flexion prevails, are very short, but high in their gross morphology (Figure 2.16. A). The maximal length/height ratio decreases from about 0.9 to 0.5 in this unit (Figure 2.16. B). The maximal vertebral length is relatively constant, but the maximal vertebral height increases. The centrum length and height show no variation. The zygapophyseal overhang decreases, whereas the vertebral arch height increases. The prezygapophyses in subregion IV are round, except the zygapophysis of C6, which is more oval (anteroposteriorly long) (Figure 2.16. C).

### Summary

In summary, the pattern of the overall vertebral shape reflects the differentiation based on the flexion analysis (Figure 2.14. A, Figure 2.15. A, Figure 2.16. A), especially in the alligator and *Plateosaurus*. In the ostrich, the coincidence is not as high as in the other archosaurs, because anterior and middle cervical vertebrae are not very distinct in their shape (Figure 2.16. A). In all analysed taxa, the vertebrae in subregions with prevalently ventral flexion show a slight tendency towards a relatively quadratic shape with a broad neural spine. In units in which dorsal flexion prevails, the vertebrae are, in general, rather high and rectangular. Accordingly, the maximal length/height ratio is higher in subregions with prevalent ventral flexion than in units in which dorsal flexion prevails (Figure 2.14. B, Figure 2.15. B, Figure 2.16. B). The gross morphology of vertebrae that reveal equal dorsoventral flexion is, mainly, longer than high. The maximal length/height ratios in these units are often relatively high. There was no significant correlation between flexion and the shape of the prezygapophysis (Figure 2.14. C, Figure 2.15. C, Figure 2.16. C).

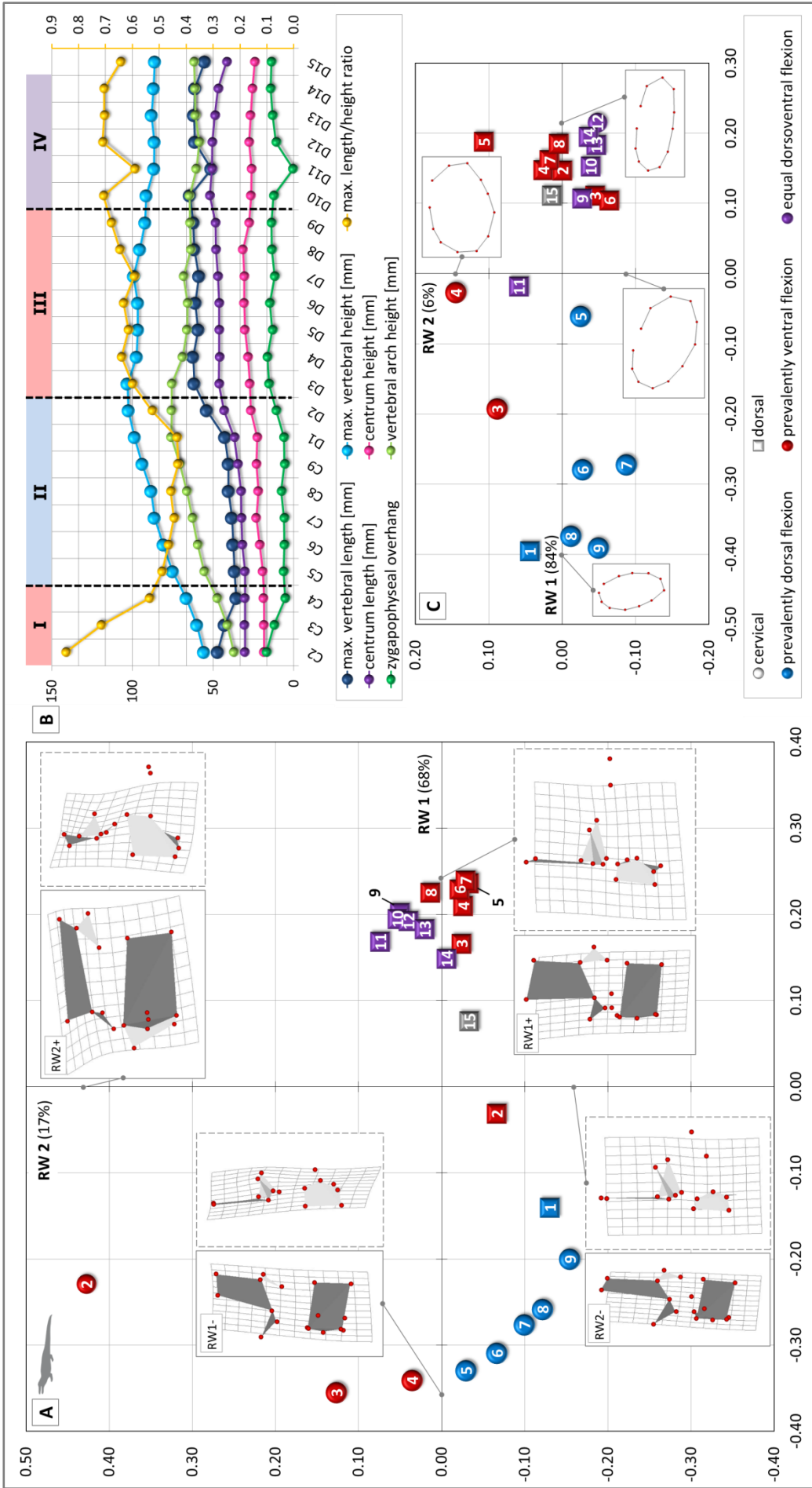
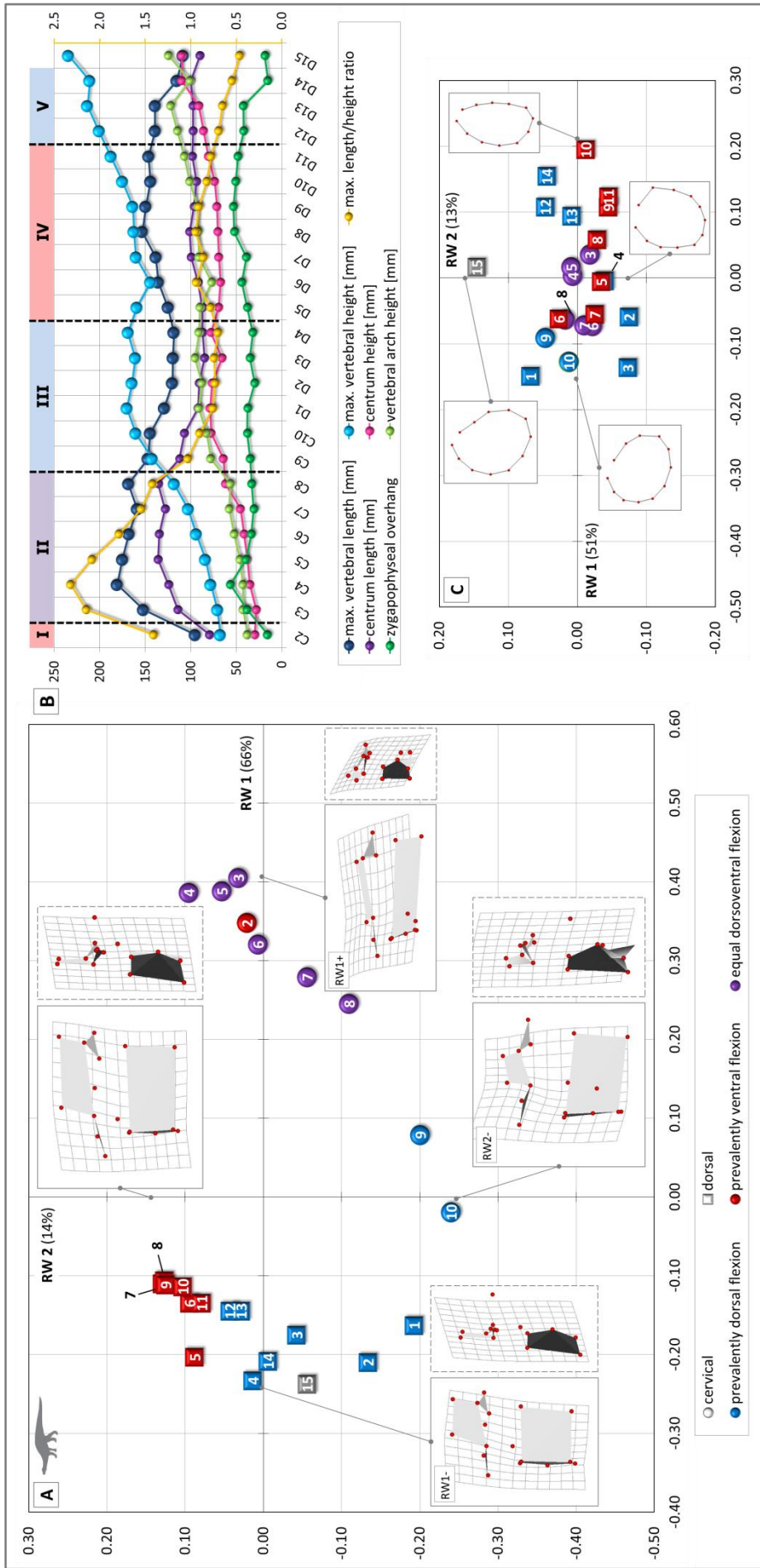
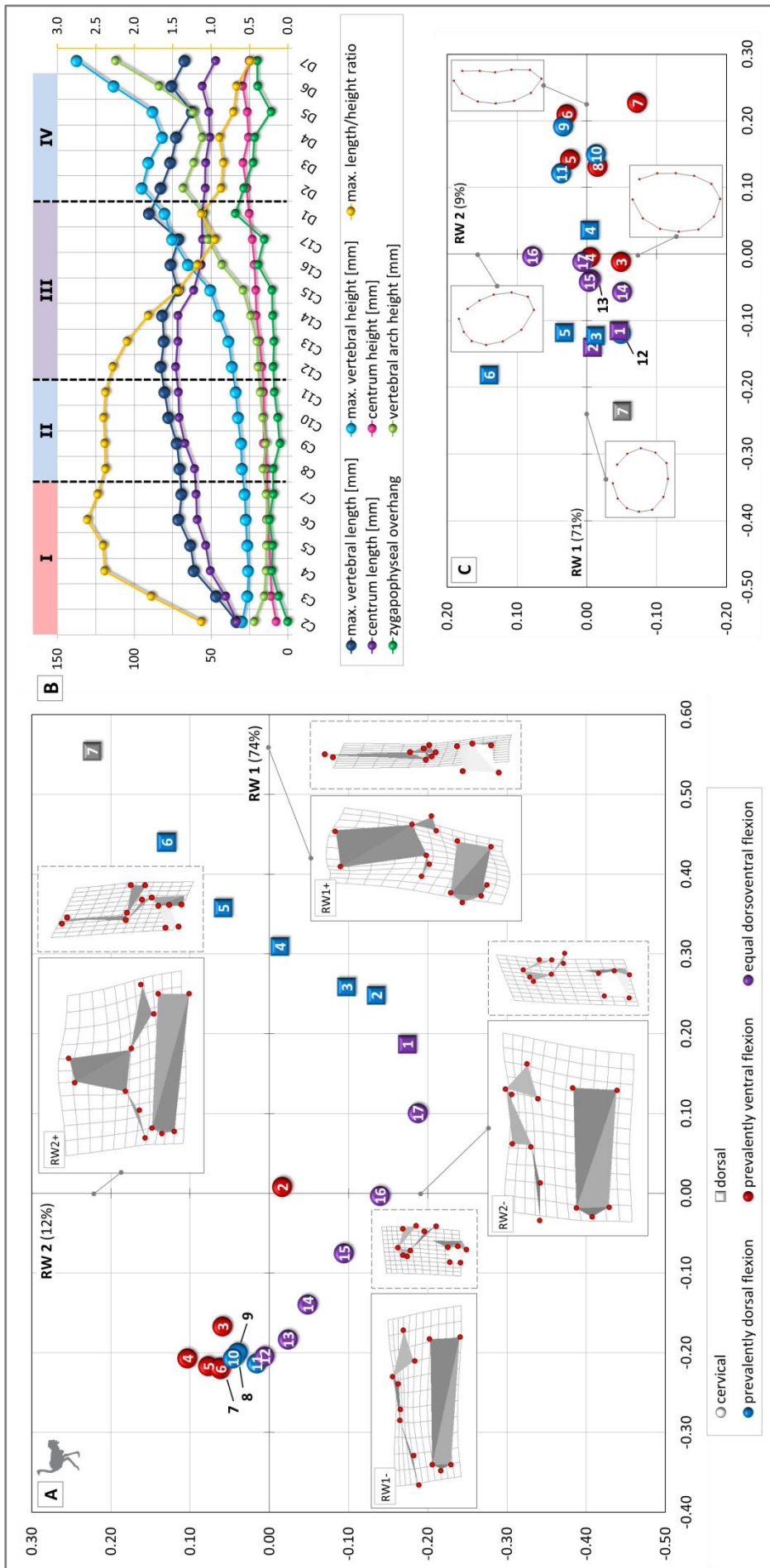


Figure 2.14.: Morphofunctional pattern in alligator. Each plot shows the prevalent flexion (indicated by colour) associated with the shape and size differences of the presacral vertebrae. (A) Relative Warps (RW) Analysis results of the overall vertebral shape, (B) linear measurements and (C) Relative Warps (RW) Analysis results of the prezygapophyseal shape. 3D thin-plate splines visualise the variation between the landmark configurations from the respective average shape as in Figure 2.8. and Figure 2.9., respectively. The last dorsal vertebra of each taxon is displayed in grey colour because its flexion to the posterior adjoining sacrum was not investigated.



**Figure 2.15.: Morphofunctional pattern in *Plateosaurus*.** Each plot shows the prevalent flexion (indicated by colour) associated with the shape and size differences of the presacral vertebrae. (A) Relative Warps (RW) Analysis results of the overall vertebral shape, (B) linear measurements and (C) Relative Warps (RW) Analysis results of the prezygapophyseal shape. 3D thin-plate splines visualise the variation between the landmark configurations from the respective average shape as in Figure 2.8. and Figure 2.9., respectively. The last dorsal vertebra of each taxon is displayed in grey colour because its flexion to the posterior adjoining sacrum was not investigated.



**Figure 2.16.: Morphofunctional pattern in ostrich.** Each plot shows the prevalent flexion (indicated by colour) associated with the shape and size differences of the presacral vertebrae. (A) Relative Warps (RW) Analysis results of the overall vertebral shape, (B) linear measurements and (C) Relative Warps (RW) Analysis results of the prezygapophyseal shape. 3D thin-plate splines visualise the variation between the landmark configurations from the respective average shape as in Figure 2.8. and Figure 2.9., respectively. The last dorsal vertebra of each taxon is displayed in grey colour because its flexion to the posterior adjoining sacrum was not investigated.

## 2.4. Discussion

Although the number of presacral vertebrae in the alligator (24 presacrals) and ostrich (24 presacrals) displays no variation, the comparative analysis of the vertebral morphology revealed fundamental structural modifications of the axial skeleton between the crocodylian and avian lineage. The results for *Plateosaurus* (25 presacrals) display an intermediate state between the representatives of the extant phylogenetic bracket. The cervical morphology and shape pattern in the dinosaur shares several similarities with the bird, whereas the dorsal morphology and shape pattern are more similar to the crocodylian.

### 2.4.1. Mobility range analysis

Although our data supports the observation that the ONP of a relatively long neck does not reflect the habitual neck posture (Christian and Dzemski 2007), the reconstructed curvature (without consideration of the absolute inclination) equals the axial form of the living animal. This corresponds with the previous description that the cervical column maintains its axial form regardless of the posture of the animal (Vidal et al. 1986). The varying curvature of the cervical and dorsal vertebral series is based on different construction principles, which affect the overall mobility in each region. Curvature and flexion reflect the different mechanical loads and functional demands on the axial system. The vertebral column plays an important role in controlling body posture against external forces, such as weight force, ground reaction force and inertia. The axial system is subjected to static and dynamic forces that cause parts of it to bend, stretch, shorten, twist and shear (Wainwright 1988). Apart from active stabilisation against these loads by muscular activity, vertebral morphology passively stabilises the axial system.

In general, the static construction of the axial system can be regarded as a string-and-bow model (Slijper 1946). The head-neck system is supported on one side, analogous to a cantilevered beam (Kummer 1959, Slijper 1946). Where the neck has a dorsally concave curvature, it forms a bow that is stringed with dorsal muscles, tendons or ligaments (Alexander 1989, Kummer 1959). The dorsally convex curvature of the trunk is part of another string-and-bow system that is braced by ventral soft tissue (Kummer 1959, Slijper 1946). Depending on the posture and curvature of the vertebral column, tensile forces act on the neural arches of the vertebrae and the vertebral centra resist to compressive forces or vice versa (Rockwell et al. 1938). Despite these basic assumptions, there are differences in the specific construction of the axial system, such as the importance of a bone-facilitated (e.g. neck of the alligator (Frey 1988)) or soft-tissue-facilitated (e.g. neck of mammals (Nickel et al. 1968)) stabilisation.

The typical dorsally concave neck of the crocodile is a ventrally self-supporting structure that accommodates the weight force and the down-bending force of the large skull (Frey 1988, Salisbury and Frey 2000, Seidel 1978). Corresponding the ventral flexibility in the neck is limited. The dorsally convex curvature of the alligator trunk is part of the string-and-bow-construction of the body bracing system (Frey 1988, Salisbury and Frey 2000). Accordingly, the dorsal series is more flexible in ventral than in dorsal direction. In the ostrich, the cervical series is actually an upward-sloping S-curve, which ensures a high overall flexibility of the neck. This construction is enabled by a combination of the more or less vertical position of the neck at rest and during locomotion, the relatively small and light head and the characteristic ligament system that acts as a brace (Dzemeski and Christian 2007, Tsuihiji 2004). The dorsally concave trunk of the bipedal bird compensates the ventral acting forces in a similar way to the lordotic neck of the alligator. Correspondingly, the ventral flexibility in the trunk is limited. The kyphotic neck of *Plateosaurus* resembles the cervical structure seen in the ostrich. The dinosaur also had a relatively small head, which reduced the ventral acting force. Additionally, it had a relatively long and heavy tail that may have acted as counterbalance. However, it is unlikely that *Plateosaurus* held its neck in an upright position to stabilise the cervical column. In contrast to the ostrich, the neck of the dinosaur would be constantly almost maximally dorsally flexed at such a vertical position. Whether or not the dinosaur had a similar ligament system as reported for ostriches is part of a further study. However, the observed dorsal widening of the neural spines starting from the sixth cervical vertebra suggests an interspinal ligament (ligamentum elasticum interspinale) similar to that in the bird. The kyphotic dorsal series is very similar to the structure of the crocodilian trunk. This may indicate a somewhat similar string-and-bow construction of the body.

#### 2.4.2. Feeding and locomotion behaviour

The flexibility along the presacral vertebral column showed a taxon-specific pattern of functional subregions. These differences can be linked to variations in feeding strategy and locomotor style.

In addition to the relationship between vertebral morphology, posture and static forces, the form of the axial system is also linked to dynamic forces that act for instance during feeding and locomotion. Morphological specialisations enhance the ability to apprehend food and, thus, the feeding strategy also depends on the posture and mobility of the neck (Schwenk 2000). In general, an elongate neck enables a greater reaching distance and, thus, increases the feeding envelope (Preuschoft et al. 2011). In order to efficiently exploit the vegetation, two feeding behaviours can be distinguished (Figure 2.17.). Either the increased feeding range is primarily used in vertical direction and, thus, the long neck enables high feeding (e.g. feeding height stratification between giraffe and smaller browsers (Cameron and du Toit 2007, du Toit 1990) and high browsing in sauropod dinosaurs (Bakker 1986, Christian 2002, Christian and Dzemeski 2007, Fastovsky and Smith 2004)). Alternatively, the

feeding range is increased in horizontal direction and, thus, the long neck enables the animal to reach a large volume of vegetation without needing to move the body (Shipley et al. 1996) (e.g. feeding overlap between kudu and impala (du Toit 1990), middle to low browsing in sauropod dinosaurs (Christian 2002, Fastovsky and Smith 2004, Martin 1987, Preuschoft et al. 2011). Considering the head trajectory as the function of the neck (van der Leeuw et al. 2001), the flexion pattern provides insights into the different neck movement mechanisms and related feeding behaviour in extant archosaurs.

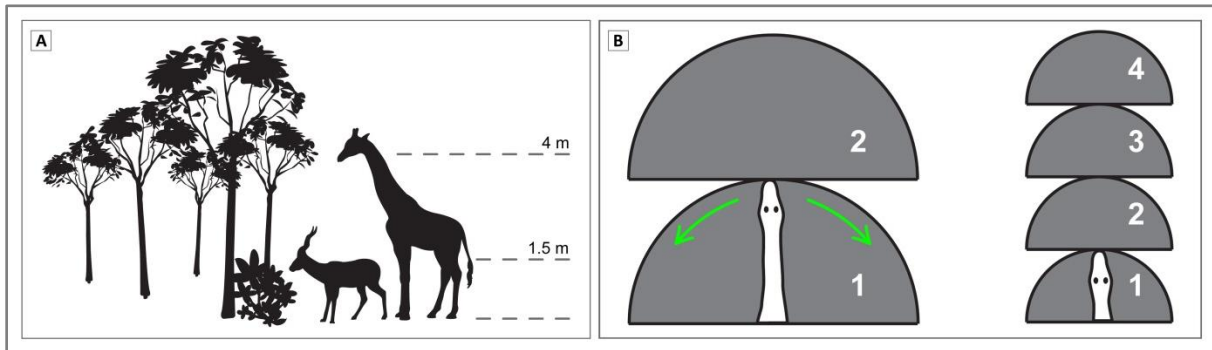


**Figure 2.17.: Different strategies of long-necked animals to exploit vegetation.** (A) Feeding height stratification between giraffe and smaller browsers. (B) Relationship between neck length and number of feeding stations (modified after Preuschoft et al. 2011). The long-necked animal on the left needs only two feeding stations to reach a large area of vegetation. The short-necked animal on the right needs about 4 feeding stations to cover the same distance, but reaches only about half of the area.

In the alligator, the cervical region is dominated by a large subregion II, in which dorsal flexion prevails (Figure 2.18. A). This indicates that the predaceous, semiaquatic crocodile mainly flexes its neck in dorsal direction and, thus, primarily catches prey that is at or above the level of its head. Indeed, the feeding strategy of the semiaquatic alligator is to capture prey by lurking in the water. Although crocodylians display several hunting techniques, most prey are taken as they approach the head (Murphy and Schlager 2004). Once within striking range, the alligator propels itself forward using its tail and limbs to grip the prey with its powerful jaw (Murphy and Schlager 2004). To pick up an item of prey off the ground, the alligator rotates its head about its long axis (Busbey 1989). Intraoral transport and swallowing are achieved only through inertial or gravitational movements of the head (Busbey 1989, Gans 1969). The prey is usually acquired by a short series of rapid head movements (Busbey 1989). The captured prey is then swallowed by raising the head and flicking the prey into the throat, under gravity (Busbey 1989, Gans 1969, Murphy and Schlager 2004).

Similar to the rhea (van der Leeuw et al. 2001), the head trajectory during feeding off the ground is a large vertical movement in the ostrich. This is a consequence of the upright posture of the neck during rest and alert, respectively, as well as the relatively long legs. Accordingly, there is a large unit of vertebrae at the base of the neck that allows equal dorsoventral flexion (subregion III) (Figure 2.18. B). The ostrich is an open-country bird that grazes on grass and browses on shrubs, succulents

and seed (Jackson et al. 2004). During feeding at ground level, the posterior cervical section is bent ventrally, whereas the middle part of the neck is dorsally flexed and the anterior cervical section is bent in ventral direction. This neck movement is reflected in subregion II, in which dorsal flexion is prevalent, and the anteriormost subregion I, in which ventral flexion prevails. The same link between the pattern of neck movement and flexibility has been previously observed in the rhea (van der Leeuw et al. 2001) (Figure 2.19.). The feeding strategy of the ostrich is to reach a large area of vegetation (mainly low-browsing) by moving the neck, but not the trunk (Dzemeski and Christian 2007). This strategy is also supported by the relatively high lateral flexibility in the neck.

The link between flexion pattern and feeding behaviour in extant archosaurs allows the inference of the feeding strategy in the extinct dinosaur *Plateosaurus*. The cervical region is dominated by a large subregion II that is characterised by uniform dorsoventral flexion (Figure 2.18. C). However, in subregion III, which includes the base of the neck, dorsal flexion prevails. This indicates that the

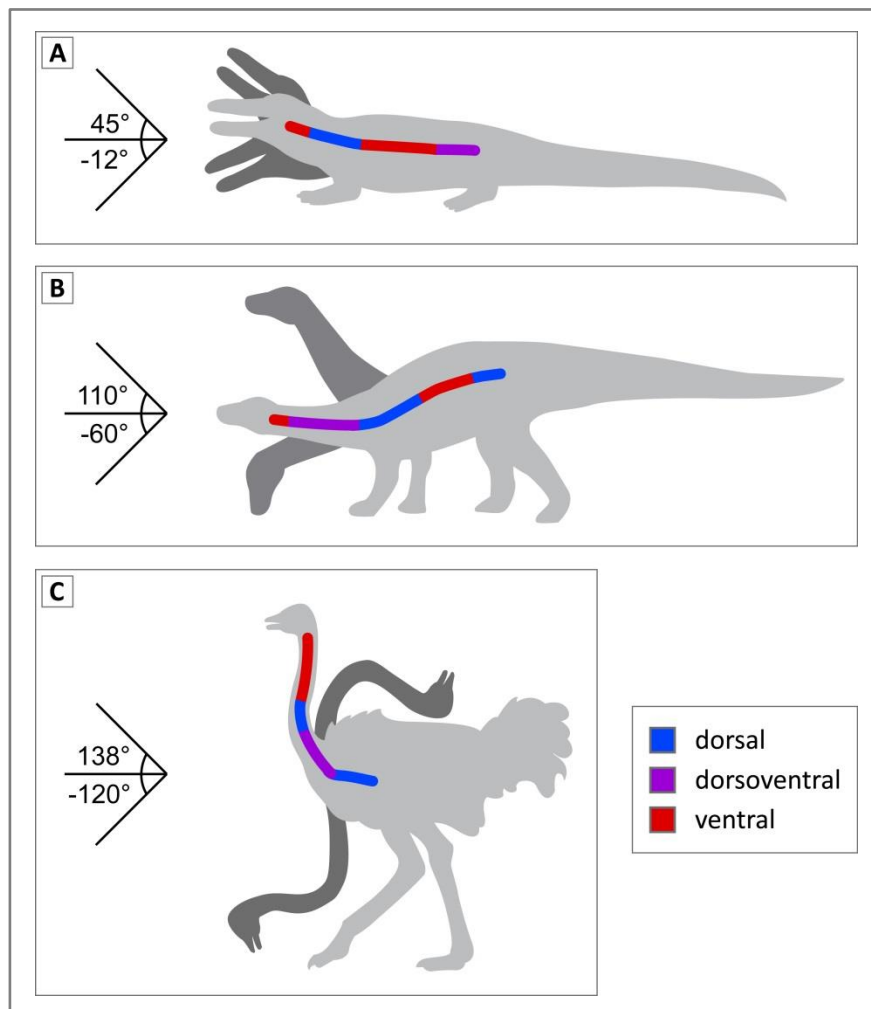


**Figure 2.18.:** Schematic illustration of the flexion pattern in the presacral vertebral column of extant and extinct archosaurs. The coloured bars represent the identified subregions in which dorsal, ventral or equal dorsoventral flexion is prevalent. The overall flexion of the neck in dorsal and ventral direction is indicated by the measured angles for (A) alligator, (B) *Plateosaurus* and (C) ostrich.

sauropodomorph dinosaur did not reach the ground in the same way as the ostrich. Instead, *Plateosaurus* moved its head up and down using more or less the whole neck as lever. Thus, the bending is mainly located in the middle and anterior part of the neck, associated with the vertical head trajectory (Figure 2.18. C). This flexion pattern somewhat resembles the behaviour observed for swans, with the major difference that the bird is adapted to reach depths in the water (van der Leeuw et al. 2001) (Figure 2.19.). This modification in the swan is revealed by the anterior and middle cervical vertebrae, in which ventral flexion is prevalent (van der Leeuw et al. 2001). In the dinosaur, dorsal flexion of the equivalent vertebrae prevails. Thus, although *Plateosaurus* is able to reach the ground, it appears to be primarily adapted to obtain food that is at or above the horizontal level of its head. The high lateral flexibility of the cervical and also first two dorsal vertebrae indicates that *Plateosaurus* was able to exploit a wide feeding envelope, therefore saving energy during feeding. The long and relatively flexible neck allowed it to reach a large area, and *Plateosaurus* had to change its feeding station less often compared with an short-necked animal. A modern analogon may be the African ruminant kudu. It has been reported that kudu allocated 33% of their feeding time to the height that they reach with almost vertically held necks (du Toit 1990). More than half of kudu

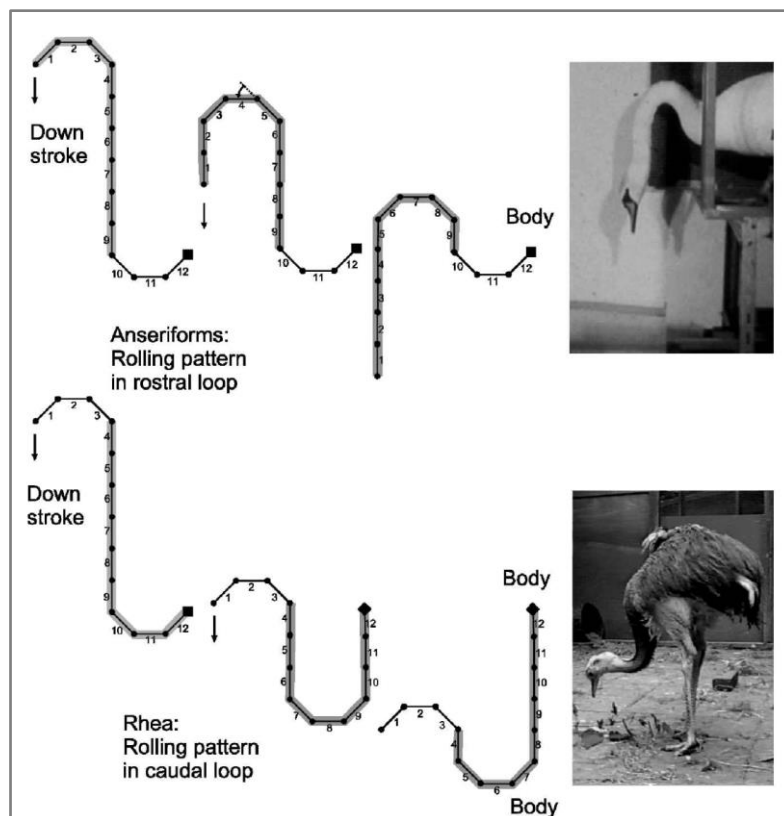


**Figure 2.19.:** Schematic illustration of the neck movement pattern in the swan and rhea. In order to move the head downward, the swan mainly bends its neck in the middle part. Accordingly this cervical sections revealed prevalent dorsal flexion. In the adjacent posterior part of the neck ventral flexion prevails, whereas the base of the cervical series is limited in its flexibility. The rhea shows a differen movement pattern. (Figure from van der Leeuw et al. 2001). See text for details.

feeding time was spent feeding below this level, which is within the reach of the shorter steenbock (du Toit 1990).

The axial skeleton is also a key skeletal component that reflects locomotor behaviour (Slijper 1946). In particular, the dorsal vertebral column contributes to body propulsion and provides the foundation for the production of mechanical work by the limbs. Variations in vertebral morphology and flexibility of the axial column are linked to locomotion styles. The way in which the bracing of the vertebral column operates against the mechanical loads governs the capacity for different locomotor modes (Salisbury and Frey 2000).

Extant crocodylians move in widely varying ways. During swimming, the semiaquatic animals generally sweep the limbs back and use primarily their powerful tail for propulsion (Murphy and Schlager 2004, Seebacher et al. 2003). Although water is their preferred domain, the modern crocodylians are also proficient in terrestrial locomotion. When travelling overland, the alligator employs different gaits, ranging from very sprawling to somewhat erect postures and including a mammal-like gallop (Frey 1988, Gatesy 1991, Reilly and Elias 1998 and references therein). This range of locomotion styles requires the axial column of the alligator to be constructed in accordance with the different functional adaptations. The crocodylian sprawl is not functionally equivalent to the sprawling behaviours exhibited by salamanders and lizards (Reilly and Elias 1998). Accordingly, the lateral flexion is relatively low throughout the axial column in the alligator. During sprawling, which is used only for short distances, and high-walk, which is the primary terrestrial locomotion style of the alligator, the dorsal vertebral column is retained in kyphosis (Frey 1988, Reilly and Elias 1998). The dorsally convex curvature of the trunk plays a particularly important role during high-speed locomotion, galloping and jumping (Frey 1988). This is also reflected in the flexion pattern of the dorsal vertebrae. In the anterior half of the trunk (subregion III) ventral flexion is prevalent, whereas the posterior part (subregion IV) is characterised by uniform dorsoventral flexion (Figure 2.18. A). The low dorsal flexibility of the thoracic region helps to passively maintain the kyphotic posture and prevents extreme dorsal flexion and deflection, respectively. In combination with the pronounced dorsoventral flexibility of the lumbar region, the dorsal series allows mobility that is necessary for sprinting performance and quick movements. A noticeable trait of crocodylians is the ability to jump almost vertically out of the water (Murphy and Schlager 2004). During a jump on land, the alligator accelerates exclusively by the thrust of its hindlimbs accompanied with the extension of the dorsal vertebral column (Frey 1988).

Birds are obligately bipedal and move in more erect postures. The ostrich lost the ability to fly, and is well adapted for high-speed terrestrial locomotion. In contrast to the long, muscular tail of bipedal dinosaurs, the tail of modern birds is ineffective at counterbalancing the anterior part of the body

(Gatesy and Dial 1996). This affects not only the morphology and posture of the hind limbs, but also the construction of the axial skeleton. Associated with the evolution of the unique avian body plan is the shortening and stiffening of the postcervical vertebral column, as well as the fusion of particular dorsal vertebrae into a notarium (Gatesy 2002). Although the ostrich is not able to fly and does not develop a notarium, the dorsal vertebral column is short and constrained in its movement. The trunk of the ostrich is dominated by subregion IV, in which dorsal flexion is prevalent (Figure 2.18. B). Corresponding to the construction principle of the cervical column of *Alligator*, the dorsal series of the ostrich passively prevents extreme ventral flexion. However, the high dorsal flexibility of the avian trunk may be somewhat artificial. The bird exhibits additional features that decrease the absolute degree of freedom of movement of the trunk skeleton. Some dorsal vertebrae of the ostrich have small, bony extensions on the anterior and posterior tip of the neural spine, which limits flexion. Birds lack a lumbar region and intermediate ribs. Thus, the avian thorax is also constrained in flexion because of the ribcage.

In *Plateosaurus*, the anterior part of the trunk is assigned to subregion III, in which dorsal flexion prevails (Figure 2.18. C). The middle part of the dorsal series is characterised by mainly ventral flexion (subregion IV). The posteriormost subregion V revealed prevalently dorsal flexion. This indicates that stabilisation of the trunk in the sauropodomorph dinosaur is not achieved by passively preventing extreme dorsal flexion, as observed in the alligator. In a quadruped posture, *Plateosaurus* stiffens its kyphotic dorsal vertebral column by hyposphene-hypantrum articulations. This is somewhat similar to the bracing system previously observed in large squamates, in which another type of accessory intervertebral articulations (zygosphene-zygantrum joints) stabilise the axial column (Virchow 1914). The hyposphene-hypantrum articulations, which are found in the dorsal vertebrae of almost all saurischian dinosaurs (excluding titanosaurian sauropods and birds), also adds rigidity to the vertebral column in bipedal animals (Langer 2004, Rauhut 2003). The hyposphene-hypantrum complex between C10 and D15 significantly restricts the mobility of the vertebrae in *Plateosaurus*. In particular, it leads to the low lateral flexibility of the dorsal series between C10 and D9. Thus, the interlocking wedge-and-notch articulation below the zygapophyses stabilises the trunk by constraining torsion and lateral flexion. Resisting these actions is important during forceful retraction of the limbs. In combination with the accessory articulations, the low ventral flexibility near the pectoral and pelvic girdle passively stabilises the trunk of *Plateosaurus*. The results of the present analysis indicate that the axial skeleton of *Plateosaurus* exhibits features that allow the stabilisation of the trunk during bipedal and quadrupedal posture. This supports the idea that the dinosaur may have extended its vertical feeding range by adopting a bipedal stance. However, this does not allow us to interpret an unambiguous locomotion style for the dinosaur.

## 2.5. Conclusion

The regionalisation of the axial skeleton into a cervical, dorsal, sacral and caudal compartment is a key attribute of amniotes, including archosaurs, reflecting an enhanced specialisation of the vertebral column to perform different functions. The first objective of the present study was to establish functional subregions based on the flexibility along the axial skeleton of alligator, *Plateosaurus* and ostrich. The presacral vertebral column of the analysed taxa was divided into units, according to the prevalence of dorsal, ventral or equal dorsoventral bending. The second goal was to evaluate the vertebral morphology with respect to the functional subregions. In summary, the pattern of the overall vertebral shape reflects the differentiation based on the flexion analysis. The cervical and dorsal elements of the archosaurian vertebral column thus form a series of morphofunctional subregions. The comparison of these units and performance of the axial column during various activities, such as feeding and locomotion, in extant archosaurs was the third objective of this work. It revealed a strong link between the taxon-specific flexion pattern and the biological role to which the vertebral mobility is adapted in the living animals. This relation enabled the use of the vertebral flexibility in the extinct dinosaur *Plateosaurus* as a function of axial movement. Although the cervical region of *Plateosaurus* shares several morphological similarities with the neck of the modern ostrich, the flexion pattern and thus the neck movement is quite different. The cervical flexibility pattern revealed that the basal sauropodomorph dinosaur was a mid-level browser that was also able to reach higher levels (Figure 2.20.). The latter may be an adaptation along with the rise of “gymnosperm” floras (Bakker 1986, Fastovsky 2000, Fastovsky and Smith 2004). The dorsal series of the sauropodomorph dinosaur shows more similarities with the trunk morphology of the extant alligator. Both share some similarities in their flexion pattern. The dorsal flexibility indicates that *Plateosaurus* was able to adopt both a quadrupedal and bipedal

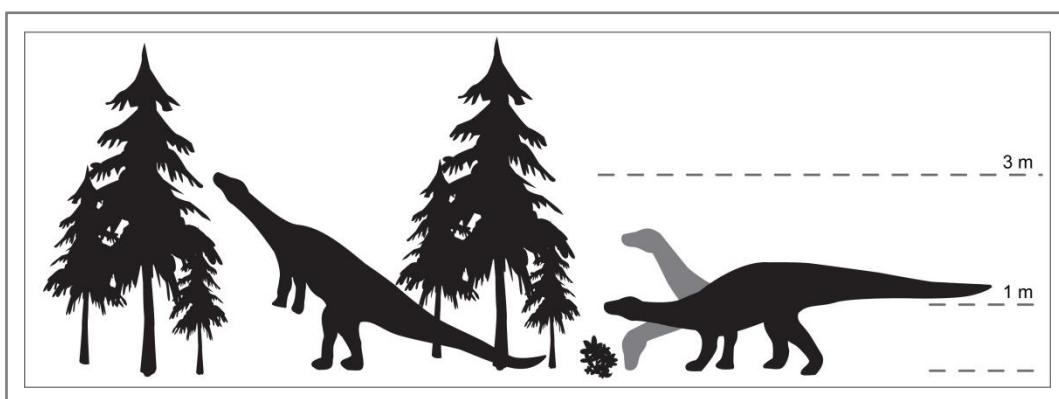


**Figure 2.20.: Schematic representation of the feeding behaviour in *Plateosaurus*.** The present study showed that the neck of the dinosaur allowed to reach the ground, but was primarily adapted to feed at or above the horizontal head level. Furthermore, the trunk of the dinosaur enabled to adopt both a quadrupedal and bipedal posture. In bipedal stance, a fully grown *Plateosaurus* could probably have reached heights around 3.0-3.5 m (according to Barrett and Upchurch 2007).

posture. However, the present study does not allow for an unambiguous interpretation of *Plateosaurus* as a facultative quadrupedal animal.

Understanding the relationship between organismal structure and function is a fundamental goal in biology. Linking morphofunctional patterns of the axial skeleton with related behaviour in modern animals enables us to enhance our knowledge about the palaeobiology of fossil taxa. Vertebral evidence thus provides new insights into the anatomy and physiology of extinct animals, such as sauropodomorph dinosaurs, which became the dominant large herbivores in terrestrial ecosystems with a nearly global distribution.

## 2.6. References

- Alexander, R.M., 1989. Dynamics of dinosaurs and other extinct giants. Columbia University Press, New York, 167 pp.
- Bakker, R.T., 1978. Dinosaur feeding behaviour and the origin of flowering plants. *Nature* **274**: 661-663.
- Bakker, R.T., 1986. The dinosaur heresies: New theories unlocking the mystery of the dinosaurs and their extinction. Zebra Books, Kensington Publishing Corporation, New York, 482 pp.
- Barrett, P.M., Upchurch, P., 2007. The evolution of feeding mechanisms in early sauropodomorph dinosaurs. *Special Papers in Palaeontology* **77**: 91-112.
- Baumel, J.J., King, A.S., Breazile, J.E., Evans, H.E., Vanden Berge, J.C., 1993. Handbook of avian anatomy: nomina anatomica avium. Nuttall Ornithological Club, Cambridge, 779 pp.
- Boas, J., E., V., 1929. Biologisch-anatomische Studien über den Hals der Vögel. *Kgl. Danske Vidensk. Skrifter* **9**: 101-222.
- Bonaparte, J.F., 1999. Evolución de las vértebras presacras en Sauropodomorpha. *Ameghiniana* **36**: 115-187.
- Busbey, A.R., 1989. Form and function of the feeding apparatus in Alligator mississippiensis. *Journal of Morphology* **202**: 99-127.
- Cameron, E.Z., du Toit, J.T., 2007. Winning by a neck: tall giraffes avoid competing with shorter browsers. *The American Naturalist* **169**: 130-135.
- Christian, A., 2002. Neck posture and overall body design in sauropods. *Mitteilungen des Museums für Naturkunde Berlin Geowissenschaftliche Reihe* **5**: 271-281.
- Christian, A., Dzemski, G., 2007. Reconstruction of the cervical skeleton posture of Brachiosaurus brancai Janensch, 1914 by an analysis of the intervertebral stress along the neck and a comparison with the results of different approaches. *Fossil Record* **10**: 38-49.
- Christian, A., Koberg, D., Preuschoft, H., 1996. Shape of the pelvis and posture of the hindlimbs in Plateosaurus. *Paläontologische Zeitschrift* **70**: 591-601.
- Christian, A., Preuschoft, H., 1996. Deducing the body posture of extinct large vertebrates from the shape of the vertebral column. *Palaeontology* **39**: 801-812.
- Claessens, L.P., O'Connor, P.M., Unwin, D.M., 2009. Respiratory evolution facilitated the origin of pterosaur flight and aerial gigantism. *PLoS One* **4**: e4497.
- Cobley, M.J., Rayfield, E.J., Barrett, P.M., 2013. Inter-vertebral flexibility of the ostrich neck: implications for estimating sauropod neck flexibility. *PLoS One* **8**: e72187.
- du Toit, J.T., 1990. Feeding-height stratification among African browsing ruminants. *Africa Journal of Ecology* **28**: 55-61.
- Dzemski, G., 2006. Funktionsmorphologische Analysen langer Hälse bei rezenten terrestrischen Wirbeltieren zur Rekonstruktion der Stellung und Beweglichkeit langer Hälse prähistorischer Tiere. Dissertation, Universität Flensburg, Flensburg, 155 pp.

- Dzemeski, G., Christian, A., 2007. Flexibility along the neck of the ostrich (*Struthio camelus*) and consequences for the reconstruction of dinosaurs with extreme neck length. *Journal of Morphology* **268**: 701-714.
- Fastovsky, D.E., 2000. Dinosaur architectural adaptations for a gymnosperm-dominated world, in: Gastaldo, R.A., DiMichele, W.A. (Eds.), *Phanerozoic Terrestrial Ecosystems*. Paleontological Society Papers, pp. 183-207.
- Fastovsky, D.E., Smith, J.B., 2004. Dinosaur Paleocology, in: Weishampel, D.B., Dodson, P., Osmólska, H. (Eds.), *The Dinosauria*. University of California Press, Berkeley, pp. 614-626.
- Fechner, R., 2009. Morphofunctional evolution of the pelvic girdle and hindlimb of Dinosauromorpha on the lineage to Sauropoda. Dissertation, Ludwig-Maximilians-Universität München, Fakultät für Geowissenschaften, Munich, 197 pp.
- Foote, M., 1993. Contributions of individual taxa to overall morphological disparity. *Paleobiology* **19**: 403-419.
- Frey, E., 1988. Das Tragsystem der Krokodile - eine biomechanische und phylogenetische Analyse. *Stuttgarter Beiträge zur Naturkunde Serie A* **426**: 1-60.
- Galton, P.M., 1985. Diet of prosauropod dinosaurs from the late Triassic and early Jurassic. *Lethaia* **18**: 105-123.
- Galton, P.M., Upchurch, P., 2004. Prosauropoda, in: Weishampel, D.B., Dodson, P., Osmólska, H. (Eds.), *The Dinosauria*. University of California Press, Berkeley, California, pp. 232-258.
- Gans, C., 1969. Comments on inertial feeding. *Copeia* **4**: 855-857.
- Gatesy, S.M., 1991. Hind limb movements of the American alligator (*Alligator mississippiensis*) and postural grades. *Journal of Zoology* **224**: 577-588.
- Gatesy, S.M., 2002. Locomotor Evolution in the Line to Modern Birds, in: Chiappe, L.M., Witmer, L.M. (Eds.), *Mesozoic Birds: above the heads of dinosaurs*. University of California Press, Berkeley, pp. 432-447.
- Gatesy, S.M., Dial, K.P., 1996. Locomotor modules and the evolution of avian flight. *Evolution* **50**: 331-340.
- Graf, W., de Waele, C., Vidal, P.P., 1995. Functional anatomy of the head-neck movement system of quadrupedal and bipedal mammals. *Journal of Anatomy* **186**: 55-74.
- Gunga, H.-C., Suthau, T., Bellmann, A., Friedrich, A., Schwanebeck, T., Stoinski, S., Trippel, T., Kirsch, K., Hellwich, O., 2007. Body mass estimations for *Plateosaurus engelhardti* using laser scanning and 3D reconstruction methods. *Naturwissenschaften* **94**: 623-630.
- Huene, F.v., 1926. Vollständige Osteologie eines Plateosauriden aus dem schwäbischen Keuper. *Geologische und Paläontologische Abhandlungen* **15**: 1-43.
- Jackson, J.A., Bock, W.J., Olendorf, D., 2004. *Grzimek's Animal Life Encyclopedia*, Vol. 8 Birds I. Gale Group, Farmington Hills, MI, 571 pp.
- Koob, T.J., Long, J.H., Jr., 2000. The vertebrate body axis: evolution and mechanical function. *American Zoologist* **40**: 1-18.

- Kummer, B., 1959. Bauprinzipien des Säugerskeletes. Georg Thieme Verlag, Stuttgart, 235 pp.
- Langer, M.C., 2004. Basal Saurischia, in: Weishampel, D.B., Dodson, P., Osmólska, H. (Eds.), *The Dinosauria*. University of California Press, Berkeley, California, pp. 25-46.
- Mallison, H., 2010a. The digital Plateosaurus I: body mass, mass distribution and posture assessed using CAD and CAE on a digitally mounted complete skeleton. *Palaeontologia Electronica* **13**: 1-26.
- Mallison, H., 2010b. The digital Plateosaurus II: An assessment of the range of motion of the limbs and vertebral column and of previous reconstructions using a digital skeletal mount. *Acta Palaeontologica Polonica* **55**: 433-458.
- Martin, J., 1987. Mobility and feeding of Cetiosaurus (Saurischia, Sauropoda) - why the long neck?, in: Currie, P.J., Koster, E.H. (Eds.), *Fourth Symposium on Mesozoic Terrestrial Ecosystems. Short Papers, Occasional Papers of the Royal Tyrrell Museum of Paleontology*, pp. 154-159.
- Mazzetta, G.V., Christiansen, P., Fariña, R.A., 2004. Giants and Bizarres: Body Size of Some Southern South American Cretaceous Dinosaurs. *Historical Biology* **16**: 71-83.
- Moser, M., 2003. Plateosaurus engelhardti MEYER, 1837 (Dinosauria: Sauropodomorpha) aus dem Feuerletten (Mittelkeuper; Obertrias) von Bayern. *Zitteliana* **B 24**: 3-186.
- Murphy, J.B., Schlager, N., 2004. Grzimek's Animal Life Encyclopedia, Vol. 7 Reptiles. Gale Group, Farmington Hills, MI, 571 pp.
- Nickel, R., Schummer, A., Seiferle, E., 1968. Lehrbuch der Anatomie der Haustiere. P. Parey, Berlin, 502 pp.
- O'Higgins, P., Jones, N., 2006. Morphologica<sup>2</sup> (2.5). Hull York Medical School. Available from <http://sites.google.com/site/hymsfme/downloadmorphologica>.
- Preuschoft, H., Hohn, B., Stoinski, S., Witzel, U., 2011. Why so huge? Biomechanical reasons for the acquisition of large size in sauropod and theropod dinosaurs, in: Klein, N., Remes, K., Gee, C.T., Sander, P.M. (Eds.), *Biology of the Sauropod Dinosaurs. Understanding the Life of Giants*. Indiana University Press, Bloomington, pp. 179-218.
- Rauhut, O.W.M., 2003. The interrelationships and evolution of basal theropod dinosaurs, *Interrelationships and Evolution of Basal Theropod Dinosaurs*. Palaeontological Association, Aberystwyth, pp. 1-213.
- Rauhut, O.W.M., Fechner, R., Remes, K., Reis, K., 2011. How to get big in the Mesozoic: the evolution of the sauropodomorph body plan, in: Klein, N., Remes, K., Gee, C.T., Sander, P.M. (Eds.), *Biology of the Sauropod Dinosaurs: Understanding the Life of Giants*. Indiana University Press, Bloomington, pp. 119-149.
- Reilly, S.M., Elias, J.A., 1998. Locomotion in Alligator mississippiensis: kinematic effects of speed and posture and their relevance to their sprawling-to-erect paradigm. *The Journal of Experimental Biology* **201**: 2559-2574.
- Remes, K., 2008. Evolution of the pectoral girdle and forelimb in Sauropodomorpha (Dinosauria, Saurischia): osteology, myology and function. Dissertation, Ludwig-Maximilians-Universität München, Fakultät für Geowissenschaften, Munich, 355 pp.

- Rockwell, H., Evans, F.G., Pheasant, H.C., 1938. The comparative morphology of the vertebrate spinal column. Its form as related to function. *Journal of Morphology* **63**: 87-117.
- Romer, A.S., 1976. *Osteology of the Reptiles*. The University of Chicago Press, Chicago, 772 pp.
- Salisbury, S., Frey, E., 2000. A biomechanical transformation model for the evolution of semi-spheroidal articulations between adjoining vertebral bodies in crocodylians, in: Grigg, G.C., Seebacher, F., Franklin, C.E. (Eds.), *Crocodylian Biology and Evolution*. Surrey Beatty & Sons, Chipping Norton, pp. 85-134.
- Sander, P.M., Christian, A., Clauss, M., Fechner, R., Gee, C.T., Griebeler, E.-M., Gunga, H.-C., Hummel, J., Mallison, H., Perry, S.F., Preuschoft, H., Rauhut, O.W.M., Remes, K., Tütken, T., Wings, O., Witzel, U., 2011. Biology of the sauropod dinosaurs: the evolution of gigantism. *Biological Reviews* **86**: 117-155.
- Sander, P.M., Klein, N., 2005. Developmental plasticity in the life history of a prosauropod dinosaur. *Science* **310**: 1800-1802.
- Schwenk, K., 2000. *Feeding. Form, function and evolution in tetrapod vertebrates*. Academic Press, New York, 537 pp.
- Seebacher, F., Elsworth, P.G., Franklin, C.E., 2003. Ontogenetic changes of swimming kinematics in a semi-aquatic reptile (*Crocodylus porosus*). *Australian Journal of Zoology* **51**: 15-24.
- Seidel, M., R., 1978. The somatic musculature of the cervical and occipital regions of *Alligator mississippiensis*. Dissertation, The City University of New York, Graduate Faculty in Biology, New York, 327 pp.
- Shiple, L.A., Spalinger, D.E., Gross, J.E., Thompson Hobbs, N., Wunder, B.A., 1996. The dynamics and scaling of foraging velocity and encounter rate in mammalian herbivores. *Functional Ecology* **10**: 234-244.
- Sivers, W., 1934. Ein Beitrag zur Kenntnis des Vogelhalses. *Morphologische Jahrbücher* **74**: 697-728.
- Slijper, E.J., 1946. Comparative biologic-anatomical investigation on the vertebral column and spinal musculature of mammals. *Verhandelingen Der Koninklijke Nederlandse Akademie Van Wetenschappen, Afdeling Natuurkunde, Tweede Sectie* **42**: 1-128.
- Stevens, K.A., Parrish, J.M., 1999. Neck posture and feeding habits of two Jurassic sauropod dinosaurs. *Science* **284**: 798-800.
- Taylor, M.P., Wedel, M.J., Naish, D., 2009. Head and neck posture in sauropod dinosaurs inferred from extant animals. *Acta Palaeontologica Polonica* **54**: 213-220.
- Tsuihiji, T., 2004. The ligament system in the neck of *Rhea americana* and its implications for the bifurcated neural spines of sauropod dinosaurs. *Journal of Vertebrate Paleontology* **24**: 165-172.
- van der Leeuw, A., H., J., Bout, R.G., Zweers, G.A., 2001. Evolutionary morphology of the neck system in ratites, fowl and waterfowl. *Netherlands Journal of Zoology* **51**: 243-262.
- Vidal, P.P., Graf, W., Berthoz, A., 1986. The orientation of the cervical vertebral column in unrestrained awake animals. I. Resting position. *Experimental Brain Research* **61**: 549-559.

Virchow, H.J.P., 1914. Mechanik der Wirbelsäule des *Varanus varius*. *Archiv für Pathologische Anatomie und Physiologie* **1914**: 69-89.

Wagner, W.M., 2002. Bildgebende Verfahren beim Strauß (*Struthio camelus*). Dissertation, Universität von Pretoria In Onderstepoort, Companion Animal Clinical Studies, Freie Universität Berlin, 69 pp.

Wainwright, S.A., 1988. Axis and Circumference. The cylindrical shape of plants and animals. Harvard University Press, Cambridge, 132 pp.

Wainwright, S.A., 2000. The animal axis. *American Zoologist* **40**: 19-27.

Wiley, D.F., 2005. Landmark (3.0). Institute for Data Analysis and Visualization (IDAV), University of California, Davis. Available from <http://graphics.idav.ucdavis.edu/research/projects/EvoMorph>.

Wilson, J.A., 1999. A nomenclature for vertebral laminae in sauropods and other saurischian dinosaurs. *Journal of Vertebrate Paleontology* **19**: 639-653.

Zelditch, M.L., Swiderski, D.L., Sheets, H.D., Fink, W.L., 2004. Geometric morphometrics for biologists: A primer. Elsevier Academic Press, New York, 443 pp.

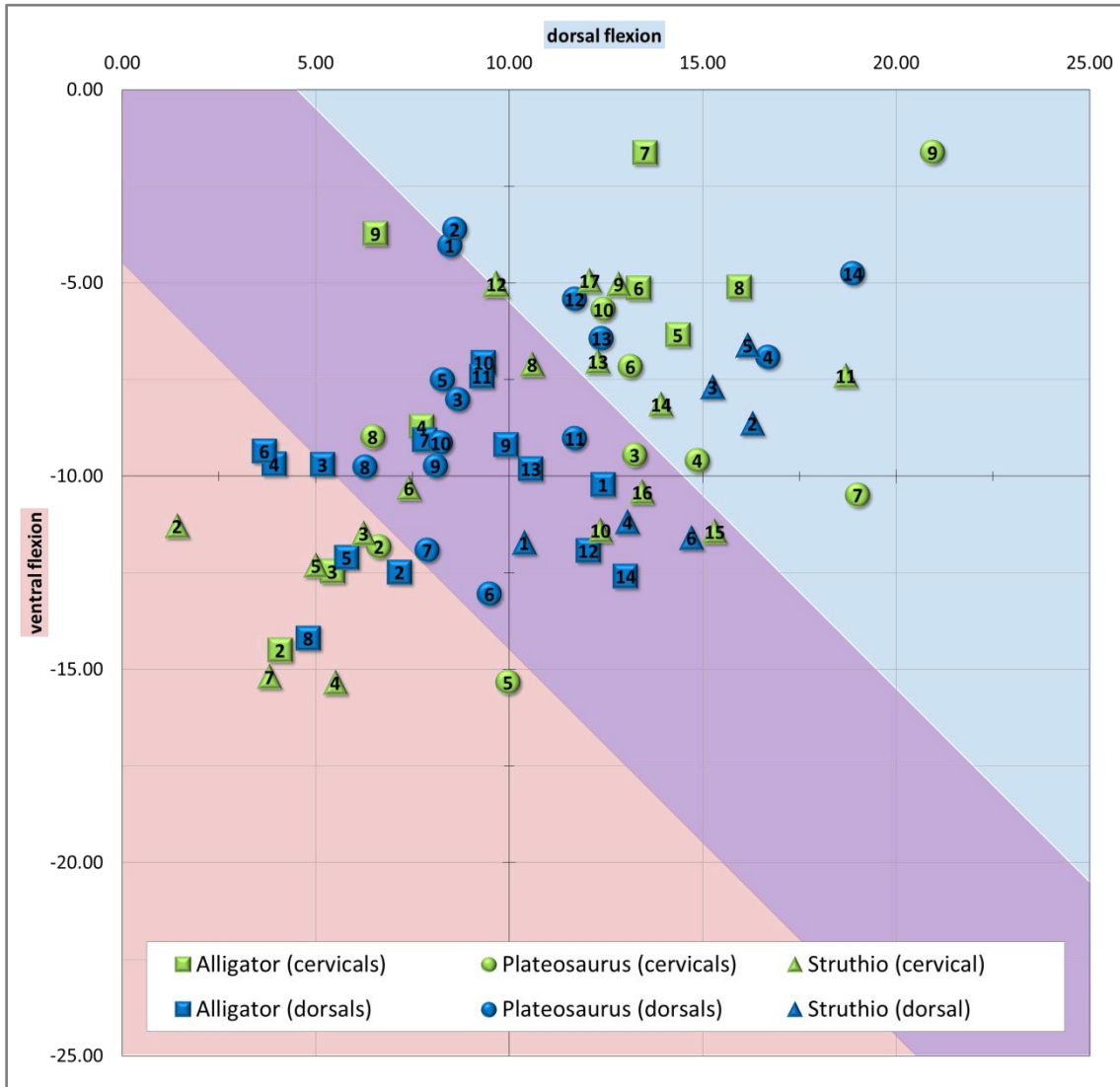
## Acknowledgements

We thank Britta Möllenkamp, Dr. Henriette Obermaier and Prof. Dr. Joris Peters of the Institut für Paläoanatomie, Domestikationsforschung und Geschichte der Tiermedizin at the Ludwig-Maximilians-Universität München (Germany) and the Staatssammlung für Anthropologie und Paläoanatomie München (Germany) for providing specimens of recent archosaurs, the Paläontologische Sammlung of the Eberhard Karls Universität Tübingen (Germany) for loan of *Plateosaurus* material and the Staatliches Museum für Naturkunde Stuttgart (Germany) for access to dinosaur specimens. Heiner Mallison (Museum für Naturkunde Berlin, Germany) kindly provided the 3D models of the dorsal vertebrae D14 and D15 of *Plateosaurus*. Jesus Marugán-Lobón (Universidad Autónoma de Madrid, Spain) is thanked for the introduction to geometric morphometrics. The manuscript has greatly benefitted from critical and helpful review by Mathew J. Wedel (Western University of Health Sciences California, USA). We acknowledge all current members of the Mesozoic Vertebrates Research Group in Munich (Germany) for discussion.

CB was supported by a doctoral fellowship of the Studienstiftung des deutschen Volkes (German National Academic Foundation) and the mentoring programme within the framework of LMUexcellent of the Ludwig-Maximilians-Universität München (Germany). This project was supported by the Deutsche Forschungsgemeinschaft (DFG, German Research Foundation) through its Research Unit 533 project E4 of OWMR and KR.

## Appendix

**Appendix 2.1.: Flexibility plot of the presacral vertebrae in extant and extinct archosaurs.** There are vertebrae that are prevalently flexible in dorsal direction (blue surface) or in ventral direction (red surface). Equally flexible vertebrae ( $x = y$ ) are indicated by the purple section (including 95% confidence limits).



## Chapter 3

### New insights into the vertebral *Hox* code of archosaurs

#### Abstract

---

Variation in axial formulae is an important feature in the evolution of vertebrates. Vertebrae at different axial positions exhibit a region-specific morphology. Key determinants for the establishment of particular vertebral shapes are the highly conserved *Hox* genes. Here, we have analysed *Hox* gene expression patterns in the Nile crocodile (*Crocodylus niloticus*) in order to complement and extend a previous examination of the alligator (*Alligator mississippiensis*) *Hox* code. We determined the expression of *HoxA-4*, *C-5*, *B-7* and *B-8*, which all revealed a crocodile-specific pattern. *HoxA-4* and *HoxC-5* characterise cervical morphologies and the latter indicates additionally the axial level of the forelimbs. *HoxB-7* and *HoxB-8* map exclusively to the dorsal vertebral region. The resulting expression patterns of these two *Hox* genes is the first description of their exact activity in the archosaurian embryo. The comparative analysis of the *Hox* code in several amniote taxa provides new evidence that evolutionary differences in the axial skeleton correspond with changes in *Hox* gene expression domains. We detect two general processes: 1) expansion and condensation, as well as 2) a shift of genetic activity corresponding to different vertebral counts. The ancestral archosaur *Hox* code was less complex and thus, may have resembled that of the crocodile. In association with the evolution of morphological traits, it may have been modified to more strongly differentiated patterns in birds and mammals.

---

### 3.1. Introduction

The axial skeleton (vertebrae and ribs) shows a striking diversity of morphology and number in extant and extinct amniotes, the clade that includes archosaurs (crocodiles, birds, dinosaurs) and mammals. It plays an essential role in body support, feeding behaviour and locomotion (see chapter 2), and it is also part of the breathing system in vertebrates. Thus, vertebral morphology and number strongly impact the physiology and ecology of animals. Axial morphology varies from the extremely heavily built vertebrae and ribs in some marine reptiles and mammals as buoyancy control (e.g. Houssaye 2009 and references therein) to the extreme lightweight construction of the vertebrae in flying birds or gigantic sauropod dinosaurs (e.g. O'Connor 2006 and references therein).

Despite these profound differences, the basic body plan of amniotes, a regionalised anteroposterior body axis, is quite conservative (Burke and Nowicki 2001). Likewise, the embryonic developmental

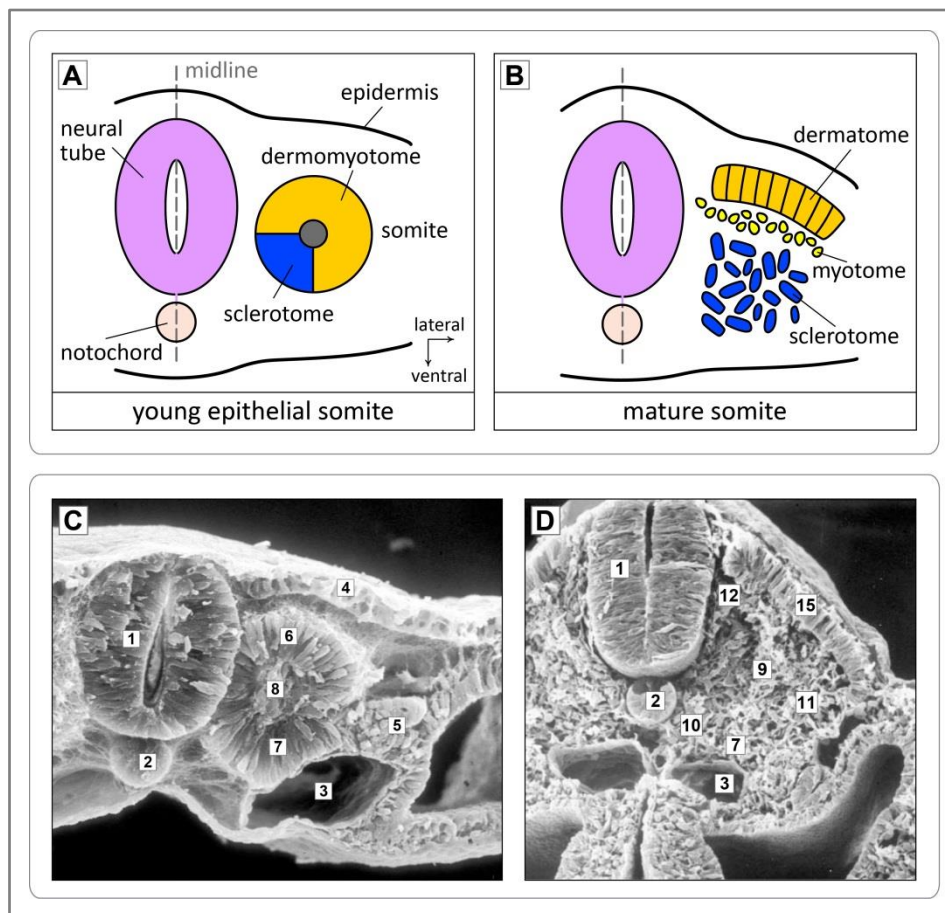


**Figure 3.1.: Somite differentiation in a vertebrate embryo.** (A) and (B) schematically illustrate the differentiation of a somite. The ventral part of the somite forms the sclerotome which will give rise to the vertebrae. The dorsal part of the somite forms the dermomyotome which differentiates into the dermatome (dermis) and the myotome (muscles). The scanning electron micrographs at the bottom (modified after Christ et al. 2004) show transverse fractures of (C) an early epithelial somite and (D) a matured somite in a chicken embryo. Abbreviations: 1 = neural tube, 2 = notochord, 3 = aorta, 4 = surface ectoderm, 5 = Wolffian duct, 6 = dorsal somite half, 7 = ventral somite half, 8 = somitocoel cells, 9 = central sclerotome, 10 = ventral sclerotome, 11 = lateral sclerotome, 12 = dorsal sclerotome, 15 = dermomyotome.

mechanisms are strongly conserved and the associated genetic patterns share an ancient structural blueprint (Gellon and McGinnis 1998, Mallo et al. 2010, Peter and Davidson 2011, Richardson et al. 1998). Early in the developing vertebrate embryo, segmentation is initiated through the formation of transient, serially homologous somites along the anteroposterior body axis (Burke and Nowicki 2001, Christ et al. 2007, Imura and Pourquie 2007, Saga and Takeda 2001). Each somite contains cells that contribute to the major axial structures: sclerotome cells give rise to the bone and cartilage of the vertebrae and ribs, myotome cells form the skeletal muscles and dermatome give rise to the dermis (Burke and Nowicki 2001, Christ et al. 2007, Wolpert et al. 2007) (Figure 3.1.). Depending on their axial level, the sclerotome cells from adjacent somites will differentiate into morphologically distinct vertebrae (Christ et al. 2007, Gomez and Pourquie 2009, Imura and Pourquie 2007, Pourquie 2003) (Figure 3.2. A). The *Hox* genes, a subset of homeobox-containing genes, are key determinants for the establishment of the positional identity of somites (Carroll 1995, Kessel and Gruss 1990, Liang et al. 2011, McGinnis and Krumlauf 1992). These highly conserved genes, like their homologues in invertebrates, encode developmentally active transcription factors that regulate the expression of numerous downstream genes involved in pattern formation of the body plan of the animal (Foronda et al. 2009, Kessel and Gruss 1990). The activity of *Hox* genes follows a spatiotemporal order, which reflects their arrangement along the chromosome (spatial and temporal colinearity) (Duboule and Dolle 1989, Kessel and Gruss 1990). Their expression is anteriorly distinct with mainly diffuse posterior boundaries, and negatively regulated by *Hox* genes posterior to them (posterior prevalence) (Duboule and Dolle 1989) (Figure 3.2. B).

In vertebrates, there are 13 paralog groups arranged in 4 clusters (named A, B, C, D) (Burke et al. 1995) (Figure 3.2. C). The same 39 *Hox* genes have been described in crocodiles, birds and placental mammals (Liang et al. 2011). Generally, *Hox* genes of the paralog groups 4 to 9 are expressed within the presacral region of the axial column in all tetrapods, irrespective of the vertebral formula. The variation in the vertebral count between taxa corresponds to changes in the pattern of *Hox* gene expression domains (Burke et al. 1995). It has been reported that specific anterior *Hox* gene expression boundaries are transposed in concert with morphological boundaries (Burke et al. 1995).

To date, the *Hox* gene expression pattern has been analysed in actinopterygian fish (Morin-Kensicki et al. 2002), placental mammals (Burke et al. 1995, Kessel and Gruss 1990), squamates (Burke et al. 1995, Cohn and Tickle 1999, Ohya et al. 2005, Woltering et al. 2009) and archosaurs (Burke et al. 1995, Mansfield and Abzhanov 2010). Apart from squamates, the archosaurian *Hox* code is by far the least completely known. This study complements and extends the previous analysis of the alligator *Hox* code (Mansfield and Abzhanov 2010), and by comparison with other amniotes we are able to discuss the evolution of the *Hox* gene expression patterns in archosaurs. In the following paragraphs,

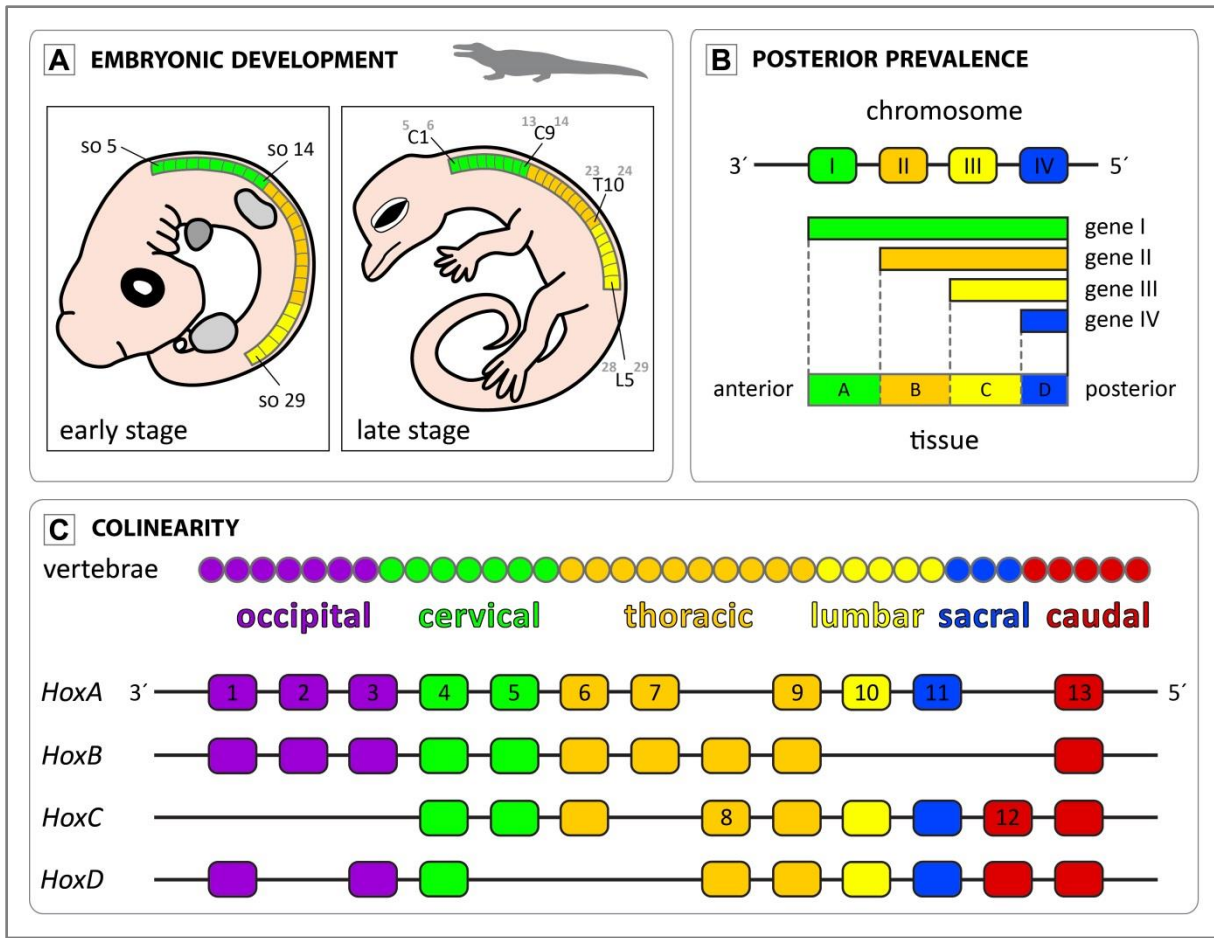


**Figure 3.2.: Axial development and *Hox* gene expression in vertebrates.** (A) The vertebrae of the axial skeleton develop from somites through resegmentation. In this way, two adjacent halves of the somites contribute to one vertebra. (B) The model illustrates how the gene expression pattern along a tissue specifies the distinct body regions A, B, C and D. The genes are expressed in overlapping domains with sharp anterior boundaries corresponding to their order on the chromosome. The posterior prevalence is defined as the hierarchical dominance of posterior over anterior gene function. (C) The 39 *Hox* genes in tetrapods are on four different chromosomes arranged in four clusters (*HoxA*, *B*, *C*, *D*). A key feature of the *Hox* genes is their spatial and temporal colinearity. The genes in each cluster are expressed in a temporal and spatial order that reflects their arrangement on the chromosome. The colour coding indicates how gene groups map to the axial regions.

the term amniote refers to crocodylian, chickens and mice, excluding squamates, because the genetic data for this group is too vague to be included within this project.

Here, we first compare the expression of *HoxB-4*, *C-4*, *D-4*, *A-5*, *C-6* and *C-8* previously analysed in the American alligator (Mansfield and Abzhanov 2010) with that in the Nile crocodile. To date, this is the only comparative analysis of *Hox* gene expression between two families (Crocodylidae and Alligatoridae) within one taxonomic order (Crocodylia). Second, with the newly determined expression patterns of the *HoxA-4*, *C-5*, *B-7* and *B-8* genes in the Nile crocodile we provide a more comprehensive view on the crocodylian *Hox* code. Furthermore, the resulting expression of *HoxB-7* and *HoxB-8* is the first description of the exact activity of these genes during archosaurian embryogenesis. Third, in order to test the hypothesis that the ancestral *Hox* code was initially less

complex or differentiated, we relate genetic data to axial body plan in the crocodile, chicken and mouse. Furthermore, this allows the reconstruction of the ancestral state of *Hox* gene expression. The requirement of *Hox* gene activity for proper organisation of the vertebrate body plan indicates its crucial role for understanding the development and evolution of the vertebral column.

The goals of this study are to 1) detect the *Hox* gene expression pattern in the Nile crocodile (*Crocodylus niloticus*) via whole-mount *in situ* hybridisation experiments, 2) compare the crocodilian *Hox* code with known *Hox* gene expression patterns in chicken and mouse and 3) analyse the obtained genetic data with respect to the different axial body plans in order to gain new insights into the underlying processes of evolutionary changes in archosaurs.

## 3.2. Materials and methods

### 3.2.1. Embryo collection

A total of 76 embryos of *Crocodylus niloticus* were collected at “La Ferme aux Crocodiles” crocodile farm in Pierrelatte, France, in May 2011 (two clutches) and May 2012 (one clutch) (Table 3.1.). The crocodile embryos were harvested after 9-15 days of embryonic development. This corresponds to stages 9-13 according to Ferguson (1985). At these stages, the somites are developed within the presacral vertebral column (Ferguson 1985). The forelimb buds map to the somites 11-16 at the cervicothoracic transition (Ferguson 1985). The buds of the hindlimbs are at the level of somite 27-32 at the lumbosacral transition (Ferguson 1985). The somitic *Hox* gene expression boundaries are thought to be well established and stable during further development (Burke et al. 1995, Mansfield and Abzhanov 2010). The embryos were dissected in 1x PBS and fixed overnight in 4% paraformaldehyde in 1x PBS at 4°C on a rocking platform (Hargrave et al. 2006) (Table 3.2.). After rinsing in 1x PBS, they were dehydrated in a sequence of ethanol concentrations and stored in fresh 100% ethanol at -20°C until use (Hargrave et al. 2006).

Embryonic day (ED)	Number of embryos	Clutch	Date of collection
ED 9	5	#19	May 07, 2011
ED 10	6	#19	May 08, 2011
ED 11	6	#19	May 09, 2011
ED 12	9	#17	May 07, 2011
ED 13	7	#17	May 08, 2011
ED 14	34	#17; #13	May 09, 2011; May 15, 2013
ED 15	9	#13	May 16, 2012

**Table 3.1.: Overview of collected Nile crocodile embryos (catalogued with Institution-No. GW4889).** Three embryos at ED9, ED12 and ED15 were transferred into RNAlater RNA stabilisation reagent after harvesting. The remaining embryos were fixed overnight in 4% paraformaldehyde in 1x PBS at 4°C for subsequent whole-mount *in situ* hybridisation.

Working step	Number/Time	Temperature
Preparation of embryos in 1x PBS	-	-
Fixation of embryos with 4% PFA in 1xPBS	overnight	4°C
Wash in 1x PBS	1x 10 min	RT
Dehydrate by steps into 100% EtOH:		RT
- 75% 1x PBS/ 25% EtOH	1x 10 min	
- 50% 1x PBS/ 50% EtOH	1x 10 min	
- 25% 1x PBS/ 75% EtOH	1x 10 min	
- 100% EtOH	1x 10 min	
Store in fresh 100% EtOH	long-term (until use)	-20°C

**Table 3.2.: Protocol for collection, fixation and storage of embryos.** Abbreviations: PBS = phosphate buffered saline, PFA = paraformaldehyde, EtOH = ethanol, RT = room temperature.

### 3.2.2. RNA extraction and cDNA synthesis

For complementary DNA (cDNA) synthesis, three embryos at ED 9, ED12 and ED15 were transferred into *RNAlater* RNA stabilisation reagent (Quiagen) after harvesting (Table 3.1.). Total RNA was extracted using the RNeasy kit (Quiagen), according to the manufacturer's instructions. The RNA concentration was measured using a NanoDrop 1000 Spectrophotometer (Thermo Fisher Scientific). A sample of the isolated RNA was checked via agarose electrophoresis.

The single-stranded RNA was reverse transcribed into cDNA with anchored-oligo(dT)<sub>18</sub> primer applying the Transcriptor First Strand cDNA Synthesis Kit (Roche), according to the manufacturer's instructions.

### 3.2.3. Primer design, sequencing and riboprobe synthesis

*Hox* genes normally consist of two exons, with the conserved 180-bp homeobox located in exon 2 (Kessel and Gruss 1990, Liang et al. 2011, Ruddle et al. 1994). Degenerate primers were designed for the *Hox* genes analysed in this study, targeting the conserved 5' region of exon one and the homeobox (Table 3.3.). The intended PCR product size ranged between 400 and 900 bp.

The specific *Hox* gene fragments were amplified from cDNA by polymerase chain reaction (PCR) using 25 µL reaction volumes of GoTaq (Promega). PCR was performed, applying the following cycling parameters: an initial denaturation step at 95°C for 3 min, 35 cycles of 95°C for 30 s, 40°C for 30 s, 72°C for 1 min and a final extension step at 72°C for 5 min. PCR products were purified by standard ammonium acetate-ethanol precipitation and sequenced by applying the BigDye Terminator v3.1 Cycle Sequencing kit (Applied Biosystems). Sequencing was performed in both directions using the same specific *Hox* primers used for PCR. Sequencing reactions were precipitated with sodium acetate-ethanol. Subsequently, the samples were analysed on the ABI 3730 Genetic Analyzer

(Applied Biosystems) at the Sequencing Service of the Department of Biology at the Ludwig-Maximilians-Universität in Munich (Germany). Trace files were assembled in the bioinformatics software suite Geneious (Drummond et al. 2011). *Hox* gene identity of all obtained sequences was verified using NCBI BLAST (Johnson et al. 2008). The new sequences were aligned in Geneious with chicken and mouse sequences obtained from GenBank database.

After successful identification of the specific *Hox* genes in the Nile crocodile, further PCR reactions under the same conditions, except for a modified reverse primer, were performed for riboprobe synthesis (PCR-based riboprobe synthesis after David and Wedlich (2001)). For each *Hox* gene, the T3 RNA polymerase promoter sequence (5'-ATTAACCCTCACTAAAGGGA-3') was artificially introduced at the 5'-end of the gene-specific reverse primer to enable antisense transcripts. The PCR fragments were cleaned using the NucleoSpin kit (Machery-Nagel), and the resulting cDNA concentration was measured with a NanoDrop 1000 spectrophotometer. Subsequently, 20-400 ng of the purified template cDNA were used for *in vitro* transcription. Antisense riboprobes were transcribed *in vitro* using T3 RNA polymerase and digoxigenin (DIG) labelled UTP (Roche), according to the manufacturer's instructions. A sample of the labelled RNA was checked via agarose electrophoresis.

Before whole-mount *in situ* hybridisation, the concentration and the binding potential of the DIG-labelled riboprobes were tested via blot hybridisation in a vial. The applied protocol follows the

<i>Hox</i> gene	Fwd sequence (5'-3')	Rev sequence (5'-3')	Reference
<i>HoxA-4</i>	GYTCGTTTTGATAAACTCC	YTTRTGRTCYTTYTTCCAYTTCAT	This study
<i>HoxB-4</i>	TTTTTGATCAACTCCAATATGT	ATCCTCCTGTTCTGGAACC	Mansfield and Abzhanov (2010)
<i>HoxC-4</i>	ATGATCATGAGCTCGTATTTG	ACGGTTTTGGAACCAGATTTTG	Mansfield and Abzhanov (2010)
<i>HoxD-4</i>	ATGGCCATGAGTTCGTATATG	GTTCTGAAACCAGATCTTGATC	Mansfield and Abzhanov (2010)
<i>HoxA-5</i>	TTTTGTAAACTCATTTTGCG	ATRCTCATRCTTTTCAGC	This study
<i>HoxC-5</i>	GCAGAGCCCCAATATCCCTGCC	TTCATNCKNCKRTTYTGRAACCA	This study, Liang et al. (2011)
<i>HoxC-6</i>	GAATTCCTACTTCACTAACC	GAACCAGATTTTGATCTGYC	This study
<i>HoxB-7</i>	GCCGCAAGTTCGGTTTTTC	TTTCCACTTCATGCGCC	This study
<i>HoxB-8</i>	CCAAATACAAAACCGGGG	CTGCTGGGAAACTGTCT	This study
<i>HoxC-8</i>	ATGAGTTCCTACTTTGTAAA	CTACCACTGCGCCTTCC	Mansfield and Abzhanov (2010)

**Table 3.3.: *Hox* gene-specific primers.** The forward (fwd) and reverse (rev) primers were used for amplification of the studied *Hox* genes in the Nile crocodile. The primers were designed based on aligned sequences of the specific *Hox* gene available for chicken and mouse (obtained from GenBank database).

procedures previously described by Farrell (2006), Chevalier et al. (1997) and Schwarzacher and Heslop-Harrison (2000). Each riboprobe was diluted to 1:10 and 1:100. For each riboprobe concentration, a sample of denatured cDNA was spotted on a nylon membrane (Table 3.4.). After crosslinking (in order to immobilise the cDNA on the membrane) with the UV Crosslinker BioLink (Biometra), each strip of the membrane contained a target cDNA to be hybridised to the labelled riboprobes. The samples were prehybridised in a vial and, subsequently, the riboprobes were added. The vials were incubated overnight at 65°C for hybridisation. The prehybridisation and the hybridisation buffer as well as the detection procedure correspond to the applied protocol for whole-mount *in situ* hybridisation (see section 3.2.4).

Working step	Number/Time	Temperature
Denature target cDNA:		
- add 0.1 volume of 1N NaOH	-	RT
- incubate	30 min	37°C
Neutralize the alkaline pH:		
add 10 volumes of ice-cold 6x SSC (pH 7)	-	on ice
Cut the membrane		
and prewet in 6x SSC (pH 7)	for each riboprobe dilution few seconds	RT RT
Spot 1 µL (2-5 µg) of denatured cDNA on membrane	for each riboprobe dilution	RT
Immobilise via UV crosslinking	254 nm, 0.5-5 min	-
Prehybridise each strip in a vial	1-5 h	65°C
Hybridisation (riboprobe and hybridisation buffer)	Overnight	65°C

**Table 3.4.: Blot hybridisation in a vial.** The labelling efficiency of the DIG-labelled riboprobes were tested via blot hybridisation in a vial. With some modifications, the protocol is based on the procedure described by Farrell (2006). Refer to section 3.2.4 for a detailed description of the prehybridisation and hybridisation step and the detection of the hybridisation. Abbreviations: NaOH = sodium hydroxide, SSC = saline sodium citrate buffer, RT = room temperature.

### 3.2.4. *In situ* hybridisation

*In situ* hybridisation is a general method with which to determine accurate spatial and temporal gene expression in tissues and whole animals. In order to interpret the genetic pattern in three dimensions, the somitic expression of *HoxB-4*, *C-4*, *D-4*, *A-5*, *C-6* and *C-8* was detected via whole-mount *in situ* hybridisation. The applied protocol is based on the procedures described by Hargrave et al. (2006), Schwarzacher and Heslop-Harrison (2000) and Wilkinson (1999), with some modifications (Table 3.5.). Embryos stored in 100% ethanol were rehydrated, washed and prehybridised. After prehybridisation, DIG-labelled riboprobes were added. The samples were incubated overnight at 60°C. Subsequently, the embryos were stained using anti DIG-fragments coupled to alkaline phosphatase (AP). After washing the colour substrates, 4-nitrobluetetrazolium

Working step	Number/Time	Temperature
<b>Day 1</b>		
Rehydrate by steps into 100% PBS:		RT
- 75% EtOH/ 25% 1x PBS	1x 5 min	
- 50% EtOH / 50% 1x PBS	1x 5 min	
- 25% EtOH / 75% 1x PBS	1x 5 min	
- 100% 1x PBS	1x 5 min	
Washes in 1xPBS.	3x 5 min	RT
Permeabilisation with 1 µg/mL proteinase K in 1x PBS	25 min	37°C
Incubate in DEPC 1x PBS	2x 5 min	RT
Refixation in 4% PFA in 1x PBS	30 min	RT
Washes in DEPC 1x PBS	3x 15 min	RT
Equilibrate in 6x SSC (pH 7)	15 min	RT
Prehybridisation	2-6 h	60°C
Hybridisation (riboprobe and hybridisation buffer)	Overnight	60°C
<b>Day 2</b>		
Incubate in prehybridisation buffer from previous step	10 min	60°C
Washes in 2x SSC (pH 7)	3x 20 min	RT
Washes in 2x SSC (pH 7)	3x 20 min	60°C
Washes in preheated 0.1x SSC (pH 7)	2x 30 min	60°C
Washes in MAB	2x 10 min	RT
Wash in MAB 2% blocking reagent	1-2 h	RT
Wash in diluted antibody (anti-DIG antibody in MAB 2% blocking reagent; 1:5000)	Overnight	4°C
<b>Day 3</b>		
Washes in MAB	3x 1h	RT
Incubate 1x Mg-free AP buffer	2x 5 min	RT
Incubate in AP buffer	2x 5 min	RT
Incubate in colour substrate solution (4.4 µL NBT and 3.3 µL BCIP per mL AP buffer)	(in dark!)	4°C
Stop reaction by		
- washes in MAB	2x 5 min	RT
- washes in 1x PBS	2x 5 min	RT
Postfixation in 4% PFA in 1x PBS	1-2 h or overnight	RT or 4°C
Washes in 1x PBS	5x 5min	RT

**Table 3.5.: Whole-mount *in situ* hybridisation.** With some modifications the applied protocol is based on the procedure described by Hargrave et al. (2006). Abbreviations: PBS = phosphate buffered saline, EtOH = ethanol, RT = room temperature, DEPC = diethyl pyrocarbonate, PFA = paraformaldehyde, SSC = saline sodium citrate buffer, MAB = maleic acid buffer, Mg = magnesium, AP buffer = alkaline phosphatase buffer, NBT = 4-nitrobluetetrazolium chloride, BCIP = 5-bromo-4-chloro-3-indoyl-phosphate.

chloride (NBT) and 5-bromo-4-chloro-3-indoyl-phosphate (BCIP) were used to detect the hybridisation patterns.

The same protocol was also used for section *in situ* hybridisation. Although postembedding *in situ* hybridisation on LR white sections was successful (as previously described by Gros and Maurin 2008, Mandry et al. 1993, or Osamura et al. 2000), the hybridisation signal was too weak to be clearly identified, probably because much of the embryonic RNA was lost during the cutting procedure (see section 3.2.5).

After whole-mount *in situ* hybridisation, the embryos were dehydrated in a sequence of ethanol concentrations and stored in fresh 100% ethanol. Photographs were taken immediately after hybridisation with the M165 FC microscope (Leica). Finally, the stained embryos were prepared for sectioning.

### 3.2.5. Sectioning

The general parts of the following sectioning procedure are 1) dehydration, 2) infiltration, 3) polymerisation and 4) cutting and mounting. The dehydrated embryos were transferred to specific tubes and gradually embedded in LR white (a polyhydroxy-aromatic acrylic resin that is hydrophilic after polymerisation). For polymerisation, the capsules were put in an incubator at 40°C for 2 hours followed by 60°C for up to 18 hours. The polymerised blocks were cut with the saw microtome SP1600 (Leica). Some samples were embedded in methyl methacrylate and sectioned with a rotation microtome HM 360 (Microm, Thermo Scientific) at the institute for veterinary pathology at the Ludwig-Maximilians-Universität in Munich (Germany).

## 3.3. Results

### 3.3.1. Sequence analysis

The comparison of the crocodile sequence data with previously published *Hox* gene sequences revealed a high degree of amino acid sequence conservation (about 60-80%) among the different species (Appendix 3.1. and Appendix 3.2.).

### 3.3.2. Histology and section analysis

Transverse sections of the Nile crocodile embryos revealed the segmentation of the anteroposterior body axis in somites (Figure 3.3.). As reported by Ferguson (1985), the forelimb buds map to the somites 11 - 16 at the cervicothoracic transition. In combination with somite counting, the limb bud was, thus, used as relative landmark for determining somite levels. Precise counting of somites can be difficult. However, the somite levels of *Hox* gene expression reported here were considered to be accurate, give or take one somite.

For the following *Hox* gene expression results, the positioning of the definitive anterior expression boundary is of decisive importance due to the hierarchical dominance of posterior over anterior *Hox* gene expression.

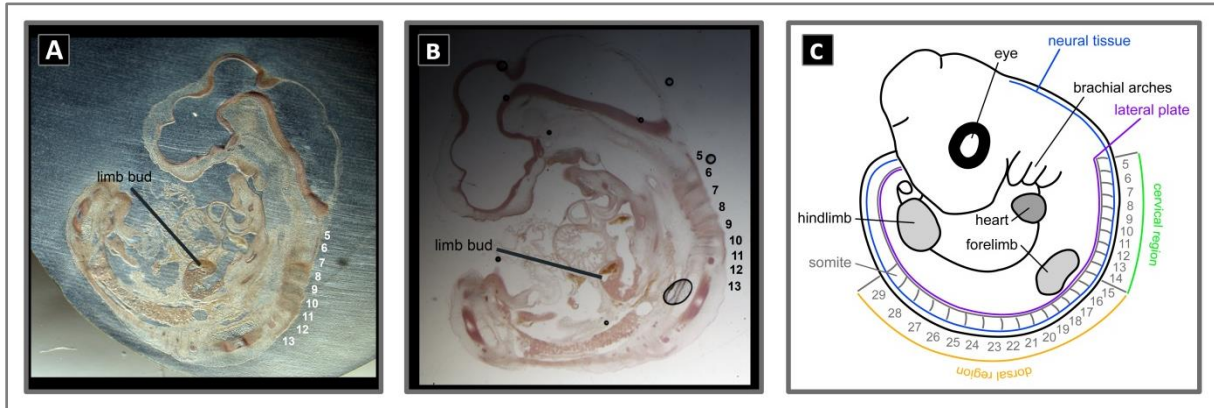


**Figure 3.3.: Nile crocodile embryo sections.** (A) and (B) Transverse sections of embryos in order to analyse the somites of the anteroposterior body axis and the forelimb bud as relative landmark for somitic level. (C) Schematic illustration of whole-mount embryo with somites along the cervical (green) and dorsal (orange) region.

### 3.3.3. *Hox* gene expression in archosaurs

The total number of presacral vertebrae, as well as the number of vertebrae within an axial region, varies significantly among amniotes (Figure 3.4.). The following description of the newly determined *Hox* gene expression pattern in the Nile crocodile and the comparison with the previously published *Hox* code in the chicken and the mouse (Table 3.6., Appendix 3.3.) reveals the spatial colinearity of *Hox* genes also in the crocodile. There is a correlation between the relative position of the *Hox* genes along the chromosome and the axial level of the vertebral column, in which they are expressed in amniotes. *Hox* genes that lie at the 3' end of the chromosome are expressed in the anterior region of the axial column, while the expression of the 5' genes is restricted to the posterior part of the

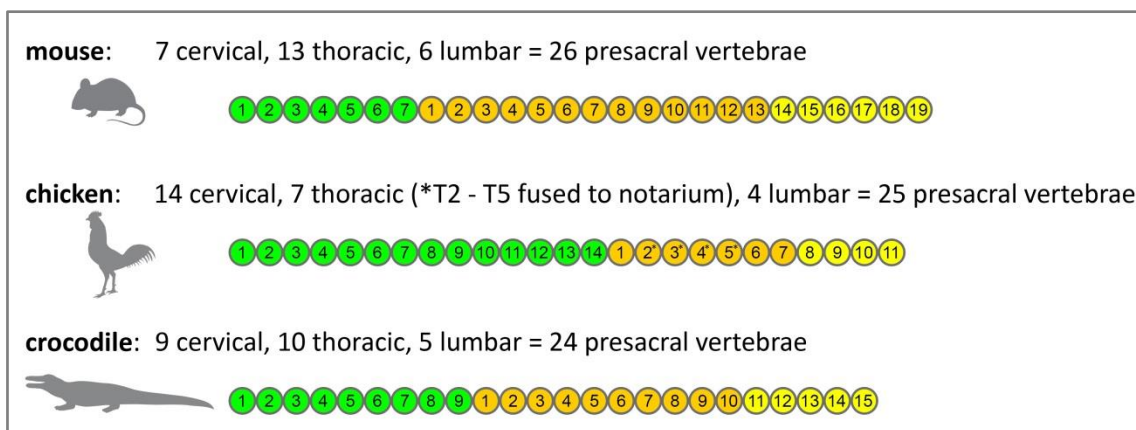


**Figure 3.4.: Vertebral formula in amniotes.** The total number of presacral vertebrae as well as the number of vertebrae within an axial region varies significantly among mouse, chicken and crocodile. Although commonly not applied to reptiles, it is possible to distinguish the dorsal series into 10 thoracic and 5 lumbar vertebrae in the crocodilian. Colour coding: green = cervical, orange = thoracic, yellow = lumbar.

primary body axis. The anterior expression limit of the *Hox* paralog groups 4-5 lie exclusively in the cervical region of crocodylians, chickens and mice. The expression of the *Hox* paralog groups 6-8 is detected only in the dorsal series of the vertebral column in these taxa.

<b>Hox cluster</b>	<b>Paralog group</b>	<b><i>C. niloticus</i></b>	<b><i>A. mississippiensis</i></b>	<b><i>G. gallus</i></b>	<b><i>M. musculus</i></b>
4	A	X	-	X	X
	B	X	X	X	X
	C	X	X	X	X
	D	X	X	X	X
5	A	X	X	X	X
	B	-	X	X	X
	C	X	-	X	X
6	A	-	not able to detect	X	X
	B	-	-	X	X
	C	X	X	X	X
7	A	-	X	X	X
	B	X	-	-	X
8	B	X	-	X	X
	C	X	X	X	X
	D	-	not able to detect	X	X

**Table 3.6.: Overview of expression data for analysed *Hox* genes.** The presence of the same 15 *Hox* genes (of paralog groups 4-8) have been described for crocodiles, birds and placental mammals (Liang et al. 2011). Expression analyses in the Nile crocodile (*Crocodylus niloticus*) were part of the present study. Expression data for the American alligator (*Alligator mississippiensis*) are from Mansfield and Abzhanov (2010). Data for the chicken (*Gallus gallus*) and for mouse (*Mus musculus*) have previously been published (Refer to Appendix 3.3. for detailed references). Abbreviations: X = data present, - = no data.

#### Paralog group 4

In the Nile crocodile, the anterior expression limits of *HoxB-4* and *HoxD-4* were both detected at C3 (so 7/8) (Figure 3.5.). This pattern is similar to that found in the American alligator (Mansfield and Abzhanov 2010) and in the chicken (Burke et al. 1995). In contrast, it has been shown that the anterior expression boundary of *HoxB-4* is at C2 (so 6/7), and *HoxD-4* expression starts at C1 (so 5/6) in the mouse (Burke et al. 1995, Gaunt et al. 1989).

*HoxA-4* is expressed in the middle and posterior part of the cervical column, starting at C5 (so 9/10) and extending to D3 (so 16/17) in the Nile crocodile (Figure 3.6. A - C). The anterior expression limit of *HoxC-4* is at C5 (so 9/10) in the crocodile as well (Figure 3.6. D - F). The latter *Hox* gene has also been analysed in the alligator, and revealed the same expression pattern (Mansfield and Abzhanov 2010). It has been reported previously that the anterior expression limit of *HoxA-4* in the chicken and

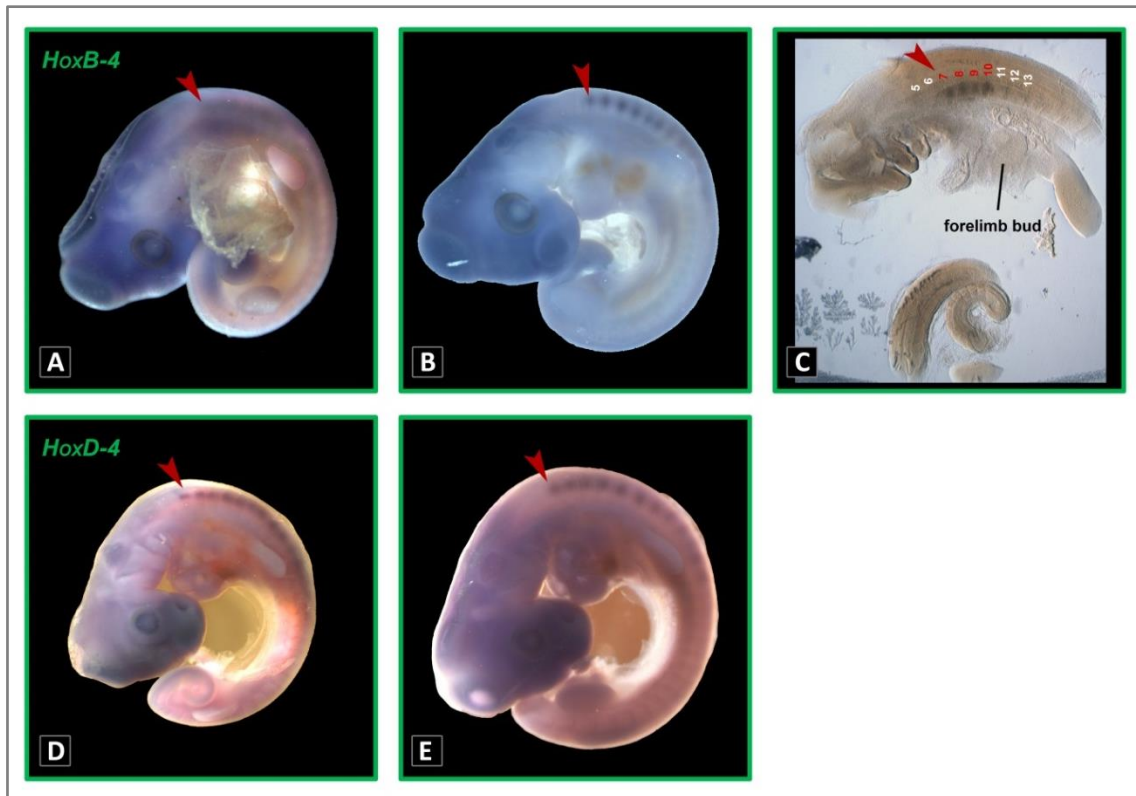


Figure 3.5.: Expression of *HoxB-4* and *HoxD-4* in the somites (so) of Nile crocodile embryos (ED 10-14). Arrowheads indicate the anterior expression boundary. (A-C) *HoxB-4* has an anterior limit at C3 (so 7/8) and extends to C6 (so 10/11). (D and E) *HoxD-4* expression starts at C3 (so 7/8) and fades out posteriorly at D1 (so 14/15).

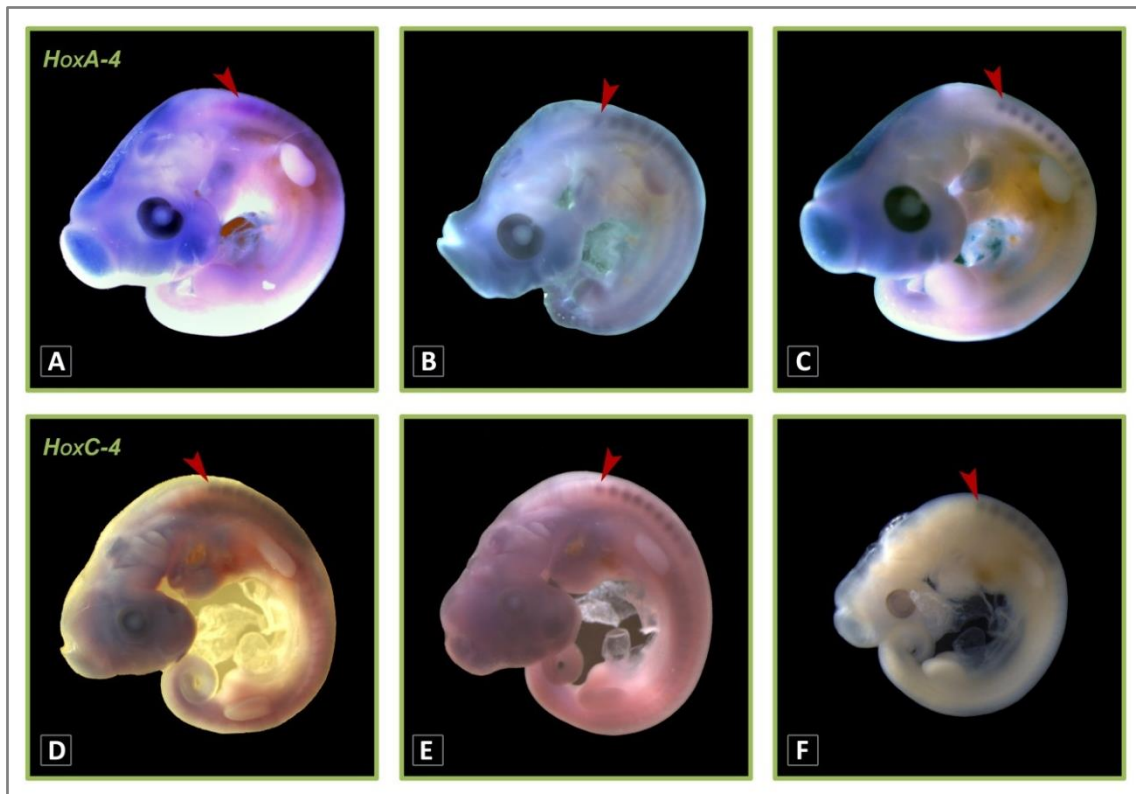


Figure 3.6.: Expression of *HoxA-4* and *HoxC-4* in the somites (so) of Nile crocodile embryos (ED 10-14). Arrowheads indicate the anterior expression boundary. (A-C) *HoxA-4* is expressed from C5 (so 9/10) to D3 (so 16/17). (D-F) *HoxC-4* has an anterior boundary at C5 (so 9/10) and extends to C9 (so 13/14).

the mouse is, for each, at a midcervical vertebra as well (Burke et al. 1995). *HoxA-4* was detected along the axial columns starting at C6 (so 10/11) in the bird and at C3 (so 7/8) in the mammal (Burke et al. 1995). *HoxA-4* shares the same anterior expression boundary with *HoxC-4* in the alligator, chicken and mouse.

#### Paralog group 5

Expression of *HoxC-5* maps near the end of the cervical series in crocodiles, chickens and mice. It starts at C8 (so 12/13) and fades out posteriorly at D1 (so 14/15) in the crocodile (Figure 3.7. A - C). The anterior expression limit of *HoxC-5* is at C13 (so 17/18) in the chicken and at C6 (so 10/11) in the mouse (Burke et al. 1995, Gaunt et al. 1990).

In the Nile crocodile, *HoxA-5* is expressed at the base of the neck, starting at C9 (so 13/14), and fades out posteriorly at D4 (so 17/18) (Figure 3.7. D - F). This is similar to the pattern observed in the alligator (Mansfield and Abzhanov 2010). In contrast, the anterior expression limit of *HoxA-5* has been detected at C8 (so 12/13) in the chicken and at C3 (so 7/8) in the mouse (Mansfield and Abzhanov 2010).

#### Paralog group 6

Expression of *HoxC-6* indicates the cervicothoracic transition. In the crocodile, this gene is expressed from D1 (so 14/15) to D9 (so 22/23) (Figure 3.8. A - C). The same anterior expression boundary has

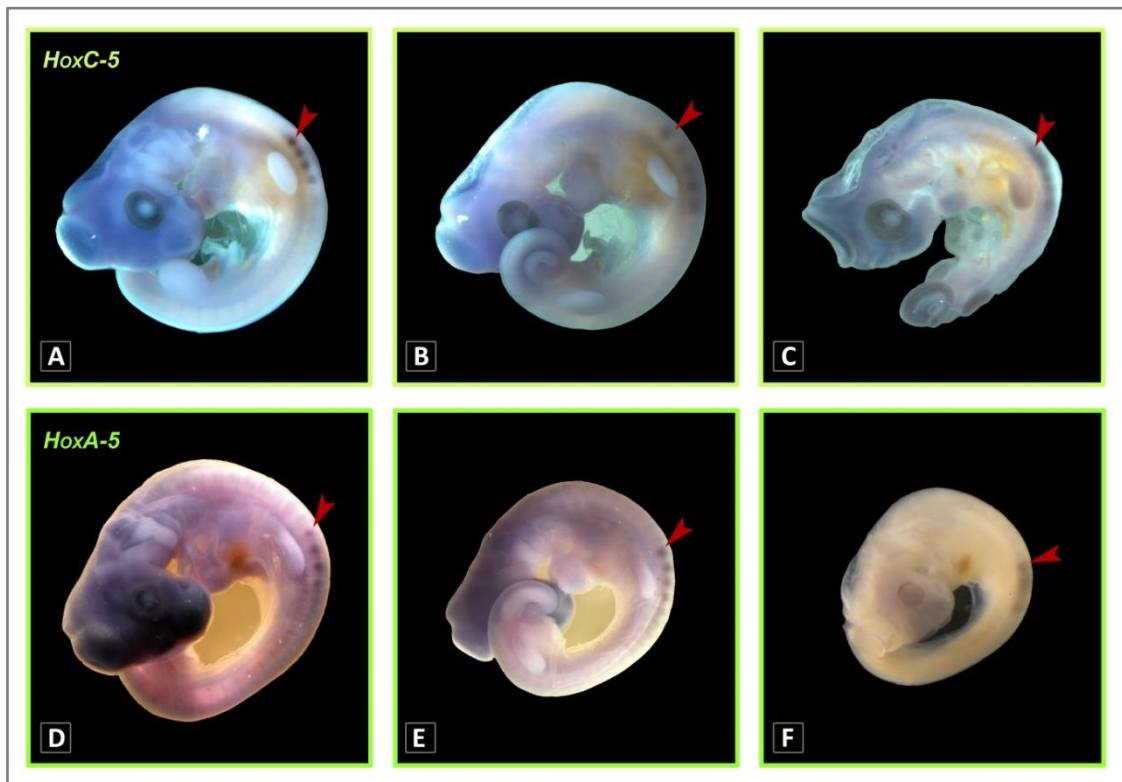


Figure 3.7.: Expression of *HoxC-5* and *HoxA-5* in the somites (so) of Nile crocodile embryos (ED 10-14). Arrowheads indicate the anterior expression boundary. (A-C) *HoxC-5* expression starts at C8 (so 12/13) and fades out posteriorly at D1 (so 14/15). (D-F) *HoxA-5* is expressed from C9 (so 13/14) to D4 (17/18).

been found in the alligator (Mansfield and Abzhanov 2010), the chicken and in the mouse (Burke et al. 1995).

#### Paralog group 7

*HoxB-7* is expressed in the dorsal region of the Nile crocodile (Figure 3.8. D - F). Its anterior expression limit is at D5 (so 18/19) and it continues to the hindlimbs at the posterior end of the trunk. To date, there is no information about the somitic expression pattern of *HoxB-7* in the chicken. In the mouse, the anterior expression boundary of *HoxB-7* is at D4 (so 15/16) (Burke et al. 1995).

#### Paralog group 8

In the Nile crocodile, the anterior expression limit of *HoxC-8* is at D1 (so 14/15) and it extends posteriorly to the end of the dorsal series (Figure 3.9. A - C). This is similar to the genetic pattern observed in the alligator (Mansfield and Abzhanov 2010). In the chicken, expression of *HoxC-8* starts at D5 (so 23/24) (Burke et al. 1995). In the mouse, the anterior expression boundary of *HoxC-8* is at D6 (so 17/18) (Burke et al. 1995).

Expression of *HoxB-8* maps exclusively to the dorsal series in several amniote taxa with varying vertebral count. *HoxB-8* is expressed in the middle and posterior part of the dorsal series, starting at D8 (so 21/22) in the Nile crocodile (Figure 3.9. D - F). In the chicken, expression of *HoxB-8* is strong in the midtrunk mesoderm, but no specific somite number could be assigned (Burke et al. 1995). Another study showed that *HoxB-8* is expressed in the dorsal series of mouse, starting at D3 (so 14/15) (van den Akker et al. 2001).

### **3.4. Discussion**

#### **3.4.1. Hox gene expression in archosaurs**

Genes provide a generative programme for embryonic development. In this study, the expression of *Hox* genes that specify the development of the vertebral column in the Nile crocodile has been analysed in order to investigate the relationship between *Hox* gene expression and vertebrate body plan (Figure 3.10.). The comparative analyses of *Hox* gene expression patterns along the presacral body axis (encompassing paralog groups 4-8) provide new insights into the archosaurian *Hox* code and reveal novel clues about the evolutionary relation of *Hox* gene expression to axial body plan.

The *in situ* hybridisation results confirmed that the same seven *Hox* genes of paralog groups 4 and 5 are expressed in the cervical region of crocodylians, as reported for chickens and mice (Burke et al. 1995, Gaunt et al. 1989). Furthermore, the present analysis showed that the expression of *Hox* paralog genes 6 to 8 is restricted to the dorsal region in crocodiles, as observed in chickens and mice.

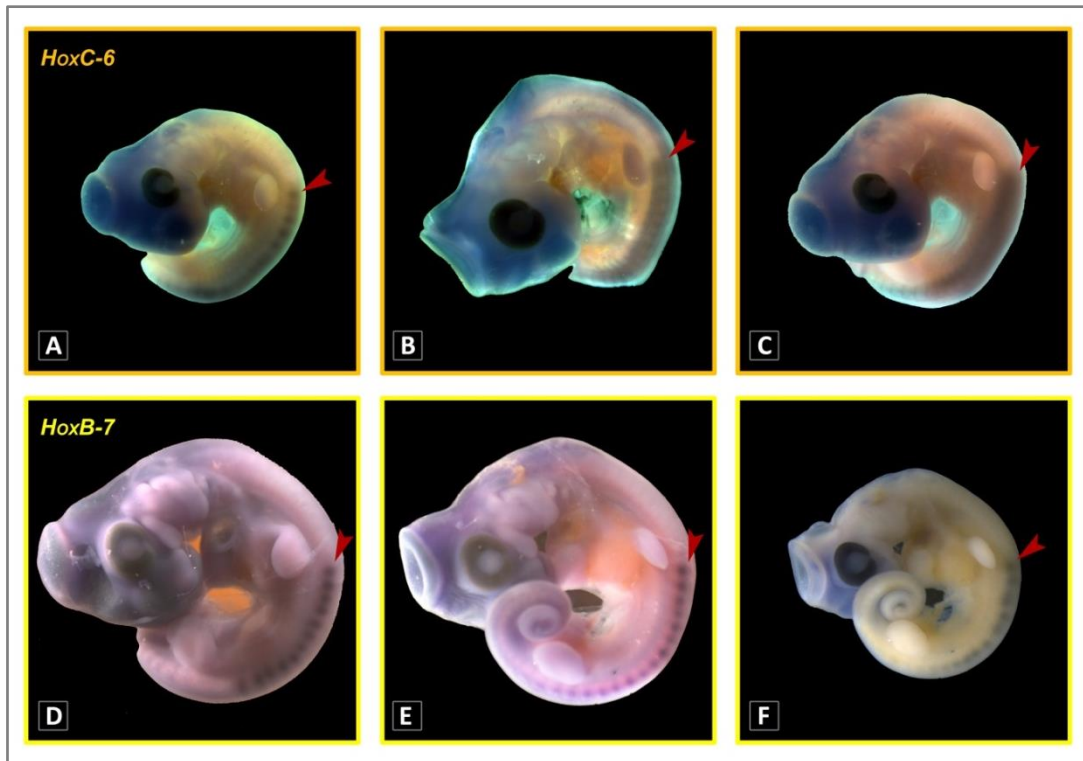


Figure 3.8.: Expression of *HoxC-6* and *HoxB-7* in the somites (so) of Nile crocodile embryos (ED 10-14). Arrowheads indicate the anterior expression boundary. (A-C) *HoxC-6* has an anterior limit at D1 (so 14/15) to D9 (so 22/23). (D-F) *HoxB-7* expression starts at D5 (so 18/19) and it continues to the hindlimbs at the posterior end of the trunk.

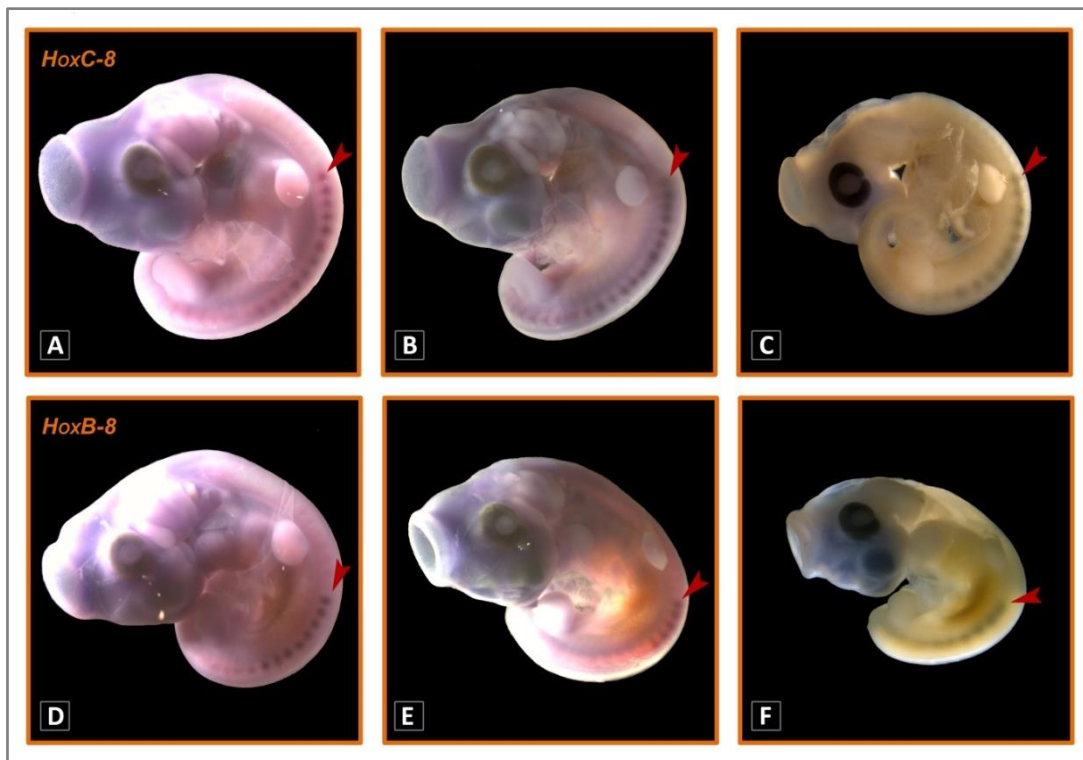


Figure 3.9.: Expression of *HoxC-8* and *HoxB-8* in the somites (so) of Nile crocodile embryos (ED 10-14). Arrowheads indicate the anterior expression boundary. (A-C) *HoxC-8* expression starts at D1 (so 14/15) and it extends posteriorly to the end of the dorsal series. (D-F) *HoxB-8* is expressed in the middle and posterior part of the dorsal series starting at D8 (so 21/22).

The comparison of the expression patterns of *HoxB-4*, *C-4*, *D-4*, *A-5*, *C-6* and *C-8* in the Nile crocodile with the previously published genetic pattern in the American alligator (Mansfield and Abzhanov 2010) revealed that there are no differences between the two families. Due to the strong correlation between *Hox* gene expression and vertebral formula (see chapter 4), it can be hypothesised that *Hox* genes maintain the same domains of expression within a taxonomic order that share the same vertebral number. However, more research is needed to test this hypothesis. This supports the evolutionary conservation of these genes, which is also reflected in the largely invariant body plan and in particular in the conservative vertebral formula among crocodylians.

A detailed discussion of the newly determined expression patterns of *HoxA-4*, *C-5*, *B-7* and *B-8* follows.

#### Hox paralog genes 4 to 5

In the mouse, *HoxA-4* has the same anterior expression limit as *HoxC-4* and *HoxA-5* in the anterior portion of the neck (Burke et al. 1995). In the chicken, only *HoxA-4* and *HoxC-4* share the same anterior expression boundary, and *HoxA-5* is confined to the posterior part of the neck (Burke et al. 1995). Our analysis revealed that the latter pattern is also true for crocodiles and appears to represent the configuration of the archosaur ancestor. Primitively, each vertebra possessed a pair of ribs, as seen in the vertebral column of crocodylians (Hoffstetter and Gasc 1969). It has been argued that *HoxA-5* was independently recruited for cervical rib repression in the mouse and turtle, where its expression starts at the anterior part of the neck (Mansfield and Abzhanov 2010, Ohya et al. 2005).

The expression of *HoxC-5* is at the base of the neck across the analysed taxa. Its expression begins at the penultimate cervical vertebra in mice and chickens (Burke et al. 1995), and it starts at the second to the last in the crocodile.

#### Hox paralog genes 6 to 8

As in the mouse, where the anterior expression limit of *HoxB-7* is in the anterior part of the dorsal series (D4), this *Hox* gene is expressed starting at D5 in the crocodile. Although there is no genetic data for chickens, we hypothesise that *HoxB-7* is also ancestrally associated with the anterior portion of the dorsal region, because its activity appears to be conservative.

The expression pattern of *HoxB-8* is more variable in amniotes. In the crocodile, it marks the mid-dorsal region (D8), whereas it is expressed in the anterior portion of the trunk (D3) in the mouse. To date, no distinct anterior expression limit has been detected in chickens, but *HoxB-8* is definitely active in the dorsal vertebral column. The shift of the anterior expression limit by 5 vertebrae between reptile and mammal appears to be a mammalian adaptation. However, more data on outgroup taxa, such as salamanders, is needed.

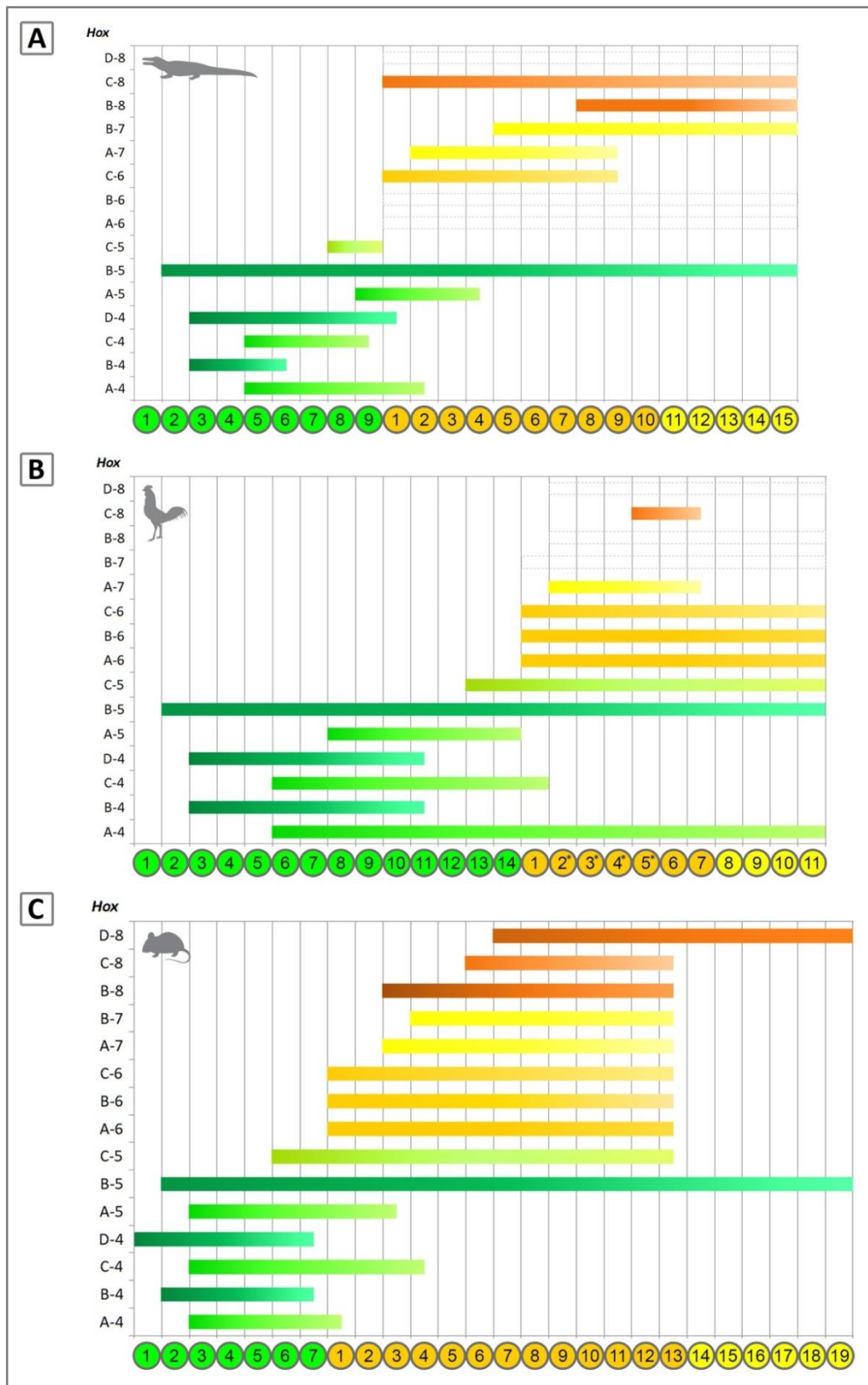


**Figure 3.10.: Summary of the somitic *Hox* code in amniotes.** (A) crocodilian, (B) chicken and (C) mouse. Anterior limits of expression were taken from determinations at relatively late stages. Posterior boundaries are not clearly defined. The partial *Hox* gene expression pattern in the alligator has previously been published by Mansfield and Abzhanov (2010) and was completed with *in situ* hybridisation experiments in the crocodile within the present study. Further references for *Hox* gene expression limits are indicated in Appendix 3.3. The circles represent the corresponding vertebral formula as given in Figure 3.4.

### 3.4.2. *Hox* gene expression domains and axial evolution

*Hox* genes are thought to act in combination in order to specify vertebral identity (*Hox* code) (Kessel and Gruss 1990). In order to test this hypothesis, the analysed *Hox* gene expression data of crocodiles (this study), chickens and mice (refer to Appendix 3.3. for references) was summarised into domains - units of vertebrae that share the same *Hox* code within a taxon (Figure 3.11.). A taxon-specific pattern of expression domains within the presacral region was revealed, and at least 10 *Hox* units can be recognised in the crocodile, with 6 units being assigned to the cervical series and 4 units being allocated in the dorsal series. In the chicken, 9 *Hox* domains could be identified. However, as we lack expression data of three *Hox* genes (*HoxB-7*, *B-8* and *D-8*) in the trunk of the bird, this may be an artefact. Similar to the crocodilian, there are 6 units in the neck, but the trunk reveals 3 units. Due to the high conservation of the *Hox* gene activity, it can be assumed that at least one of the unknown genes is expressed in the dorsal series and would produce a further expression domain. In the mouse, 9 *Hox* domains were recognised. Only 4 units are assigned to the cervical region, whereas 5 units are detectable in the dorsal region.

This genetic pattern and, thus, the differing activity of specific *Hox* genes are reflected by the axial skeleton of the analysed taxa, which may allow inference of the changes that occurred during the evolution of the vertebral column in amniotes. Comparatively, crocodilians reveal a relatively uniform body axis. There are vertebral regions that exhibit a specialised morphology, such as the atlas-axis complex (C1, C2) and the cervicodorsal transition (C8, C9, D1), but the remaining vertebrae - in particular, the dorsal series - are not very morphologically variable. Thus, an originally crocodile-like *Hox* gene expression pattern may have been modified in birds that have undergone significant modifications to their axial skeleton. Chickens have the same specialised vertebral regions at the anterior and posterior part of the neck as crocodiles. Additionally, they have a relatively long neck and a short trunk that displays fusion of several vertebrae. Corresponding to the morphological pattern, the *Hox* gene expression domains are expanded in the cervical series of the chicken since we recognised the same number of genetic units as in the crocodilians. Although to date, the expression pattern of three *Hox* genes of the paralog group 7 and 8 is unknown, there are at least 3 *Hox* domains in the dorsal series, reflecting the highly specialised anatomy of birds, whereas the dorsal region of crocodiles, which exhibits only 4 genetic units, is longer. Irrespective of the absolute neck length, almost all mammals have 7 cervical vertebrae. This number of vertebrae is reflected in the reduced number of *Hox* domains in the neck of mice, and is accompanied with a condensation and particular shifts of the genetic pattern. Mammals reveal the highest regional differentiation of the dorsal vertebral column, which is further subdivided into a thoracic and lumbar section. Associated with this very specialised body plan we recognise a higher number of *Hox* units in the dorsal series of mice.



**Figure 3.11.: Hox gene expression domains.** The expression data of *Hox* gene paralog groups 4-8 were summarised into units of vertebrae that share the same *Hox* code within a taxon. The colour coding indicates in which vertebrae the same *Hox* genes are expressed in each taxon. In the crocodile and the chicken, other than the analysed *Hox* genes are active at the first cervical vertebra (C1) indicated by grey colour.

In general, we detected two evolutionary processes concerning *Hox* domains and axial patterning: 1) expansion and condensation of genetic expression and 2) shift of genetic activity corresponding to different vertebral counts.

This comparative analysis of the genetic and morphological pattern allows inference of the ancestral amniote *Hox* code. It has been previously reported that the vertebral formula of the amniote ancestor may have included 6 cervical and 20 dorsal vertebrae (Müller et al. 2010). Accompanied by the relatively uniform body plan, the underlying genetic program may have resembled that of the crocodile, considering the two identified processes of evolutionary *Hox* expression change. However, *Hox* gene expression analyses in snakes, caecilians and lizards that exhibit a highly specialised body plan have shown that there are also some *Hox* genes that are not directly linked to morphology in the axial skeleton in the dorsal region (Woltering et al. 2009). Despite these uncertainties, the last common ancestor of crocodiles, chickens and mice probably had a less complex body plan and thus, a relatively conservative *Hox* gene expression pattern.

### 3.5. Conclusion

The present study is consistent with the hypothesis that the *Hox* code in the amniote ancestor was initially less complex or differentiated. Associated with and probably facilitating the evolutionary development of the higher complexity of the axial skeleton, the genetic pattern changed. Initially, the *Hox* genes were expressed in broad overlapping domains. During evolution the expression pattern has differentiated into additional distinct domains. These discrete domains coincide with the morphological boundaries between axial levels.

The crocodylian *Hox* code may be close to the configuration of the amniote ancestor. We observed a fairly differentiated genetic expression pattern in the crocodile (5 *Hox* subdomains in the neck and 4 *Hox* subdomains in the trunk) that resembles the pattern in birds (5 *Hox* subdomains in the neck and

3 *Hox* subdomains in the trunk) and appears to be less complex than in mammals (4 *Hox* subdomains in the neck and 5 *Hox* subdomains in the trunk) (refer to Appendix 3.3. for references). Accompanied by a higher number of vertebrae in an axial region, the *Hox* gene expression domains expand and there is less overlap (e.g. neck of chicken vs. crocodile), whereas the domains of expression are condensed in association with a lower number of vertebrae or a fusion of axial bones (e.g. trunk of chicken vs. crocodile, as well as neck of mouse vs. crocodile).

In summary, the analysis of the previously undescribed crocodylian *Hox* genes supports and extends the observation that differences in the somitic *Hox* gene expression pattern correlate with morphological changes within the vertebral column (Burke et al. 1995, Gaunt 1994). In amniotes, all *Hox* genes of paralog groups 4 and 5 possess a well-conserved expression domain in the cervical region, whereas the activity of the genes of paralog groups 6-8 is restricted to the dorsal region. The comparison of *Hox* gene expression patterns in different taxa is a useful tool to link gene activity and morphology of the vertebral column. The overall *Hox* code allows tracking of evolutionary changes associated with modifications of the amniote axial body plan. It appears that the evolution of the amniote *Hox* gene expression pattern is linked to the development of an increased regionalisation of the vertebral column. Analogous to the increase in *Hox* gene number that happened after the split between vertebrates and cephalochordates (Garcia-Fernandez and Holland 1994), the *Hox* gene expression pattern changed during evolution in association with evolutionary changes in the body plan.

Additionally, the results of this study stimulated a further project, in which the correlation between the genetic and morphological pattern was analysed in more detail. The significance of this link for the study of the evolution of the vertebral column in archosaurs was investigated in order to trace the *Hox* code via vertebral morphology in fossil taxa (refer to chapter 4). It is not possible to directly study the genetic expression in extinct animals, but proxies may allow us to infer the genetic complexity of fossil archosaurs.

### 3.6. References

- Burke, A.C., Nelson, C.E., Morgan, B.A., Tabin, C., 1995. *Hox* genes and the evolution of vertebrate axial morphology. *Development* **121**: 333-346.
- Burke, A.C., Nowicki, J.L., 2001. *Hox* genes and axial specification in vertebrates. *American Zoologist* **41**: 687-697.
- Carroll, S.B., 1995. Homeotic Genes and the Evolution of Arthropods and Chordates. *Nature* **376**: 479-485.
- Chevalier, J., Yi, J., Michel, O., Tang, X.-M., 1997. Biotin and Digoxigenin as Labels for Light and Electron Microscopy in Situ Hybridization Probes: Where Do We Stand? *Journal of Histochemistry & Cytochemistry* **45**: 481-491.
- Christ, B., Huang, R., Scaal, M., 2004. Formation and differentiation of the avian sclerotome. *Anatomy and Embryology* **208**: 333-350.
- Christ, B., Huang, R., Scaal, M., 2007. Amniote somite derivatives. *Developmental Dynamics* **236**: 2382-2396.
- Cohn, M.J., Tickle, C., 1999. Developmental basis of limblessness and axial patterning in snakes. *Nature* **399**: 474-479.
- David, R., Wedlich, D., 2001. PCR-based RNA probes: a quick and sensitive method to improve whole mount embryo in situ hybridizations. *Biotechniques* **30**: 769-772, 774.
- Drummond, A.J., Ashton, B., Buxton, S., Cheung, M., Cooper, A., Duran, C., Field, M., Heled, J., Kearse, M., Markowitz, S., Moir, R., Stones-Havas, S., Sturrock, S., Thierer, T., Wilson, A., 2011. Geneious R6 (Version 6.0.3) created by Biomatters. Available from <http://www.geneious.com>.
- Duboule, D., Dolle, P., 1989. The structural and functional organization of the murine HOX gene family resembles that of *Drosophila* homeotic genes. *The EMBO journal* **8**: 1497-1505.
- Farrell, R.E., 2006. RNA Methodologies. A Laboratory Guide for Isolation and Characterization. Elsevier Academic Press, Amsterdam, 767 pp.
- Ferguson, M.W., 1985. Reproductive Biology and Embryology of the Crocodylians, in: Gans, C., Billet, F., Maderson, P.F.A. (Eds.), *Biology of the Reptilia, Development A*. John Wiley & Sons, New York, pp. 329-492.
- Foronda, D., de Navas, L.F., Garaulet, D.L., Sanchez-Herrero, E., 2009. Function and specificity of Hox genes. *The International Journal of Developmental Biology* **53**: 1404-1419.
- Garcia-Fernandez, J., Holland, P.W., 1994. Archetypal organization of the amphioxus Hox gene cluster. *Nature* **370**: 563-566.
- Gaunt, S.J., 1994. Conservation in the *Hox* code during morphological evolution. *International Journal of Developmental Biology* **38**: 549-552.
- Gaunt, S.J., Coletta, P.L., Pravtcheva, D., Sharpe, P.T., 1990. Mouse Hox-3.4: homeobox sequence and embryonic expression patterns compared with other members of the Hox gene network. *Development* **109**: 329-339.

- Gaunt, S.J., Dean, W., Sang, H., Burton, R.D., 1999. Evidence that *Hoxa* expression domains are evolutionarily transposed in spinal ganglia, and are established by forward spreading in paraxial mesoderm. *Mechanisms of Development* **82**: 109-118.
- Gaunt, S.J., Krumlauf, R., Duboule, D., 1989. Mouse homeo-genes within a subfamily, Hox-1.4, -2.6 and -5.1, display similar anteroposterior domains of expression in the embryo, but show stage- and tissue-dependent differences in their regulation. *Development* **107**: 131-141.
- Gellon, G., McGinnis, W., 1998. Shaping animal body plans in development and evolution by modulation of *Hox* expression patterns. *Bioessays* **20**: 116-125.
- Gomez, C., Pourquie, O., 2009. Developmental control of segment numbers in vertebrates. *Journal of Experimental Zoology Part B Molecular and Developmental Evolution* **312**: 533-544.
- Gros, O., Maurin, L.C., 2008. Easy flat embedding of oriented samples in hydrophilic resin (LR White) under controlled atmosphere: Application allowing both nucleic acid hybridizations (CARD-FISH) and ultrastructural observations. *Acta Histochemica* **110**: 427-431.
- Hargrave, M., Bowles, J., Koopman, P., 2006. In Situ Hybridization of Whole-Mount Embryos, in: Darby, I.A., Hewitson, T.D. (Eds.), *In Situ Hybridization Protocols*. Humana Press Inc., Totowa, pp. 103-113.
- Hoffstetter, R., Gasc, J.-P., 1969. Vertebrae and Ribs of Modern Reptiles, in: Gans, C. (Ed.), *Biology of the Reptilia*, pp. 201-310.
- Houssaye, A., 2009. "Pachyostosis" in aquatic amniotes: a review. *Integrative Zoology* **4**: 325-340.
- Iimura, T., Pourquie, O., 2007. *Hox* genes in time and space during vertebrate body formation. *Development, Growth and Differentiation* **49**: 265-275.
- Johnson, M., Zaretskaya, I., Raytselis, Y., Merezuk, Y., McGinnis, S., Madden, T.L., 2008. NCBI BLAST: a better web interface. *Nucleic Acids Research* **36**: W5-9.
- Kessel, M., Gruss, P., 1990. Murine developmental control genes. *Science* **249**: 374-379.
- Liang, D., Wu, R., Geng, J., Wang, C., Zhang, P., 2011. A general scenario of Hox gene inventory variation among major sarcopterygian lineages. *BMC Evolutionary Biology* **11**: 25.
- Mallo, M., Wellik, D.M., Deschamps, J., 2010. *Hox* genes and regional patterning of vertebrate body plan. *Developmental Biology* **344**: 7-15.
- Mandry, P., Murray, A.B., Rieke, L., Becke, H., Höfler, H., 1993. Postembedding Ultrastructural In situ Hybridization on Ultrathin Cryosections and LR White Resin Sections. *Ultrastructural Pathology* **17**: 185-194.
- Mansfield, J.H., Abzhanov, A., 2010. *Hox* expression in the American alligator and evolution of archosaurian axial patterning. *Journal of Experimental Zoology Part B Molecular and Developmental Evolution* **314**: 1-16.
- McGinnis, W., Krumlauf, R., 1992. Homeobox genes and axial patterning. *Cell* **68**: 283-302.
- Morin-Kensicki, E.M., Melancon, E., Eisen, J.S., 2002. Segmental relationship between somites and vertebral column in zebrafish. *Development* **129**: 3851-3860.

- Müller, J., Scheyer, T.M., Head, J.J., Barrett, P.M., Werneburg, I., Ericson, P.G.P., Pol, D., Sánchez-Villagra, M.R., 2010. Homeotic effects, somitogenesis and the evolution of vertebral numbers in recent and fossil amniotes. *Proceedings of the National Academy of Sciences* **107**: 2118-2123.
- Nowicki, J.L., Burke, A.C., 2000. *Hox* genes and morphological identity: axial versus lateral patterning in the vertebrate mesoderm. *Development* **127**: 4265-4275.
- O'Connor, P.M., 2006. Postcranial pneumaticity: an evaluation of soft-tissue influences on the postcranial skeleton and the reconstruction of pulmonary anatomy in archosaurs. *Journal of Morphology* **267**: 1199-1226.
- Ohya, Y.K., Kuraku, S., Kuratani, S., 2005. *Hox* code in embryos of Chinese soft-shelled turtle *Pelodiscus sinensis* correlates with the evolutionary innovation in the turtle. *Journal of Experimental Zoology Part B Molecular and Developmental Evolution* **304**: 107-118.
- Osamura, R.Y., Yltoh, Y., Matsuno, A., 2000. Applications of Plastic Embedding to Electron Microscopic Immunocytochemistry and In Situ Hybridization in Observations of Production and Secretion of Peptide Hormones. *Journal of Histochemistry & Cytochemistry* **48**: 885-891.
- Peter, I.S., Davidson, E.H., 2011. Evolution of gene regulatory networks controlling body plan development. *Cell* **144**: 970-985.
- Pourquie, O., 2003. The segmentation clock: converting embryonic time into spatial pattern. *Science* **301**: 328-330.
- Puschel, A.W., Balling, R., Gruss, P., 1990. Position-specific activity of the *Hox1.1* promoter in transgenic mice. *Development* **108**: 435-442.
- Rancourt, D.E., Tsuzuki, T., Capecchi, M.R., 1995. Genetic interaction between *hoxb-5* and *hoxb-6* is revealed by nonallelic noncomplementation. *Genes & Development* **9**: 108-122.
- Richardson, M.K., Allen, S.P., Wright, G.M., Raynaud, A., Hanken, J., 1998. Somite number and vertebrate evolution. *Development* **125**: 151-160.
- Ruddle, F.H., Bartels, J.L., Bentley, K.L., Kappen, C., Murtha, M.T., Pendleton, J.W., 1994. Evolution of *Hox* genes. *Annual Review of Genetics* **28**: 423-442.
- Saga, Y., Takeda, H., 2001. The making of the somite: molecular events in vertebrate segmentation. *Nature Reviews Genetics* **2**: 835-845.
- Schwarzacher, T., Heslop-Harrison, P., 2000. Practical in situ hybridization. BIOS Scientific Publishers Limited, Oxford, 250 pp.
- Toth, L.E., Slawin, K.L., Pintar, J.E., Nguyen-Huu, M.C., 1987. Region-specific expression of mouse homeobox genes in the embryonic mesoderm and central nervous system. *Proceedings of the National Academy of Sciences* **84**: 6790-6794.
- van den Akker, E., Fromental-Ramain, C., de Graaff, W., Le Mouellic, H., Brulet, P., Chambon, P., Deschamps, J., 2001. Axial skeletal patterning in mice lacking all paralogous group 8 *Hox* genes. *Development* **128**: 1911-1921.
- Wilkinson, D.G., 1999. In situ hybridization. A practical approach. Oxford University Press, Oxford, 224 pp.

Wolpert, L., Jessel, T., Lawrence, P., Meyerowitz, E., Robertson, E., Smith, J., 2007. Principles of Development. Spektrum Akademischer Verlag, Heidelberg, 559 pp.

Woltering, J.M., Vonk, F.J., Müller, H., Bardine, N., Tuduca, I.L., de Bakker, M.A.G., Knöchel, W., Sirbu, I.O., Durston, A.J., Richardson, M.K., 2009. Axial patterning in snakes and caecilians: evidence for an alternative interpretation of the *Hox* code. *Developmental Biology* **332**: 82-89.

## **Acknowledgements**

The crocodile embryos were donated by Jean-Yves Sire (Université Pierre et Marie Curie Paris, France), Samuel Martin and Eric Ferrandez from the crocodile farm “La Ferme aux Crocodiles” in Pierrelatte (France). We thank Cathleen Witzemberger (Bayerische Staatssammlung für Paläontologie und Geologie München, Germany), Heike Sperling and Prof. Dr. Walter Hermanns from the Institut für Tierpathologie of the Ludwig-Maximilians-Universität München (Germany) for support with sectioning and methodological discussions. All current members of the Molecular Geo- & Palaeobiology Lab in Munich (Germany), especially Claire Larroux, Oliver Voigt, Astrid Schuster, Gabriele Büttner, Simone Schätzle and Dirk Erpenbeck is thanked for help with laboratory work. The manuscript has greatly benefitted from critical and helpful review by Sergio Vargas (Ludwig-Maximilians-Universität München, Germany). We acknowledge Nadia Fröbisch (Humboldt Universität zu Berlin, Germany), Igor Schneider (Universidade Federal do Para, Belem, Brazil) and Neil Shubin (University of Chicago, USA) for fruitful discussions.

CB was supported by a DAAD fellowship, a doctoral fellowship of the Studienstiftung des deutschen Volkes (German National Academic Foundation) and the mentoring programme within the framework of LMUexcellent of the Ludwig-Maximilians-Universität München (Germany).

## **Appendix**

Appendix 3.1.: Amino acid sequence conservation of *Hox* 4-8 paralog genes among amniotes.

Appendix 3.2.: Amino acid sequence alignment of *Hox* 4-8 paralog genes among amniotes.

Appendix 3.3.: References for *Hox* gene expression limits.

**Appendix 3.1.: Amino acid sequence conservation of Hox 4-8 paralog genes among amniotes.** Hox protein sequences of mouse, chicken, alligator and crocodile (at least 190 amino acids including the homeodomain; if less then too short for meaningful comparison) were aligned applying ClustalW in the software Geneious (Drummond et al. 2011). Percentage of amino acid sequence conservation was calculated. If not otherwise referenced, mouse and chicken sequences were obtained from NCBI database. Alligator sequences were published by Mansfield and Abzhanov (2010). Crocodile sequences are the result of the present study.

<b><u>HoxA-4</u></b>	mouse (NP_032291)	chicken (NP_001025517)	crocodile
mouse (NP_032291)	-	52.7%	48.1%
chicken (NP_001025517)	52.7%	-	45.0%
crocodile	48.1%	45.0%	-

<b><u>HoxB-4</u></b>	mouse (NP_034589)	chicken (NP_990624)	alligator	crocodile
mouse (NP_034589)	-	65.5%	68.6%	67.9%
chicken (NP_990624)	65.5%	-	92.9%	92.3%
alligator	68.6%	92.9%	-	99.5%
crocodile	67.9%	92.3%	99.5%	-

<b><u>HoxC-4</u></b>	mouse (AAI44779)	chicken	alligator	crocodile
mouse (AAI44779)	-	77.3%	82.5%	82.0%
chicken	77.3%	-	88.0%	87.9%
alligator	82.5%	88.0%	-	100.0%
crocodile	82.0%	87.9%	100.0%	-

<b><u>HoxD-4</u></b>	mouse (AAI39207)	chicken (NP_001012293)	alligator	crocodile
mouse (AAI39207)	-	74.8%	74.3%	73.5%
chicken (NP_001012293)	74.8%	-	90.8%	90.5%
alligator	74.3%	90.8%	-	100.0%
crocodile	73.5%	90.5%	100.0%	-

<b><u>HoxA-5</u></b>	mouse (NP_034583)	chicken (AAT90845)	alligator	crocodile
mouse (NP_034583)	-	84.1%	81.0%	78.3%
chicken (AAT90845)	84.1%	-	92.7%	91.7%
alligator	81.0%	92.7%	-	100.0%
crocodile	78.3%	91.7%	100.0%	-

Appendix 3.1. continued:

<b><u>HoxB-5</u></b>	mouse (NP_032294)	chicken (NP_001020526)	alligator
mouse (NP_032294)	-	82.9%	82.0%
chicken (NP_001020526)	82.9%	-	94.2%
alligator	82.0%	94.2%	-

<b><u>HoxC-8</u></b>	mouse (EDL03944)	chicken (NP_990224)	alligator	crocodile
mouse (EDL03944)	-	93.4%	93.0%	90.8%
chicken (NP_990224)	93.4%	-	98.5%	98.0%
alligator	93.0%	98.5%	-	100.0%
crocodile	90.8%	98.0%	100.0%	-

**Appendix 3.2.: Amino acid sequence alignment of Hox 4-8 paralog genes among amniotes.** Hox amino acid sequences of mouse, chicken, alligator and crocodile (at least 190 amino acids including the homeodomain; if less then too short for meaningful comparison) were aligned applying ClustalW in the software Geneious (Drummond et al. 2011). Sequence positions with different amino acids are highlighted. If not otherwise referenced, mouse and chicken sequences were obtained from NCBI database. Alligator sequences were published by Mansfield and Abzhanov (2010). Crocodile sequences are the result of the present study.

**HoxA-4:**



**HoxB-4:**







Appendix 3.2. continued:

HoxA-6:

1. mouse (NP_034584)	1	10	20	30	40
2. chicken (NP_001026158)	MSSYFVNPTTFPGSLP	SGQDS	ELGQL	PLYPAGYDALR	PFPA
3. alligator	MSSYFVNPTTFPGSLP	AGQDS	ELGQL	PLYPAGYDALR	HFFP
1. mouse (NP_034584)	50	60	70	80	90
2. chicken (NP_001026158)	KTYTSPCFYQQSN	SVLACNRAS	YEYEGASC	FYS	DKDLS
3. alligator	KTYTSPCFYQQSN	TVILACNRAS	YEYEGASC	FYS	DKDLS
1. mouse (NP_034584)	100	110	120	130	140
2. chicken (NP_001026158)	PGDYLFHFSPEQQYK	PDG	SVQ	KA	LH
3. alligator	QGDYLFHFSPEQQYK	SN	GVQ	KA	LH
1. mouse (NP_034584)	150	160	170	180	190
2. chicken (NP_001026158)	AVYGS	HGRRGRQ	TYTRYQ	TLELEKE	FHNRYL
3. alligator	TVYGA	HGRRGRQ	TYTRYQ	TLELEKE	FHNRYL
1. mouse (NP_034584)	200	210	220	230	232
2. chicken (NP_001026158)	QIKIWFQNR	RMKWK	KKENK	L	INSTQ
3. alligator	QIKIWFQNR	RMKWK	KKENK	F	INSTQ

HoxC-6:

1. mouse (NP_034595)	1	10	20	30	40	50
2. chicken (XP_003643502)	MNSYFTNPSLS	SCHLAG	GQD	VLPNVALN	STAYDPVR	H
3. alligator	MNSYFTNPSLS	SCHL	TSG	QVLPNVALN	STAYDPVR	H
1. mouse (NP_034595)	60	70	80	90	100	
2. chicken (XP_003643502)	S	T	P	F	Y	
3. alligator	S	S	P	F	Y	
1. mouse (NP_034595)	110	120	130	140	150	
2. chicken (XP_003643502)	AQDF	S	S	E	Q	
3. alligator	AQDF	T	S	D	Q	
1. mouse (NP_034595)	160	170	180	190	200	
2. chicken (XP_003643502)	YQ	T	L	E	L	
3. alligator	YQ	T	L	E	L	
1. mouse (NP_034595)	210	220	230	238		
2. chicken (XP_003643502)	NL	T	S	T	L	
3. alligator	NL	S	T	L	S	

HoxA-7:

1. mouse (NP_034585)	1	10	20	30	40	50
2. chicken (NP_989926)	MSSSYVNALFS	KYTAGAS	L	FQNAEPT	S	C
3. alligator	MSSSYVNALFS	KYTAGAS	L	FQNAEPT	S	C
1. mouse (NP_034585)	60	70	80	90	100	
2. chicken (NP_989926)	M	P	G	L	Y	
3. alligator	M	P	G	L	Y	
1. mouse (NP_034585)	110	120	130	140	150	
2. chicken (NP_989926)	D	K	A	D	E	
3. alligator	E	K	A	E	S	
1. mouse (NP_034585)	160	170	180	190	200	
2. chicken (NP_989926)	N	R	Y	L	T	
3. alligator	N	R	Y	L	T	
1. mouse (NP_034585)	210	220	229			
2. chicken (NP_989926)	D	A	M			
3. alligator	E	P	T			

HoxB-7:

- (less than 190 amino acids)



**Appendix 3.3.: References for *Hox* gene expression limits.** The data of the described *Hox* gene expression patterns in mouse (*Mus musculus*) and chicken (*Gallus gallus*) were collected from previously published works. To date no expression data was available for *HoxB-7* in the chicken.

<i>Hox</i> gene	<i>G. gallus</i>	<i>M. musculus</i>
<i>HoxA-4</i>	Burke et al. (1995)	Burke et al. (1995)
<i>HoxB-4</i>	Burke et al. (1995)	Burke et al. (1995)
<i>HoxC-4</i>	Burke et al. (1995)	Burke et al. (1995)
<i>HoxD-4</i>	Burke et al. (1995)	Gaunt et al. (1989)
<i>HoxA-5</i>	Mansfield and Abzhanov (2010)	Mansfield and Abzhanov (2010)
<i>HoxB-5</i>	Mansfield and Abzhanov (2010)	Rancourt et al. (1995)
<i>HoxC-5</i>	Burke et al. (1995)	Burke et al. (1995)
<i>HoxA-6</i>	Nowicki and Burke (2000)	Toth et al. (1987)
<i>HoxB-6</i>	Woltering et al. (2009)	Rancourt et al. (1995)
<i>HoxC-6</i>	Burke et al. (1995)	Burke et al. (1995)
<i>HoxA-7</i>	Gaunt et al. (1999)	Puschel et al. (1990)
<i>HoxB-7</i>	-	Burke et al. (1995)
<i>HoxB-8</i>	Burke et al. (1995)	van den Akker et al. (2001)
<i>HoxC-8</i>	Burke et al. (1995)	Burke et al. (1995)
<i>HoxD-8</i>	Burke et al. (1995)	Burke et al. (1995)

## Chapter 4

### **Correlation between *Hox* code and vertebral morphology in archosaurs: implications for vertebral evolution in sauropodomorph dinosaurs**

#### **Abstract**

---

The relationship between regulation of developmental genes and phenotypic variation is of central interest in evolutionary biology. A classic example of this relationship is the role of *Hox* genes in the anteroposterior patterning in metazoans and regionalisation of the vertebral column in vertebrates. Archosaurs (crocodiles, birds and dinosaurs) display a variety of vertebral morphologies and number. However, it appears that equivalent *Hox* genes are active in the neck during embryonic development. This implies that variation in the cervical column is due to modifications in the pattern of gene expression.

Here, we first demonstrate the direct correlation between vertebral *Hox* code and quantifiable vertebral morphology in modern archosaurs, where morphological clusters can be linked to anterior *Hox* gene expression boundaries. The correlation observed in modern crocodiles and birds allows a reconstruction of the vertebral *Hox* code in extinct taxa, suggesting that important modifications in the expression of *Hox* genes have occurred. For the first time, the present findings allow to confidently infer the genetic basis for vertebral evolution in sauropodomorph dinosaurs, a fossil group with highly variable vertebral counts.

---

#### 4.1. Introduction

The regionalisation of the axial skeleton in a cervical, dorsal, sacral and caudal compartment is a key attribute of amniotes (Figure 4.1.). The number of axial elements varies significantly among different groups of vertebrates. In mammals, there is a remarkably low level of variation in the number of cervical vertebrae (Galis 1999). Almost all mammals have seven cervicals, irrespective of the neck length. In contrast, reptiles and birds as well as sauropodomorph dinosaurs often have highly variable numbers of cervical vertebrae (Müller et al. 2010). Vertebral morphology and number have far-reaching consequences for organismal function and ecology. The vertebral column, or at least parts thereof, serves many different functions, from food acquisition via sustaining the body posture to locomotion. Since the form of the axial column is related to its function, the vertebral morphology results from multiple mechanical stimuli simultaneously (Koob and Long 2000), resulting in a high variability of anatomical structures. The total number of postembryonic vertebrae is determined by the process of somitogenesis (Carroll 1995, Kmita and Duboule 2003, Krumlauf 1994, Pourquie 2003, Wellik 2009). The rhythmic formation of somites continues until the total species-specific number of transient embryonic segments is reached (Gomez et al. 2008, Gomez and Pourquie 2009, Imura and Pourquie 2007, Pourquie 2003). Subsequently, the vertebral precursors differentiate, through resegmentation, into vertebrae, exhibiting

distinct morphologies depending on their position along the anteroposterior body axis (Gomez and Pourquie 2009, Imura and Pourquie 2007, Pourquie 2003). Since the pioneering discovery of eight homeotic genes distributed among two complexes in *Drosophila* (Kaufman et al. 1980, Lewis 1978), intensive work spanning three decades has shown that the specific temporal and spatial expression pattern of the highly conserved *Hox* genes determines the anteroposterior organisation and segmentation of all metazoans, including chordates (Carroll 1995, Krumlauf 1994, McGinnis and Krumlauf 1992, Pearson et al. 2005, Wellik 2007). *Hox* genes are organised in four clusters, and their expression/function

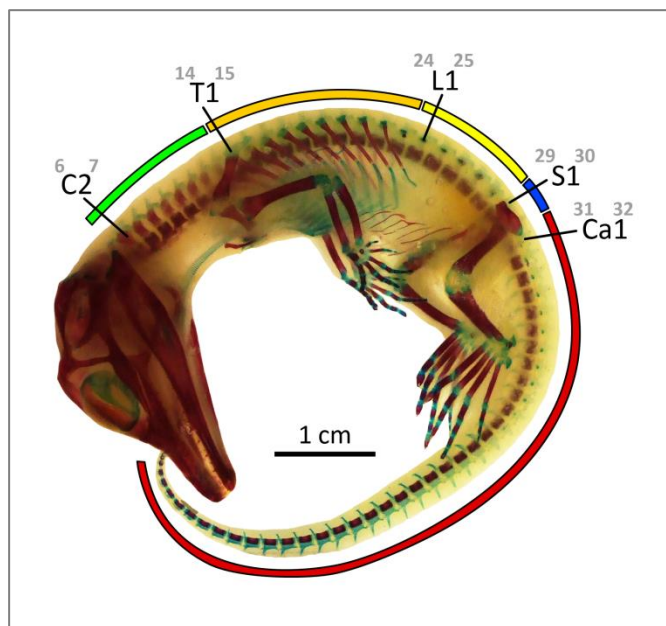


**Figure 4.1:** Axial skeleton of the crocodile. An alcian blue (cartilage)/alizarin red (ossified bone) stained embryo at embryonic day 46 (#260590 of the Field Museum of Natural History Chicago, USA). There are nine cervical vertebrae (green), ten thoracic (orange), five lumbar (yellow), two sacral (blue), and several caudal vertebrae (red). The first vertebra of each anatomical region is indicated and flanked by the associated somites (grey numbers). Two somites contribute to one vertebra.

along the main body axis (anterior to posterior) correlates with their spatial order along the chromosome (reviewed in Carroll 1995, Krumlauf 1994) (Figure 4.2.). In terms of chromosomal arrangement, sequence and most importantly function, amniotes share almost identical complements of these homeotic genes. This implies that the variation in the relative vertebral count is due to modifications in the pattern of the *Hox* gene activity.

*Hox* genes are key determinants of vertebrae identity (Burke et al. 1995, Carroll 1995, Kessel and Gruss 1990, Kmita and Duboule 2003, Krumlauf 1994, Pourquie 2003, Wellik 2009) and it has been proposed that a unique or highly distinctive *Hox* code expressed in each somite specifies different vertebral morphologies (Gaunt 1994). Vertebral *Hox* codes have been established for fish (Morin-Kensicki et al. 2002), mammals (Burke et al. 1995, Kessel and Gruss 1990), squamates (Burke et al. 1995, Cohn and Tickle 1999, Ohya et al. 2005, Woltering et al. 2009) and birds (Burke et al. 1995),

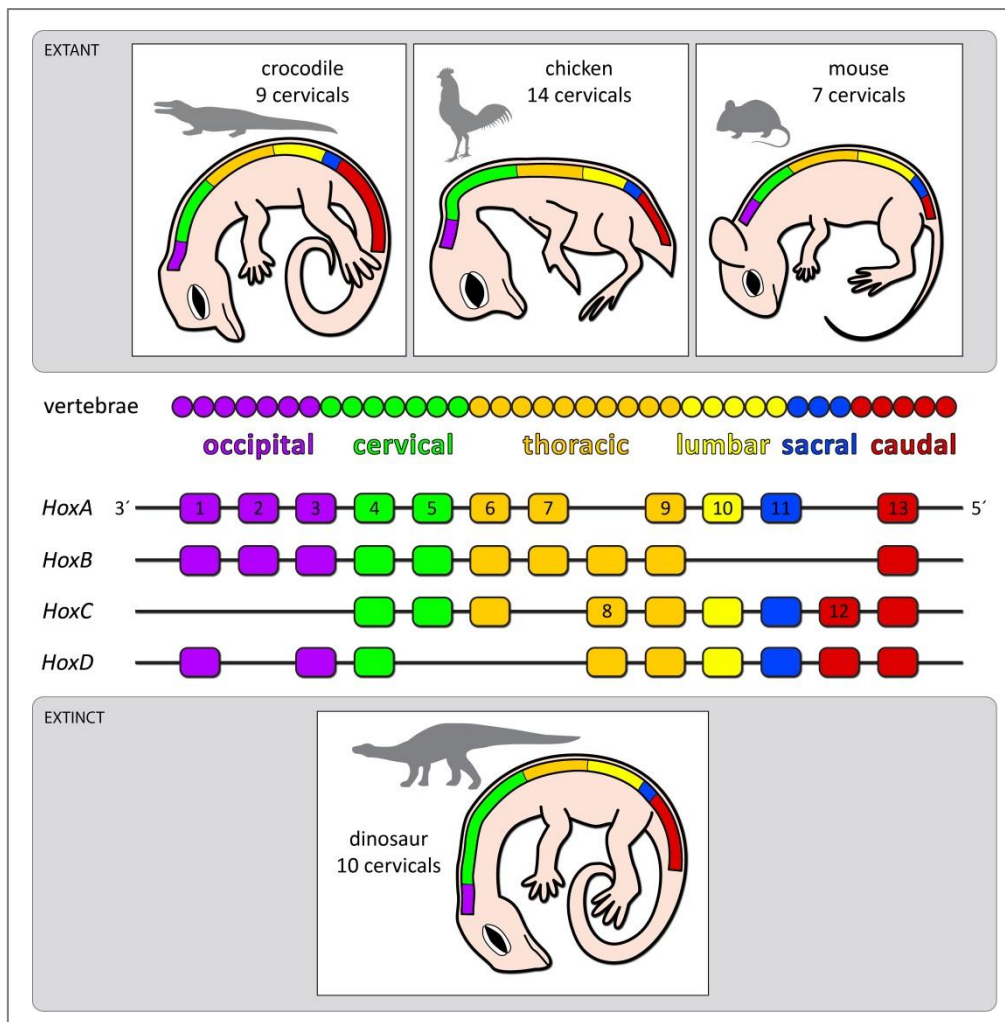


**Figure 4.2.: Schematic representation of the association between *Hox* genes and vertebral regions in extant and extinct amniotes.** There are 39 *Hox* genes arranged in four clusters (*HoxA*, *B*, *C*, *D*) in tetrapods. The order of the genes from 3' to 5' in the DNA corresponds to the order in which they are expressed along the anteroposterior body axis. The colour coding indicates how gene groups map to the axial regions. The differentiation of the morphological divisions along the axial column is mainly governed by *Hox* genes and thus, differences in the body plan correspond to changes in the *Hox* code.

but not yet fully for reptiles. In crocodiles, only a partial *Hox* code (8 out of 19 *Hox* genes) for the American alligator (*Alligator mississippiensis*) has been proposed so far (Mansfield and Abzhanov 2010). Previous analyses have shown that the vertebral *Hox* code in amniotes is highly conserved, and several *Hox* gene expression boundaries can be used as markers for different regions of the axial skeleton (Burke et al. 1995). For example, the anterior expression boundary of *HoxC-6* marks the cervicothoracic transition in a variety of vertebrate species that differ in cervical number (Burke et al. 1995). Likewise, *Hox-10* and *Hox-11* paralogs regulate the formation of the lumbosacral boundary in amniotes (Wellik and Capecchi 2003). Studies of *Hox* gene expression patterns promise to reveal homology between vertebrate body plans and constitute an additional set of characters to homologize segments between organisms (Burke et al. 1995). Because morphological similarity within an individual vertebral column seems to be directly and causally related to *Hox* gene expression (Johnson and O'Higgins 1996), the study of morphological variation of vertebrae as an expression pattern proxy provides an opportunity to re-examine long-problematic aspects of morphology, such as the establishing of the exact homologies of different body sections in related taxa with varying vertebral counts.

The objectives of the present study are 1) to investigate the *Hox* gene expression pattern in the Nile crocodile (*Crocodylus niloticus*) via whole-mount *in situ* hybridisation experiments, 2) to test the correlation between *Hox* gene expression and vertebral morphology in the cervical vertebral column of extant archosaurs as a case study for a comprehensive understanding of patterns of vertebral evolution in amniotes and 3) to identify for the first time the exact modifications in *Hox* gene expression in extinct archosaurs such as the basal sauropodomorph *Plateosaurus* in order to elucidate how evolutionary changes of the axial column occurred.

## 4.2. Materials and methods

### 4.2.1. Whole-mount *in situ* hybridisation

First, we examined the *Hox* genes that are expressed in the cervical region of modern archosaurs. In order to establish the extant phylogenetic bracket (Witmer 1995), the *Hox* gene expression patterns were analysed in crocodylians (American alligator and Nile crocodile) and birds (domestic chicken) - the closest living relatives of dinosaurs. Besides a literature survey, whole-mount *in situ* hybridisations (ISH) were performed in order to complete the cervical *Hox* code for crocodylians. Nile crocodile eggs were collected at “La Ferme aux Crocodiles” crocodile farm in Pierrelatte, France. The crocodile embryos were harvested after 9-15 days of embryonic development (ED), dissected in 1x PBS and fixed overnight in 4% paraformaldehyde in 1x PBS at 4°C. After rinsing in 1x PBS, they were dehydrated in a sequence of ethanol concentrations and stored in fresh 100% ethanol at -20°C until

use. For cDNA synthesis, three embryos were transferred into RNAlater RNA stabilisation reagent after harvesting. Total RNA was extracted using the RNeasy kit from Qiagen according to the manufacturer's instructions.

Degenerate primers were designed for the *Hox* genes analysed in this study (*HoxA-4*, *B-4*, *C-4*, *D-4* and *A-5*, *C-5*), targeting the conserved 5' region of exon one and the homeobox. To generate antisense-riboprobes for *in situ* hybridisation, the promotor sequence for T3 RNA polymerase was added to the 5' end of each gene-specific reverse primer sequence. From purified cDNA templates, antisense RNA probes were transcribed *in vitro* using T3 RNA polymerase and digoxigenin (DIG)-labelled UTP (Roche). Before whole-mount *in situ* hybridisation, the DIG-labelled riboprobes were tested via blot hybridisation in a vial.

Embryos stored in 100% ethanol were rehydrated, washed and prehybridised. After prehybridisation, DIG-labelled riboprobes were added. The samples were incubated overnight at 60°C. The embryos were stained using anti-DIG fragments coupled with alkaline phosphatase (AP). After washing the colour substrates, 4-nitrobluetetrazolium chloride (NBT) and 5-bromo-4-chloro-3-indoyl-phosphate (BCIP) were used to detect the hybridisation patterns. With some modifications, the applied ISH protocol is based on that described by Hargrave et al. (2006). The detailed protocol for blot hybridisation and whole-mount *in situ* hybridisation is described in chapter 3 (see section 3.2.1.).

#### 4.2.2. Morphological analysis

The morphological variability of the cervical vertebrae of the extant and extinct archosaurs was comprehensively evaluated by a combined shape analysis (Table 4.1.). First, a set of qualitative

Taxon	Cervical vertebrae	Specimen	3D model
<i>Alligator mississippiensis</i>	9	SAPM No. 4	X
<i>Alligator mississippiensis</i>		SAPM No. 3	-
<i>Crocodylus niloticus</i>	9	SAPM No. 2	X
<i>Gallus gallus domesticus</i>	14	SAPM No. 133	X
<i>Gallus gallus domesticus</i>		SAPM No. 134	-
<i>Mus musculus</i>	7	TMM M-8671	X*
† <i>Plateosaurus engelhardti</i>	10	GPIT/RE/7288	X
† <i>Plateosaurus engelhardti</i>		SMNS 13200	-

**Table 4.1.: List of modern and fossil taxa analysed in the present study.** The amniotes differ in number of cervical vertebrae. Cross (†) denotes extinct taxon. Institutional abbreviations: SAPM = Staatliche Sammlung für Anthropologie und Paläoanatomie München, Germany; TMM = Texas Memorial Museum; GPIT = Geologisches und Paläontologisches Institut der Universität Tübingen, Germany; SMNS = Staatliches Museum für Naturkunde Stuttgart, Germany.

\*Dr. Timothy Rowe, Ms. Megan Demarest, 2007, "Mus musculus" (On-line), Digital Morphology, Accessed May 09, 2012 at [http://www.digimorph.org/specimens/Mus\\_musculus/heterozygous/adult/whole/](http://www.digimorph.org/specimens/Mus_musculus/heterozygous/adult/whole/).

characteristics that varied within each cervical series were collected and coded, as binary or multistate characters in a data matrix. The characters that could not be captured by homologous landmarks include the presence and absence of osteological features such as a ventral keel, a bifurcated neural spine and muscle insertion points. Second, the morphological differences between the vertebrae were quantitatively analysed via 3D landmark-based geometric morphometrics. Three-dimensional scans of the cervical vertebrae of *A. mississippiensis*, *C. niloticus*, *G. gallus domesticus* and *P. engelhardti* were generated using the laser scanner ModelMaker Z35 integrated with the FaroArm Platinum (Table 4.1.). The software packages KUBE and Geomagic Studio 9.0 were used for post-processing of the raw data. Applying the software Landmark Version 3.0 (Wiley 2005), a series of 17 homologous landmarks (Figure 4.3., Table 4.2.) were digitised on the 3D models. The homologous points abstract the vertebral shape and characterise important osteological features. The first cervical vertebra is not included in the geometric morphometric analysis, because it lacks specific homologies and thus, several landmarks cannot be applied to the atlas. The coordinates of all landmark sets were superimposed using General Procrustes Analysis (GPA) in Morphologika (O'Higgins and Jones 2006). The subsequent Relative Warps Analysis (RWA) summarised the multidimensional information. With the applied settings, this method is equivalent to a Principal Components Analysis. The shape differences were visualised with 3D thin-plate splines.

In order to find the similarity relationships among the vertebrae, the superimposed landmark coordinates assembled with the qualitative character matrix were analysed with a Principal

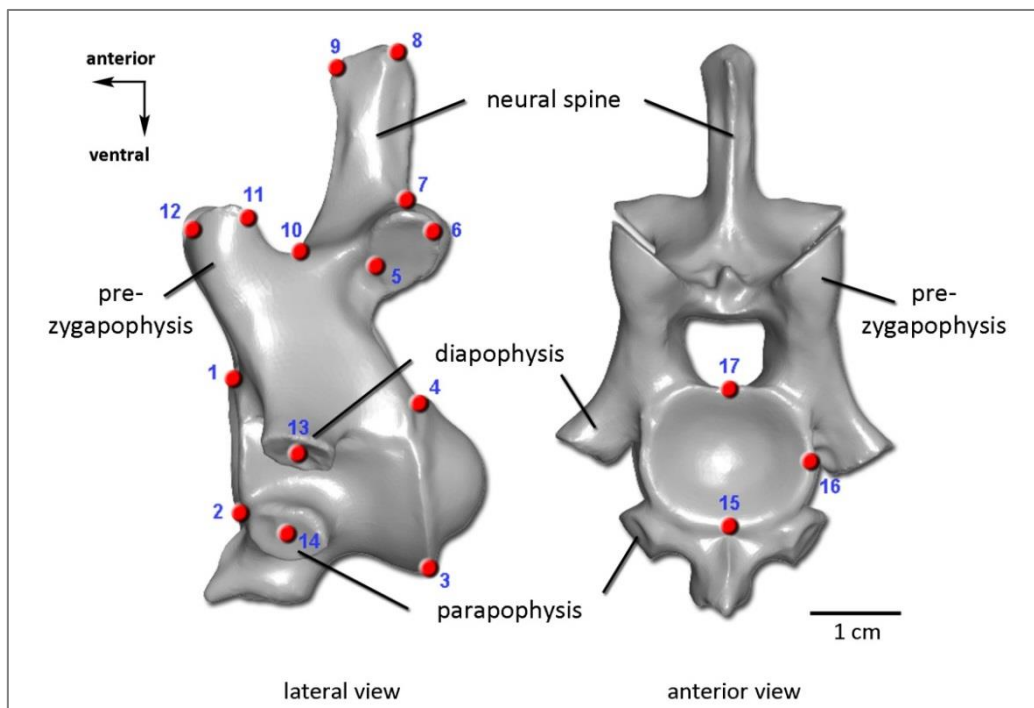


**Figure 4.3.:** Landmark set used in the geometric morphometric analysis. The 3D landmarks (red points) are shown on the fourth cervical vertebra of the American alligator (3D model of specimen SAPM No. 4). Refer to Table 4.2. for detailed description of the homologous points.

View	Landmark (LM)	Definition
lateral	1	dorsal-anterior edge of the centrum
	2	ventral-anterior edge of the centrum
	3	ventral-posterior edge of the centrum
	4	dorsal-posterior edge of the centrum
	5	anteriormost edge of the articular facet of the postzygapophysis
	6	dorsal-posterior edge of the articular facet of the postzygapophysis
	7	point of maximum curvature between postzygapophysis and neural spine
	8	posterior edge of the neural spine
	9	anterior edge of the neural spine
	10	point of maximum curvature between neural spine and prezygapophysis
	11	posteriormost point of the articular facet of the prezygapophysis
	12	dorsal-anterior edge of the articular facet of the prezygapophysis
	13	centre of the diapophysis
	14	centre of the parapophysis
anterior	15	ventralmost point of the centrum
	16	lateralmost point of the centrum
	17	dorsalmost point of the centrum

**Table 4.2.: Description of the 3D landmarks.** The same landmark sets were applied to all analysed taxa in order to provide a comparable basis for the morphological study. Although there are transverse processes connecting the cervical ribs with the vertebral centrum, LM 13 and 14 are not applied in the analysis of the chicken and the mouse because their placement is not exactly repeatable.

Coordinates Analysis (PCO) applying the Gower index (Gower 1966, 1971) with the software PAST (Hammer et al. 2001). In comparison to a PCA, this method allows the processing of both quantitative and qualitative data. The vertebrae were joined based on the smallest distance between them via the cluster analysis using the single linkage algorithm in combination with the Gower similarity index. This resulted in the morphological subdomain patterns of the cervical series for the analysed taxa.

The osteological terms used in the present study are based on the nomenclature proposed by Baumel et al. (1993) for bird, Huene (1926) and Wilson (1999) for dinosaur and Romer (1976) for crocodile.

## 4.3. Results

### 4.3.1. Hox gene expression in modern archosaurs

The present sequence analyses on cDNA (alignments see chapter 3, section 3.3.1.) confirmed that the Nile crocodile possesses the same *Hox* genes (*HoxA-4*, *B-4*, *C-4*, *D-4* as well as *A-5*, *C-5*) found in the

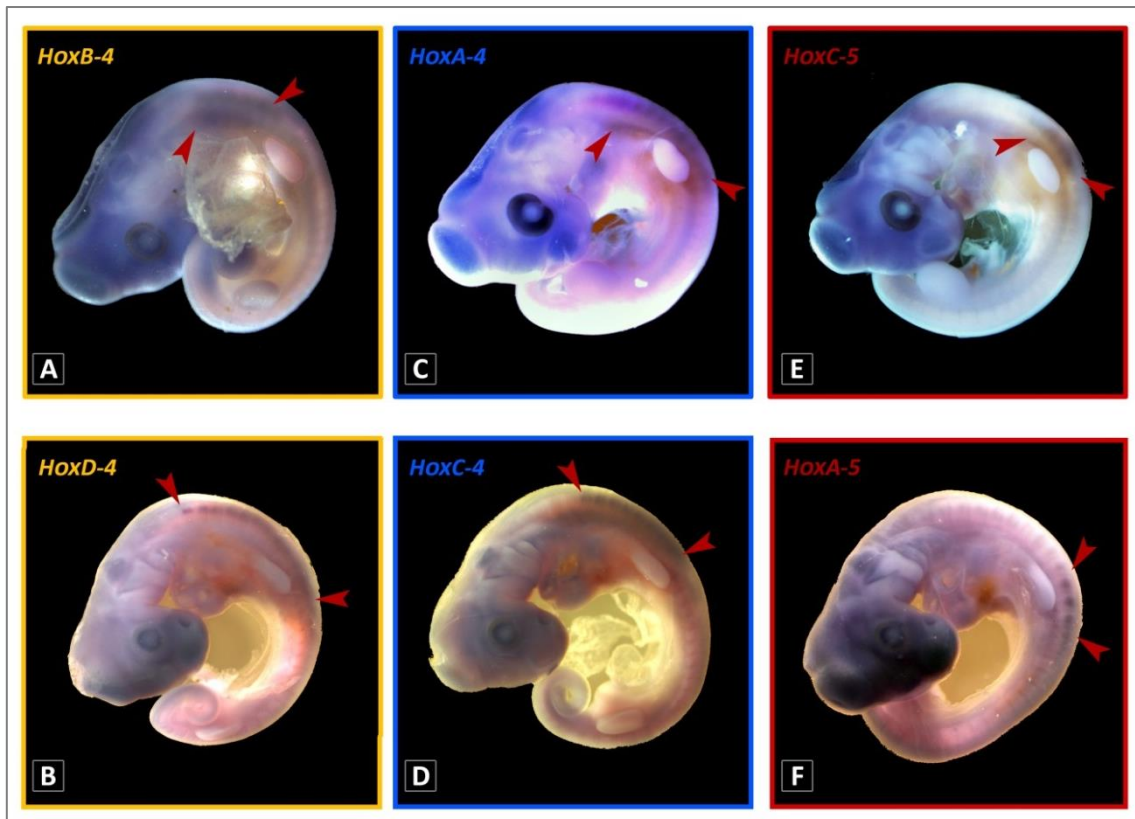


**Figure 4.4:** *Hox* gene expression in the somites (so) of Nile crocodile embryos (ED 10-14). Arrowheads indicate the anterior and posterior expression boundary. (A) *HoxB-4* has an anterior limit at C3 (so 7/8) and extends to C6 (so 10/11). (B) *HoxD-4* expression starts at C3 (so 7/8) and fades out posteriorly at D1 (so 14/15). (C) *HoxA-4* is expressed from C5 (so 9/10) to D3 (so 16/17). (D) *HoxC-4* has an anterior boundary at C5 (so 9/10) and extends to C9 (so 13/14). (E) *HoxC-5* expression starts at C8 (so 12/13) and fades out posteriorly at D1 (so 14/15). (F) *HoxA-5* is expressed from C9 (so 13/14) to D4 (so 17/18).

neck of other amniotes (Burke et al. 1995, Cohn and Tickle 1999, Kessel and Gruss 1990, Mansfield and Abzhanov 2010, Ohya et al. 2005, Woltering et al. 2009). The comparison of the new crocodile sequence data with previously published *Hox* gene sequences revealed a high degree of amino acid sequence conservation (about 60-80%) among the different species (alignments see chapter 3, section 3.3.1.).

The *in situ* hybridisation results revealed that in crocodiles, the anterior expression limit of *HoxB-4* and *D-4* is at the third cervical vertebra (C3) (Figure 4.4. A and B). *HoxB-4* is only active until C6, whereas *HoxD-4* is expressed to the end of the neck. The expression of *HoxA-4* and *C-4* begins at the fifth cervical vertebra, extending to the thoracic region (Figure 4.4. C and D). *HoxC-5* is expressed at the last two cervical vertebrae (Figure 4.4. E). *HoxB-5* expression already starts at C2 (Mansfield and Abzhanov 2010), whereby the anterior expression boundary of *HoxA-5* is at the last cervical vertebra (C9) (Figure 4.4. F). The complete pattern of cervical *Hox* expression differs between crocodiles, birds and mammals (Figure 4.5.). Although the general expression pattern of the *Hox-4* paralogs is relatively similar in all taxa, there is some variation in their anterior expression limits, in relation to the number of cervical vertebrae. The same is seen in the *Hox-5* paralogs, with *HoxA-5* showing the

highest variability. Similar to the crocodile, the anterior expression limit of the chicken *HoxB-4* and *D-4* (Burke et al. 1995) is at the third cervical vertebra (Figure 4.5. B). The expression of *HoxA-4* and *C-4* in the chicken (Burke et al. 1995) is posteriorly shifted by one vertebra in comparison to the crocodile and, thus, begins at the sixth cervical (Figure 4.5. B). The *HoxC-5* expression pattern (Burke et al. 1995) begins at the penultimate cervical vertebra (C13) in the chicken and the anterior expression limit of *Hox B-5* is at C2 as previously observed in crocodilians (Mansfield and Abzhanov 2010) (Figure 4.5. B). *HoxA-5* is expressed at the eighth cervical vertebra (Mansfield and Abzhanov 2010). It is shifted anteriorly by one vertebra in comparison to the crocodilian pattern (Figure 4.5. B). In the mouse, the *Hox* gene expression pattern is quite condensed and there is more overlap of specific *Hox* gene activity. The anterior expression boundary of *HoxB-4* (Burke et al. 1995) is at C2 and coincides with *HoxB-5* (Rancourt et al. 1995) (Figure 4.5. C). *HoxD-4* (Gaunt et al. 1989) is shifted anteriorly and expression starts at C1 (Figure 4.5. C). The expression of *HoxA-4* and *HoxC-4* (Burke et al. 1995) starts at C3 and coincides with the anterior expression limit of *HoxA-5* (Mansfield and Abzhanov 2010), due to an anterior shift in comparison with the crocodilian and avian pattern (Figure 4.5. C). *HoxC-5* (Burke et al. 1995) is expressed at the penultimate cervical vertebra (C6) of the mouse (Figure 4.5. C).

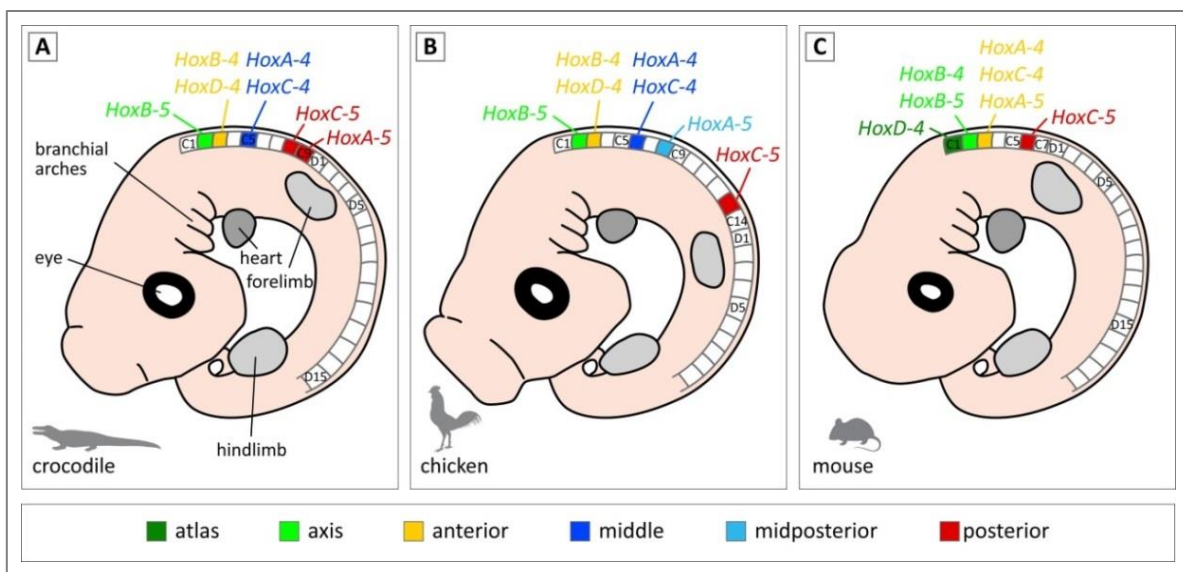


**Figure 4.5.:** Schematic representation of the anterior *Hox* expression limits in modern amniotes. The same *Hox-4* and *Hox-5* paralogs are active in the cervical vertebrae of (A) crocodile, (B) chicken and (C) mouse. In relation to the number of vertebrae, there are differences in the position of the anterior *Hox* expression limits (indicated by colour). Except for *HoxB-5* the *Hox* gene expression analysis in crocodiles was part of the present study. Refer to section 4.3.1. for detailed references of the *Hox* code in chicken and mouse. Abbreviations: C = cervical vertebra, D = dorsal vertebra.

## 4.3.2. Vertebral morphology in modern archosaurs

### 4.3.2.1. Qualitative morphology

The study of the qualitative characteristics of the vertebrae revealed significant morphological differences within the cervical series in the crocodilians and chickens (Figure 4.6.). The distribution of

the osteological features indicates the morphological differentiation of the cervical vertebral region in each taxon. The complete data matrix is provided in Appendix 4.1. (crocodile), Appendix 4.2. (alligator) and Appendix 4.3. (chicken). The detailed description of the morphological characters is provided in Table 4.3. The qualitative morphology of the mouse has not been investigated, because the landmark-based geometric morphometric analysis conclusively revealed the morphological pattern of the cervical vertebrae and the identical regionalisation has been independently identified by a previous study (Buchholtz et al. 2012).

In crocodylians, the second cervical vertebra is unique in its morphology as it develops a dens which articulates with the atlas. Additionally, the axis has a rounded hypapophysis (Figure 4.6. A). Furthermore, it lacks morphological characteristics that are present in the majority of the successive vertebrae. The third and fourth cervical vertebra share several osteological features. They possess a truncated hypapophysis, a lateral concavity on the centrum and a rugosity on the latero-dorsal edge of the condylar fossa in anterior view (Figure 4.6. A). The latter character can solely be identified in C3 and C5. The adjacent vertebrae C5, C6 and C7 are characterised by an anteriorly-pointing, sickle-shaped hypapophysis, a ventral keel extending from the hypapophysis and ending in a rugosity on the ventral posterior surface of the centrum as well as a rugosity on the dorsal posterior surface of the postzygapophysis and a lateral concavity on the centrum (Figure 4.6. A). The last two cervical vertebrae differ in their morphology from the other vertebrae because they develop a prominent knob on the tip of the neural spine, which is a muscle insertion point (Figure 4.6. A). Additionally, the longitudinal axes of the diapophysis and the parapophysis have an orientation of about 45° posterior from the vertical line. They lack a rugosity on the dorsal posterior surface of the postzygapophysis, but show a rugose concavity on the lateral surface of the prezygapophysis.

In the chicken, the second cervical vertebrae has no ribs (Figure 4.6. B). In addition to the dens, the absence of tubercula anae, as well as of a transverse and pneumatic foramen, clearly distinguishes the axis from the successive cervical vertebrae in the bird. The vertebrae C3, C4 and C5 have two tubercula anae and several cristae laterales (Figure 4.6. B). The torus dorsalis is near the tip of the postzygapophysis and the shape of the foramen transversarium is round. The sixth and seventh vertebrae of the neck lack a hypapophysis, which is present in most other cervical vertebrae (Figure 4.6. B). Furthermore, both vertebrae have three tubercula anae and cristae laterales and they develop a processus caroticus. The torus dorsalis is shifted anteriorly and lies near the base of the neural spine. The shape of the transverse foramen is oval. C8 is the first vertebra that develops a bifurcated neural spine (Figure 4.6. B). It has four tubercula anae and cristae laterales. The torus dorsalis is shifted posteriorly and lies near the base of the postzygapophysis. The adjacent vertebrae share most of these osteological features. However, the last two cervical vertebrae (C13 and C14)

differ in some characters, such as they lack a processus caroticus and a pneumatic foramen. Additionally, the shape of the foramen transversarium is round.

Although there are minor differences between the Nile crocodile and the American alligator, the variation in the qualitative characters indicates four morphological subregions in the crocodilian neck. Five cervical subunits are recognised in the chicken.

Character	Abbreviation	Description
ribs	-	presence or absence of ribs
hypapophysis <sup>1</sup>	hyp	presence or absence and shape (rounded, truncated, pointed anteriorly) of the ventral process
neural spine	spin	development of a prominent knob on the tip of the neural spine (muscle insertion) <sup>1</sup> ; development of bifurcation <sup>2</sup>
diapophysis <sup>1</sup>	dia	orientation of the longitudinal axis (45°, 90°, 315° posterior from vertical line)
parapophysis <sup>1</sup>	para	orientation of the longitudinal axis (45°, 90°, 315° posterior from vertical line)
tubercula ansae <sup>2</sup>	tub	number of the knob-like surface features of the ansa costotransversaria
cristae laterales <sup>2</sup>	crist	number of the linear crests extending from tuberculae ansae
ventral keel <sup>1</sup>	keel	presence or absence of a ventral keel extending from the hypapophysis and ending in a posterior ventral rugosity on the centrum
processus caroticus <sup>2</sup>	caro	presence or absence of the paired ventral processes
postzygapophysis <sup>1</sup>	poz	presence or absence of rugosity on dorsal posterior surface of the posterior zygapophysis
centrum <sup>1</sup>	cent	presence or absence of a lateral concavity on the centrum
torus dorsalis <sup>2</sup>	tor	presence or absence of the dorsal process on the crista transverso-obliqua between the neural spine and the postzygapophysis
condylar fossa <sup>1</sup>	cond	presence or absence of a rugosity on the latero-dorsal edge of the condylar fossa in anterior view (kidney shape)
prezygapophysis <sup>1</sup>	prez	presence or absence of a (rugose) concavity on the lateral surface of the anterior zygapophysis
foramen transversarium <sup>2</sup>	trans	shape of the transverse foramen
pneumatic foramen <sup>2</sup>	pneu	presence or absence of a pneumatic foramen

**Table 4.3.: Description of the qualitative characters identified in the cervical vertebrae of extant archosaurs.** The same abbreviations provided in this table are used in Figure 4.6. Note that there are morphological features that can solely be identified in the <sup>1</sup>crocodilian or the <sup>2</sup>bird.

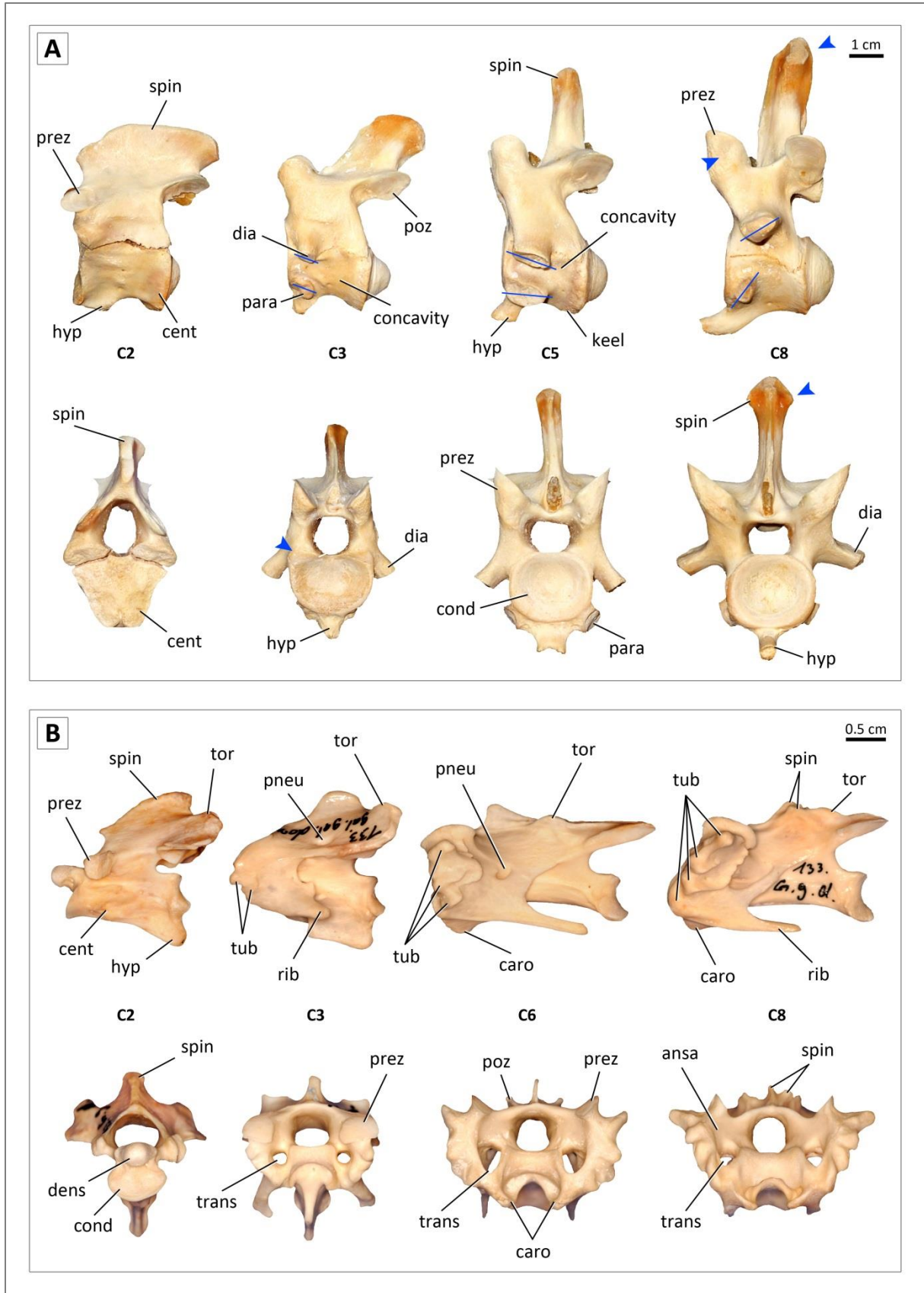


**Figure 4.6: Qualitative morphology of representative cervical vertebrae in extant archosaurs.** The structural features indicate the morphological differentiation of the neck in (A) alligator (SAPM No. 3) and (B) chicken (SAPM No. 133). The vertebrae are represented by photographs in left lateral view (first row) and in anterior view (second row). Blue lines and arrows mark important osteological characters. Refer to Table 4.3. for abbreviations and description. Note that the dens of C2 is not shown in the alligator.

#### 4.3.2.2. Quantitative morphology (landmark analysis)

The landmark-based geometric morphometric study allowed the quantitative assessment of the varying morphology of the cervical vertebrae, to gain additional insights into the regionalisation of the neck. The Relative Warps Analysis summarised the vertebral shape differences and 3D thin-plate splines visualised the morphological changes from the average (Figure 4.7.). The first two RWs explained about 70-90% of the variation in the sample for each examined taxon. In all examined amniotes, the morphological groups separate along the axes. The morphologically clearly distinct second cervical vertebra always occupies a unique region of the morphospace (Figure 4.7.). A group of following anterior cervicals clusters away from posterior vertebrae. In between is a cluster of middle cervical vertebrae. In general, the morphological differences within each cervical region involve variation in the shape of the vertebral centrum, the pre- and postzygapophysis and the neural spine (Figure 4.7.). As well as in the relative position of the diapophysis and the parapophysis, which is only detected in the crocodylians (Figure 4.7. A and B), because the vertebrae of the mouse and the chicken lack unambiguous diapophyseal and parapophyseal landmarks.

The morphological differences of the cervical vertebrae, observed along the RW axes, are not a function of size. The size regression analysis (log centroid size vs. RWs) revealed no significant correlation between shape variation and size in all analysed taxa.

#### 4.3.2.3. Morphological pattern (Principal Coordinates and Cluster Analysis)

The morphospace occupation along the first two PCOs (which account for about 70-90% of the explained variation) for each examined amniote shows substantial differences between the cervical vertebrae. The combined morphological analysis allowed the comprehensive discrimination of vertebrae at different cervical levels, revealing the pattern of the functional segmental units of the vertebral column. The grouping of the vertebrae corresponds to their position in one of the four quadrants of the coordinate system. The discrimination of the respective clusters is based on the highest distance between successive vertebrae in the PCO morphospace, which is visualised by the Cluster Analysis. Thus, the amniote neck (excluding the atlas) can be subdivided into three, four or five morphological subdomains, depending on the total number of cervical vertebrae (Figure 4.8.). The general units are the axis complex, an anterior section and a posterior group. Depending on the cervical number, an additional subdomain can be recognised in the mid-cervical series, which is the main difference between different groups of archosaurs.

The Principle Coordinate Analysis of both morphometric and qualitative morphological characters recovered four subregions for the crocodylian neck, corresponding to the axis, two anterior, three middle and two posterior cervical vertebrae as morphological subdomains (Figure 4.8. A and B, Appendix 4.5. A and B).

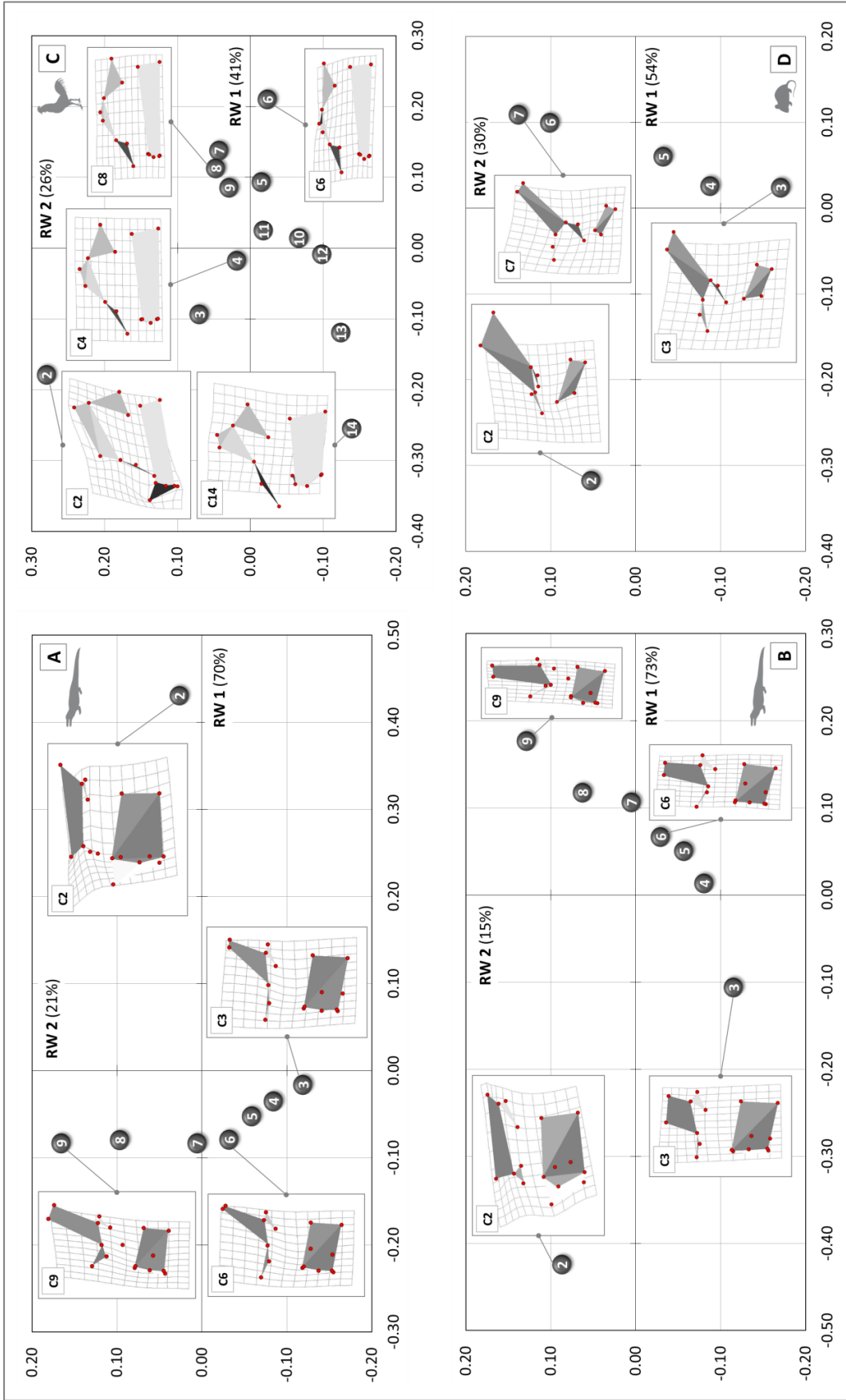


**Figure 4.7.: Relative Warps (RW) Analysis results for modern amniotes.** Each plot shows the shape differences of the cervical vertebrae along RW 1 and RW 2. Thin-plate splines (3D in left lateral view) visualise the variation between landmark configurations of the vertebrae from the respective average shape (zero point). (A) crocodile, (B) alligator, (C) chicken, (D) mouse.

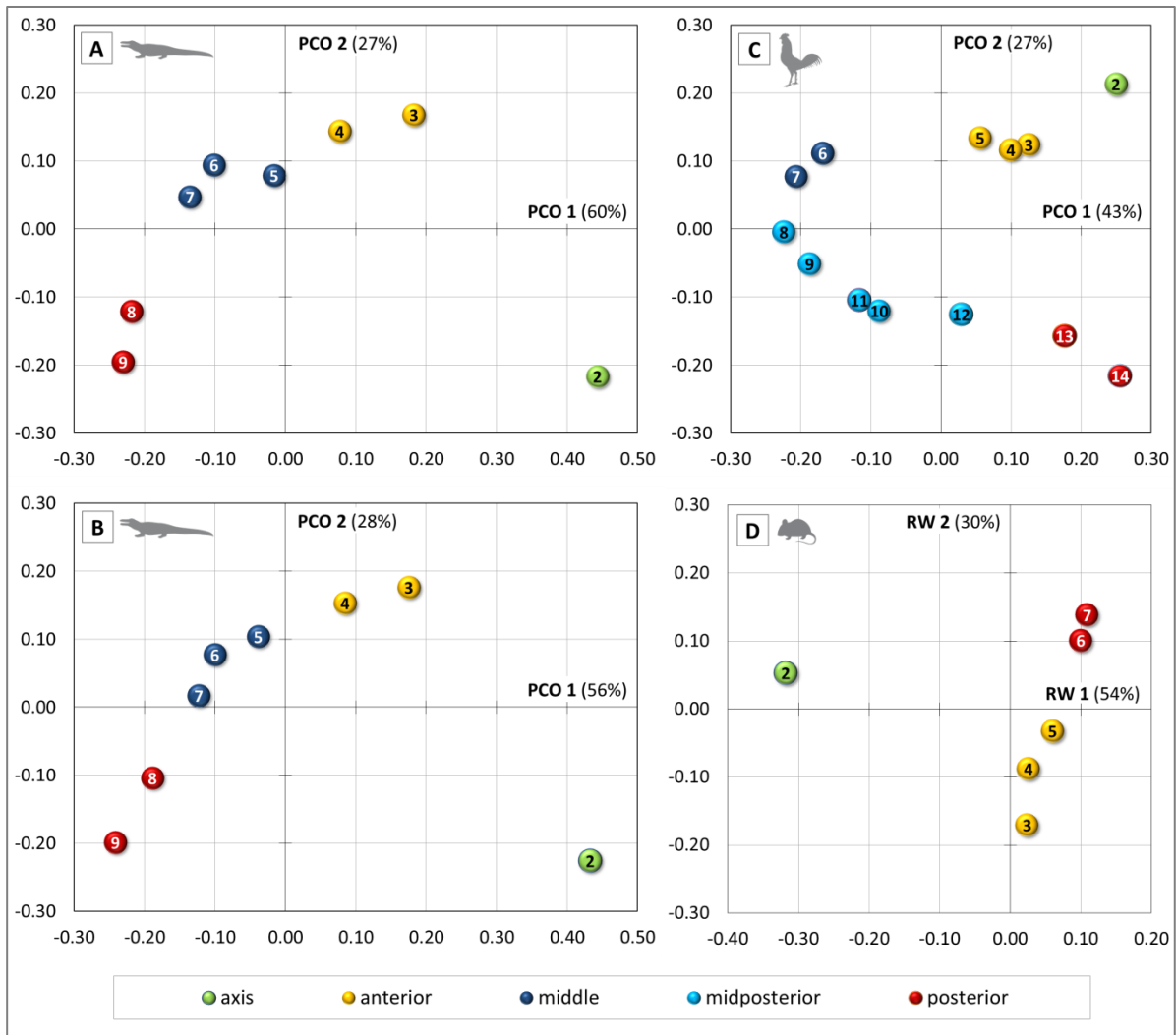


**Figure 4.8.: Principal Coordinates (PCO) Analysis results for modern amniotes.** The plots for (A) crocodile, (B) alligator and (C) chicken show the discrimination of the cervical vertebrae along PCO1 and PCO 2. The morphological pattern of the cervical vertebrae in (D) mouse is represented by the Relative Warps Analysis plot because the it conclusively revealed the regionalisation. The pattern of the segmental units corresponds between the crocodylians, but is different in the bird and the mammal.

The relatively long neck of chicken is subdivided into five morphological subregions (Figure 4.8. C, Appendix 4.5. C). Additional to the axis, three anterior, two middle and two posterior cervical vertebrae, there is also a midposterior cervical compartment, comprising C8 to C12. Another difference between the morphological pattern of crocodiles and chickens is that the number of cervical vertebrae that form the anterior subdomain is higher and that of the middle subregion is lower in birds.

In the mouse, the previous landmark analysis conclusively revealed the regionalisation of the cervical vertebrae. A three-subunit pattern in cervical morphology is detected, which includes one axis, three anterior and two posterior vertebrae as functional segments (Figure 4.8. D). This pattern appears to be typical for the mammalian neck (Böhmer et al. 2011, Buchholtz et al. 2012).

### 4.3.3. Correlation between *Hox* gene expression and vertebral morphology

Comparing the *Hox* gene expression pattern with the morphological subdomains of the amniote neck reveals that vertebrae that form clusters in the morphological analysis have identical patterns of *Hox* gene expression. Thus, distinct shape changes in cervical vertebrae (that is the first vertebra of each subregion) coincide with differences in the activity of cervical *Hox* genes.

In the crocodilian neck, the morphological analysis revealed that the vertebrae C2, C3, C5 and C8 show significant changes in morphology. The anterior expression limits of the *Hox-4* and *Hox-5* paralog genes coincide with the boundaries of distinct shape change (Figure 4.9. A). *HoxB-5* expression is associated with the development of the second cervical vertebra. The expression of *HoxB-4* and *D-4* correlates with the anterior subdomain comprising C3 and C4. The middle subregion (C5, C6, C7) is related to the expression of *HoxA-4* and *C-4*. The anterior expression limit of *HoxC-5*

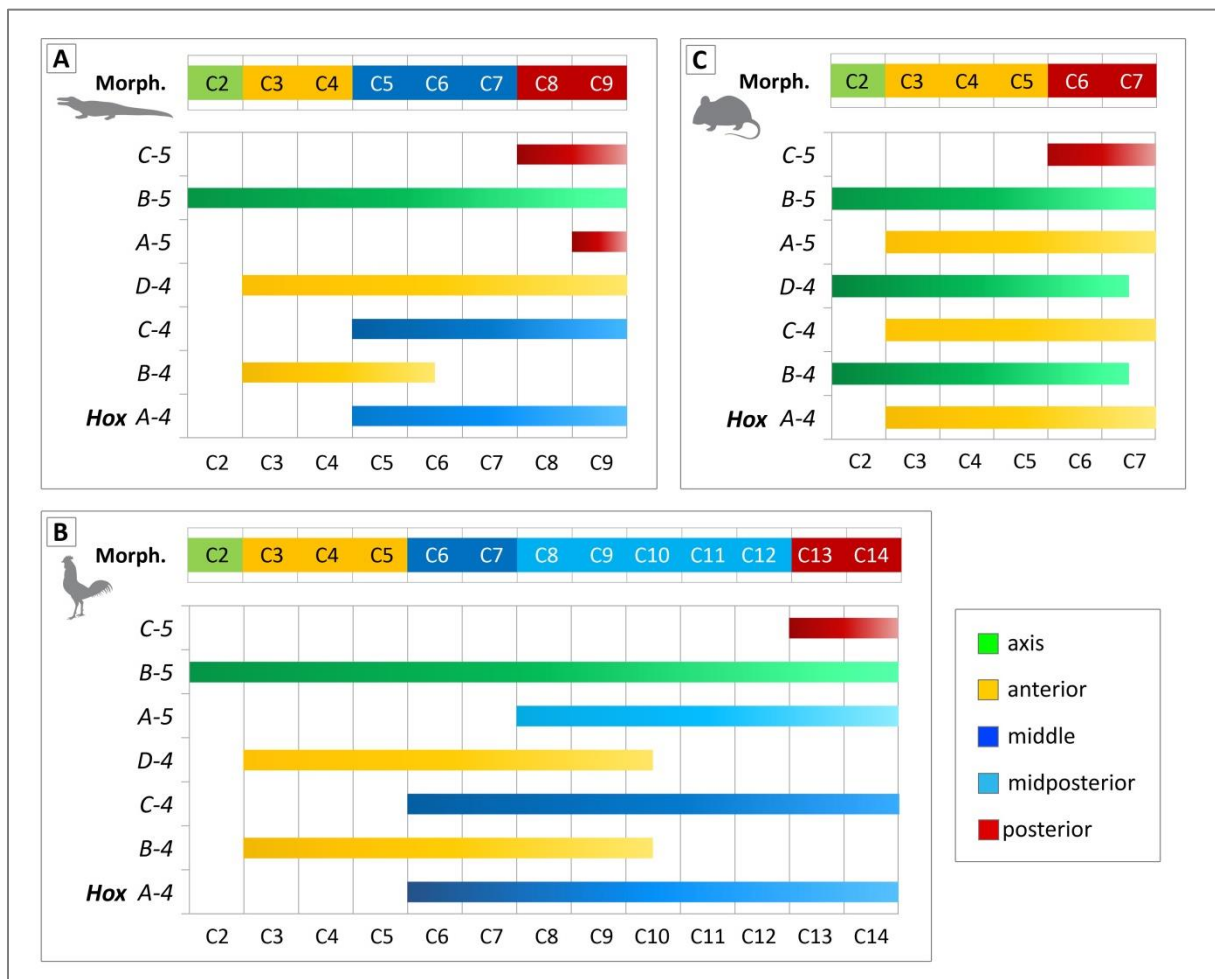


**Figure 4.9.: Morphological subdomains and *Hox* gene expression pattern in the neck of modern amniotes.** Vertebrae that share a common morphology form a morphological subregion. Comparing this pattern with the genetic activity reveals that distinct shape changes in cervical vertebrae coincide with differences in the *Hox* gene expression in (A) crocodilians, (B) chicken and (C) mouse. Note that the anterior expression limit of *HoxD-4* in the mouse lies at C1 which is not depicted in the illustration. Except for *HoxB-5* the *Hox* gene expression analysis in crocodiles was part of the present study. Refer to section 4.3.1. for detailed references of the *Hox* code in chicken and mouse.

coincides with the posterior subdomain (C8, C9). In contrast to the fact that *HoxA-5* expression starts at the last cervical vertebra (C9), the morphological analysis did not discriminate C8 and C9.

For the longer neck of the chicken, the shape investigation detected distinct changes in morphology at the vertebrae C2, C3, C6, C8 and C13. Corresponding to the boundaries of significant shape change, the anterior expression limits of the *Hox-4* and *Hox-5* paralog genes have been detected at the respective vertebrae (Figure 4.9. B). Similar to the crocodile, *HoxB-5* expression is related to the development of the second cervical vertebra. The expression of *HoxB-4* and *D-4* is associated with the anterior subdomain (C3, C4, C5). The anterior expression limits of *HoxA-4* and *C-4* are shifted posteriorly by one vertebra in comparison to crocodylians, which correlates with the middle subregion (C6, C7). *HoxA-5* expression coincides with the midposterior subdomain comprising C8 to C12. The expression of *HoxC-5* is related to the posterior subregion (C13, C14).

The morphological analysis of the neck in mice showed significant shape changes at the vertebrae C2, C3 and C6. The anterior expression boundaries of the *Hox-4* and *Hox-5* paralog genes correlate with the limits of distinct change in morphology (Figure 4.9. C). As previously observed in the crocodile and the chicken, the expression of *HoxB-5* is associated with the development of the second cervical vertebra. The anterior expression limit of *HoxB-4* is shifted anteriorly and correlates with C2 as well. In contrast to the analysed archosaurs, *HoxD-4* expression is related to the first cervical vertebra. The expression of *Hox A-4* and *C-4* coincides with the anterior subdomain (C3, C4, C5). Additionally, the anterior expression limit of *HoxA-5* is also associated with this subregion. *HoxC-5* expression is related to the posterior subdomain comprising C6 and C7.

In summary, changes in the number of vertebrae are associated with changes in the morphological grouping of the cervical region. The *Hox* gene expression pattern significantly correlates with the pattern of the morphological subdomains in the neck of the analysed amniote taxa. The expression of each *Hox* gene maintains a definite, gene-specific anterior limit that is associated with vertebrae at which distinct shape changes occur.

#### 4.3.4. Vertebral morphology and *Hox* gene expression in extinct archosaur

The correlation of vertebral morphology and *Hox* gene expression patterns thus enables the hypothesis of the latter from morphological changes. The morphological pattern appears to serve as a proxy for the underlying *Hox* code in taxa where the genetic information is not directly retrievable, that is fossils. To test such a hypothesis, we analysed the morphological changes in the cervical vertebrae of an extinct relative of modern crocodiles and birds, the basal sauropodomorph dinosaur *Plateosaurus*.

#### 4.3.4.1. Vertebral morphology in *Plateosaurus*

The examination of the qualitative characteristics of the vertebrae in *Plateosaurus* revealed distinct morphological differences within the cervical region (Figure 4.10.). The distribution of the osteological features points towards the morphological differentiation of the cervical vertebral region. The complete data matrix is provided in Appendix 4.4. The detailed description of the morphological characters is provided in Table 4.4.

The second cervical vertebra of the sauropodomorph dinosaur shows a unique morphology; it has dens which articulates with the atlas. The neural spine is even and displays no thickening. The epiphysis extends over the postzygapophysis and there is a rugosity on the latero-dorsal edge of the condylar fossa in anterior view (Figure 4.10.). It lacks some morphological characteristics that are present in the majority of the successive vertebrae, such as a ventral keel on the centrum, an anterior and posterior centrodiaepophyseal lamina as well as a concavity on the lateral surface of the prezygapophyses. The vertebrae C3, C4 and C5 have several osteological features in common. They possess a small knob on the tip of the neural spine, a concavity on the lateral surface of the prezygapophysis and the epiphysis extends over the postzygapophysis (Figure 4.10.). The adjacent

Character	Abbreviation	Description
ventral keel	keel	presence or absence of a ventral keel
neural spine	spin	development of a prominent knob on the tip of the neural spine (muscle insertion)
diapophysis	dia	orientation of the longitudinal axis (45°, 90°, 315° posterior from vertical line)
parapophysis	para	orientation of the longitudinal axis (45°, 90°, 315° posterior from vertical line)
epiphysis	epi	bony projection extends over postzygapophysis or does not extend over postzygapophysis
anterior centrodiaepophyseal lamina	acd1	presence or absence of the lamina that connects the diapophysis to the anterior aspect of the neurocentral junction
posterior centrodiaepophyseal lamina	pcdl	presence or absence of the lamina that projects from the diapophysis to the posterior portion of the neurocentral junction
condylar fossa	cond	presence or absence of a rugosity on the latero-dorsal edge of the condylar fossa in anterior view (kidney shape)
prezygapophysis	prez	presence or absence of a (rugose) concavity on the lateral surface of the anterior zygapophysis

**Table 4.4.:** Description of the qualitative characters identified in the cervical vertebrae of the extinct archosaur *Plateosaurus*. The same abbreviations provided in this table are used in Figure 4.10.

vertebrae C6, C7 and C8 are characterised by a ventral keel on the centrum (Figure 4.10.). Additionally, they have an anterior and posterior centrodiaepophyseal lamina. The last two vertebrae C9 and C10 develop a prominent knob on the tip of the neural spine and the epiphysis does not extend over the postzygapophysis (Figure 4.10.). They have a concavity on the lateral surface of the prezygapophysis, as previously observed in the other cervical vertebrae (except C2).

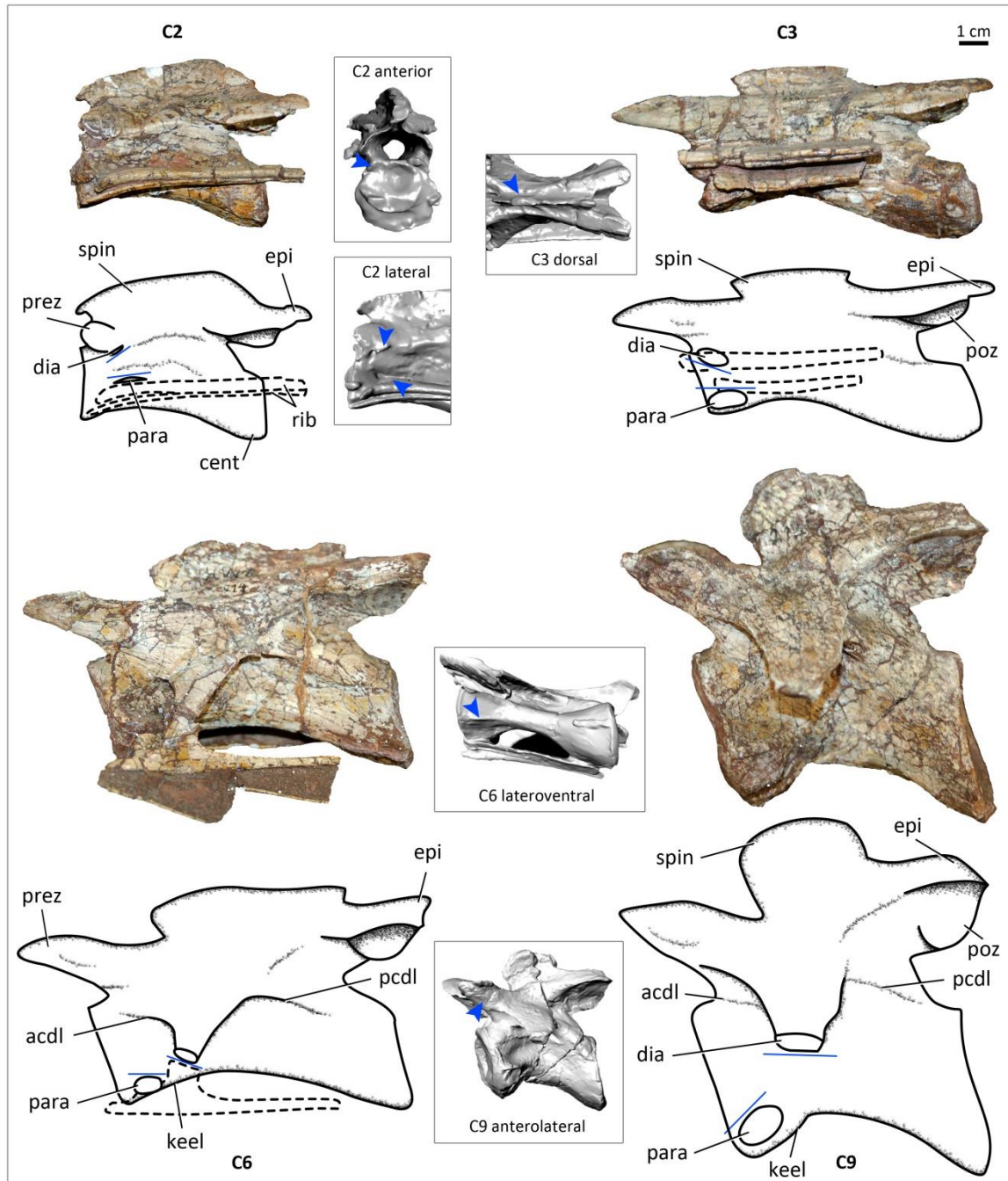


**Figure 4.10.: Qualitative morphology of representative cervical vertebrae in the extinct archosaur.** The structural features indicate the morphological differentiation of the neck in *Plateosaurus* (GPIT/RE/7288). Each vertebra is represented by a photograph in left lateral view and an interpretative line drawing. Details (not to scale) of the 3D model of the respective vertebrae illustrate morphological characters that are not precisely visible in the lateral photographs. Blue lines and arrows mark important osteological characters. Refer to Table 4.4. for abbreviations and description. Note that the dens of C2 is not shown.

The regionalisation of the dinosaur cervical vertebrae is also indicated by quantitative shape differences as revealed by the landmark analysis (Figure 4.11.). The first two RWs explained about 80% of the variation in the vertebrae of *Plateosaurus*. As previously observed for the modern amniotes, the morphological groups separate along the axes. The morphologically unique second cervical vertebra is distant from the other vertebrae in the morphospace (Figure 4.11.). There is a cluster of anterior cervicals that is separate from the posterior vertebrae. In between is a group of middle cervical vertebrae. Corresponding to the Relative Warps Analysis in the extant taxa, the morphological variations within each cervical subregion include differences in the shape of the vertebral centrum, the pre- and postzygapophysis and the neural spine (Figure 4.11.). There is also variation in the relative position of the diapophysis and the parapophysis, as previously observed for the crocodylians.

The morphological differences of the cervical vertebrae in *Plateosaurus*, observed along the RW axes, are not a function of size. The size regression analysis (log centroid size vs. RWs) revealed no significant correlation between shape variation and size.

Combining the qualitative and quantitative morphological data via the Principal Coordinates Analysis showed substantial differences between the cervical vertebrae of *Plateosaurus*. The morphospace

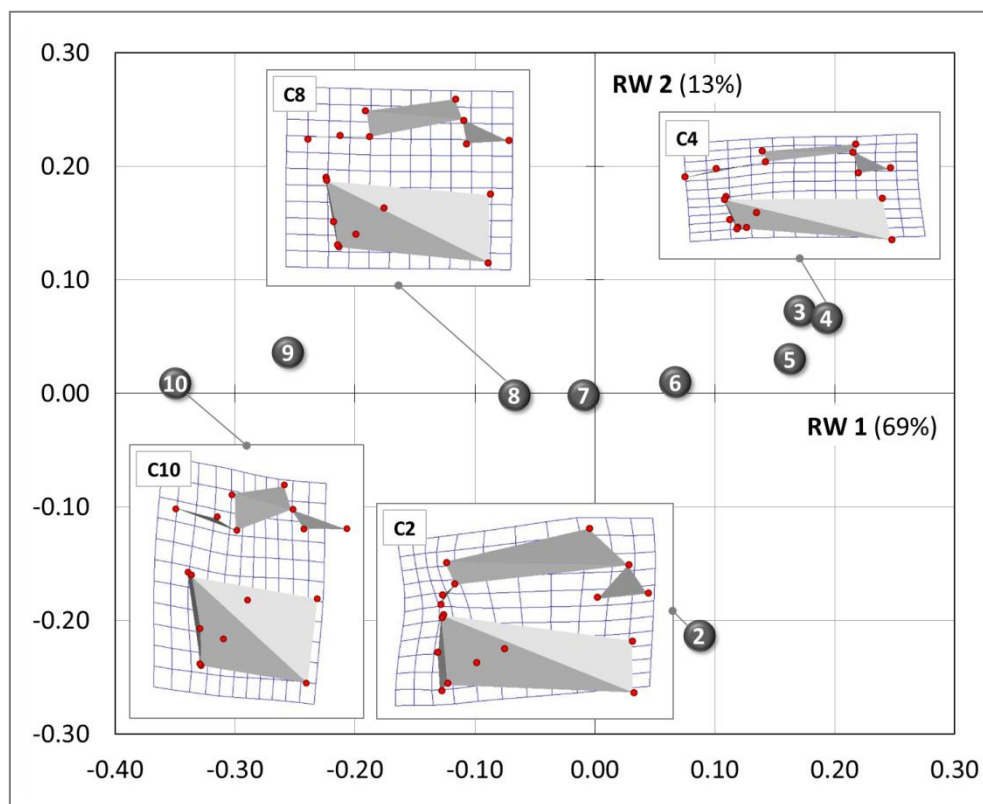
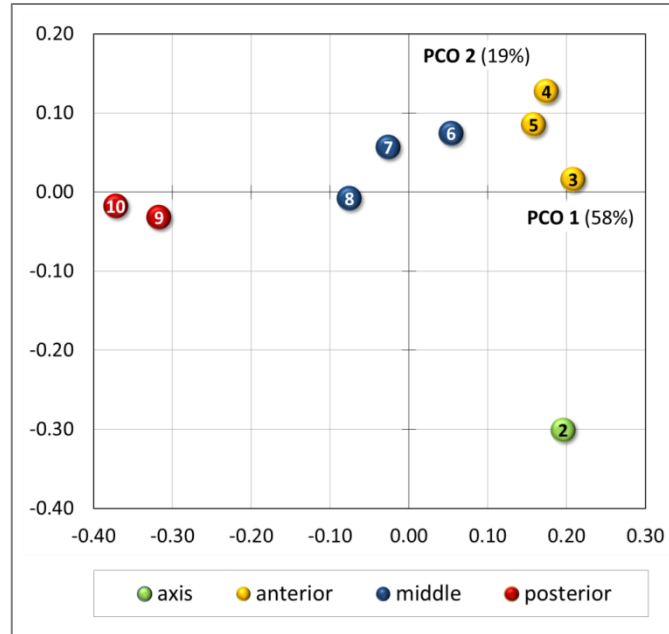


Figure 4.11.: Relative Warps (RW) Analysis results for the extinct archosaur *Plateosaurus*. The plot shows the shape differences of the cervical vertebrae along RW 1 and RW 2. Thin-plate splines (3D in left lateral view) visualise the variation between landmark configurations of the vertebrae from the average shape (zero point).

occupation along the first two PCOs (account for almost 80% of the explained variation) indicates four morphological subregions in the neck: the axis, three anterior, three middle and two posterior cervical vertebrae (Figure 4.12., Appendix 4.6.). This pattern of segmental units resembles that seen in crocodylians, but with the variation that the anterior cervical subdomain is expanded by one vertebra, as observed in the chicken.



**Figure 4.12.: Principal Coordinates (PCO) Analysis results for the extinct archosaur *Plateosaurus*.** The plot shows the discrimination of the cervical vertebrae along PCO1 and PCO 2. The morphological pattern of the cervical vertebrae is similar to the pattern previously observed in crocodylians, but with the variation that the anterior subdomain is expanded by one vertebra as observed in chicken. Refer to Figure 4.8. for comparison with PCO results of extant archosaurs.

#### 4.3.4.2. *Hox* gene expression in *Plateosaurus*

On the basis of the correlation between vertebral morphology and *Hox* gene expression noted above (see section 4.3.3), a hypothetical *Hox* code for the extinct dinosaur *Plateosaurus* can be established. The hypothetical segment-specific *Hox* code for *Plateosaurus* is reconstructed via the extant phylogenetic bracket approach and the use of the vertebral shape changes as *Hox* gene expression pattern proxy, and it appears to be generally similar to the genetic pattern observed in crocodylians (Figure 4.13.). The distinct morphology of the second cervical vertebra is associated with *HoxB-5* expression. The anterior subdomain comprising C3, C4 and C5 is related to the expression of *HoxB-4* and *D-4*. The middle subregion (C6, C7, C8) correlates with the expression of *HoxA-4* and *C-4*. The posterior subdomain is associated with *HoxC-5* and *A-5* expression. These results indicate that the posterior shift of the expression boundary of *HoxA-4* and *HoxC-4* seen in modern birds is already present in the basal saurischian dinosaur (Figure 4.13.). The anterior shift of the expression boundary of *HoxA-5* cannot yet be recognised in *Plateosaurus* because the morphological study did not reveal a midposterior subdomain (Figure 4.13.). However, the anterior expression limits of *HoxA-5* and *C-5* are shifted posteriorly because the posterior subregion in the dinosaur comprises C9 and C10 (in contrast to C8 and C9 in crocodylians) (Figure 4.13.).

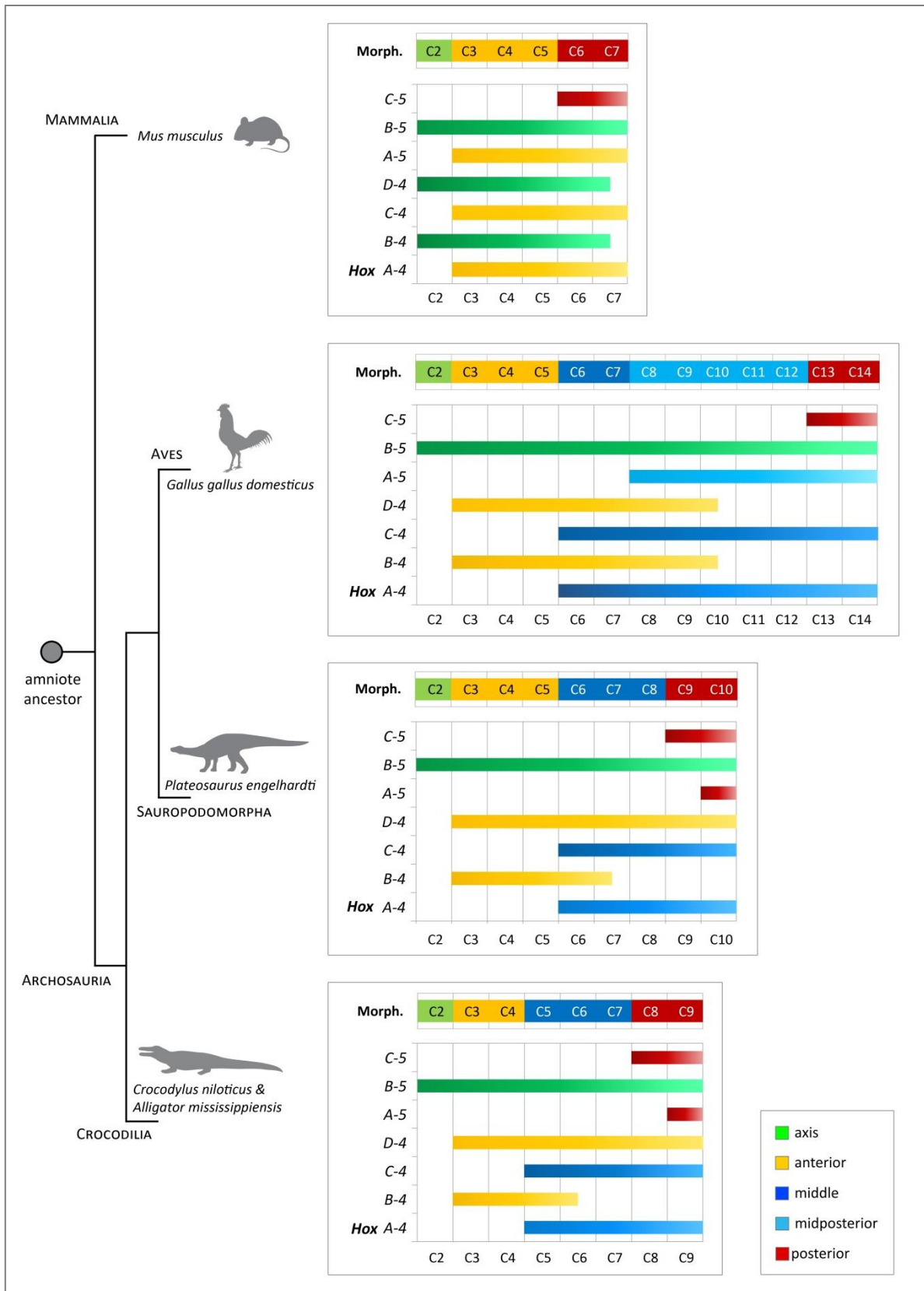


Figure 4.13.: Phylogenetic distribution of morphological subdomains and Hox gene expression pattern in the neck among extant and extinct amniotes. The correlation between Hox code and vertebral morphology in modern crocodiles and birds allows a reconstruction of the Hox code in the extinct archosaur *Plateosaurus* on the basis of the morphological subdomain pattern. Note that the anterior expression limit of *HoxD-4* in the mouse lies at C1 which is not depicted in the illustration. Except for *HoxB-5* the Hox gene expression analysis in crocodiles was part of the present study. Refer to section 4.3.1. for detailed references of the Hox code in chicken and mouse.

## 4.4. Discussion

### 4.4.1. *Hox* gene expression correlates with vertebral morphology

Whole-mount *in situ* hybridisation experiments in various amniote taxa, including the Nile crocodile analysed here, revealed that the *Hox* genes are key determinants for the establishment of vertebral segments along the primary body axis. The activity of these highly conserved genes is required for proper organisation of the amniote body plan. *Hox* mutation experiments in mice supported this requirement during animal development (reviewed in Wellik 2009). Mutating one or more *Hox* paralogs has dramatic effects on the axial column, and reveals abnormalities affecting the vertebral region in which they are expressed. For instance, *HoxA-4* expression is necessary for proper development of the third cervical vertebra in mice because mutation of this gene results in an anterior morphological transformation of C3 to C2 (Horan et al. 1994, Kostic and Capecchi 1994). The vertebra C3 acquires characteristics that are normally associated with C2, such as a prominent neural spine (Figure 4.14.). Although final evidence of the role of *Hox* genes in specifying the axial skeleton in non-mammalian amniotes would involve mutation analyses in these taxa, the high spatial, temporal and functional conservatism of these genes make them a very strong candidate for vertebral development.

By specifying the differential morphology of vertebrae, *Hox* genes are responsible for the regionalisation of the axial column. There is a striking correspondence between sets of *Hox* genes and distinct vertebral regions along the body axis of modern amniotes (Figure 4.2.). As indicated by earlier analyses (e.g. Burke et al. 1995, Mansfield and Abzhanov 2010), this study showed that the same seven *Hox* genes (*Hox-4* and *Hox-5* paralog groups) are expressed during development of the neck in different taxa. Despite this exceptional genetic uniformity there are significant variations

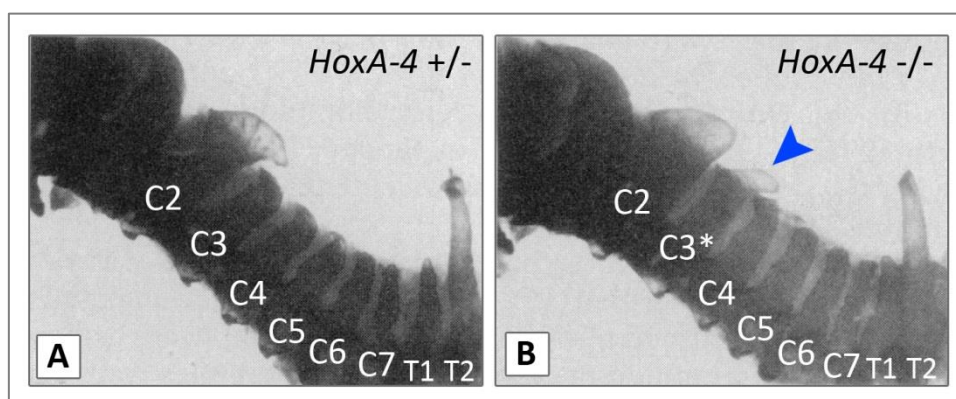


**Figure 4.14.: *HoxA-4* mutation in adult mice.** Dorsolateral view of the cervical (C2-C7) and anterior thoracic vertebrae (T1, T2) in (A) a heterozygote and (B) a homozygous mutant. The heterozygote corresponds to the wild-type mouse because it does not possess a prominent neural spine on C3. In the *HoxA-4* homozygous mutant, an anterior transformation of C3 to C2 occurs (indicated by asterisk). The blue arrow points to the ectopic neural spine on C3 which now resembles the shape of C2. (Modified after Horan et al. 1994)

in the number of cervical vertebrae among different groups of amniotes. These morphological differences are detectable in the taxon-specific subunit pattern of vertebral shape within the cervical series. Similarities and variations in the shape of successive vertebrae are already visible to the unaided eye, which was apparent by the investigation of the qualitative characters of the cervical vertebrae in extant and extinct amniotes. The landmark-based geometric morphometric analysis allowed the quantitative assessment of the vertebral morphology, which is also a method with which to objectively evaluate the shape of bones. Combining both data sets via the Principal Coordinates Analysis revealed the morphological pattern of the cervical vertebral column. The differences between the cervical subunit patterns among the analysed amniotes correlate with variations in the *Hox* gene expression. Although there is one discrepancy in crocodylians regarding the association of *HoxA-5* expression and the posterior cervical vertebrae (Figure 4.9. A), changes in segmental organisation are driven by changes in function of *Hox* genes. *HoxA-5* is the most dynamic in its expression in amniote taxa (Mansfield and Abzhanov 2010). This may suggest a secondary role in the patterning of the axial skeleton, and therefore allows the evolution of varying functions in different animals. In the chicken, the expression of *HoxA-5* is anteriorly shifted and correlates with the morphological midposterior subdomain of the avian neck (Figure 4.9. C).

The present study showed that the anterior *Hox* gene expression limits shift together with the displacement of cervical subdomains. This provides a reasonable mechanism for evolutionary patterns along the axial column. Because morphological similarity is directly causally related to *Hox* gene expression, it seems to be possible to use axial shape variation in modern archosaurs with varying vertebral count as a proxy for *Hox* gene expression. In order to further prove this correlation between the *Hox* code and vertebral morphology, future studies on additional taxa should provide further insights into the genetic mechanisms that drive morphological evolution. Using the vertebral shape pattern to infer the *Hox* code not only in extant animals, but more importantly, in extinct ones, it seems to be possible to study the previously unknown genomic mechanisms driving morphological evolution in extinct lineages, such as sauropodomorph dinosaurs. The *Hox* gene expression pattern in the extinct archosaur *Plateosaurus* was established on the basis of quantifiable changes in vertebral morphology. We lack conclusive proof because fossil taxa do not preserve the soft tissue that would allow to directly analyse the *Hox* gene expression pattern. However, the congruence of the results as intermediate between the representatives of the extant phylogenetic bracket (Figure 4.13.) indicates the utility of morphological analysis as a proxy for the underlying genomic foundation of the vertebral column in archosaurs. For the first time, profound insights into the evolutionary development of the axial column in an extinct archosaur are gained.

#### 4.4.2. Modification of *Hox* gene expression associated with vertebral evolution

Vertebral morphology and number have far-reaching consequences for organismal function and ecology. The different functional anatomy of the head-neck system yields potential selective advantages. Although a great variety in the number of vertebrae can be recognised in amniotes, there is little diversity in terms of options for functional axial units. The general morphological groups of the neck include: the atlas-axis complex forming a functional unit that carries the head, the anterior and the middle subdomain and the posterior subgroup which forms the junction from the highly mobile cervical column to the relatively stiff thoracic spine. Additionally, a midposterior subdomain can be recognised if the neck is relatively long. The ancestral archosaur *Hox* code may be similar to that of crocodylians (Figure 4.13.). With an increasing number of cervical vertebrae and therefore an increasing anatomical complexity (due to a longer neck) the *Hox* gene expression patterns were expanded and shifted relatively to each other, respectively. The first step towards the elongation of the cervical vertebral column as seen in chicken in comparison to crocodiles may have been the addition of one vertebra to the anterior section of the neck (Figure 4.13.). The next step may have involved the further addition of vertebrae to the middle region. The present morphological analysis showed that in the basal sauropodomorph dinosaur *Plateosaurus* the anterior cervical subregion is expanded by one vertebra and may thus represent the first step towards neck elongation. Changes in the number of cervical vertebrae associated with changes in the morphological subdomains of the neck suggest that important modifications in the expression of *Hox* genes have occurred during amniote evolution. Ultimately, this may have facilitated the extraordinary evolution of the sauropodomorph dinosaurs towards extreme neck lengths that remain unsurpassed in all other terrestrial animals.

#### 4.5. Conclusion

Determination of the number and morphological identity of vertebrae are subjects of major importance in the evolution of amniotes. The highly conserved *Hox* genes play a fundamental role in the development of the axial column, because they specify vertebral shape and thus are responsible for the regionalisation of the primary body axis. The first objective of this study involved the investigation of the *Hox* gene expression pattern in the Nile crocodile. The whole-mount *in situ* hybridisation experiments revealed that the same *Hox-4* and *Hox-5* paralog genes are active in the crocodylian neck. The second goal was to test the link between *Hox* code and vertebral morphology of extant archosaurs as a case study for a comprehensive understanding of patterns of vertebral evolution in amniotes. In order to establish vertebral homologies in taxa with different vertebral count, the cervical series was differentiated into morphological subdomains. By comparing the anterior expression boundaries of the *Hox* genes in modern amniotes, a correlation between these

expression limits and the boundaries of morphologically distinct subregions in the cervical column was demonstrated here. Using the axial bone shape pattern as a proxy for the *Hox* code in extinct animals, it is possible to hypothesise the *Hox* code in fossil taxa lacking direct genetic information, which was the third objective of this work. Neck elongation is a prominent feature in the evolution of ornithodiran archosaurs, both on the lineage towards modern birds and also in sauropodomorph dinosaurs, in which the extremely elongated neck has been directly linked to their ecological success (Sander et al. 2011). On the basis of the results presented here, an evaluation of the importance of modifications in *Hox* gene expression patterns in relation to this neck elongation appears feasible, leading to new insights into the genetic mechanisms that shaped dinosaur evolution. For the first time, the exact modifications in *Hox* gene expression in extinct archosaurs, such as the basal sauropodomorph *Plateosaurus*, were identified in order to elucidate how evolutionary changes of the axial column occurred.

The integration of genes, morphology and fossils allows for the comprehensive analysis of the evolution of life (Slater et al. 2012, Thewissen et al. 2012). A better understanding of vertebral development provides new insights into the evolutionary mechanisms responsible for the great morphological flexibility of the axial column. The highly variable cervical region has provided an illuminating model for the study of the relationship between genomic control and phenotypic changes. The evolution of *Hox* genes and associated changes in the axial column has been crucial in mediating the major transitions in the archosaurian body plan.

#### 4.6. References

- Baumel, J.J., King, A.S., Breazile, J.E., Evans, H.E., Vanden Berge, J.C., 1993. Handbook of avian anatomy: nomina anatomica avium. Nuttall Ornithological Club, Cambridge, 779 pp.
- Böhmer, C., Rauhut, O.W.M., Wörheide, G., 2011. Comparative shape analysis of the neck in extinct and extant archosaurs: implications for vertebral evolution in sauropodomorph dinosaurs. *Journal of Vertebrate Paleontology* **61A**: 73-74.
- Buchholtz, E.A., Bailin, H.G., Laves, S.A., Yang, J.T., Chan, M.Y., Drozd, L.E., 2012. Fixed cervical count and the origin of the mammalian diaphragm. *Evolution & Development* **14**: 399-411.
- Burke, A.C., Nelson, C.E., Morgan, B.A., Tabin, C., 1995. *Hox* genes and the evolution of vertebrate axial morphology. *Development* **121**: 333-346.
- Carroll, S.B., 1995. Homeotic genes and the evolution of arthropods and chordates. *Nature* **376**: 479-485.
- Cohn, M.J., Tickle, C., 1999. Developmental basis of limblessness and axial patterning in snakes. *Nature* **399**: 474-479.
- Galis, F., 1999. Why do almost all mammals have seven cervical vertebrae? Developmental constraints, *Hox* genes, and cancer. *Journal of Experimental Zoology Part B Molecular and Developmental Evolution* **285**: 19-26.
- Gaunt, S.J., 1994. Conservation in the *Hox* code during morphological evolution. *International Journal of Developmental Biology* **38**: 549-552.
- Gaunt, S.J., Krumlauf, R., Duboule, D., 1989. Mouse homeo-genes within a subfamily, *Hox*-1.4, -2.6 and -5.1, display similar anteroposterior domains of expression in the embryo, but show stage- and tissue-dependent differences in their regulation. *Development* **107**: 131-141.
- Gomez, C., Ösbudak, E.M., Wunderlich, J., Baumann, D., Lewis, J., Pourquié, O., 2008. Control of segment number in vertebrate embryos. *Nature* **454**: 335-339.
- Gomez, C., Pourquie, O., 2009. Developmental control of segment numbers in vertebrates. *Journal of Experimental Zoology Part B Molecular and Developmental Evolution* **312**: 533-544.
- Gower, J.C., 1966. Some Distance Properties of Latent Root and Vector Methods Used in Multivariate Analysis. *Biometrika* **53**: 325-338.
- Gower, J.C., 1971. A General Coefficient of Similarity and Some of Its Properties. *Biometrics* **27**: 857-871.
- Hammer, Ø., Harper, D.A.T., Ryan, P.D., 2001. PAST: Palaeontological Statistics software package for education and data analysis. *Palaeontologia Electronica* **4**: 1-9.
- Hargrave, M., Bowles, J., Koopman, P., 2006. In Situ Hybridization of Whole-Mount Embryos, in: Darby, I.A., Hewitson, T.D. (Eds.), *In Situ Hybridization Protocols*. Humana Press Inc., Totowa, pp. 103-113.
- Horan, G.S., Wu, K., Wolgemuth, D.J., Behringer, R.R., 1994. Homeotic transformation of cervical vertebrae in *Hoxa*-4 mutant mice. *Proceedings of the National Academy of Sciences* **91**: 12644-12648.

- Huene, F.v., 1926. Vollständige Osteologie eines Plateosauriden aus dem schwäbischen Keuper. *Geologische und Paläontologische Abhandlungen* **15**: 1-43.
- Imura, T., Pourquie, O., 2007. *Hox* genes in time and space during vertebrate body formation. *Development, Growth and Differentiation* **49**: 265-275.
- Johnson, D.R., O'Higgins, P., 1996. Is there a link between changes in the vertebral "*hox* code" and the shape of vertebrae? A quantitative study of shape change in the cervical vertebral column of mice. *Journal of Theoretical Biology* **183**: 89-93.
- Kaufman, T.C., Kewis, R., Wakimoto, B., 1980. Cytogenetic analysis of chromosome 3 in *Drosophila melanogaster*: the homeotic gene complex in polytene chromosome interval 84A-B. *Genetics* **94**: 115-133.
- Kessel, M., Gruss, P., 1990. Murine developmental control genes. *Science* **249**: 374-379.
- Kmita, M., Duboule, D., 2003. Organizing axes in time and space; 25 years of colinear tinkering. *Science* **301**: 331-333.
- Koob, T.J., Long, J.H., Jr., 2000. The vertebrate body axis: evolution and mechanical function. *American Zoologist* **40**: 1-18.
- Kostic, D., Capecchi, M.R., 1994. Targeted disruptions of the murine *Hoxa-4* and *Hoxa-6* genes result in homeotic transformations of components of the vertebral column. *Mechanisms of Development* **46**: 231-247.
- Krumlauf, R., 1994. *Hox* genes in vertebrate development. *Cell* **78**: 191-201.
- Lewis, E.B., 1978. A gene complex controlling segmentation in *Drosophila*. *Nature* **276**: 565-570.
- Mansfield, J.H., Abzhanov, A., 2010. *Hox* expression in the American alligator and evolution of archosaurian axial patterning. *Journal of Experimental Zoology Part B Molecular and Developmental Evolution* **314**: 1-16.
- McGinnis, W., Krumlauf, R., 1992. Homeobox genes and axial patterning. *Cell* **68**: 283-302.
- Morin-Kensicki, E.M., Melancon, E., Eisen, J.S., 2002. Segmental relationship between somites and vertebral column in zebrafish. *Development* **129**: 3851-3860.
- Müller, J., Scheyer, T.M., Head, J.J., Barrett, P.M., Werneburg, I., Ericson, P.G.P., Pol, D., Sánchez-Villagra, M.R., 2010. Homeotic effects, somitogenesis and the evolution of vertebral numbers in recent and fossil amniotes. *Proceedings of the National Academy of Sciences* **107**: 2118-2123.
- O'Higgins, P., Jones, N., 2006. Morphologica<sup>2</sup> (2.5). Hull York Medical School. Available from <http://sites.google.com/site/hymsfme/downloadmorphologica>.
- Ohya, Y.K., Kuraku, S., Kuratani, S., 2005. *Hox* code in embryos of Chinese soft-shelled turtle *Pelodiscus sinensis* correlates with the evolutionary innovation in the turtle. *Journal of Experimental Zoology Part B Molecular and Developmental Evolution* **304**: 107-118.
- Pearson, J.C., Lemons, D., McGinnis, W., 2005. Modulating *Hox* gene functions during animal body patterning. *Nature Reviews Genetics* **6**: 893-904.
- Pourquie, O., 2003. The segmentation clock: converting embryonic time into spatial pattern. *Science* **301**: 328-330.

- Rancourt, D.E., Tsuzuki, T., Capecchi, M.R., 1995. Genetic interaction between *hoxb-5* and *hoxb-6* is revealed by nonallelic noncomplementation. *Genes & Development* **9**: 108-122.
- Romer, A.S., 1976. *Osteology of the Reptiles*. The University of Chicago Press, Chicago, 772 pp.
- Sander, P.M., Christian, A., Claus, M., Fechner, R., Gee, C.T., Griebeler, E.-M., Gunga, H.-C., Hummel, J., Mallison, H., Perry, S.F., Preuschoft, H., Rauhut, O.W.M., Remes, K., Tütken, T., Wings, O., Witzel, U., 2011. Biology of the sauropod dinosaurs: the evolution of gigantism. *Biological Reviews* **86**: 117-155.
- Slater, G.J., Harmon, L.J., Alfaro, M.E., 2012. Integrating fossils with molecular phylogenies improves inference of trait evolution. *Evolution* **66**: 3931-3944.
- Thewissen, J.G.M., Cooper, L.N., Behringer, R.R., 2012. Developmental biology enriches paleontology. *Journal of Vertebrate Paleontology* **32**: 1223-1234.
- Wellik, D.M., 2007. *Hox* patterning of the vertebrate axial skeleton. *Developmental Dynamics* **236**: 2454-2463.
- Wellik, D.M., 2009. *Hox* genes and vertebrate axial pattern, in: Pourquie, O. (Ed.), *Hox* genes. Academic Press, pp. 257-278.
- Wellik, D.M., Capecchi, M.R., 2003. *Hox10* and *Hox11* genes are required to globally pattern the mammalian skeleton. *Science* **30**: 363-367.
- Wiley, D.F., 2005. Landmark (3.0). Institute for Data Analysis and Visualization (IDAV), University of California, Davis. Available from <http://graphics.idav.ucdavis.edu/research/projects/EvoMorph>.
- Wilson, J.A., 1999. A nomenclature for vertebral laminae in sauropods and other saurischian dinosaurs. *Journal of Vertebrate Paleontology* **19**: 639-653.
- Witmer, L.M., 1995. The extant phylogenetic bracket and the importance of reconstructing soft tissues in fossils, in: Thomason, J. (Ed.), *Functional morphology in vertebrate paleontology*. Cambridge University Press, Cambridge, pp. 19-33.
- Woltering, J.M., Vonk, F.J., Müller, H., Bardine, N., Tuduice, I.L., de Bakker, M.A.G., Knöchel, W., Sirbu, I.O., Durston, A.J., Richardson, M.K., 2009. Axial patterning in snakes and caecilians: evidence for an alternative interpretation of the *Hox* code. *Developmental Biology* **332**: 82-89.

## Acknowledgements

The crocodile embryos were donated by Jean-Yves Sire (Université Pierre et Marie Curie Paris, France), Samuel Martin and Eric Ferrandez from the crocodile farm “La Ferme aux Crocodiles” in Pierrelatte (France). We thank Britta Möllenkamp, Dr. Henriette Obermaier and Prof. Dr. Joris Peters of the Institut für Paläoanatomie, Domestikationsforschung und Geschichte der Tiermedizin at the Ludwig-Maximilians-Universität München (Germany) and the Staatssammlung für Anthropologie und Paläoanatomie München (Germany) for providing specimens of recent archosaurs, the Paläontologische Sammlung of the Eberhard Karls Universität Tübingen (Germany) for loan of *Plateosaurus* material and the Staatliches Museum für Naturkunde Stuttgart (Germany) for access to dinosaur specimens. Dr. Timothy Rowe (University of Texas at Austin, USA) and Ms. Megan Demarest kindly provided CT data of the studied mouse skeleton. Dr. Jennifer Olori and Dr. Jessica A. Maisano (High-Resolution X-ray CT Facility & DigiMorph.org, Department of Geological Sciences, The University of Texas, USA) for creating and adding the STL file of the studied mouse skeleton to the DigiMorph website. Jesus Marugán-Lobón (Universidad Autónoma de Madrid, Spain) is thanked for introduction to geometric morphometrics. The manuscript has greatly benefitted from critical and helpful review by Nadia Fröbisch (Humboldt-Universität zu Berlin, Germany). All current members of the Molecular Geo- & Palaeobiology Lab in Munich (Germany), especially Claire Larroux, Sergio Vargas, Oliver Voigt, Astrid Schuster, Gabriele Büttner, Simone Schätzle and Dirk Erpenbeck is thanked for help with laboratory work. We acknowledge all current members of the Mesozoic Vertebrates Research Group in Munich (Germany), especially Adriana López-Arbarello, Richard Butler and Christian Foth for fruitful discussions.

CB was supported by a DAAD fellowship, a doctoral fellowship of the Studienstiftung des deutschen Volkes (German National Academic Foundation) and the mentoring programme within the framework of LMUexcellent of the Ludwig-Maximilians-Universität München (Germany).

## Appendix

Appendix 4.1.: Qualitative characteristics of the cervical vertebrae of *Crocodylus niloticus*.

Appendix 4.2.: Qualitative characteristics of the cervical vertebrae of *Alligator mississippiensis*.

Appendix 4.3.: Qualitative characteristics of the cervical vertebrae of *Gallus gallus domesticus*.

Appendix 4.4.: Qualitative characteristics of the cervical vertebrae of *Plateosaurus engelhardti*.

Appendix 4.5.: Cluster Analysis results of the cervical vertebrae in modern archosaurs.

Appendix 4.6.: Cluster Analysis results of the cervical vertebrae in *Plateosaurus engelhardti*.

**Appendix 4.1.: Qualitative characteristics of the cervical vertebrae of *Crocodylus niloticus*.** Note that all cervical vertebrae of the Nile crocodile have ribs. It was not possible to identify homologous landmarks on the hypapophysis because its geometry varies considerably from a rounded tubercle (C2) to a truncated process (C3, C4) and an anteriorly pointing, sickle-shaped process (C5-C9). The detailed description of the characters is provided in the results (section 4.3.2.).

Abbreviations: hyp = hypapophysis, spin = neural spine, dia = diapophysis, para = parapophysis, keel = ventral keel, poz = postzygapophysis, cent = centrum, cond = condylar fossa, prez = prezygapophysis; if not otherwise indicated 0 = absent, 1 = present.

Character	hyp	spin	dia	para	keel	poz	cent	cond	prez
			0 = no axis 1 = 45° or less posterior from vertical line 2 = 90° from vertical line	0 = no axis 1 = 45° or less posterior from vertical line 2 = 90° from vertical line					
vertebra	1 = rounded 2 = truncated 3 = pointed, anteriorly								
C2	1	0	0	0	0	1	0	0	0
C3	2	0	0	2	0	1	1	1	0
C4	2	0	2	2	0	1	1	1	0
C5	3	0	2	2	1	1	1	0	1
C6	3	0	2	2	1	1	1	0	1
C7	3	0	2	2	1	1	1	0	1
C8	3	1	1	1	1	0	1	0	1
C9	3	1	1	1	1	0	1	0	1

**Appendix 4.2.: Qualitative characteristics of the cervical vertebrae of *Alligator mississippiensis*.** Note that all cervical vertebrae of the American alligator have ribs. It was not possible to identify homologous landmarks on the hypapophysis because its geometry varies considerably from a rounded tubercle (C2) to a truncated process (C3, C4) and an anteriorly pointing, sickle-shaped process (C5-C9). The detailed description of the characters is provided in the results (section 4.3.2.).  
 Abbreviations: hyp = hypapophysis, spin = neural spine, dia = diapophysis, para = parapophysis, keel = ventral keel, poz = postzygapophysis, cent = centrum, cond = condylar fossa, prez = prezygapophysis; if not otherwise indicated 0 = absent, 1 = present.

Character	hyp	spin	dia	para	keel	poz	cent	cond	prez
			0 = no axis						
	1 = rounded	1 = 45° or less posterior from vertical line	1 = 45° or less posterior from vertical line						
	2 = truncated	2 = 90° from vertical line	2 = 90° from vertical line						
	3 = pointed, anteriorly	3 = 315° from vertical line	3 = 315° from vertical line						
C2	1	0	0	0	0	1	0	0	0
C3	2	0	3	3	0	1	1	1	0
C4	2	0	3	3	0	1	1	1	0
C5	3	0	3	2	1	1	1	0	0
C6	3	0	2	2	1	1	1	0	1
C7	3	0	2	2	1	1	1	0	1
C8	3	1	1	1	1	0	0	0	1
C9	3	1	1	1	1	0	0	0	1

**Appendix 4.3.: Qualitative characteristics of the cervical vertebrae of *Gallus gallus domesticus*.** Note that all cervical vertebrae of the domestic chicken have a diapophysis and a parapophysis. However, it was not possible to identify homologous landmarks on these transverse processes because they are completely fused with the cervical ribs. In order to consider the morphology of the ansa costotransversaria, we analysed its tubercles and crests. The detailed description of the characters is provided in the results (section 4.3.2.). Abbreviations: hyp = hypapophysis, spin = neural spine, tub = tuberculum ansae, crist = cristae laterales, caro = processus caroticus, tor = torus dorsalis, trans = foramen transversarium, pneu = pneumatic foramen, poz = postzygapophysis; if not otherwise indicated 0 = absent, 1 = present.

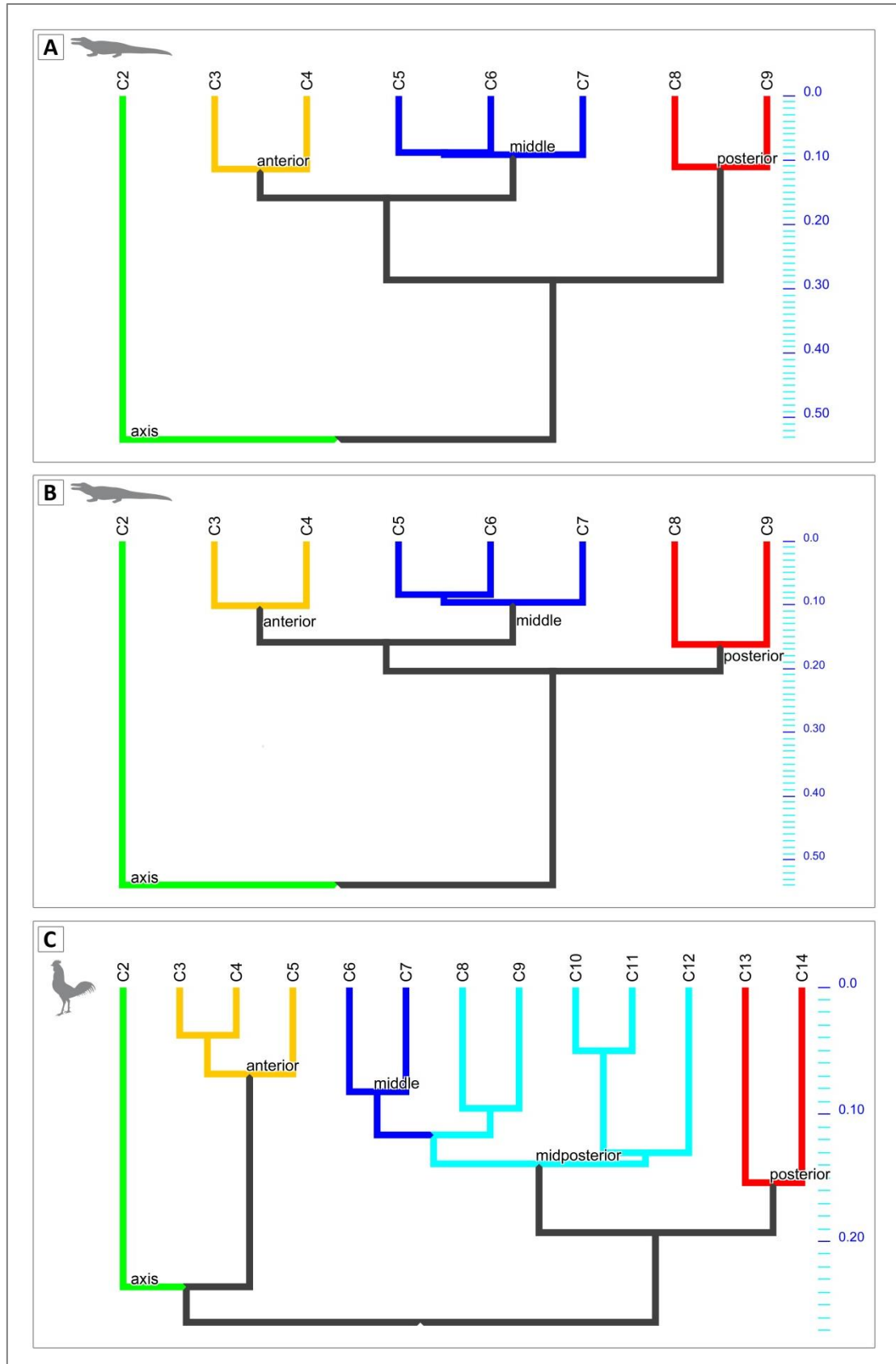
Character	ribs	hyp	spin	tub	crist	caro	tor	trans	pneu
vertebra				[0; 1; 2; 3; 4] = number	[0; 1; 2; 3; 4] = number		1 = near the tip of poz 2 = near the base of spin 3 = near the base of poz	0 = none 1 = round 2 = oval	
C2	0	1	0	0	0	0	1	0	0
C3	1	1	0	2	2	0	1	1	1
C4	1	1	0	2	2	0	1	1	1
C5	1	1	0	2	3	0	1	1	0
C6	1	0	0	3	3	1	2	2	1
C7	1	0	0	3	3	1	2	2	1
C8	1	0	1	4	4	1	3	2	1
C9	1	0	1	4	4	1	3	2	1
C10	1	0	1	4	4	1	1	2	1
C11	1	0	1	4	4	1	1	2	1
C12	1	1	1	4	4	0	1	2	1
C13	1	1	1	4	3	0	1	1	0
C14	1	1	1	4	3	0	1	1	0

**Appendix 4.4.: Qualitative characteristics of the cervical vertebrae of *Plateosaurus engelhardti*.** Note that all cervical vertebrae of the sauropodomorph dinosaur have ribs. The detailed description of the characters is provided in the results (section 4.3.2.).

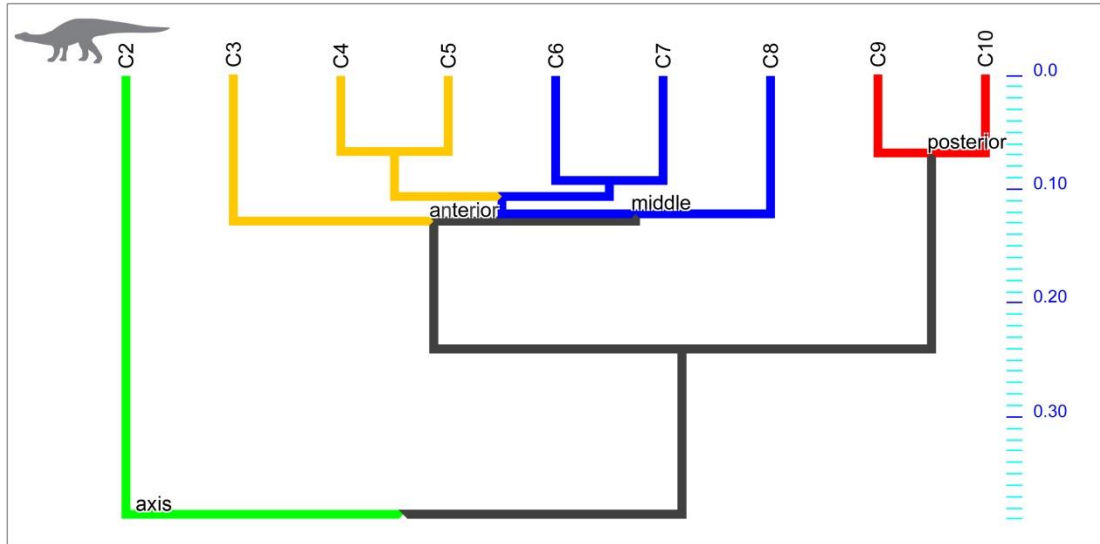
Abbreviations: keel = ventral keel, spin = neural spine, dia = diapophysis, para = parapophysis, epi = epipophysis, acdl = anterior centrodiapophyseal lamina, pcdl = posterior centrodiapophyseal lamina, cond = condylar fossa, prez = prezygapophysis, poz = postzygapophysis; if not otherwise indicated 0 = absent, 1 = present.

Character	keel	spin	dia	para	epi	acdl	pcdl	cond	prez
vertebra		0 = absent 1 = small 2 = prominent	1 = 45° or less posterior from vertical line 2 = 90° from vertical line 3 = 315° from vertical line	1 = 45° or less posterior from vertical line 2 = 90° from vertical line 3 = 315° from vertical line	1 = extends over poz 2 = does not extend over poz				
C2	0	0	1	2	1	0	0	1	0
C3	0	1	3	2	1	0	0	1	1
C4	0	1	2	2	1	1	1	0	1
C5	0	1	2	2	1	1	1	0	1
C6	1	1	3	2	1	1	1	0	1
C7	1	1	3	2	2	1	1	0	1
C8	1	1	3	2	2	1	1	0	1
C9	1	2	2	1	2	1	1	0	1
C10	1	2	2	1	2	1	1	0	1

**Appendix 4.5.: Cluster Analysis results of the cervical vertebrae in modern archosaurs.** The grouping of the vertebrae corresponds to their position in one of the four quadrants of the coordinate system revealed by the Principal Components Analysis (section 4.3.2.3). The discrimination of the respective clusters is based on the highest distance between successive vertebrae in the PCO morphospace which is visualised by the Cluster Analysis for (A) *Crocodylus niloticus*, (B) *Alligator mississippiensis* and (C) *Gallus gallus domesticus*.



**Appendix 4.6.: Cluster Analysis results of the cervical vertebrae in *Plateosaurus engelhardti*.** The grouping of the vertebrae corresponds to their position in one of the four quadrants of the coordinate system revealed by the Principal Components Analysis (section 4.3.4.1). The discrimination of the respective clusters is based on the highest distance between successive vertebrae in the PCO morphospace which is visualised by the Cluster Analysis.



## Chapter 5

### Conclusion

#### 5.1. Synopsis

The vital importance of the axial skeleton for vertebrate life is clearly evident, as its basic functions, that is the protection of the neural structures as well as providing a healthy balance between stability and mobility, remained the same in a huge variety of species (Gadow 1933). It is also the site of lethal disorders and ubiquitous diseases that severely affect the organism's physiology (e.g. Oostra et al. 2005, Pang and Thompson 2011). During evolution, the vertebral column experienced extensive morphological changes and an increased regionalisation, reflecting different additional adaptations to specific functions that have strong impacts on the biology of the animal.

##### 5.1.1. Morphology

The first section of this thesis (chapter 2) revealed a strong link between the digitally simulated flexion pattern of the presacral vertebral column and the axial movements of the living crocodile and ostrich during related activities, such as feeding and locomotion. This correlation, observed in modern animals, enabled the enhancement of knowledge about the palaeobiology of the extinct relative *Plateosaurus*.

Although the ostrich and the sauropodomorph dinosaur *Plateosaurus* share a very long neck, they differ in their cervical flexion pattern and, by association, in their neck movement. The dinosaur was able to reach the ground, but it appears to be primarily adapted as mid-level browser, obtaining food that is at or above the horizontal level of its head.

Despite some functional differences with respect to passive stabilisation of the vertebral column, the dorsal series of *Plateosaurus* displayed several similarities with the alligator. Although this supports a quadrupedal posture for the dinosaur, the morphofunctional pattern of the trunk also indicates that a bipedal posture was possible. This study did not allow an unambiguous interpretation of the locomotion style of *Plateosaurus*.

##### 5.1.2. Genes

The development of an embryo appears to be controlled by the expression of a hierarchy of regulatory genes, such as *Hox* genes. The second section of the present thesis (chapter 3) demonstrates the *Hox* gene expression pattern of the paralog groups 4 to 8 in the Nile crocodile (*Crocodylus niloticus*). *HoxA-4*, *B-4*, *C-4* and *D-4* as well as *HoxA-5* and *C-5* are expressed in the cervical region of the crocodile. The anterior expression limit of *HoxC-6* marks the cervicothoracic

transition. The expression of *HoxA-7* and *B-7* as well as *HoxB-8* and *C-8* are restricted to the dorsal series.

The comparative analysis of the *Hox* code in the crocodile, chicken and mouse revealed that changes in the spatial pattern of *Hox* gene expression along the presacral vertebral column are associated with morphological differences in these modern taxa.

Although the same *Hox* genes are expressed in the cervical region, the pattern of expression is different, because reptile, bird and mammal vary in the number of neck vertebrae. In the relatively long-necked chicken (14 cervical vertebrae), the *Hox* gene expression domains are expanded, whereas the relatively short neck of the mouse (7 cervical vertebrae) revealed a highly condensed and overlapping *Hox* gene expression pattern.

The dorsal series of the crocodile (15 dorsal vertebrae) showed 4 *Hox* gene expression domains. In the mouse, 5 domains were identified in the dorsal vertebral column (19 dorsal vertebrae). The difference in the genetic expression pattern between these two taxa is due to shifts in the *Hox* code, which reflects the increased specialisation of the mammalian axial skeleton. In the dorsal series of the chicken (11 dorsal vertebrae with 4 of them fused to the notarium), another mechanism was observed. There are 3 *Hox* gene expression domains because of condensation and increased overlap of the genetic activity.

### 5.1.3. Fossils

Research on the expression pattern of *Hox* genes (including this study, chapter 3) in a variety of vertebrate species revealed a strong association between morphological boundaries along the vertebral column and specific *Hox* gene expression limits (e.g. Burke et al. 1995, Mansfield and Abzhanov 2010, Wellik and Capecchi 2003). Furthermore, mutation experiments reinforced the significant importance of *Hox* gene activity for proper organisation of the vertebrate body plan, and thus for the regionalisation of the axial column (e.g. Horan et al. 1994, Jeannotte et al. 1993). The potential of the correlation between anterior *Hox* gene expression and vertebral morphology was demonstrated in the third section of the present thesis (chapter 4).

In the cervical vertebral column of crocodile, chicken and mouse, morphological clusters were linked to anterior *Hox* gene expression boundaries. This direct correlation between vertebral *Hox* code and quantifiable vertebral morphology showed that the genetic code can be deduced from vertebral morphology in modern taxa. The highly variable cervical region provides an illuminating model for the study of the relationship between genomic control and phenotypic changes.

These findings were applied to a fossil archosaur in order to establish the *Hox* code for the extinct relative *Plateosaurus*, on the basis of quantifiable changes in vertebral morphology. The

morphometric investigations revealed a pattern of cervical morphology that is intermediate between the morphological pattern observed in the crocodile and the bird. Via the extant phylogenetic bracket approach plus the use of the vertebral shape changes as morphological marker, the hypothetical *Hox* code for *Plateosaurus* was reconstructed. It is generally similar to the crocodylian *Hox* gene expression pattern, but with the variation that the anterior region is expanded as in birds.

These results demonstrate that it is indeed possible to indirectly trace the evolution of *Hox* gene expression patterns in the vertebral column of amniotes through an analysis of quantifiable morphology. This opens up new approaches to establish vertebral homologies in taxa with different vertebral numbers, and to comprehensively analyse the morphological and genetic evolution of the axial skeleton including both extant and extinct taxa.

## 5.2. Concluding remarks

The evolution of vertebrate life, ranging from fish to mammals, including humans, happened over the incredibly long period of 500 million years. The origin of biodiversity is one of the great challenges in science. Recent research has shown that, in addition to Darwinian variation and selection, the function of regulatory genes during development plays a major role in the evolution of disparate morphologies. Methods of integrating data from evolutionary developmental biology and palaeontology can greatly enhance our understanding of trait evolution (Slater et al. 2012, Thewissen et al. 2012).

As this study showed, an integrative analysis (morphology, genes and fossils) of the vertebrae provides valuable information about the possible reasons, the genetic basis and the pattern for evolutionary changes of the vertebral column. On one hand, it is necessary to infer the specific biological roles of the axial skeleton on the basis of functional differences that may be associated with modifications in the morphology of the axial skeleton. On the other hand, these phenotypic variations are related to the expression of regulatory genes in modern animals. Furthermore, the strong correlation between modifications in vertebral morphology and *Hox* gene expression allows the tracing of the pattern of vertebral evolution including fossil taxa where the genetic information is not retrievable.

## 5.3. Future directions

Geological and fossil records form one piece of information about the evolutionary history of life on Earth. They reveal the actual environments, contemporary species and transitional structures that existed throughout the history of life. The record of the diversity of life provides insights into the patterns of evolution. The more data is available, the more information can be collected in order to understand evolution. Thus, it is highly important to achieve a rich fossil record by intensive field

work. In order to draw all the secrets from skeletal remains, it is necessary to apply a comprehensive approach by combining palaeontological and developmental data. In addition to the study of the morphology of bones in extant and extinct animals, the study of genetic activity and embryonic development provides growing knowledge of the molecular basis of evolution. A detailed understanding of evolutionary patterns and the underlying genetic mechanisms will allow to widely open the window into the past. Winston Churchill once said: "*The farther backward you can look, the farther forward you are likely to see.*" If we investigate the past, we are able to understand the present, which may even allow predictions for the future.

## 5.4. References

- Burke, A.C., Nelson, C.E., Morgan, B.A., Tabin, C., 1995. *Hox* genes and the evolution of vertebrate axial morphology. *Development* **121**: 333-346.
- Gadow, H.F., 1933. The evolution of the vertebral column. A contribution to the study of vertebrate phylogeny. Cambridge University Press, London, 356 pp.
- Horan, G.S., Wu, K., Wolgemuth, D.J., Behringer, R.R., 1994. Homeotic transformation of cervical vertebrae in *Hoxa-4* mutant mice. *Proceedings of the National Academy of Sciences* **91**: 12644-12648.
- Jeannotte, L., Lemieux, M., Charron, J., Poirier, F., Robertson, E.J., 1993. Specification of axial identity in the mouse: role of the *Hoxa-5* (*Hox1.3*) gene. *Genes & Development* **7**: 2085-2096.
- Mansfield, J.H., Abzhanov, A., 2010. *Hox* expression in the American alligator and evolution of archosaurian axial patterning. *Journal of Experimental Zoology Part B Molecular and Developmental Evolution* **314 B**: 1-16.
- Oostra, R.J., Hennekam, R.C., de Rooij, L., Moorman, A.F., 2005. Malformations of the axial skeleton in Museum Vrolik I: homeotic transformations and numerical anomalies. *American Journal of Medical Genetics. Part A* **134**: 268-281.
- Pang, D., Thompson, D.N., 2011. Embryology and bony malformations of the craniovertebral junction. *Child's Nervous System* **27**: 523-564.
- Slater, G.J., Harmon, L.J., Alfaro, M.E., 2012. Integrating fossils with molecular phylogenies improves inference of trait evolution. *Evolution* **66**: 3931-3944.
- Thewissen, J.G.M., Cooper, L.N., Behringer, R.R., 2012. Developmental biology enriches paleontology. *Journal of Vertebrate Paleontology* **32**: 1223-1234.
- Wellik, D.M., Capecchi, M.R., 2003. *Hox10* and *Hox11* genes are required to globally pattern the mammalian skeleton. *Science* **30**: 363-367.

## Acknowledgments

First, I would like to extend my deepest gratitude to PD Dr. Oliver W. M. Rauhut (Bayerische Staatssammlung für Paläontologie und Geologie München, Germany) and Prof. Dr. Gert Wörheide (Ludwig-Maximilians-Universität München and Bayerische Staatssammlung für Paläontologie und Geologie München, Germany), the first and second supervisor of this thesis, for leaving the research on the present subject to me. I am very grateful for all of their help, valuable advice, enduring support and encouragement.

Thanks to the constant support of my colleagues that have been involved during my work on the manuscripts which make up this thesis. I have listed the detailed acknowledgements at the end of each chapter.

I thank Prof. Dr. Martin Sander (Universität Bonn, Germany) for his help and the opportunity to be part of the DFG Research Unit 533 “Biology of the Sauropod Dinosaurs: The Evolution of Gigantism”. Without the support of Prof. Dr. Hans-Ulrich Pfretzschner (Universität Tübingen, Germany) this project would not have been possible.

Financial support for this study was provided by the DAAD (German Academic Research Exchange Service), the Studienstiftung des deutschen Volkes (German National Academic Foundation) and the mentoring programme within the framework of LMUexcellent of the Ludwig-Maximilians-Universität München (Germany).